UNIVERSIDADE D
COIMBRA

Getachew Debas Belew

FRUCTOSE METABOLISM AND LIPOGENESIS FLUXES IN MICE MODELS OF DIET-INDUCED NON-ALCOHOLIC FATTY LIVER DISEASE

Tese no âmbito do Doutoramento em Biologia Experimental e Biomedicina, ramo de Biotecnologia e Saúde, orientada pelo Doutor John G. Jones e coorientada pela Professor Doutor Piero Portincasa e pelo Professor Doutor João Ramalho Santos, apresentada ao Instituto de Investigação Interdisciplinar da Universidade de Coimbra

Julho de 2021

Institute for Interdisciplinary Research,
University of Coimbra

FRUCTOSE METABOLISM AND LIPOGENESIS FLUXES IN MICE MODELS OF DIET-INDUCED NON-ALCOHOLIC FATTY LIVER DISEASE

Getachew Debas Belew

Doctoral thesis submitted to the Institute of Interdisciplinary Research of the University of Coimbra to apply for the degree of Doctor of Philosophy in Experimental Biology and Biomedicine, specialization in Biotechnology and Health.

July 2021

1 2 9 0

UNIVERSIDADE D
COIMBRA

Horizon2020
European Union Funding
for Research & Innovation

CENTER FOR NEUROSCIENCE
AND CELL BIOLOGY
UNIVERSITY OF COIMBRA
PORTUGAL

This doctoral thesis is part of a project that has received funding from the European Union's Horizon 2020 research and innovation programme under the Marie Skłodowska-Curie grant agreement No 722619.

Also, this work was supported by the Portuguese Foundation for Science and Technology (research grant FCT-FEDER-02/SAICT/2017/028147). Structural funding for the Center for Neurosciences and Cell Biology and the UC-NMR facility is supported in part by FEDER – European Regional Development Fund through the COMPETE Programme, Centro 2020 Regional Operational Programme, and the Portuguese Foundation for Science and Technology through Grants UIDB/04539/2020; POCI-01-0145-FEDER-007440; REEQ/481/QUI/2006, RECI/QEQ QFI/0168/2012, CENTRO-07-CT62-FEDER-002012, and Rede Nacional de Ressonancia Magnética Nuclear.

PUBLICATIONS

Part of the work included in this Thesis is already published in international peer-reviewed scientific journal, and is referred below:

1. **Belew GD,** Silva J, Rito J, Tavares L, Viegas I, Teixeira J, Oliveira PJ, Macedo MP, Jones JG. **Transfer of 2H from glucose to specific sites of newly synthesized triglyceride fatty acids in feeding mice.** *J Lipid Res.* 2019Dec;60(12):2050-2056. http://doi.org/10.1194/jlr.RA119000354. PMID: 31575642; PMCID: PMC6889712.

2. **Getachew D. Belew**[#], Giada Di Nunzio[#], Joao Gabriel Silva, Alejandra N. Torres, Ludgero Tavares, and John G. Jones. **Estimating Pentose Phosphate Pathway Activity From the Analysis of Hepatic Glycogen ^{13}C-Isotopomers Derived From [U-^{13}C]Fructose and [U-^{13}C]Glucose.** *Magn Reson Med.* 2020;00:1–7. http://doi.org/10.1002/mrm.28286.

3. **Getachew Debas Belew**, Ludgero Tavares, Maria Joao Meneses, Paula Macedo, John G. Jones. **Quantifying the effects of high fat, high sugar and a combination of high fat and high sugar feeding on hepatic triglyceride synthesis and sources in the mouse model (2021).** Manuscript in-preparation (Included in the thesis)

4. Giada Di Nunzio[#], **Getachew D. Belew**[#], Alejandra N. Torres, Joao Gabriel Silva, Luis P. Silva, Cristina Barosa, Ludgero Tavares, and John G. Jones. **Determining the Contribution of a High-Fructose Corn Syrup Formulation to Hepatic Glycogen Synthesis during ad-libitum feeding in mice.** *Sci Rep.* 2020 (10):12852. https://doi.org/10.1038/s41598-020-69820-3.

5. Diego O Borges, Rita S Patarrão, Rogério T Ribeiro, Rita Machado de Oliveira, Nádia Duarte, **Getachew Debas Belew**, Madalena Martins, Rita Andrade, João Costa, Isabel Correia, José Manuel Boavida, Rui Duarte, Luís Gardete-Correia, José Luís Medina,

João F Raposo, John G Jones, Carlos Penha-Gonçalves, M Paula Macedo. **Loss of postprandial insulin clearance control by Insulin-degrading enzyme drives dysmetabolism traits.** *Metabolism.* 2021 (118): 154735 https://doi.org/10.1016/j.metabol.2021.154735

6. Hu Huang, Seung-Hwan Lee, Inês Sousa-Lima, Sang-Soo Kim, Won Min Hwang, Yossi Dagon, Won-Mo Yang, Sungman Cho, Min-Cheol Kang, Ji A. Seo, Munehiko Shibata, Hyunsoo Cho, **Getachew Debas Belew**, Jinhyuk Bhin, Bhavna N. Desai, Min Jeong Ryu, Minho Shong, Peixin Li, Hua Meng, Byung-Hong Chung, Daehee Hwang, Min Seon Kim, Kyong Soo Park, Maria Paula Macedo, Morris White, John Jones, and Young-Bum Kim. **Rho-kinase is a novel regulator of hepatic lipogenesis during overnutrition.** *J Clin Invest*. 2018;128(12):5335-5350. https://doi.org/10.1172/JCI63562.
7. Ivana Jarak, Cristina Barosa, Fatima O. Martins, Joao C. P. Silva, Cristiano Santos, **Getachew Debas Belew**, Joao Rito, Ivan Viegas, Jose Teixeira, Paulo J. Oliveira, John G. Jones. **Sources of hepatic glycogen synthesis in mice fed with glucose or fructose as the sole dietary carbohydrate**. *Magn Reson Med*, 2018;00:1-6. https://doi.org/10.1002/mrm.27378.

Review Papers

8. Caroline D Veloso, **Getachew D Belew**, Luciana L Ferreira, Luís F Grilo, John G Jones, Piero Portincasa, Vilma A Sardão, Paulo J Oliveira. **A Mitochondrial Approach to Cardiovascular Risk and Disease.** *Curr Pharm Des*. 2019;25(29):3175-3194. https://doi.org/10.2174/1389203720666190830163735.
9. Getachew D Belew and John G Jones. ***De novo* lipogenesis in NAFLD: quantification with stable isotope tracers**. Manuscript in-preparation (included in the thesis)

PRESENTATIONS

The results exhibited in this Thesis were presented in national and international scientific meetings in the form of oral or poster communication.

- The 54th Annual Scientific Meeting of the European Society of Clinical Investigation (**Virtual ESCI 2021 meeting**), 9-11 June 2021. **Getachew D. Belew**, Ludgero Tavares, Maria J. Meneses, Paula Macedo, and John G. Jones. **Increased contribution of fructose to de novo synthesis of saturated over mono-unsaturated fatty acids in mice fed high-sugar and high fat-high sugar diets**. In *EUROPEAN JOURNAL OF CLINICAL INVESTIGATION* (Vol. 51, pp. 77-78). 111 RIVER ST, HOBOKEN 07030-5774, NJ USA: WILEY.
- The 56th European Association for the Study of Diabetes (**Virtual EASD 2020 meeting**) Annual Meeting, 21-25th September 2020. **Belew, G. D.,** Tavares, L., Torres, A. N., Nunzio, G. D., & Jones, J. G. (2020, September). **Estimating pentose phosphate pathway activity from the analysis of hepatic glycogen ^{13}C-isotopomers from [U-^{13}C]fructose.** In *DIABETOLOGIA* (Vol. 63, No. SUPPL 1, pp. S201-S201). ONE NEW YORK PLAZA, SUITE 4600, NEW YORK, NY, UNITED STATES: SPRINGER.
- The 54th Annual Scientific Meeting of the European Society of Clinical Investigation (**Virtual ESCI 2020 meeting**), 20-30 September 2020. **Belew, G. D**., Tavares, L., Nunzio, G. D., Torres, A. N., & Jones, J. G. (2020, September). **Estimating pentose phosphate pathway activity from the analysis of hepatic glycogen ^{13}C-isotopomers from [U-^{13}C]fructose**. In *EUROPEAN JOURNAL OF CLINICAL INVESTIGATION* (Vol. 50, pp. 19-20). 111 RIVER ST, HOBOKEN 07030-5774, NJ USA: WILEY.

- The 16th Annual Diabetes Congress of the SPD (Portuguese Society of Diabetology), 6-8 March 2020. Vilamoura, Algarve, Portugal. **Getachew D. Belew**, Ludgero Tavares, Alejandra N. Torres, Giada Di Nunzio, & John Jones**. Estimating pentose phosphate pathway activity from the analysis of hepatic glycogen ^{13}C-isotopomers from [U-^{13}C]fructose**.
- The 55th European Association for the Study of Diabetes (EASD) Annual Meeting, 16-20th September 2019, Barcelona, Spain. **Belew, G.,** Texeira, J., Oliveira, P., Rito, J., Silva, J., Viegas, I., & Jones, J. (2019, September). **Pentose pathway oxidation of glucose is a significant source of NADPH for de novo lipogenesis as evidenced by extensive transfer of glucose hydrogens into fatty acid position 3.** In *DIABETOLOGIA* (Vol. 62, pp. S266-S266). 233 SPRING ST, NEW YORK, NY 10013 USA: SPRINGER.
- 53rd Annual Scientific Meeting of the European Society of Clinical Investigation (ESCI), 22-24 May 2019. Coimbra, Portugal. **Belew, G.,** Silva, J., Rito, J., Viegas, I., Texeira, J., Oliveira, P., & Jones, J. (2019, April). **Transfer of ^{2}H from glucose to fatty-acids during *de novo* lipogenesis in feeding mice.** In *EUROPEAN JOURNAL OF CLINICAL INVESTIGATION* (Vol. 49, pp. 214-214). 111 RIVER ST, HOBOKEN 07030-5774, NJ USA: WILEY.
- The 15th Annual Diabetes Congress of the SPD (Portuguese Society of Diabetology), 8-10 March 2019. Vilamoura, Algarve, Portugal. **Getachew Debas Belew**, Joao Silva, Joao Rito, Ivan Viegas, Jose Teixeira, Paulo J. Oliveira, John G. Jones. **Transfer of Glucose Hydrogens to Fatty Acids during Lipogenesis.**
- The 7th annual meeting of the European Association for the Study of Diabetes – Non-alcoholic Fatty Liver Disease (EASD-NAFLD) study group and 27th European Group for the study of Insulin Resistance (EGIR) meeting, 8-10 May 2019. Lisbon, Portugal.

Belew G., Silva, J., Rito, J. Viegas, I, Texeira, J., Oliveira, P. Tavares, L. Jones, J. **^{13}C NMR of hepatic triglyceride from mice fed fructose plus [U-^{13}C]glucose informs the contribution of glucose to de novo lipogenesis and elongation of specific fatty acid classes.**

- The 6th annual meeting of the ESAD_NAFLD study group, 19-20 April 2018. Oxford, UK. **Getachew Debas Belew**, Joao Silva, Joao Rito, Ivan Viegas, Jose Teixeira, Paulo J. Oliveira, John G. Jones. **Transfer of ^{2}H from glucose to specific sites of newly synthesized triglyceride fatty acids in feeding mice.**
- The 26th European Group for the study of Insulin Resistance (EGIR) meeting, 7-8 June 2018. Lille, France. **Getachew Debas Belew**, Joao Silva, Joao Rito, Ivan Viegas, Jose Teixeira, Paulo J. Oliveira, John G. Jones. **Transfer of ^{2}H from glucose to specific sites of newly synthesized triglyceride fatty acids in feeding mice.**

COMPLEMENTARY TRAININGS

Formations within the Doctoral School and Institute:

a) **Laboratory animal science course**, "**Federation of European Laboratory Animal Science Associations"** (FELASA Category C) (80hrs), May 7-19, 2018, i3s-Porto, Porto, Portugal

b) **NMR Basics-2018**, April 11-14, 2018, UC-NMR, University of Coimbra, Coimbra, Portugal

Formations within the Foie Gras consortium:

- **1st FOIE GRAS Networking School**: "Tools and Rationale for measuring mitochondrial function in intact cells and isolated mitochondria" – 18th-23th September 2017, Coimbra, Portugal.
- **2nd FOIE GRAS Networking School**: "Tools for the study of Gut-Liver crosstalk and energy fluxes in NAFLD" – 3rd-5th July 2018, Pisa, Italy.
- **3rd FOIE GRAS Networking School:** "Biomarkers for NAFLD staging, prognosis and treatment" – 10th-12th July 2019, Lisbon, Portugal.
- **4th FOIE GRAS Networking School**: "NAFLD: modulation by lifestyles and therapies" – May 26th, online
- Short course on public communication given by Dr. Marisa Azul from the Center for Neuroscience and Cell Biology (Coimbra, Portugal) – 12th-13th July 2018, Coimbra, Portugal (18h).

ACKNOWLEDGEMENTS

First and foremost, I would like to thank the Almighty God and his mother Virgin Mary for their mercy and blessings in all my life.

I would like to extend my heart-felt gratitude to my supervisor, Dr. John Jones, whose expertise, understanding, and guidance, added greatly to my knowledge. Under his supervision I have learned a great deal about what it really means to do science. I recognize you an endless capacity for work and an enormous sense of kindness. Thank you for believing in me and the opportunities you gave me, for having supported me unconditionally and for all the knowledge transmitted over these years. His door is always open and his mind is always ready for discussing science. I won't forget all the extracurricular activities we had together; making beer, golfing, playing football, fishing etc.

I owe the deepest gratitude to my lab mates in the Intermediary Metabolism group: João Silva, João Rito, Catia Marques, Cristina Barosa, Ivan Viegas, Mariana Palma, Ludgero Tavares, Margarida Coelho, Giada Di Nuzio, for their kind welcoming, technical and administrative support in the laboratory work as well as for providing me so important information about the academic environment and expert opinion throughout my stay. Thank you so much for supporting, caring and challenging me for the last four years.

I also would like to thank Dr. Paulo Oliveira and his lab group members, for the constant availability, friendship, and technical and material support throughout the program.

To Professor João Ramalho-Santos, for his kind help and support whenever I need, his fast reaction for my requests make things very simple and smooth during the program. To the CNC, in particular the UC Biotech which made possible my work, and also to the UC for the NMR facilities.

I thank you all the members of the Foie Gras advisory board and PI team, for all the professional advice and scientific debates you provided. More than a researcher, this program has made me grow as an individual. To Professor Piero Portincasa for welcoming me into his lab and clinic at the University of Bari Medical school where I got the opportunity to acquire hands on experience on clinical aspects of NAFLD patients, and for treating me as part of the team during my stay. To Dr. Amalia Gastadelli for your kind willingness to welcome me in your lab though interrupted by the COVID-19 pandemic.

To my fellow ESRs at project FOIE GRAS. Looking back, I cannot think of a more spectacular group of people with whom I could have shared this experience. Even if time and distance take us apart, be sure that I will always hold you dear in my heart. Ameseginalehu, Obrigado. Gracias. Gràcies. Grazie. Hvala. Dhanyavaad. Tomake Donnobadh.

I thank the European Union's Horizon 2020 research and innovation programme and Portuguese Foundation for Science and Technology for the financial support of the program.

I owe special thanks to my Portuguese family Mr. and Mrs. Carlos, Joao Silva, Cesar Silva, Diana, etc for your kind hospitality, family treatment, caring, and unconditional love. You are more than a family. I will always remember you to the rest of my life. Thank you.

Finally, I would like to owe many thanks to my family for their endless support and love. To my dearest wife (**SELAMIE**), the strongest woman I have known and had the lion-share in this PhD success, my lovely kids and sisters, and other members of my family, without your unconditional love and support none of this would have been possible. I am grateful and blessed for having a wonderful wife and family. I would like to thank all my friends and colleagues for their love and continuous encouragement.

DEDICATION

This thesis is dedicated to my father, the late soldier Debas Belew, who passed away peacefully six years ago, and to my mother Aselef Tenaw, who did not only raise and nurture me but also scarified themselves for years for my personal and academic development. I missed you badly, Father! May God rest your soul in peace!

To my amazing wife, Selamawit Mulugeta, to my lovely children, Solyana and Nehimiya who are born in the middle of this PhD program and became part of the story, to my parents, with my gratitude for their support, scarifies, tolerance, inspiration, and endless love throughout my study.

CONTENTS

LIST OF FIGURES 18

LIST OF TABLES 20

LIST OF ABBREVIATIONS 22

ABSTRACT 28

RESUMO 30

CHAPTER ONE 33

NON-ALCOHOLIC FATTY LIVER DISEASE (NAFLD) 34

1. INCIDENCE, RISK FACTORS, TREATMENT AND STUDY OF NAFLD 34

1.1. Dietary factors in NAFLD development 37

1.2. Genetic factors in NAFLD development 41

1.3. NAFLD Treatment 45

1.4. Study of NAFLD 53

2. METABOLIC BASIS OF NAFLD 59

2.1. The role of DNL in NAFLD 62

2.2. DNL regulation, substrates and co-factors 64

2.3. How DNL is measured: 67

2.4. How contributions of individual substrates to DNL are measured 73

3. RESEARCH OBJECTIVES 76

1. RESEARCH METHODOLOGY 77

CHAPTER TWO 80

TRANSFER OF GLUCOSE HYDROGENS VIA ACETYL-COA, MALONYL-COA AND NADPH TO FATTY ACIDS DURING *DE NOVO* LIPOGENESIS.....81

1. INTRODUCTION.....81

2. METHODS.....84

2.1. Materials.....84

2.2. Animal studies.....84

2.3. Triglyceride extraction and purification.....85

2.4. NMR analysis.....86

2.5. Quantification of triglyceride positional ^{2}H and ^{13}C enrichments.....87

2.6. Statistics.....89

3. RESULTS.....90

4. DISCUSSION.....95

4.1. Exchange of glucose ^{2}H during the formation of acetyl-CoA and malonyl-CoA.........95

4.2. ^{2}H transfer from glucose to fatty acids via NADPH.....97

4.3. Fatty acid enrichment from $^{2}H_2O$.....100

4.4. Implications for estimating the number of deuterium atoms incorporated per fatty acid.....101

CHAPTER THREE.....103

ESTIMATING PENTOSE PHOSPHATE PATHWAY ACTIVITY FROM THE ANALYSIS OF HEPATIC GLYCOGEN ^{13}C-ISOTOPOMERS DERIVED FROM [U-^{13}C]FRUCTOSE AND [U-^{13}C]GLUCOSE.....104

1. INTRODUCTION.....104

2. METHODS.....107

2.1. Materials:.....107

2.2. Animal Studies.....107

2.3. Glycogen extraction and monoacetone glucose synthesis.....108

2.4. NMR analysis:.....109

2.5. Quantification of PPP fluxes.....109

2.6. Statistics.....114

3. RESULTS.....115

4. DISCUSSION.....119

CHAPTER FOUR.....122

QUANTIFYING THE EFFECTS OF HIGH FAT, HIGH SUGAR AND A COMBINATION OF HIGH FAT AND HIGH SUGAR FEEDING ON HEPATIC TRIGLYCERIDE SYNTHESIS AND SOURCES IN THE MOUSE MODEL.....123

1. INTRODUCTION.....123

2. MATERIALS AND METHODS.....126

2.1. Materials.....126

2.2. Animal Studies.....126

2.3. Liver triglyceride extraction and purification.....127

2.4. NMR analysis.....128

2.5. Estimation of body fat fraction.....130

2.6. ^{13}C-chemical shift assignments and quantification of FAs abundance.....131

2.7. Quantification of TG positional ^{2}H-enrichments and estimates of FA and glycerol fractional synthetic rates: 131

2.8. Statistics 134

3. RESULTS 135

3.1. Effects of the diets on body weight, adiposity and liver TG 135

3.2. Effects of the diets on hepatic triglyceride lipidomics 137

3.3. Effects of the diets on hepatic triglyceride lipid fluxes 146

3.4. Effects of a high fat background on HFCS-55 fructose metabolism into hepatic triglyceride fatty acids and glycerol. 150

4. DISCUSSION 153

4.1. Influence of the diet on liver adiposity and fat levels 153

4.2. Influence of the diets on hepatic triglyceride lipidomics: 153

4.3. Influence of the diets on hepatic lipogenesis and triglyceride synthesis rates: 154

4.4. Contribution of dietary fructose to hepatic TG synthesis during high sugar and high sugar + high fat feeding: 156

CHAPTER FIVE 159

GENERAL CONCLUSIONS AND FUTURE PERSPECTIVES 160

1. GENERAL CONCLUSION 160

2. FUTURE PERSPECTIVES 163

BIBLIOGRAPHY 165

LIST OF FIGURES

Figure 1: The spectrum of non-alcoholic fatty liver disease (NAFLD). 35

Figure 2: The estimated prevalence of NAFLD and the PNPLA3 genotypes distribution across the globe.....36

Figure 3: Metabolic pathways leading to hepatic steatosis.....60

Figure 4: Integration of $^{2}H_2O$ and [U-^{13}C]sugar substrates to quantify the contribution of exogenous sugar as part of a glucose/fructose mixture to de novo synthesis of TG fatty acid and glycerol moieties 74

Figure 5: Sources of hydrogens for the synthesis of palmitoyl-CoA from glucose and body water via fatty acyl-CoA synthase, with the butyryl acyl carrier protein (Butyryl-ACP) intermediate.....82

Figure 6: Representative ^{13}C NMR spectrum of liver triglyceride isolated from a mouse that ingested glucose enriched with [U-^{13}C]- and [U-^{2}H]glucose. 88

Figure 7: A: A representative ^{2}H NMR spectrum of purified liver triglyceride acquired from a mouse provided with glucose enriched with equimolar amounts of [U-^{2}H]glucose and [U-^{13}C]glucose. **B:** A ^{2}H NMR spectrum of triglyceride acquired from a mouse provided with glucose enriched with equimolar amounts of [3-^{2}H]glucose and [U-$^{13}C_6$]glucose. **C**: A ^{2}H NMR spectrum of triglyceride acquired from a mouse provided with $^{2}H_2O$ and [U-^{13}C]glucose.....92

Figure 8: Schematic of intracellular NADPH hydrogen sources.....99

Figure 9: Schematic of glycogen isotopomer formation from exogenous [U-^{13}C]glucose and [U-^{13}C]fructose, including TCA cycle and Pentose-P effects. 106

Figure 10: Schematic of [U-^{13}C]glucose-6-P conversion to fructose-6-P through the PPP with the carbon skeleton passing via xylulose-5-phosphate **(A)** or ribose-5-phosphate **(B)**. 111

Figure 11: Schematic of glycogen enrichment from exogenous [U-^{13}C]fructose, via the pentose phosphate pathway.....112

Figure 12: Carbon 2 and carbon 5 resonances of glycogen following derivatization to MAG from a mouse administered with [U-^{13}C]glucose (top) and a mouse administered with [U-^{13}C]fructose (bottom).....116

Figure 14: ^{2}H (upper) and ^{1}H (lower) NMR spectra of a purified triglyceride fraction obtained from a high fat and high sugar diet (**HFHSD**) mouse provided with a mixture of $^{2}H_2O$ and a combination of [U-^{13}C]fructose and unlabelled glucose. 138

Figure 15: ^{13}C NMR spectrum of hepatic triglyceride obtained from a high fat and high sugar diet **(HFHSD**) mouse provided with a mixture of [U-^{13}C]fructose and unlabeled glucose. .139

Figure 16: Hepatic triglyceride fatty acid profiles for mice fed normal chow (**CTRL),** high fat chow (**HFD)**, high sugar diets (**HSD)**, and high fat and high sugar diet (**HFHSD)** : 140

Figure 17: The distribution of different fatty acid classes in the glycerol *sn*1,3 and *sn*2 positions of hepatic triglyceride resolved by ^{13}C NMR for mice fed normal chow (**CTRL**), high fat chow (**HFD**), high sugar diets (**HSD**), and high fat and high sugar diet (**HFHSD**): 143

Figure 18: Fractional rates of fatty acid synthesis **(A)**, fatty acid elongation **(B)**, fatty acid desaturation **(C)** and glycerol synthesis **(D)** of hepatic triglyceride for mice fed normal chow **(CTRL)**, high fat chow **(HFD)**, high sugar diets **(HSD)**, and high fat and high sugar diet **(HFHSD)** :.....147

Figure 19: Fractional mass of newly synthesized fatty acid **(A)**, fatty acid elongation mass **(B)**, desaturated fatty acid mass **(C)** and newly synthesized glycerol mass **(D)** of hepatic triglyceride for mice fed normal chow **(CTRL)**, high fat chow **(HFD)**, high sugar diets **(HSD)**, and high fat and high sugar diet **(HFHSD)** : 149

Figure 20: Contribution of dietary fructose to the synthesis of fatty acid **(A)** and glycerol **(B)** components of hepatic triglyceride for mice fed high sugar diets **(HSD)**, and high fat and high sugar diet **(HFHSD)** : 151

LIST OF TABLES

Table 1: Most commonly used animal models (mice and rats) of NAFLD.....55

Table 2: Fatty acid ^{13}C and ^{2}H enrichments from mice provided with glucose enriched with [U-^{13}C]- and [U-^{2}H]glucose and [U-^{13}C]- and [3-^{2}H]glucose. 91

Table 3: $^{2}H/^{13}C$ enrichment ratios for fatty acid position 2, position 3, and terminal methyl.94

Table 4: Selected liver glycogen ^{13}C-isotopomers from mice provided with fructose/glucose mixture in their drinking water enriched with either [U-^{13}C]fructose or [U-^{13}C]glucose. 118

Table 5: Results from one-way ANOVA (*p*-values) applied to data representing on Figure 16 representing hepatic triglyceride fatty acid profiles.....141

Table 6: Results from one-way ANOVA (*p*-values) applied to data on Figure 17 representing fatty acids distribution in each position – *sn*2 or *sn*1,3 –.....145

Table 7: Results from one-way ANOVA (*p*-values) applied to data on Figure 18 representing the effect of diets on hepatic triglyceride lipid fluxes (%).....146

Table 8: Results from one-way ANOVA (*p*-values) applied to data on Figure 19 representing the effect of diets on hepatic triglyceride lipid fluxes (g/100g of tissue) 148

Table 9: ^{2}H Enrichment of the TG ω-1 and glycerol *sn*1, *sn*3 hydrogens in mice provided with $^{2}H_2O$ and the combinations of [U-^{13}C]fructose and unlabeled glucose in their drinking water.....150

Table 10: Results from one-way ANOVA (*p*-values) applied on data from specific contributions [U-^{13}C]fructose to newly synthesized fractions of fatty acids in each diet group (high sugar diets (**HSD**), and high fat and high sugar diet (**HFHSD**)), and two-tailed t-tests on specific contributions [U-^{13}C]fructose to newly synthesized fractions of glycerol and fatty acids between the diets (HSD vs HFHSD). 152

LIST OF ABBREVIATIONS

^{13}C: Carbon-13

^{19}F: Fluorine-19

^{1}H: Proton

^{2}H: Deuterium

$^{2}H_2O$: Deuterated water

AASLD: American Association for the Study of Liver Diseases

ACC: Acetyl-Coenzyme A Carboxylase

ACC1: Acetyl-CoA carboxylase 1

ACC2: Acetyl-CoA carboxylase 2

ALDH1L1: Aldehyde Dehydrogenase 1 Family Member L1

ALT: alanine aminotransferase

ApoE: Apolipoprotein E

ASK 1: Apoptosis Signal-regulating Kinase 1

ATGL: adipose triglyceride lipase

ATP: adenosine triphosphate

BMI: body mass index

C57BL/6: C57 black 6

C_6F_6: Hexafluorobenzene

CCl_4: Carbon tetrachloride/ tetrachloromethane

CCR2: C-C chemokine receptor type 2

CCR5: C-C chemokine receptor type 5

CDAA: Choline-deficient L-amino acid-defined diet

$CHCl_3$: Chloroform/trichloromethane

ChREBP: carbohydrate response element binding protein

CM: chylomicron

CVD: cardiovascular disease

FFA: free fatty acid

CTL: Control

db/db: diabetic mouse model

DGAT diacylglycerol O-acyltransferase

DGAV: Direção-Geral de Alimentação e Veterinária/ Portuguese National Authority for Animal Health

DHA: Docosahexaenoic acid

DNL: *de novo* lipogenesis

EASD: European Association for the Study of Diabetes,

EASL: European Association for the Study of the Liver

EASO: European Association for the Study of Obesity

ER: Endoplasmic reticulum

FA: fatty acid

FAS: fatty acid synthase

FFM: fat-free mass

FGF19: Fibroblast Growth Factor 19

FGF21: Fibroblast Growth Factor 21

FID: free-induction decay

FM: fat mass

FSR: Fractional synthetic rates

FXR: Farnesoid X Receptor

F-1-P: Fructose 1-phophate

F-1,6-P: Fructose 1,6-bisphosphate

F-6-P: Fructose 6-phosphate

G-3-P: Glyceraldehyde 3-phosphate

GCKR: glucokinase regulator

GC-MS: Gas chromatography–mass spectrometry

GIP: gastric inhibitory polypeptide

GLP-1: glucagon-like peptide 1

GLP-1RA: GLP-1 receptor agonist

glucose-6-P: glucose-6-phosphate

Gly: glycerol

GR-MD-02: Galectin-3 protein inhibitors

HCC: hepatocellular carcinoma

HCl: Hydrochloric acid

HDL: high-density lipoprotein

HFCS-55: High-fructose corn syrup-55

HFD: high fat diet

HFHSD: high-fat and high-sugar diet

HPLC: High-performance liquid chromatography

HSD: high-sugar diet

HSL: hormone-sensitive lipase

Hz: hertz

IDH1: isocitrate dehydrogenase 1

IHL: intrahepatic lipids

IP: Intraperitoneal

IR: insulin resistance

kHz: kilohertzù

KOH: potassium hydroxide

LDLR: low-density lipoprotein receptor

MAFLD: metabolic dysfunction associated fatty liver disease

MAG: Monoacetone glucose

MBOAT7: membrane bound O-acyltransferase domain-containing protein 7

MCD: Methionine and choline deficiency

ME1: malic enzyme 1

MET: metabolic equivalents

mg/dL: Milligrams per deciliter

MHz: MegaHertz

MIDA: Mass isotopomer distribution analysis

MS: Mass Spectroscopy

MTBE: methyl-*tert*-butyl ether

MUFA: monounsaturated fatty acids

MUP-uPA: Major urinary protein-urokinase type plasminogen activator

N: the number of deuterium atoms incorporated per fatty acid molecule

ω-3: omega-3

ω-6: omega-6

Na_2SO_4 Sodium sulfate

NaCl: Sodium chloride

$NADP^+$ Non-protonated nicotinamide adenine dinucleotide phosphate

NADPH: Protonated nicotinamide adenine dinucleotide phosphate

NAFL: Non-Alcoholic Fatty Liver

NAFLD: Non-Alcoholic Fatty Liver Disease

NASH: Nonalcoholic steatohepatitis

NEFA: non-esterified fatty acids

NMR: nuclear magnetic resonance

ob/ob: leptin deficient

OGTT: oral glucose tolerance test

ORBEA: Orgão de Bem-Estar e Ética Animal/the Animal Ethics Committee at University of Coimbra

PCSK9: Proprotein convertase subtilisin/kexin type 9

PNPLA2: Patatin-like phospholipase domain-containing protein 2

PNPLA3: Patatin-like phospholipase domain-containing protein 3

PPAR: peroxisome proliferator-activated receptor

PPARα: peroxisome proliferator-activated receptor alpha

PPARγ: peroxisome proliferator-activated receptor gamma

PPP: pentose phosphate pathway

PTEN: Phosphatase and tensin homolog

PUFA: polyunsaturated fatty acids

RCT: randomized controlled trial

S: second

SCAP: SREBP cleavage-activating protein

SCD1: Stearoyl coenzyme A desaturase 1

SCFA: short-chain fatty acids

SFA: saturated fatty acids

SGLT1: Sodium glucose co-transporter 1

SGLT2: Sodium glucose co-transporter 2

SNR: signal-to-noise ratios

SPE: solid phase extraction

SREBP: sterol regulatory element-binding proteins

SREBP1c: sterol regulatory element binding protein 1c

T2D: Type 2 diabetes

TBW: total body water

TCA: tricarboxylic acid cycle

TG: triglyceride

THR-β: Thyroid Hormone Receptor-β

TIMP1: metalloproteinase 1

TLC: thin layer chromatography

TM6SF2: transmembrane 6 superfamily member 2

Triose-P: triose phosphate

VLDL: very low-density lipoprotein

WD: western diet

ABSTRACT

Non-alcoholic fatty liver disease, characterised as an abnormal accumulation of triglyceride in hepatocytes, is one of the most prevalent chronic liver disease globally in current times. It is associated with many metabolic disorders related to overfeeding including type 2 diabetes mellitus, insulin resistance, and hyperlipidemia. NAFLD represents a spectrum of liver diseases ranging from simple steatosis to steatohepatitis, fibrosis, cirrhosis and ultimately, hepatocellular carcinoma or liver failure. NAFLD has a multifactorial cause with genetic susceptibility and an unhealthy lifestyle playing a central role in its development. Hepatic *de novo* lipogenesis (DNL) may play an important role in the accumulation of lipids in the liver during NAFLD. Deuterated water (^2H_2O) is a widely used tracer for quantifying DNL rates in both animal models and humans. A major uncertainty of this method is that exchange of water hydrogens with those of fatty acid precursors and/or NADPH may be incomplete, resulting in under-estimates of DNL. In mice, we measured the ^2H enrichment of fatty acid hydrogens in positions 2, 3 and terminal methyls from [U-$^2H_7$]glucose to determine ^2H transfer from glucose to fatty acid via malonyl-CoA, NADPH, and acetyl-CoA, respectively. Our study indicates that glucose ^2H are transferred at different fractional rates into the different fatty-acid sites during lipogenesis. Transfer of hydrogen from unlabeled glucose to fatty acids via NADPH was the most important factor in the non-stoichiometric incorporation of ^2H into fatty acids during DNL. This information allows better modelling of lipid enrichment from ^2H_2O and also provides insight on NADPH sources for lipogenesis.

The pentose phosphate pathway (PPP) is an important component of hepatic intermediary metabolism, and is a key requirement for *de novo* lipogenesis since it generates NADPH equivalents for fatty acid synthesis and/or elongation. Recently, Jin et al developed an elegant ^{13}C-NMR method for measuring hepatic PPP flux by quantifying the distribution of glucose

^{13}C-isotopomers formed from [U-^{13}C]glycerol. In chapter 3, we demonstrate this approach can be extended to exogenous [U-^{13}C]fructose and [U-^{13}C]glucose precursors by ^{13}C-NMR analysis of glycogen. Our study revealed that the PPP preferentially utilized the glucose-6 phosphate generated via glucokinase and the direct pathway as compared to glucose-6-P obtained from indirect pathway precursors, such as [U-^{13}C]fructose.

An excessive consumption of fat and/or fructose either as part of sucrose or in the form of high-fructose corn syrup results a higher accumulation of lipid in the liver, implicated in the surge of NAFLD development and pathogenesis. In chapter 4, we established mouse models to determine the contribution of fructose in high sugar and/or high fat diets to *de novo* synthesis of liver triglyceride in diet induced mice models of NAFLD. Mice were provided with a combination of deuterated water and [U-^{13}C]fructose tracers. Our study showed that high-fat, high sugar and a combination of high fat and high sugar diets provided over an 18 week period resulted in significant increases in adiposity over standard chow for adult male C57BL6/J mice. Moreover, high sugar and high fat plus high sugar feeding resulted in significant increased hepatic TG levels that associated with elevated lipogenesis rates in which the fructose component contributed sizable fractions of both acetyl-CoA and glycerol-3-phosphate precursors. Thus, both the fat and sugar components of this diet contribute to hepatic steatosis in an additive manner.

Keywords: Non-alcoholic fatty liver disease, *De novo* lipogenesis, Stable isotope tracers, High-fat and/or High-sugar diets, Pentose Phosphate Pathway, NMR, NADPH

RESUMO

O Fígado Gordo Não-Alcoólico (NAFLD), caracterizado por uma acumulação anormal de triglicerídeos nos hepatócitos, é uma das doenças crónicas associadas ao fígado mais prevalentes à escala global. É uma condição normalmente associada com diversas patologias metabólicas especialmente as relacionadas com dietas excessivas tais como Diabetes Mellitus tipo 2, resistência a insulina e hiperlipidémia. A NAFLD representa o espectro das doenças de fígado desde esteatose simples até esteatohepatite, fibrose, cirrose e, nos estágios mais avançados, em carcinoma hepatocelular e falência hepática. As causas para NAFLD são multifatoriais, tendo a suscetibilidade genética e estilos de vida menos saudáveis um papel central no seu desenvolvimento. A lipogénese *de novo* hepática (DNL) pode desempenhar um papel crucial de acumulação de lípidos no fígado durante progressão de NAFLD. A água deuterada (^2H_2O) é amplamente utilizada como marcador para quantificação das taxas de DNL em diversos modelos animais e também em humanos. Uma das maiores subjetividades deste método relaciona-se com a troca de hidrogénios da água com os ácidos gordos percursores e/ou o NADPH, que pode ser incompleta resultando em sub-estimação da DNL. Em modelos de ratinho, medimos o enriquecimento em ^2H nos hidrogénios dos ácidos gordos, nas posições 2, 3 e grupos metilo terminais, provenientes do substrato externo [U-^2H]glucose, por forma a determinar a transferência de ^2H da glucose para os ácidos gordos, via malonil-coA, NADPH e acetil-CoA respetivamente. O nosso estudo indica que os ^2H da glucose são transferidos para as diferentes posições dos ácidos gordos durante a lipogénese, a taxas fracionais diferentes. A transferência de hidrogénio da glucose não marcada para os ácidos gordos via NADPH, revelou-se o fator mais relevante na incorporação não-estequiométrica de ^2H nos ácidos gordos durante a DNL. Esta informação permite assim uma modelação melhorada do enriquecimento lipídico do ^2H_2O providenciando ainda evidência das fontes de NADPH para a lipogénese.

A via das pentoses fosfato (PPP) é um importante componente do metabolismo intermédio hepático, sendo um requisito crucial para a lipogénese *de novo,* uma vez que gera equivalentes NADPH para a síntese de ácidos gordos e/ou elongação dos mesmos. Recentemente, Jin et al. desenvolveram um elegante método de ^{13}C-NMR, para medir os fluxos PPP hepáticos, através da quantificação da distribuição de isotopómeros de glucose ^{13}C formados através de [U-^{13}C]glicerol. No capítulo 3 desta dissertação, demonstramos que este desenho experimental pode ser estendido e aplicado aos percursores exógenos [U-^{13}C]glucose e [U-^{13}C]frutose por análise ^{13}C-NMR de glicogénio. Os nossos estudos revelaram que a PPP utiliza preferencialmente a glucose-6-fosfato gerada via glucokinase por via direta quando comparado com glucose-6-P obtida pela via dos percursores indiretos, tal como a [U-^{13}C]frutose.

O consumo excessivo de gordura e/ou frutose, como parte da sacarose ou "high-fructose corn syrup" resulta no incremento da acumulação lipídica no fígado, que está presente no surgimento e progressão de NAFLD e evolução patológica. No capítulo 4, estabelecemos modelos de ratinho por forma a determinar a contribuição da frutose em dietas enriquecidas em açúcar e/ou gordura, para a síntese *de novo* de triglicerídeos no fígado, em modelos de ratinho NAFLD induzida por dieta. Aos ratinhos foi administrada uma combinação de marcadores de água deuterada e [U-^{13}C]frutose. Os nossos resultados demonstraram que dietas enriquecidas em gordura, açúcar e uma combinação destes dois, providenciados durante um período de 18 semanas, resultaram num aumento significativo da adiposidade em comparação com ratinhos adultos C57BL6/J alimentados com dieta standard. Adicionalmente, dietas enriquecidas em açúcar e gordura mais açúcar, levaram a um incremento significativo dos níveis de TG hepáticos, correlacionando-se com taxas de lipogénese aumentadas, em que a frutose se revelou como componente contributivo significativo para as frações dos percursores

acetil-CoA e glicerol-3-fosfato. Desta forma, ambos os substratos, açúcar e gordura, nestas dietas, contribuíram para a esteatose hepática de modo aditivo.

Palavras-chave: Doença hepática gordurosa não alcoólica, lipogênese de novo, traçadores de isótopos estáveis, dietas com alto teor de gordura e / ou açúcar, via da pentose fosfato, RMN, NADPH

CHAPTER ONE

NON-ALCOHOLIC FATTY LIVER DISEASE (NAFLD)

1. INCIDENCE, RISK FACTORS, TREATMENT AND STUDY OF NAFLD

Non-Alcoholic Fatty Liver Disease (NAFLD) is the condition of a liver, which has an abnormal accumulation of fat in the absence of causes such as substantial use of alcohol or any drugs that can induce fatty liver or other chronic diseases of the liver: for instance chronic viral hepatitis, autoimmune hepatitis, Wilson's disease or haemochromatosis (Marjot et al., 2020). NAFLD commonly coexists with insulin resistance, obesity, and dyslipidaemia (Marjot et al., 2020). The term NAFLD refers to a spectrum of fatty liver conditions, which range from non-alcoholic fatty liver (NAFL), also called simple steatosis, to non-alcoholic steatohepatitis (NASH). These conditions can also involve fibrosis, cirrhosis and the development of hepatocellular carcinoma (HCC) (Figure 1). These diseases start with the accumulation of fat in the liver (NAFL), without any histological indications of inflammation or hepatocellular injury (hepatic steatosis), but it can potentially progress to non-alcoholic steatohepatitis (NASH), a condition in which hepatic steatosis is accompanied by hepatocyte ballooning, inflammation, and onset of fibrosis. The disease can further progress to cirrhosis and/or HCC (Chalasani et al., 2018a; Friedman et al., 2018; Marjot et al., 2020) (Figure 1). Recently, a panel of international experts proposed a new term for NAFLD: metabolic dysfunction associated fatty liver disease (MAFLD) (Eslam et al., 2020)

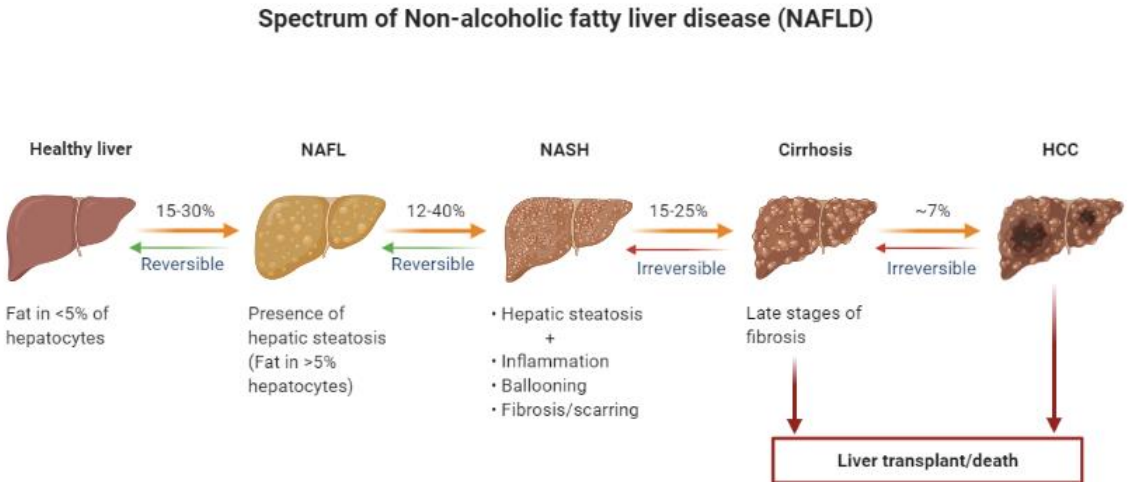

Figure 1: *The spectrum of non-alcoholic fatty liver disease (NAFLD). It starts when a healthy liver has an abnormal accumulation of fat (hepatic steatosis), and possibly progressed to NASH when hepatic steatosis accompanied by hepatic inflammation and fibrosis, and further developed to cirrhosis and HCC. Abbreviations: HCC, Hepatocellular carcinoma; NAFL, Non-alcoholic fatty liver; NASH, Non-alcoholic steatohepatitis.*

Meta-analysis of studies from 1989-2015 has confirmed that NAFLD is a global disease in which the overall prevalence has now reached one-quarter of the global population (Younossi et al., 2016). Its prevalence ranges from 13% in Africa to 24% in Europe and North America, 27% in Asia, 30% in South America, with the Middle East having the highest at 32% (see Figure 2) (Younossi et al., 2018, 2016). The current prevalence of NAFLD represents a rapid increase over a relatively short interval: from 15% in 2005 to 25% in 2010 (Younossi et al., 2016). From 7 to 30% of NAFLD patients confirmed by ultrasound will have NASH verified by biopsy (Younossi et al., 2016), hence the overall prevalence of NASH is estimated to be 1.5-6.5% of the general population. Moreover, around 40% of patients with NASH will have developed fibrosis, with a corresponding mean fibrosis annual progression rate of 0.09 per 1000 person-years (Younossi et al., 2016).

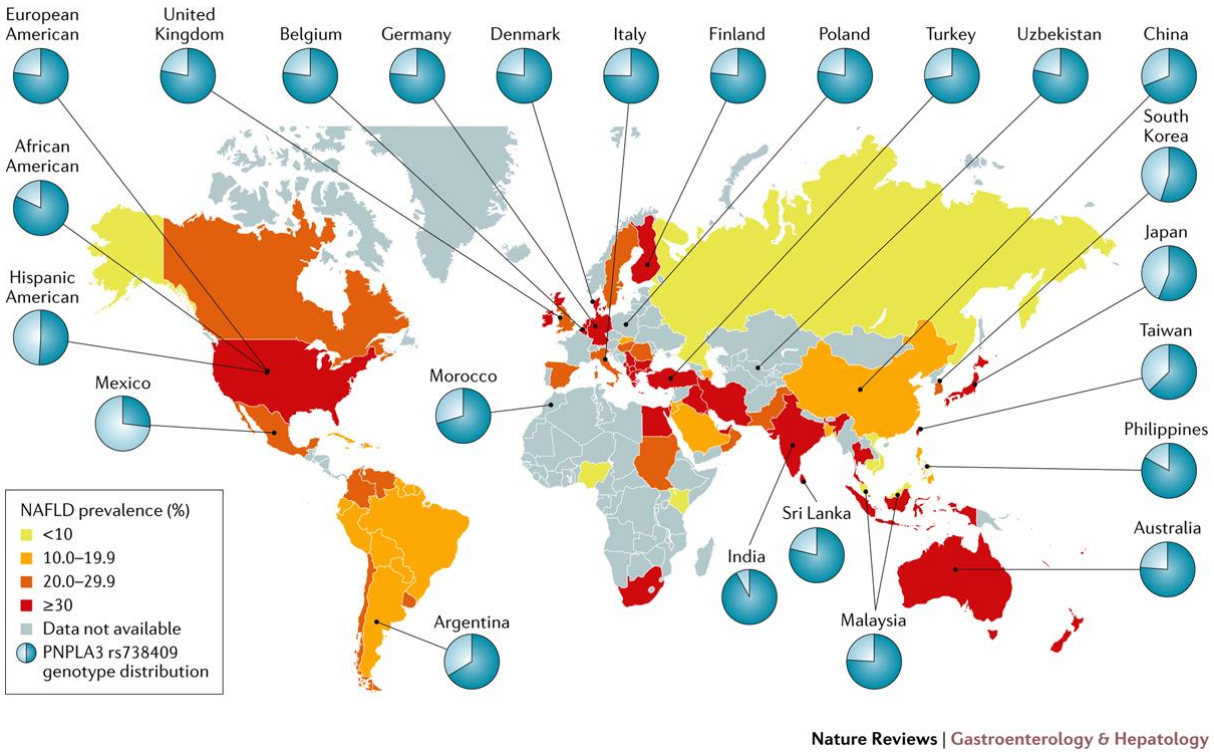

Figure 2: *The estimated prevalence of NAFLD and the PNPLA3 genotypes distribution across the globe. PNPLA3 is presented as minor allele frequency (light blue section of the pie chart adapted from (Younossi et al., 2018). Abbreviations: NAFLD, Non-alcoholic fatty liver disease; PNPLA3, Patatin-like phospholipase domain-containing protein 3.*

Although the role of ethnicity on NAFLD prevalence and severity remains ambiguous, in the USA population Hispanic patients have a higher prevalence of NAFLD in comparison with Caucasian and African-American populations (Rich et al., 2018). Males have a considerably higher prevalence of NAFLD compared to females in the general population (Ballestri et al., 2017) although women may have higher NAFLD prevalence among normal weight or lean people (BMI < 25 kg/m^2) (Younossi et al., 2012). Also, there seem to be gender-specific variations in respect to age; men have relatively little differences in NAFLD prevalence across age groups (S. H. Park et al., 2006) while the prevalence in women older than 50 years of age is considerably higher than younger women (J. G. Fan et al., 2005; S. H. Park et al., 2006).

1.1. Dietary factors in NAFLD development

1.1.1. Excess caloric intake

Dietary factors, both in terms of caloric intake as well as nutrient composition, play a key role in NAFLD and NASH development. A study of 18 healthy individuals showed significant elevations in alanine aminotransferase (ALT) and increased hepatic fat after doubling the regular caloric intake with fast-food based meals in less than 4 weeks (Kechagias et al., 2008). NAFLD is highly associated with consumption of high-calorie diets, typically high in carbohydrate (mainly refined sugars) and fat (primarily saturated fats). Sweetened beverages that comprised of fructose-containing sugars, for example high fructose corn syrup or sucrose, are associated with increased risk of NAFLD and NASH development, particularly in overweight/obese individuals (Ma et al., 2015). The total energy intake share from such sugars has increased from 3.9% to 9.2% between 1977 and 2001 (Nielsen & Popkin, 2004). Moreover, Zelber-Sagi *et al.* have showed that patients with NAFLD consume a higher quantity of soft drinks and meat than healthy individuals (Zelber-Sagi et al., 2007). Thus, soft drinks are a significant source of added sugar globally and their intake is associated with the development of NAFLD (Abid et al., 2009; Assy et al., 2008). Diets that are high in refined sugar promote hyperinsulinemia and arouse the activity of lipogenic enzymes in the liver resulting in increased *de novo* synthesis of fatty acids, and augmented secretion of very low-density lipoprotein (VLDL) (Bourgeois et al., 1995; J. Park et al., 1997; Wiggins et al., 1995). Also, Musso *et al.* established that NAFLD patients have an increased dietary protein intake compared to healthy individuals (Musso et al., 2003). Moreover, in comparison to the healthy individuals, NAFLD patients were inclined to ingest dietary lipids with a higher proportion of saturated fat and cholesterol, and with lower amounts of polyunsaturated fatty acids (PUFAs) (Cortez-Pinto et

al., 2006; Musso et al., 2003). Furthermore, individuals with NAFLD tended to have a lower intake of fish rich in omega-3 fatty acids (Capanni et al., 2006; Zelber-Sagi et al., 2007).

1.1.2. More sedentary lifestyle vs exercise interventions

Physical activity results in increased expenditure of energy above the resting metabolic rate and can be characterised by modality, intensity, frequency, duration and framework of practice (Thivel et al., 2018). Exercise is a sub-class of physical activity that is scheduled, organized and repetitive, and results in the development and maintenance of physical fitness (Thivel et al., 2018). Meanwhile, sedentary behaviour has been defined as waking actions that expend ≤ 1.5 metabolic equivalents (MET) of resting metabolic rate in a sitting or reclining position (Thivel et al., 2018). Recent studies have revealed an association of sedentary behaviour with adverse health outcomes (Thivel et al., 2018). Moreover, a strong association between sedentary lifestyle and NAFLD prevalence has been found in an observational study (Ryu et al., 2015). Furthermore, Pälve *et al*. has reported that fit obese persons were at a significantly lower risk of NAFLD than unfit obese indicating that sedentary behaviour is an independent risk factor for NAFLD (Pälve et al., 2017). A number of studies have been conducted to study the effect of exercise on liver fat content in sedentary, obese individual with NAFLD, and overall results showed that exercising training substantially decreased the liver fat content without notable body weight/body fat loss (Johnson et al., 2009; Keating et al., 2012; Sullivan et al., 2012). Other studies showed reversals in liver fat content and circulating markers of liver injury (Baba et al., 2006; Bassuk & Manson, 2005; Lamonte et al., 2005; Suzuki et al., 2005). Hickman *et al.* studied 31 NASH patients over a 3 month interval who undertook well-structured moderate exercise (150 min/week of aerobic exercise) in combination with dietary modifications (55% carbohydrate, 15% protein, and 30% fat diets). They found a 4% mean

weight loss accompanied by a marked reduction in serum alanine aminotransferase (ALT) (Hickman et al., 2004). In a randomized controlled trial (RCT), Vilar Gomez *et al*. studied 60 liver biopsy-proven NAFLD patients allocated into two groups (n = 30 each), where the first group assigned to a daily aerobic exercise plus hypocaloric diet and three Viusid[1] sachets, and the other group only exercise and hypocaloric diet for a period of six months. They showed a notable improvement in histological features of NAFLD if the NAFLD patients treated with a combination of diet and exercise (Vilar Gomez et al., 2009).

1.1.3. High intake of saturated fat

The amount and composition of dietary lipid plays a significant role in NAFLD development and progression (Zivkovic et al., 2007). Dietary lipid is absorbed as chylomicrons via the lymphatic system which does not directly perfuse the liver thereby explaining its relatively small direct contribution to intrahepatic triglyceride in the postprandial state (Donnelly et al., 2005). Nevertheless, saturated fatty acids (SFAs) and trans-fatty acids have adverse systemic effects on insulin-mediated control of hepatic glucose and lipid metabolism thereby potentiating NAFLD, while polyunsaturated fatty acids (PUFA) and monounsaturated fatty acids (MUFA) appear to reduce insulin resistance, liver steatosis and inflammation in NAFLD patients (Capanni et al., 2006; McCarthy & Rinella, 2012; Vallim & Salter, 2010). Saturated fatty acids and trans-fatty acids may promote hepatic inflammation directly through intracellular processes. Endoplasmic reticulum (ER) stress induced by an increase in saturated fatty acids leads to cellular dysfunction and apoptosis (Leamy et al., 2013). The lipotoxicity of an increased load of saturated fatty acids is not only visited on the liver, but also in other tissues

[1] A nutritional supplement with recognised antioxidant and immunomodulatory properties which could have beneficial effects on cirrhosis-related clinical outcomes such as survival, disease progression and development of hepatocellular carcinoma (HCC).

such as endothelial cells, pancreatic beta cells, cardiomyocytes and skeletal muscle (Nolan & Larter, 2009; Suvitaival et al., 2018). Saturated fatty acids can also indirectly provoke hepatic inflammation prior to absorption through the perturbation of intestinal microflora resulting in dysbiosis, impaired intestinal barrier function and subsequent exposure of the liver to pro-inflammatory bacterial components (Estadella et al., 2013).

In contrast to saturated fatty acids, PUFA generally have beneficial effects on both hepatic lipid levels and inflammation. They reduce the overall hepatic lipid burden in part by modulating the expression of numerous genes involved in fatty acid oxidation and hepatic lipogenesis, including sterol regulatory element-binding proteins (SREBP) and peroxisome proliferator-activated receptor (PPAR) alpha (Clarke & Jump, 1996; H. J. Kim et al., 1999). PUFA are precursors to eicosanoids that have roles in immunity and inflammation control, of which ω-3 PUFA (also known as omega-3) are anti-inflammatory, whereas ω-6 PUFA (omega-6) have pro-inflammatory properties (Patterson et al., 2012). Since eicosanoids play a significant role in the regulation of inflammation, they involved in several diseases, including atherosclerosis, cancer, obesity, and NAFLD (Azrad et al., 2013; Simopoulos, 2002).

1.1.4. High sugar intake – fructose

Consumption of fructose in the USA has risen from around 15 g per day in 1900 to 54.7 g in 2008 (Lim et al., 2010; Y. K. Park & Yetley, 1993; Vos et al., 2008), and now accounts for around 15% of dietary caloric intake (Welsh et al., 2011). NAFLD patients consume nearly 3 times more fructose compared to control subjects with matching BMI, age and sex (Ouyang et al., 2008) while daily intake of soft drinks sweetened with sucrose is associated with significantly higher levels of visceral and hepatic fat compared to intake of water, milk, or diet

cola (Maersk et al., 2012). A study of 427 adults recruited in the NASH Clinical Research Network showed that consumption of fructose was associated with a higher stage of fibrosis (Abdelmalek et al., 2010). Accordingly, NAFLD development in obese subjects may be protected by low intake of fructose (O'Sullivan et al., 2014).

In addition to its caloric contribution, fructose may also augment hepatocellular metabolic dysfunction and oxidative stress. Its uncontrolled phosphorylation by fructokinase leads to an acute depletion of ATP. This is thought to contribute to mitochondrial dysfunction, oxidative stress, and protein synthesis impairment (Choi et al., 2014; Lanaspa et al., 2012). It also triggers purine catabolism resulting in the generation of uric acid, which has been also associated with NAFLD pathogenesis through impaired β-oxidation and oxidative stress (Choi et al., 2014; Lanaspa et al., 2012). Epidemiological researches have revealed an association between NAFLD and hyperuricemia (Zhou et al., 2016) with a meta-analysis study indicated that in every 1mg/dL rise in serum uric acid is associated with a 3% upsurge in NAFLD incidence (Z. Liu et al., 2015).

1.2. Genetic factors in NAFLD development

There exists a considerable inter-individual variation in the NAFLD spectrum regardless of shared environmental risk factors, for instance, individuals with morbid obesity can have a normal liver histology (Xanthakos et al., 2006) and only a minority of NAFLD patients will develop NASH, fibrosis and HCC. This leaves open the possibility of genetic components that promote NAFLD progression (Marjot et al., 2020). Several variants of genes that encode proteins involved in hepatic lipid metabolism have emerged out of genome-wide association studies, which have strong association with NAFLD development and progression

(Dongiovanni, Romeo, et al., 2015). The most robust and genetic variant associated with NAFLD is the Patatin-like phospholipase domain-containing protein 3 (PNPLA3) isoleucine to methionine substitution at position 148 (rs738409 C>G encoding for PNPLA3 I148M) (Dongiovanni et al., 2013; Romeo et al., 2008; Singal et al., 2014). The worldwide distribution of PNPLA3 genotypes are presented in Figure 2 (Younossi et al., 2018). Romeo and colleagues, screening adults with diverse ethnicity from the Dallas Heart Study, were the first to identify the association between excess hepatic fat and PNPLA3 I148M independently of other determinants of the metabolic syndrome (Romeo et al., 2008). Subsequently, several studies confirmed the association of this single nucleotide polymorphism with liver disease, including NASH, fibrosis, cirrhosis and HCC, yet the mechanistic basis of its association with NAFLD remains to be fully characterized (Dai et al., 2019; Huang et al., 2019; Shen et al., 2015). Functional PNPLA3 has a hydrolase activity towards triglycerides and retinyl esters (Pingitore et al., 2014; Pirazzi et al., 2014). The loss-of-function induced by the substitution of 148M variant protein results in its accumulation on the lipid droplets, where it escapes proteasome degradation and obstructs the actions of other lipases (mostly Adipose triglyceride lipase (ATGL/PNPLA2)) activity, thereby resulting in an entrapment of triglycerides in lipid droplets within hepatocytes (BasuRay et al., 2017; Pingitore et al., 2014). This not only promotes fatty liver disease (BasuRay et al., 2017; Pingitore et al., 2014) but also potentiates fibrosis through hepatic stellate cell (HSC) activation (Pingitore et al., 2016). This has been supported by mouse model studies showing that PNPLA3 deletion has no distinctive hepatic phenotype (Chen et al., 2010), whereas knock-in or over-expression of the I148M mutation renders mice more susceptible to the accumulation of hepatic fat by high carbohydrate diet feeding. Additionally, the reduced expression of PNPLA3 148M due to the co-presence of the 434K variant ameliorates liver damage in patients with the 148M mutant protein (Donati et al.,

2016) emphasising the down-regulation of PNPLA3 148M as a prospective target in NAFLD treatment (Valenti & Dongiovanni, 2017).

The other significant gene variant is the transmembrane 6 superfamily 2 (TM6SF2 rs58542926) that is involved in the transfer of triglycerides to apolipoprotein B100 in the VLDL pathway. A guanine to adenine substitution at position 167 (rs58542926 E>K encoding for TM6SF2 E167K) results in loss-of-function, which promotes steatosis by preventing the clearance of hepatocyte triglyceride via VLDL (Kim et al., 2017; Kozlitina et al., 2014; Liu et al., 2014). Interestingly, carriers of this mutation are protected against cardiovascular risks and circulating dyslipidaemia (Dongiovanni, Petta, et al., 2015; Pirola & Sookoian, 2015). Studies in humans also suggested that this gene variant regulates not only the qualitative enrichment of liver triglycerides but also the synthesis of lipids and amount of secreted lipoprotein particles (Luukkonen et al., 2017). Additionally, the gene variant with moderate effect in association with the NAFLD risk include loss-of-function polymorphisms in membrane bound O-acyltransferase domain containing 7 (MBOAT7), a protein that involves in the phosphatidylinositol remodelling with arachidonic acid in the Lands cycle. The downregulated MBOAT7 (the rs641738 C>T variant) appears to associate with hepatic steatosis, inflammation and fibrosis (Luukkonen et al., 2016; Mancina et al., 2016) and NAFLD progression to carcinogenesis (Donati et al., 2017) through impaired incorporation of polyunsaturated fatty acids into hepatocyte phospholipids. Moreover, the gene locus variant glucokinase regulator (GCKR) has been associated with NAFLD in which GCKR regulates *de novo* lipogenesis (DNL) by controlling glucose influx in hepatocytes (Petta et al., 2014; Santoro et al., 2012). Indeed, the loss-of-function GCKR mutation (rs1260326) causes hepatic fat accumulation (Beer et al., 2009) through preventing glucokinase inhibition by fructose-6-phosphate, such that hepatic glucose uptake and conversion to glucose-6-Phosphateee is enhanced (Valenti et

al., 2012). This in turn promotes glycolytic glucose utilization resulting in increased malonyl-CoA production that drives hepatic *de novo* lipogenesis (DNL) while inhibiting fatty acid oxidation (Santoro et al., 2012). These studies highlight the high degree of interaction between genes and environment that characterize NAFLD onset and progression. Further work is required to cross-examine the precise molecular mechanisms behind the association between genetic variants and progressive liver diseases including NAFLD so as to spot on novel and customized therapeutic targets.

Aside from the aforementioned gender and genetic factors: high caloric intake in a diet, low level of physical exercise, and subsequent development of obesity are the main risk factors for NAFLD development. It has a multifactorial etiology and yet not known completely, however, it consists of alterations of energy metabolism, intrahepatic lipids (IHL) accumulation, inflammatory processes, and insulin resistance (IR) (Tilg et al., 2017). A number of studies have now revealed that individual subjects with NAFLD or NASH are at a greater risk of Type 2 diabetes (T2D) development (Anstee et al., 2016; Gastaldelli & Cusi, 2019; Mantovani et al., 2018; Marchesini et al., 2016). Furthermore, both T2D and NAFLD patients share metabolic syndrome associated co-morbidities, including low high-density lipoprotein-cholesterol (HDL) and/or abdominal fat accumulation as well as hypertriglyceridemia, fasting hyperglycaemia, and hypertension (Vernon et al., 2011; Yki-Järvinen, 2014).

1.3. NAFLD Treatment

1.3.1. Life-style modification to treat NAFLD

As NAFLD has no approved pharmacological treatment agents at the current time (2020), lifestyle alteration has been recommended as the first approach to its mitigation, according to a consensus statement by the European Association for the Study of Diabetes (EASD), European Association for the Study of the Liver (EASL), and European Association for the Study of Obesity (EASO) (Marchesini et al., 2016). This intervention entails a 500–1000 kcal energy shortfall that leads to 7–10% weight loss accompanied by moderate-intensity aerobic exercise with other resistance training, low-to-moderate fat and high-protein diets or low-carbohydrate ketogenic diets (Marchesini et al., 2016). Also, NAFLD practice guidelines from the American Association for the Study of Liver Diseases (AASLD) recommend body-weight reduction of a minimum of 3% for hepatic steatosis improvement, and a better (≥ 7%) body-weight reduction for improving the histological features of NASH including fibrosis (Chalasani et al., 2018a). The guideline recommends, hypocaloric diet (daily reduction of 500-100 kcal) accompanied with moderate-intensity exercise (Chalasani et al., 2018b). Both the EASL-EASD-EASO and AASLD guidelines report the beneficial effects of the Mediterranean diet. Nevertheless, even though there is strong evidence demonstrating the efficacy of weight loss in decreasing IHL levels, in reality only a small proportion of NAFLD patients are able to attain and maintain the modest weight loss described in the clinical practice guidelines (El-Agroudy et al., 2019; Romero-Gómez et al., 2017).

1.3.2. Pharmacotherapy for NAFLD treatment

The development of the therapeutic landscape in NAFLD is progressing rapidly although there are still no currently approved drugs specifically for this condition. A number of therapeutic modalities are currently in Phase 2 and 3 development, yet while it is still too early to prioritize the most promising therapeutics, it is highly likely that the first approved therapies specifically licensed for the treatment of NAFLD will become available within the next few years.

A large and diverse number of agents are currently being investigated for the treatment of NAFLD. They include glucose lowering agents/anti-diabetic agents (e.g. Pioglitazone, Biguanides, Glucagon-like peptide 1 analogues, Dipeptidyl peptidase IV inhibitors, and Sodium glucose co-transporter 2 inhibitors), lipid lowering agents (e.g. Hydroxy-3-methyl-glutaryl-coenzyme A reductase inhibitors, Omega-3 poly-unsaturated fatty acids, Peroxisome proliferator-activated receptor alpha agonists, and Proprotein convertase subtilisin kexin type 9 (PCSK9) inhibitors). Moreover, there are also several drugs that target the liver; including FXR-agonists (Obeticholic acid), dual and pan-PPAR agonist (Elafibranor, Lanifibranor, Saroglitazar), C-C chemokine receptor type 2 (CCR2) and type 5 (CCR5) dual antagonist (Cenicriviroc), Vitamin E, Galectin-3 protein inhibitors (GR-MD-02), Fibroblast Growth Factor 19 (FGF19) analogues (NGM282), FGF21 analogues, Thyroid Hormone Receptor-β (THR-β) Agonists (MGL-3196), Apoptosis Signal Regulating Kinase 1 (ASK 1) inhibitors (Selonsertib), Pentoxifyline, Caspase inhibition (Emricasan). In addition, some of the therapies target hepatic lipid synthesis (e.g. Acetyl-Coenzyme A Carboxylase (ACC) Inhibition, Stearoyl coenzyme A desaturase 1 (SCD1) inhibition, for the treatment of NAFLD (Marjot et al., 2020). Those medications that have demonstrated the most robust effects on counteracting NAFLD at the population level are discussed in more detail below.

A. Pioglitazone

Pioglitazone is a member of the thiazolidinedione class of drugs currently used as an anti-diabetic therapeutic agent as it improves insulin sensitivity in type 2 diabetes, thereby improving both fasting and postprandial glycemic control. It has shown improvement of both NAFLD and NASH in several studies (Aithal et al., 2008; Belfort et al., 2006; Cusi et al., 2016; Sanyal et al., 2010). Pioglitazone acts by binding and activating the peroxisome proliferator-activated receptor gamma (PPARγ), a nuclear receptor superfamily member that plays an important role in regulation of glucose and lipid metabolism (Gross et al., 2017; Liss & Finck, 2017). Its activation improves insulin sensitivity, which in turn improves the metabolism of glucose and lipid. Systemically, it promotes the redistribution of ectopic lipid, including that of the liver, into adipose tissue. Thus, it improves steatosis, inflammation and hepatocellular ballooning as well as hepatic fibrosis (Mahady et al., 2011; Sanyal et al., 2010). This may in part be mediated by a 2-3 fold increase in plasma adiponectin (Soccio et al., 2014) as well as its partial agonism of hepatic peroxisome proliferator-activated receptor alfa (PPAR-α) (Kintscher, 2008; Orasanu et al., 2008). This promotes hepatocyte fatty acid oxidation, a decrease in plasma triglyceride levels, and an increase in HDL-cholesterol concentrations. The land-mark PIVENS study undertaken on NASH patients without T2D compared the role of pioglitazone to vitamin E and placebo (Sanyal et al., 2010). Reductions in hepatic steatosis and inflammation and resolution of NASH were observed in 47%, 34% and 18% of patients given pioglitazone, vitamin E and placebo respectively. More recent studies have demonstrated the benefits of pioglitazone treatment in mitigating fibrosis (Belfort et al., 2006). Four Randomized Controlled Trial studies (RCTs) have delivered a supporting evidence of the clinical practice guidelines in the United States (Chalasani et al., 2018b) and Europe (Marchesini et al., 2016) in which pioglitazone has been recognised and may be prescribed for

biopsy proven NASH patients (Aithal et al., 2008; Belfort et al., 2006; Cusi et al., 2016; Sanyal et al., 2010). However, its side effects, including weight gain (up to 5kg over 3 years), fluid retention, osteopenia and increased fracture risk - especially in older women - has limited its therapeutic use (Viscoli et al., 2017). While there were initial concerns about increased risk of bladder cancer from Pioglitazone therapy, more recent studies have failed to demonstrate a significant association (Filipova et al., 2017). Nevertheless, it is likely that an increase use of pioglitazone in patients with NASH will continue to prevent fibrosis progression and other accompanied healthy effects. Interestingly, with the purpose of achieving a better safety and efficacy profile, a number of novel insulin sensitizers are being studied for NASH treatment (Khan et al., 2019).

B. Sodium glucose co-transporter 2 inhibitors

Sodium glucose co-transporter 2 (SGLT2) inhibitors are the most recent class of glucose-lowering agents to obtain approval for clinical use. They have demonstrated improved glucose homeostasis, as well as conferring cardio-renal protection via several mechanisms in both pre-clinical models and clinical studies including large multicentre RCTs (Verma & McMurray, 2018). They prevent renal reabsorption of >90% of glucose and are therefore not only extremely effective as glucose lowering agents *per se* but also promote weight loss (Zinman, et al., 2015; Neal et al., 2017; Wiviott et al., 2019). Accordingly, SGLT2 inhibitors (along with GLP-1RAs) have been placed as second-line agents for the management of T2D (Davies et al., 2018). As recently reviewed (Khan et al., 2019), several recent *in vivo* studies report substantial benefits of SGLT2 inhibitors, including reversal of liver steatosis, hepatocyte necrosis, inflammation and/or fibrosis. Therefore, there is ongoing expectation on deploying these agents for the treatment of NASH. In addition, although the mechanisms are not yet fully

elucidated, many studies have revealed the association of SGLT2 use with significant improvements in cardiovascular risk outcomes (Zinman et al., 2015; Neal et al., 2017; Wiviott et al., 2019). While several small studies have between them shown evidence of improvements in body weight, liver chemistry, glycaemic control, and liver triglyceride content, to date there have been no double-blinded clinical trials of SGLT2 inhibitors with liver histology as the primary endpoint (Bajaj et al., 2018; Ito et al., 2017; Kuchay et al., 2018; Sattar et al., 2018; Seko et al., 2018; Shibuya et al., 2018). Recently, controlled and double-blind placebo studies using dapagliflozin (Eriksson et al., 2018; Latva-Rasku et al., 2019), and canagliflozin (Cusi et al., 2019) in patients with T2D reported that canagliflozin but not dapagliflozin significantly improved hepatic insulin sensitivity - however both medications caused modest reductions of intrahepatic triglyceride (Cusi et al., 2019; Latva-Rasku et al., 2019). Moreover, a single uncontrolled study of canagliflozin treatment for 24-weeks in patients with T2D revealed histological improvements in the severity of NAFLD as well as improvements in hepatic insulin sensitivity (Akuta et al., 2019). However, studies in NAFLD patients without T2D have not yet been reported (Cusi et al., 2019).

While there is potential that SGLT2 inhibitors may convey significant clinical benefits including reduction of plasma ALT concentrations, weight loss, hepatic steatosis, as well as cardiovascular risk reduction, the clinical translation of these findings to the treatment of NASH is yet to be determined. Therefore, there is an urgent need for prospective and well-structured clinical studies to address this. Of note, these agents are generally well tolerated but up to 5% of individuals have reported genitourinary infections and there is the potential to develop increased urinary frequency, postural hypotension and dehydration (Donnan et al., 2019; Hamblin et al., 2019). Also, worries have been raised about development of diabetic

ketoacidosis (although rare in patients with T2D) (Lupsa & Inzucchi, 2018), and while recent data appears to be promising, there is still a need to look out for potentially life-threatening risks (Donnan et al., 2019; Hamblin et al., 2019). Currently, studies are examining the impact of Licogliflozin, a dual SGLT1 and 2 inhibitor that promotes weight loss in patients with and without T2D on hepatic steatosis (He et al., 2019).

C. Glucagon-like peptide 1 analogues

Incretins potentiate the secretion of insulin in response to meal glucose with glucagon-like peptide 1 (GLP-1) released from the intestinal L-cells being the best known example. Currently, GLP-1 receptor agonist (GLP-1RA) therapy has been recognised as a highly effective approach for decreasing glucose levels and promoting weight loss. GLP-1RAs also reduce the risk of CVD and chronic kidney disease, thus along with SGLT2 inhibitors, are used as a second-line therapy for T2D patients (metformin being the first-line medication) (Armstrong et al., 2013; Davies et al., 2018). A retrospective study showed that Liraglutide resulted in a dose-dependent reduction of circulating alanine aminotransferase (ALT) in study subjects with abnormal liver blood chemistry at baseline, whereas it had no impact in individuals with normal liver blood chemistry (Armstrong et al., 2013). Prospective studies of Liraglutide revealed improvements in liver histological outcomes and resolution of NASH in 36% of subjects compared with 9% within the placebo treated group (Armstrong et al., 2016). Other GLP-1RA studies including those of Lixisenatide and Exenatide, as well as Liraglutide, revealed improvements in liver biochemistry, hepatic insulin sensitivity and hepatic lipid content (Feng et al., 2017; Frøssing et al., 2018; Gastaldelli et al., 2016; Gluud et al., 2014; Petit et al., 2017). The GLP-1 analogues mechanism of action for improving NAFLD remains unclear. Although an *in vitro* study in the primary cultures of human hepatocytes revealed that

hepatic DNL was decreased by GLP-1 agonism, there is still controversy surrounding the expression levels of the GLP-1 receptor in human hepatocytes (Armstrong et al., 2016). Nevertheless, several studies have failed to detect the GLP-1 receptor in rodent and human hepatocytes (Panjwani et al., 2013; Pyke et al., 2014). The confounding issue of weight loss and enhancements in glycaemic control remain to be untangled from the potential direct benefit of GLP-1 analogue therapy and thus a mechanism of action that obliquely benefits the liver remains entirely acceptable.

While initial studies suggested that GLP-1 analogues mediated a direct beneficial effect on hepatic lipid metabolism via GLP-1 signalling (Ben-Shlomo et al., 2011; Svegliati-Baroni et al., 2011), this mechanism was not supported by data from subsequent follow-up studies (Panjwani et al., 2013; Pyke et al., 2014). Therefore, the current view is that the hepatic effects of GLP-1 analogues are indirectly mediated through both acute and long-term actions on other tissues, including modulation of glucagon and insulin levels and improvement of IR through body weight loss. The hepatic effect of Exenatide (one of a short-acting GLP-1RA) is acute and noticeable from the first dose (Gastaldelli et al., 2016). It acutely reduces hepatic IR by enhancing uptake of hepatic glucose during an OGTT and decreasing hepatic glucose output (Gastaldelli et al., 2016). A recent study on a NASH animal model has reported that Exenatide reversed mitochondrial dysfunction and lipotoxicity, but was accompanied by only minor loss of body weight (Kalavalapalli et al., 2019). Improvement of hepatic IR following treatment with GLP-1RA has not only been observed in T2D patients (Cersosimo et al., 2011), but also in individuals with morbid obesity (Camastra et al., 2017) as well as in NASH patients (Armstrong et al., 2016). This therapy has also showed reductions in chronic kidney disease and CVD risks, but the mechanisms remain unclear (Nauck et al., 2017). Considering that NAFLD is an important risk factor for CVD, there is mounting evidence that GLP-1RA would

provide clinical benefits to NAFLD patients whether or not they have T2D. In general, GLP-1RA are well tolerated and the gastrointestinal side effects are diminished with careful titration. Finally, the potential role of "dual agonists", combining GLP-1RAs with glucagon (Soni, 2016) for treatment of NASH and T2D are also being explored. Recently, novel compounds with multiple agonist properties have been developed. As an example, HM1522 is a GLP-1/GIP/glucagon triple agonist that is currently being tested as a therapy for NAFLD in obese subjects (*NCT03744182*, www.clinicaltrials.gov) (accessed date 21/02/2020).

D. Acetyl-Coenzyme A Carboxylase (ACC) Inhibition

Acetyl-CoA carboxylase (ACC) is a rate limiting enzyme for the endogenous synthesis of fatty acids from acetyl-CoA via *de novo* lipogenesis (DNL). Its product, malonyl-CoA, is also a potent inhibitor of mitochondrial long-chain fatty acid oxidation. Therefore, ACC is a target for inhibiting the *de novo* synthesis of hepatic triglyceride fatty acids while at the same time promoting hepatic fatty acid oxidation. Firsocosta (GS-0976), a small molecular inhibitor of ACC, has been studied in a small number of clinical studies. In an uncontrolled, open label, prospective study of 10 subjects treated with GS-0976 for 12-weeks, where hepatic fatty acid synthesis was measured by incorporation of deuterated water into palmitate, this activity was decreased by 22%. This was accompanied by reductions in hepatic lipid levels and liver stiffness, a marker of fibrosis, as well as circulating ALT (Lawitz et al., 2018). However, in a larger placebo-controlled randomized study (n=126), hepatic steatosis was decreased only at the highest doses of GS-0976 (20mg), with no alteration in liver stiffness. Circulating levels of tissue inhibitor of metalloproteinase 1 (TIMP1), a marker of tissue wounding, were decreased (Loomba et al., 2018) Although all the groups treated with GS-0976 showed increased levels of serum triglyceride, the drug was otherwise well tolerated.

1.4. Study of NAFLD

1.4.1. Animal Models

Of the rodent species and strains used as models for NAFLD, Sprague Dawley and Wistar rats and C57BL/6 mice have been preferred due to their higher susceptibility for developing NAFLD, obesity and insulin resistance compared to other strains (Y. Takahashi et al., 2012). Animal models for NAFLD can be grouped as diet-induced, genetic, or a combination of more than one intervention (Santhekadur et al., 2018). Accordingly, the commonly used animal models for NAFLD are listed in the table below as reviewed by Friedman *et al*. (see Table 1) (Friedman et al., 2018). While accumulation of lipid in the liver is a common feature, other aspects of human NAFLD/NASH such as the development of fibrosis secondary to lipid accumulation, have not been fully recapitulated (Friedman et al., 2018). Additionally, many metabolic, proteomic and transcriptomic changes that characterize NAFLD progression in humans have not been fully reproduced in animal models (Tsuchida et al., 2018).

For induction of NAFLD by diet, rodents are fed for several weeks on a high fat diet (HFD), in which saturated fats account for 50-60% of caloric content, compared to ~10% for standard chow. While this is effective in inducing hepatic steatosis in most mice strains, there is usually no subsequent development of inflammation or fibrosis (Nakagawa et al., 2014). Recently, studies have also shown that chow supplementation with fructose promotes NAFLD development, primarily through the induction of liver ER stress and increased DNL (Softic et al., 2016). Mice provided with high in *trans*-fats and high-fructose corn syrup diet as well as a sedentary lifestyle developed liver inflammation and associated fibrosis after one year (Dowman et al., 2014). A substantially higher degree of hepatic injury can be produced by supplying western diet (WD) in which the highest calorie compositions are carbohydrates

(about 40-50%) an fat (20-35%) and is aimed at recapitulating the average caloric composition of fast foods, confectionary, soft drinks, refined grains, red and processed meats, and full-fat dairy products (Oddy et al., 2013; Trovato et al., 2018).

Table 1: Most commonly used animal models (mice and rats) of NAFLD reviewed by and adapted from (Friedman et al., 2018)

Reference		Descriptions	Phenotypic outcomes relevance to human disease
Diet	High-fat, fructose and cholesterol (AMLN diet) (Clapper et al., 2013)	Diet high in fat (40%, of which 18% is trans-fat), plus fructose (22%) and cholesterol (2%) administered for 30 weeks	Animals develop both histologic and metabolic features of human NASH with diffuse fibrosis but no cirrhosis.
	Methionine and choline deficiency (MCD) (Matsumoto et al., 2013)	High-fat and sucrose diet, deficient in methionine and choline	The histologic appearance in 2–4 weeks resembles human NASH, but animals lose weight and are not insulin resistant, with lack of concordance of the liver transcriptome with human NASH.
	Choline-deficient, l-amino acid–defined supplemented, high-fat diet (CDAA) (Matsumoto et al., 2013)	High-fat, choline-deficient, reduced-methionine diet for 24 weeks	Like the MCD diet, animals do not gain weight or exhibit insulin resistance, but can develop fibrosis within 6–8 weeks.
	ob/ob (Hummel et al., 1966)	Leptin-deficient mice	Animals develop severe insulin resistance and steatosis but are resistant to fibrosis without a second insult (e.g., LPS). Unlike this model, humans with NASH have normal or elevated serum leptin.

Genetic	db/db (Hummel et al., 1966)	Leptin receptor–deficient mouse	Severe glucose intolerance, obesity and hepatic steatosis; susceptible to fibrosis with a second insult (e.g., MCD or high-fat diet).
	Obese (fa/fa) Zucker rat (Oana et al., 2005)	Nonfunctional leptin receptor due to mutation	Severe hyperphagia, insulin resistance and obesity on a high-fat diet, with hepatic steatosis but modest fibrosis.
	foz/foz (Arsov et al., 2006)	Truncating mutation in Alstrom syndrome I (ALMS1) protein, a ciliary protein	Severe obesity, insulin resistance, hepatic steatosis and mild fibrosis on a high-fat diet for 300 days, with hypoadiponectinemia. Phenotype may be strain-dependent.
	SREBP-1c transgenic (Nakayama et al., 2007)	Hepatocyte-specific overexpression of SREBP-1c	Severe insulin resistance and spontaneous steatohepatitis with oxidant stress at 30 weeks, with some perivenular fibrosis.
	MUP-uPA transgenic (Nakagawa et al., 2014)	Hepatocyte-specific overexpression of urokinase plasminogen activator	Severe ER stress, hepatic steatosis, mild fibrosis and HCC on high-fat diet (60% of calories), with TNF-α-driven inflammation
	LDLR knockout (Subramanian et al., 2011)	LDL receptor global knockout	Marked steatosis on a diabetogenic diet for 24 weeks, made worse with addition of dietary cholesterol, and association with inflammation, oxidant stress, increased fatty acid production and mild fibrosis.
	Phosphatase and tensin homolog	Alb-Cre-mediated hepatocyte-specific knockout of PTEN	Spontaneous hepatomegaly, steatohepatitis and triglyceride accumulation with lipogenic gene induction at 40 weeks and

	(PTEN) knockout (Horie et al., 2004)		high penetrance of ademomas, then carcinomas at 74–78 weeks.
	Streptozotocin plus high fat-diet (STAM) model (Fujii et al., 2013)	Streptozotocin administered at 2 days, followed by high-fat diet	Steatohepatitis and mild fibrosis with occasional HCCs at 20 weeks. However, animals have type 1 not type 2 diabetes, do not gain weight, and the liver transcriptome is discordant from human NASH.
	DIAMOND mouse (Asgharpour et al., 2016)	Inbred isogenic strain of C57Bl6/J and S129S1/svlmj fed a high-fat, high-carbohydrate diet	Progressive steatohepatitis, fibrosis then cirrhosis and HCC at 1 year. High transcriptomic concordance to human NASH.
Combinations	Western diet plus CCl_4 addition (Tsuchida et al., 2018)	High-fat, high-fructose, high-cholesterol diet with weekly intraperitoneal CCl_4 dosing	Progressive steatosis, insulin resistance and fibrosis at 12 weeks, with cirrhosis and frequent HCC at 24 weeks. High transcriptomic concordance to human NASH.
	High-fat diet with thermoneutral housing (Giles et al., 2017)	Animals housed at thermoneutral (30 °C) conditions, high-fat diet for 8 weeks	Greatly amplified steatohepatitis compared to standard (22 °C) housing, with altered microbiome, increased inflammatory signaling but modest fibrosis.

Mice models fed the methionine and choline deficient (MCD) or choline deficient (CD) alone defined diet develop histologically more severe NASH-like appearance with fat inflammation and fibrosis (Machado et al., 2015). The lack of these essential nutrients, especially deficiency of choline, result in impaired hepatic β-oxidation and VLDL production, which in turn results in accumulation of liver lipids, oxidative stress, changes in adipokines and cytokines, and death for a portion of hepatocytes (Ibrahim et al., 2016; Library et al., 2017). Moreover, these diets result in rapid weight loss for both lean and fat mass, decreases in fasting circulating glucose and lipids, and maintenance of insulin sensitivity (Kammoun et al., 2017). Thus systemically, this model shows little similarity to the metabolic and pathogenesis features of NAFLD patients (Febbraio et al., 2019). A combination of CD with HFD (CD+HFD) does not result in weight loss and NAFLD progresses to HCC in about 25% of the mice (Wolf et al., 2014). Mice that have been made deficient in ApoE, a protein structural component of lipoprotein transport particles, showed symptoms of NASH and modest fibrosis after feeding with WD (Schierwagen et al., 2015). Moreover, animal models administered WD with weekly CCl_4 (a hepatotoxin that promotes liver injury and fibrosis), also showed a close resemblance to the human NASH (Tsuchida et al., 2018). Thus, the whole spectrum of NAFLD ranging from simple steatosis via NASH to cirrhosis and HCC can be modelled by combinations of diet, diet or genetic manipulation of lipid transport components, and non-carcinogenic hepatotoxic agents (Friedman et al., 2018).

The *db/db* (leptin receptor deficient) and *ob/ob* (leptin deficient) mice, the Zucker (*fa/fa*) rat, foz mice (deficient in the Alstrom syndrome 1 gene) and several transgenic or conditional knockout mice are among the main genetic animal models of NAFLD/NASH (Table 1) (Friedman et al., 2018). Recently, studies done on the mice model obtained by crossing a stable isogenic C57Bl/6J with s129/SvlmJ (a strain used to create targeted mutations) have shown the

development of many metabolic disorders including NAFLD that progressed to NASH, fibrosis and HCC with similar transcriptomic, lipidomic and cell signalling changes to human NASH. Moreover, they showed dyslipidemia, adipose tissue inflammation, hypoadiponectinemia, obesity, and insulin resistance (Asgharpour et al., 2016; Sanyal & Pacana, 2015).

Other animal models, ranging from zebrafish (Lai et al., 2018) and fruit flies (Musselman et al., 2013) to the Ossabaw pig (L. Lee et al., 2009), have also been used for the study of NAFLD/NASH. Factors that limit their general use include the relevance to human NAFLD (for example zebrafish and flies) as well as logistics (for example increased lifespan and NAFLD development time for pig models) (Friedman et al., 2018). Nevertheless, they can provide important data for specific disease parameters. For instance, compared to mice and rats, guinea pigs have a much closer lipid profile to the humans that may be useful for studying the cardiovascular co-morbidities of NAFLD (Ye et al., 2013). New Zealand white rabbits are well-suited for investigating pediatric NAFLD as they have a long pre-pubertal period (Fu et al., 2009). Tree shrews tend to develop NAFLD induced by a high-fat diet (HFD) in the absence of obesity, thus they could be a suitable model to study non-obese NAFLD, which has high prevalence in Asia (L. Zhang et al., 2016).

2. METABOLIC BASIS OF NAFLD

In comparison to adipose tissue depots, the hepatic triglyceride pool is very small, even with well-developed steatosis[2]. However, there is a substantial flux of lipid entering and exiting the liver alongside a significant capacity for both *de novo* synthesis and oxidation of fatty acids

[2] Assuming a liver weight of 1.5 kg, and advanced steatosis (20% of liver weight as triglyceride), the total liver triglyceride mass is 0.3 kg

within the organ itself (Figure 3). Therefore, relatively small imbalances in net lipid inflow and/or synthesis *versus* outflow and/or oxidation can have major effects on hepatic lipid levels. This is important in both pathogenesis and resolution of NAFLD.

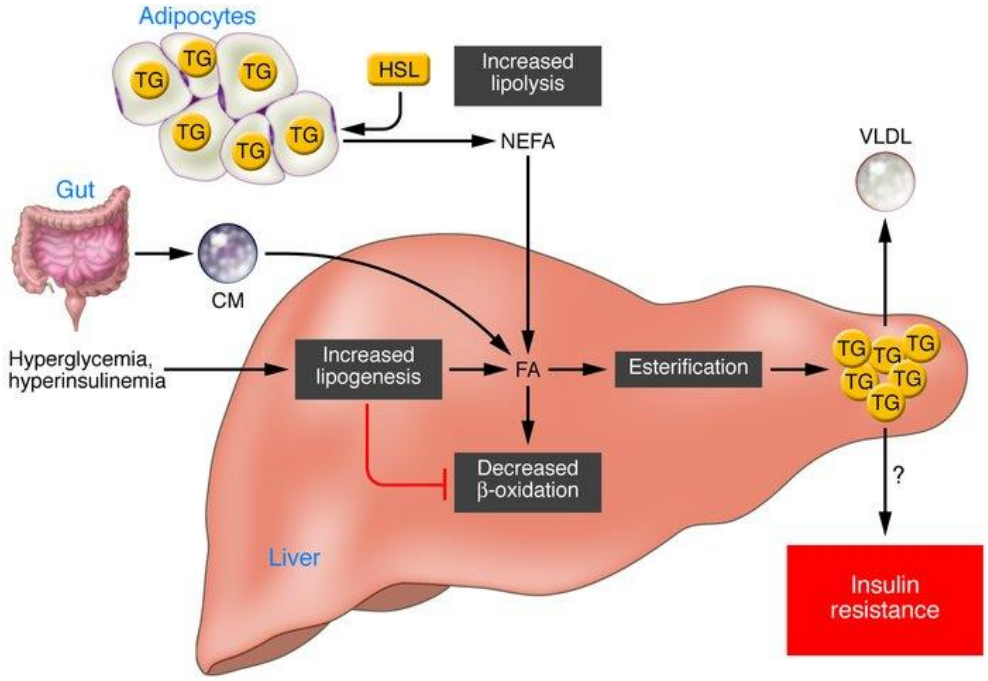

Figure 3: *Metabolic pathways leading to hepatic steatosis adapted from Postic and Girard et al. (Postic & Girard, 2008). Abbreviations: CM, Chylomicron; DNL, de novo lipogenesis; FA, Fatty acids; HSL, hormone-sensitive lipase; NEFA, Non-esterified fatty acids; TG, Triglycerides; VLDL, Very low density lipoprotein.*

There are sources of fatty acids that contribute to the development of fatty liver (NAFLD) (see Figure 3) (Postic & Girard, 2008). Under insulin resistance conditions, insulin does not sufficiently inhibit the hormone sensitive lipase (HSL), and lipolysis is not suppressed in the white adipose tissue. As a result, adipose tissue lipid is transported to the liver via plasma non-esterified fatty acids (NEFA). A portion of dietary fatty acids are also transferred to the liver via intestinally-derived chylomicron remnants. Additionally, hyperglycemia and hyperinsulinemia promote hepatic DNL. Consequently, these excesses of lipid inflow and

synthesis over clearance and oxidation lead to the development of hepatic steatosis (Friedman et al., 2018; Lomonaco et al., 2012; Postic & Girard, 2008). Once fatty acids are esterified to triglyceride (TG), the TG can then be either accumulated within hepatocytes as lipid droplets or secreted as VLDL into the circulation. They can also be saponified with the fatty acids products serving as precursors for β-oxidation . Therefore, TG accumulation in the liver can occur as a result of elevated fat synthesis, decreased fat oxidation, increased fat delivery, and/or reduced exportation of fat in the form of VLDL (Figure 3) (Postic & Girard, 2008). Studies of both humans and rodent models have revealed that excessive hepatic triglyceride levels are predominantly associated with increased NEFA delivery into the liver from TG lipolysis in peripheral adipose tissues and increased hepatic *de novo* synthesis of TG, while lipid clearance via β-oxidation and VLDL export are only moderately impaired (G. F. Lewis et al., 2002). Moreover, these studies strongly indicate that insulin does not suppress peripheral adipose tissue lipolysis as efficiently in NAFLD patients compared to healthy individuals (G. F. Lewis et al., 2002). Since insulin has a strong inhibitory effect on HSL (Ginsberg et al., 2005), this has raised the question of whether HSL resistance to insulin *per se* explains the elevated flux of NEFA from adipose tissue. Accordingly, studies have documented that there is increased hepatic insulin sensitivity in HSL-knockout mice that is associated with decreased plasma NEFA and liver triglyceride concentrations (S. Y. Park et al., 2005; Voshol et al., 2003). Thus, these studies indicate that targeting NEFA "spill-over" from adipose tissue could be an effective strategy for improving hepatic insulin resistance and steatosis.

2.1. The role of DNL in NAFLD

The accumulation of triglyceride within hepatocytes defines NAFLD (Donnelly et al., 2005) and involves contributions from lipolysis of peripheral free fatty acids as well as from hepatic DNL (Ameer et al., 2014; Kawano & Cohen, 2013). The measured contribution of hepatic DNL to liver TG levels is highly sensitive to the study design, in particular whether subjects are studied after overnight fasting or following a defined meal (Paglialunga & Dehn, 2016). In healthy lean individuals, it was estimated that DNL contributed < 5 % of total TG synthesis after overnight fasting (Hellerstein, 1999; Parks et al., 1999; J. M. Schwarz et al., 1995), whereas in the fed state the DNL rate increases by ~25 % over fasting levels (Barrows & Parks, 2006; Donnelly et al., 2005; Marques-Lopes et al., 2001; Jean Marc Schwarz et al., 2003). Moreover, although the number of studies reported to date are very limited (F. Diraison et al., 2003; Donnelly et al., 2005; Lambert et al., 2014), DNL rates were increased approximately 3-fold in individuals with NAFLD as compared to BMI-matched healthy subjects fasted for 18hrs after the last meal (Lambert et al., 2014). This is consistent with the augmented presence of DNL-derived triglycerides in very-low-density lipoproteins (VLDLs) produced in NAFLD, accounting for 15% of total VLDL TG (F. Diraison et al., 2003), in comparison to 2–5% for healthy subjects (F. Diraison et al., 1997). The impact of diet on DNL rates even in the absence of NAFLD was demonstrated in a study where DNL accounted ~20% of VLDL TG in healthy subjects following a meal high in carbohydrate (Aarsland et al., 1996). For NAFLD subjects, Donnelly *et al.* estimated that 26% of hepatic triglyceride was derived from DNL, 15% from the diet, and 59% from NEFA generated by endogenous lipolysis (Donnelly et al., 2005). This is supported by the study undertaken the triglycerides fatty acid composition in individuals with and without NAFLD. Individuals with NAFLD have shown increased levels of saturated fatty acids (Kotronen, Peltonen, et al., 2009; Kotronen, Velagapudi, et al., 2009), pointing

towards DNL as the contributor of NAFLD. Since saturated fatty acids are the major products of DNL and thus, high rates of DNL may lead to an increased proportion of hepatic saturated fatty acids that possibly explaining why DNL is associated with metabolic diseases including NAFLD. However, the DNL-derived TG contribution to the total TG content in both healthy and diseased states is still the minority but connects with the overall production of VLDL (G. F. Lewis et al., 2002).

In addition to the above measurements of the DNL products in NAFLD, transcriptional data for ACC1 (Acetyl-CoA carboxylase 1), FAS (fatty acid synthase), and SREBP1c display an elevation in expression of these key regulatory enzymes of DNL in NAFLD patients (Higuchi et al., 2008). The role of SREBP1c in the pathogenesis of NAFLD is further indicated by mouse studies where the expression of the transcriptionally active form of SREBP1c in a liver-specific way results in accumulation of hepatic lipid droplets (Knebel et al., 2012). Deletion of SREBP1c in the *ob/ob* mouse, a hyperphagic mouse model that develops harsh hepatic steatosis (Y. Zhang et al., 1994), showed a ~50% reduction in hepatic TG accumulation (Moon et al., 2012). Moreover, deletion of SCAP (SREBP cleavage-activating protein), the companion protein for immature SREBP1c, also protected against the accumulation of TG in *ob/ob* mice (Moon et al., 2012). As well as directly contributing to TG increase, DNL may also prevent the clearance of lipid by β-oxidation through its malonyl-CoA intermediate (Foster, 2012; McGarry et al., 1977, 1978). Malonyl-CoA hinders carnitine palmitoyltransferase 1 activity and therefore the translocation of long-chain fatty acids (> 8 carbon chain length) for the initiation of *β*-oxidation in the mitochondrial matrix (Ruderman et al., 2003). A second isoform of ACC, ACC2, is proposed to be more functionally orientated to β-oxidation inhibition since it is associated with the mitochondrial outer membrane (Abu-Elheiga et al., 2000).

2.2. DNL regulation, substrates and co-factors

Hepatic *de novo* lipogenesis (DNL) is a constitutive pathway that transforms acetyl-CoA into long-chain fatty acids. In humans, DNL occurs primarily in the liver, (Frédérique Diraison et al., 2003) while in rodents and other mammals, adipose tissue can also have significant activity (Bergen & Mersmann, 2005; Frédérique Diraison et al., 2003). A widely accepted teleological function of this pathway is the conversion of excess nutrient carbons into an inert and energy-dense triglyceride product that can be stored and mobilized at a later time for energy generation in times of nutrient scarcity. Among the possible mechanisms for lipid deposition, DNL is the most energetically costly with the synthesis of one equivalent of palmitate from acetyl-CoA expending 7 ATP and 14 NADPH (Chwalibog & Thorbek, 2001). Due to this, DNL activity is highly regulated both allosterically and transcriptionally such that it normally only operates during conditions of nutrient and energy satiety. For the liver, this corresponds to the absorptive and early post-absorptive feeding phase where there are high portal vein levels of simple sugars and amino acids coupled with peak levels of insulin. The transcriptional regulation of DNL has two major activating pathways: sterol regulatory element binding protein 1c (SREBP1c) and carbohydrate response element binding protein (ChREBP). These two pathways are activated by increased insulin signalling and increased glucose concentrations respectively, conditions that are associated with feeding (Kawano & Cohen, 2013; Oosterveer & Schoonjans, 2014). The loss of regulation of hepatic DNL flux secondary to excess nutrient consumption may be an important early event in the development of fatty liver and hypertriglyceridemia. Given the steep parallel increases in obesity rates and NAFLD in most Westernized societies, there is a pressing need for a better understanding of the metabolic mechanisms that contribute to lipid overload, of which DNL is likely a key component. Over-nutrition, accompanied by hyperinsulinemia and hyperglycemia, drives DNL activity. Lipogenic transcription factors

including carbohydrate response element binding protein (ChREBP) and sterol regulatory element binding protein-1c (SREBP-1c) are upregulated, leading to increased expression of lipogenic genes, increased flux through ACC, and elevations in hepatic malonyl-CoA (Hooper et al., 2011). This promotes increased hepatic DNL and suppressed hepatic fatty acid oxidation, which together potentiate steatosis (Hooper et al., 2011). Hepatic SREBP1c has also been reported to be upregulated in patients with NAFLD (Kohjima et al., 2007; Pettinelli et al., 2009) and elevated rates of hepatic DNL have been found to be a distinctive characteristic of NAFLD (Lambert et al., 2014). Humans with elevated liver fat showed a >3-fold increase in hepatic DNL relative to subjects with normal liver fat, while endogenous free fatty acid (FFA) influx from peripheral adipose tissue lipolysis and production of very low-density lipoprotein (VLDL) were not different (Lambert et al., 2014).

However, despite the clear association between elevated DNL activity and increased hepatic triglyceride levels, surprisingly little is known about the sources of acetyl-CoA that fuel this process. For nutrients that are widely held to be "lipogenic," such as fructose and ethanol, the handful of studies performed to date indicate that their contribution to the lipogenic acetyl-CoA pool is unexpectedly low. In reality, the liver has a wide choice of potential acetyl-CoA sources that in addition to dietary carbohydrates and ethanol, can also include ketogenic amino acids as well as products of intestinal microflora fermentation such as short-chain fatty acids (SCFA) and ethanol. SCFA (the relative amounts of acetate, propionate and butyrate), among the most abundant microbiota-derived metabolites, can be synthesised through the fermentation of dietary carbohydrates by the gut microbiota (Tan et al., 2014). Even if the exact mechanisms in which SCFA contribute to metabolic diseases including obesity remain unclear, one among the hypothesis is that they contribute as substrates for hepatic DNL and result in augmented capacity for energy yield from diet (Goffredo et al., 2016; Turnbaugh et al., 2006).

SCFA have been proposed to increase liver triglyceride levels and promote weight gain (Lepage et al., 2011) as they are involved in both fatty acid synthesis and gluconeogenesis (K. Takahashi et al., 2016). Also, a study has found that when gut microbiota produced acetate in higher quantities, it could stimulate the parasympathetic nervous system, thereby leads to increased ghrelin secretion, glucose-activated insulin secretion, hyperphagia, and obesity (Perry et al., 2016). The study also documented that the rats directly infused with acetate showed an impaired disposal of glucose and impaired insulin suppression of hepatic gluconeogenesis throughout a hyperglycemic-euglycemic clamp. These rats also revealed an increased triglyceride content in the liver, plasma, and skeletal muscle (Perry et al., 2016). On the other hand, supplementation of high fiber diets both to rodent models and human showed tremendous effect on weight loss, hepatic glucose and lipid control as well as maintained insulin sensitivity when compared with individual baselines (De Vadder et al., 2014; Fechner et al., 2014). Thus, these data of the study display that SCFAs derived from microbes are bioactive by-products, yet they have complex ways of interaction with the host metabolism so that the end effect being negative or positive is likely highly context-dependent.

Production of ethanol by the gut microbiota could also play a part in NAFLD pathophysiology. In children, the gut microbiota of individuals with NAFLD were more enriched with ethanol producing bacteria compared with those from either obese children with no NAFLD, or healthy lean children (Ding et al., 2010). A study performed in mice and further validated in humans identified bacteria (namely *Klebsiella pneumoniae*) that were able to produce ethanol from glucose endogenously (Alang & Kelly, 2015). Moreover, under conditions of dysregulated metabolism, where the tight reciprocal regulation of fat oxidation and fat synthesis pathways is loosened, endogenous substrates such as fatty acids and ketone bodies that would normally not contribute lipogenic acetyl-CoA may augment the more conventional dietary sources.

In addition to acetyl-CoA precursors, DNL is also dependent on NADPH: a cofactor that is required for many other cellular metabolic activities including the regeneration of reduced glutathione. The pentose phosphate pathway (PPP) is an important component of glucose metabolism. In many tissues including the liver, the PPP is thought to be the major source of NADPH. Two NADPH equivalents are generated through the stepwise oxidation of glucose-6-phosphate via glucose-6-phosphate dehydrogenase and 6-phosphogluconate dehydrogenase. Thus, the PPP is often assumed to be essential for both DNL and glutathione reduction. This suggests that PPP activity should be elevated in NAFLD, where DNL is active and oxidative stress may also be present. However, little is known about the activity of the PPP in the evolution of fatty liver. Recently, Jin et al. demonstrated that hepatic PPP flux was associated with DNL activity, but was independent of oxidative stress burden suggesting that the reducing equivalents generated by the PPP were dedicated to fatty acid biosynthesis (Jin et al., 2018). NADPH can be generated by three other cytoplasmic enzymes: isocitrate dehydrogenase 1 (IDH1), malic enzyme 1 (ME1) and 10-formyltetrahydrofolate dehydrogenase (ALDH1L1) (Bradshaw, 2019) hence it is possible that these might contribute NADPH for glutathione reduction.

2.3. How DNL is measured:

Due to the importance of lipid biosynthetic fluxes in NAFLD, T2D and cancer metabolism, multiple tracer methodologies have been developed for their study and quantification. The use of stable isotopes to study DNL dates back more than 80 years to the pioneering work of Schoenheimer and Rittenberg (Schoenheimer & Rittenberg, 1936). However, it had been not

until relatively recently that it has been routinely applied for human and animal model studies. Among the complications of stable isotope studies is determining of the correct precursor pool enrichment when that precursor is biochemically unavailable (for instance, cytosolic acetyl coenzyme-A for fatty acid synthesis). Historically, tracer experiments for measuring the lipids synthesis were first developed using radioisotope tracers, such as ^{3}H-labelled water, ^{14}C-labelled acetate, and ^{3}H- and ^{14}C- labelled fatty acids (Murphy, 2006). The metabolic information gained from radioisotope tracer research laid the groundwork for stable isotope tracer research. With stable isotopes, it became possible to carry out routine studies in both pre-clinical and clinical settings without the safety and ethical constraints associated with the use of radioisotopes.

With isotopic tracers, the fraction of hepatic or VLDL lipid that was synthesized via DNL can be measured. The principal tracer approaches for quantifying fractional DNL rates have involved carbon-based tracers such as ^{13}C- or ^{14}C-acetate as well as labelled water ($^{2}H_2O$ or $^{3}H_2O$) (J. G. Jones, 2014). Carbon-based tracers result in obligatory enrichment of the acetyl-CoA precursor pool followed by passage of the carbon label through subsequent intermediates of the DNL pathway. In the case of the labelled hydrogens of water (which from this point on will focus on the stable ^{2}H isotope), these are partially incorporated at the level of acetyl-CoA or precursor substrates as well as in the subsequent hydration and reduction steps of fatty acyl synthase (FAS). The terminal methyl hydrogens of synthesized fatty acyls are directly descended from the initial acetyl-CoA molecule that became bound to FAS and therefore reflects the isotopic enrichment of acetyl-CoA at the moment of recruitment by DNL (J. G. Jones, 2014).

^{13}C-Enriched acetate was developed as a tracer for DNL studies in both animal models and humans. Acetate is directly converted in the cytosol to the acetyl-CoA precursor. Infusion with either [1-^{13}C]acetate or [2-^{13}C]acetate yield similar results (Hellerstein et al., 1991), therefore the less costly [1-^{13}C]acetate has been the most widely used. For determining the fatty acid fractional synthetic rate from plasma triglyceride enriched with ^{13}C following infusion of [1-^{13}C]acetate, an approach known as Mass Isotopomer Distribution Analysis (MIDA) was developed by Hellerstein and Neese (Hellerstein & Neese, 1992). Essentially, MIDA considers that, in the synthesis of polymers (fatty acids can be considered a polymer of acetyl-CoA) the enrichment of the final polymer follows a binomial distribution which is a function of the enrichment of the monomers (the *p* value) and the number of monomers that constitute the polymer (the *n* value). Therefore, if both the *p* and the *n* value are known, the synthesis rate of the polymer can be determined based on the polymer's enrichment ratio. MIDA has also been applied to the analysis of fatty acid enrichment from deuterated water (F. Diraison et al., 1996, 1997; W. N. P. Lee, Bassilian, Ajie, et al., 1994; W. N. P. Lee, Bassilian, Guo, et al., 1994; Leitch & Jones, 1993). ^{13}C-Acetate administration requires a lengthy intravenous infusion period prior to sampling of ^{13}C-enrichment in the lipid product because turnover and appearance rates for lipid products are usually much slower than for other metabolites such as glucose. Even for lipid pools with relatively fast turnover such as liver and VLDL triglyceride, 8-hour infusions yield fractional synthetic rates of <5 % with 24 hour infusions yielding ~3-fold higher values (Parks et al., 1999; Timlin et al., 2005). These lengthy infusion times require several grams of [1-^{13}C]acetate per subject but are essential for achieving quantifiable enrichment levels of the lipid products (Vedala et al., 2006). In addition, zonation across the liver may result in gradients of precursor enrichment that can lead to underestimates of fatty acid fractional synthetic rates (I. R. Bederman, Kasumov, et al., 2004; I. R. Bederman, Reszko, et al., 2004). In any event, this method becomes impractical for the study of lipid metabolites

with slow turnover, such as the triglyceride fatty acids of peripheral adipose tissues, since infusion times of several days would be required to achieve measurable ^{13}C-enrichment of the product.

Deuterated water (^2H_2O) is an alternative lipogenesis tracer that is being increasingly used due to several advantages over carbon-based tracers. In addition to being relatively inexpensive, ^2H_2O quickly equilibrates with the total body water (TBW) pool, is easily administered over long periods (necessary for adipose TG and fatty acid kinetics), requires no intravenous infusion, and allows for the simultaneous measurement of several processes, notably the synthesis of both fatty acid and glycerol components of triglyceride. In animal models, an initial loading dose of ^2H_2O is given orally or via intraperitoneal injection to achieve a target body water enrichment of 3-5%. This enrichment level can then be maintained indefinitely by enriching the drinking water with ^2H_2O. The steady-state body water enrichment is systematically lower than that of the drinking water, presumably due to dilution from unlabeled metabolic water generated from food and due to water exchange through respiration (W. N. P. Lee, Bassilian, Ajie, et al., 1994). Because of this, enrichment of the drinking water is usually set to be higher than that of the target body water (i.e. for a target body water of 4%, a drinking water enrichment of 5% would be prepared). For human studies, body water enrichment levels of 0.3-0.5% are typically achieved by drinking 250-350 ml of 70-99% enriched ^2H_2O. Since a single of ingestion of >200 ml of highly-enriched deuterated water induces vertigo (Brandt, 1990), the loading dose is typically divided into 3 portions and ingested over a 1-hour interval.

^2H from water is incorporated into the triglyceride fatty acid acyl chain and glycerol moiety by several mechanisms as follows: 1), chemical exchange of water and precursor metabolite hydrogens catalyzed by enzymes of glycolysis, TCA cycle and aminotransferases; 2), direct

addition of water hydrogen to the growing fatty acid chain via the enoyl-CoA reductase step, and 3), exchange of water hydrogens with NADPH followed by reductive incorporation into the growing fatty acid chain at the 3-ketoacyl-ACP reductase and enoyl-CoA reductase steps. Exchange between water and NADPH hydrogens in turn will depend on whether NADPH was formed via the pentose pathway, malic enzyme or 10-formyl tetrahydrofolate routes.

A principal uncertainty in the use of $^{2}H_2O$ for measuring of lipid biosynthesis is the lack of information on the efficacy of these various exchange processes in transferring ^{2}H from body water to the lipid product via the precursors and metabolic intermediates. It has been previously assumed that acetyl-CoA enrichment is equivalent to that of body water; that is, exchange of acetyl-CoA methyl and water hydrogens is complete at the point of ACC and FAS (T. C. Delgado et al., 2009; Soares et al., 2012). However from analysis of hepatic glutamine hydrogen 4 to hydrogen 3 enrichments from $^{2}H_2O$ in humans, the estimated acetyl-CoA ^{2}H-enrichment was only 66% of its theoretical value (Barosa et al., 2010) while the same methodology applied to *in situ* and perfused rat livers revealed enrichments that were 71% and 53% of theoretical values, respectively (A. M. Silva et al., 2011). On the other hand, analysis of cytosolic acetyl-CoA enrichment via *N*-acetyl *p*-amino benzoic acid (*N*-acetyl-PABA) in feeding mice reported enrichments that were equivalent to that of body water (F Carvalho et al., 2011; Duarte et al., 2014). In rodents administered $^{2}H_2O$, GC-MS analyses of liver triglyceride palmitate reported ^{2}H enrichment levels that were only ~70% of the theoretical value (F. Diraison et al., 1996; W. N. P. Lee, Bassilian, Ajie, et al., 1994; W. N. P. Lee, Bassilian, Guo, et al., 1994). Based on these data, a correction factor (N) representing the average number of palmitate hydrogens enriched with ^{2}H is used to adjust the measured molar ^{2}H-enrichment of palmitate. Since GC-MS does not resolve different fatty acid ^{2}H-enrichment sites, it does not reveal to what degree the different mechanisms of ^{2}H labeling (i.e., reductive

NADPH transfer, hydration, acetyl-CoA and malonyl-CoA incorporation) contribute to the incomplete stoichiometry of fatty acyl ^{2}H enrichment. Factors that might be involved include discrimination of ^{2}H versus ^{1}H incorporation into metabolites due to kinetic isotope effects and/or slow exchange rates of body water and metabolite hydrogens relative to the rate of flow of metabolic intermediates through the DNL pathway. In the case of palmitate, three of its 31 hydrogens are derived from acetyl-CoA, with the remainder originating from NADPH (14), malonyl-CoA (7) and directly from body water (7) (Duarte et al., 2014). While the reducing hydrogen of NADPH does not directly undergo spontaneous exchange with that of water, redox cycling between NADPH and intracellular flavin enzymes such as glutathione reductase enable exchange between water and NADPH hydrogens (Z. Zhang et al., 2017). Whether this (or indeed any other exchange process) is sufficiently rapid to fully equilibrate ^{2}H-enrichment of body water and intracellular NADPH between the time it was generated from $NADP^{+}$ and then utilized for DNL is not currently known. Malonyl-CoA is generated from acetyl-CoA via ACC, hence its methylene hydrogens are derived from the methyl hydrogens of acetyl-CoA. Therefore, ^{2}H-enrichment of the malonyl-CoA methylene hydrogens is assumed to be at least equal to that of the acetyl-CoA methyl hydrogens. For studies where the level of excess ^{2}H enrichment from administered $^{2}H_2O$ is not substantially above background levels, the background ^{2}H enrichment level of the analyte must be directly measured since it may differ considerably from the benchmark Vienna Standard Mean Ocean Water value of 0.015576% (Leitch & Jones, 1993).

Enrichment of lipid hydrogens from $^{2}H_2O$ can also be resolved and quantified by ^{2}H NMR spectroscopy of isolated lipids (Belew et al., 2019; T. C. Delgado et al., 2009; Duarte et al., 2014; J. C. P. Silva et al., 2019; Soares et al., 2012; Viegas et al., 2016). This method has much lower sensitivity compared to MS, requiring 5-50 μmol of analyte in the typical experimental

setting for $^{2}H_2O$ studies (0.5-5.0 % body water enrichment). However, in addition to being non-destructive to the sample, NMR provides a much higher level of positional enrichment information compared to MS which yields a more detailed picture of lipid biosynthetic. Resolution of ^{2}H enrichment in the fatty acid position 2 and 3 hydrogens provides a direct measure of fatty acid elongation activity since enrichment of position 2 is the sum of elongation and DNL while that of position 3 is from DNL only (Duarte et al., 2014). Resolution of the ^{2}H NMR signal representing the allyl hydrogens of monounsaturated fatty acids (principally oleate and palmitoleate) gives a measure of fatty acid desaturation activity (Duarte et al., 2014). Finally for intact triglyceride, signals representing the methylene hydrogens of glycerol inform the fractional rate of triglyceride glycerol synthesis (Duarte et al., 2014).

In addition to providing positional ^{2}H-enrichment information, NMR analysis can also be used to quantify low levels of lipid ^{13}C-enrichment from a second tracer such as [U-^{13}C]fructose with minimal interference of one tracer with the other (J. C. P. Silva et al., 2019). This combination provides a means of determining contributions of individual substrates such as fructose and glucose to lipid biosynthesis.

2.4. How contributions of individual substrates to DNL are measured

Acetyl-CoA can be generated from a diversity of precursors including glucose, fructose and microbially-generated acetate (Figure 4). Profiling the sources of lipogenic acetyl-CoA in the liver is challenging for three principal reasons. First, the diversity of potential acetyl-CoA sources hinders the identification and quantification of contributing substrates by conventional tracer methods. Second, hepatic intermediary metabolism features a number of substrate and metabolite recycling pathways that, among other things, randomize the positional ^{13}C-

enrichment during conversion of a ^{13}C-enriched substrate to ^{13}C-enriched acetyl-CoA. Thirdly, there is substantial evidence that hepatocytes have distinctive intracellular acetyl-CoA pools that are enriched to different levels by ^{13}C-enriched acetyl-CoA precursors (J. G. Jones, 2014). Thus, for determining ^{13}C-enriched substrate contributions to DNL, either the true cytosolic acetyl-CoA precursor pool must be selectively sampled (F Carvalho et al., 2011; Filipa Carvalho et al., 2013), or alternatively, enrichment of acetyl-CoA units within newly synthesized fatty acids needs to be measured (J. C. P. Silva et al., 2019). This is achieved by integrating lipid ^{2}H-enrichment NMR data which informs the fraction of newly-synthesized fatty acid or glycerol moieties within tissue triglyceride, with ^{13}C-NMR isotopomer analysis which precisely measures the enrichment of the fatty acid chain from [U-^{13}C]acetyl-CoA generated from a [U-^{13}C]sugar substrate (Figure 4) (J. C. P. Silva et al., 2019).

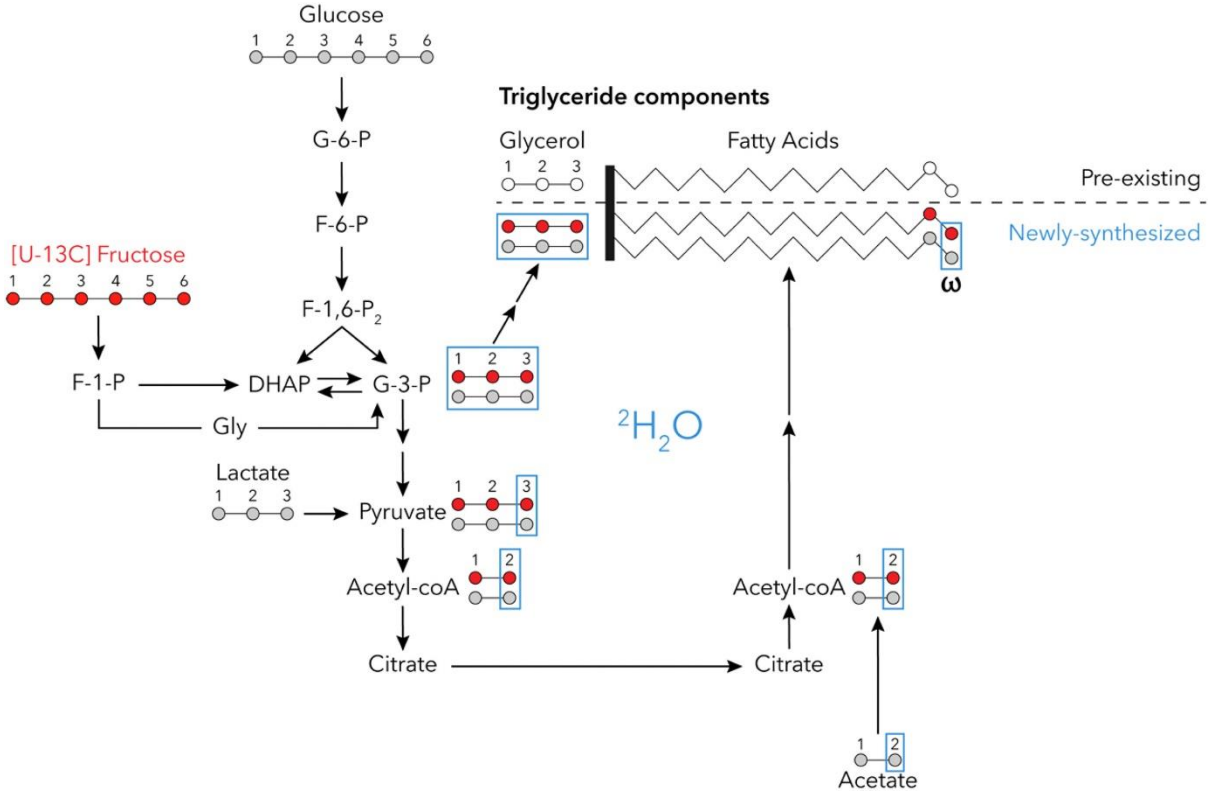

Figure 4: *Integration of $^{2}H_2O$ and [U-^{13}C]sugar substrates to quantify the contribution of exogenous sugar as part of a glucose/fructose mixture to de novo synthesis of TG fatty acid and glycerol moieties adapted from Silva et al. (J. C. P. Silva et al., 2019). The [U-^{13}C]fructose*

carbon skeleton and selected metabolic intermediates are represented as red filled circles while the carbon skeletons of unlabeled glucose and other endogenous metabolites (lactate and microbially-generated acetate) are represented by light gray circles. Pre-existing FA and glycerol carbons are represented by unfilled circles. ^{2}*H-enrichment of triose-P and glycerol hydrogens, the methyl hydrogens of pyruvate, acetate, acetyl-CoA, and the terminal (**ω**) hydrogens of TG fatty acyls, are represented by blue boxes. Note that the combination of unlabeled fructose and [U-*^{13}*C]glucose generates the same set of triose-P and FA* ^{13}*C-isotopomers (J. C. P. Silva et al., 2019). Some metabolic intermediates were omitted for clarity. Abbreviations:* $^{2}H_2O$*, Deuterated water; F-1-P, Fructose 1-phophate; F-6-P, Fructose 6-phosphate; F-1,6-P, Fructose 1,6-bisphosphate; G-3-P, Glyceraldehyde 3-phosphate; G-6-P, Glucose 6-phosphate.*

3. RESEARCH OBJECTIVES

Hepatic steatosis is a result of an over accumulation of lipids within the liver secondary to excess consumption of carbohydrate and/or fat. Since refined sugar, and in particular, fructose, is assumed to be largely metabolized in liver, its role in promoting NAFLD has been to date explained by its unregulated conversion to fatty acids via DNL. In the Western diet, high sugar ingestion is typically accompanied by high levels of saturated fat. To what extent high sugar *per se* accentuates the already high NAFLD risk from high fat feeding is unclear. In addition, many mouse models of high sugar feeding fail to induce weight gain and adiposity and only develop relatively mild NAFLD. Moreover, different mouse strains show different susceptibilities to developing NAFLD from high sugar diets. The C57BL/6J mouse strain has been shown to be more susceptible to diet-induced obesity compared to other strains. In order to better understand the relationship between high sugar feeding and DNL in this setting, we will clarify some current uncertainties in quantifying DNL rates from deuterated water in order to obtain more precise estimates of these fluxes. We will also determine the role of dietary fructose and glucose in sustaining PPP activity – an essential requirement for DNL. Finally, the effects of high dietary fat on sugar-induced DNL activity in this mouse model will be evaluated.

1. RESEARCH METHODOLOGY

This is distributed among four main tasks as follows:

Task 1 Validation of NAFLD development from high sugar and/or high fat feeding in mouse models: The aim was to verify NAFLD in the C57BL/J6 mouse by high sugar and/or high fat feeding. The C57BL/J6 mouse is reported to develop NAFLD when fed a normal chow diet supplemented with 30% sucrose in the drinking water for 8 weeks (Bedogni et al., 2006; Bergheim et al., 2008). To confirm NAFLD onset in our experimental setting, adult mice were placed on this diet and compared to controls fed normal chow only. Food intake and body weight were periodically monitored. In order to fully validate and confirm the development of NAFLD and NASH the high-sugar feeding was continued for 18 weeks until these NAFLD markers reach significance. Cohorts of mice fed with high fat and high fat + 30% sucrose in drinking water diets were undergo the same evaluations. The details of the animal studies are discussed in the following chapters.

Task 2 Implementing tracer administration and tissue analysis protocols on the NAFLD mouse model: The aim is to implement tracer and permeability measurements in the NAFLD mouse models under natural feeding conditions and develop post-mortem tissue sampling protocols for liver and portal vein blood such that all of the proposed tracer, intestinal permeability, and microbiota measurements are performed for each animal. At the onset of the final evening, the mice were placed in metabolic cages and intraperitoneally injected with 99.9% $^{2}H_2O$ in saline (40 mg/g body mass). The drinking water was replaced with water enriched to 5% with $^{2}H_2O$ and containing 30% sucrose (a mixture of 45% glucose and 55% fructose) where one or the other sugar was enriched with [U-^{13}C]hexose. The next morning,

the mice were euthanized and dissected for harvesting of portal vein blood and liver into liquid nitrogen. The details of tracer implementation and administrations are discussed in each research works of the following chapters.

Task 3 Tissue processing and analysis: the freeze-clamped liver tissues were processed for extracting and purifying the liver triglyceride as previously described (Belew et al., 2019; J. C. P. Silva et al., 2019; Viegas et al., 2016). Then, analysed sequentially by ^{1}H, ^{2}H and ^{13}C NMR to obtain overall metabolite profiles and to assess metabolite ^{13}C-enrichment from [U-^{13}C] fructose and glucose, and profiling the triglyceride as well as measuring the DNL and glyceroneogensis. The details of liver tissue processing and analysis method are covered in the following chapters.

Task 4: Data Processing, Statistics & Power analysis: The objectives were to define significance levels of alterations in metabolic, physiological and microbiological parameters for sugar-fed and/or high-fat versus control mice and also examine correlations between different sets of variables within groups (i.e. lipogenic fluxes and intestinal permeability). All data were presented in tables using appropriate and accepted units and accompanied with standard errors of mean. In this work, parameters between different conditions (i.e. control versus high sugar feeding) were compared. Also, longitudinal changes in certain parameters within individual animals were evaluated (for example weight). Statistical significance between different subject groups were evaluated using the appropriate ANOVA tests. *P* values of less than 0.05 were considered as significant. From previous experience, the metabolic flux measurements were associated with the highest amount of variability compared to other parameters such as metabolite levels etc., hence the minimum number of animals per group were based on the predicted variances of the proposed lipid metabolic flux data. Based on the

means and coefficients of variation of our previously published data (Duarte et al., 2014), we predicted that to resolve a 20 % difference in metabolic flux parameters required 12-16 animals per study group to achieve a study power of 80% at a significance level of 5%.

CHAPTER TWO

TRANSFER OF GLUCOSE HYDROGENS VIA ACETYL-COA, MALONYL-COA AND NADPH TO FATTY ACIDS DURING *DE NOVO* LIPOGENESIS

1. INTRODUCTION

There is currently high interest in the measurement of *de novo* lipogenesis (DNL) to better understand its role in the dyslipidemia of diseases such as type 2 diabetes and fatty liver disease (F. Diraison et al., 2003; Forcheron et al., 2002; Saponaro et al., 2015). Fractional DNL rates can be measured from incorporation of deuterated water (^2H_2O) into fatty acids (F. Diraison et al., 1997; Duarte et al., 2014), an inexpensive and simple method that can be applied to humans, animal models, and cell cultures. ^2H enrichment of fatty acids from ^2H_2O is conventionally measured by MS, where all the fatty acid chain hydrogens are considered as a single traceable entity (F. Diraison et al., 1997). While this provides amplification of the m+1 signal arising from ^2H incorporation, it does not resolve the carbon-bound fatty acid hydrogens according to their metabolic sources (see Figure 5). It was reported that in rats, about 30% of plasma triglyceride palmitate hydrogens had not exchanged with ^2H body water (F. Diraison et al., 1996; W. N. P. Lee, Bassilian, Ajie, et al., 1994), while for palmitate derived from cultured cells, this non-exchanged fraction was even higher (W. N. P. Lee, Bassilian, Guo, et al., 1994). Therefore, for DNL measurement, the ^2H enrichment of fatty acids measured by MS needs to be corrected by a predetermined factor related to the number of deuterium atoms that were incorporated per molecule of fatty acid, referred to as N (F. Diraison et al., 1996). Stoichiometric ^2H enrichment of fatty acids from ^2H_2O is conditional on full exchange between the hydrogens of water and those of the acetyl-CoA methyls, the malonyl-CoA methylenes, and the reducing hydrogen of NADPH.

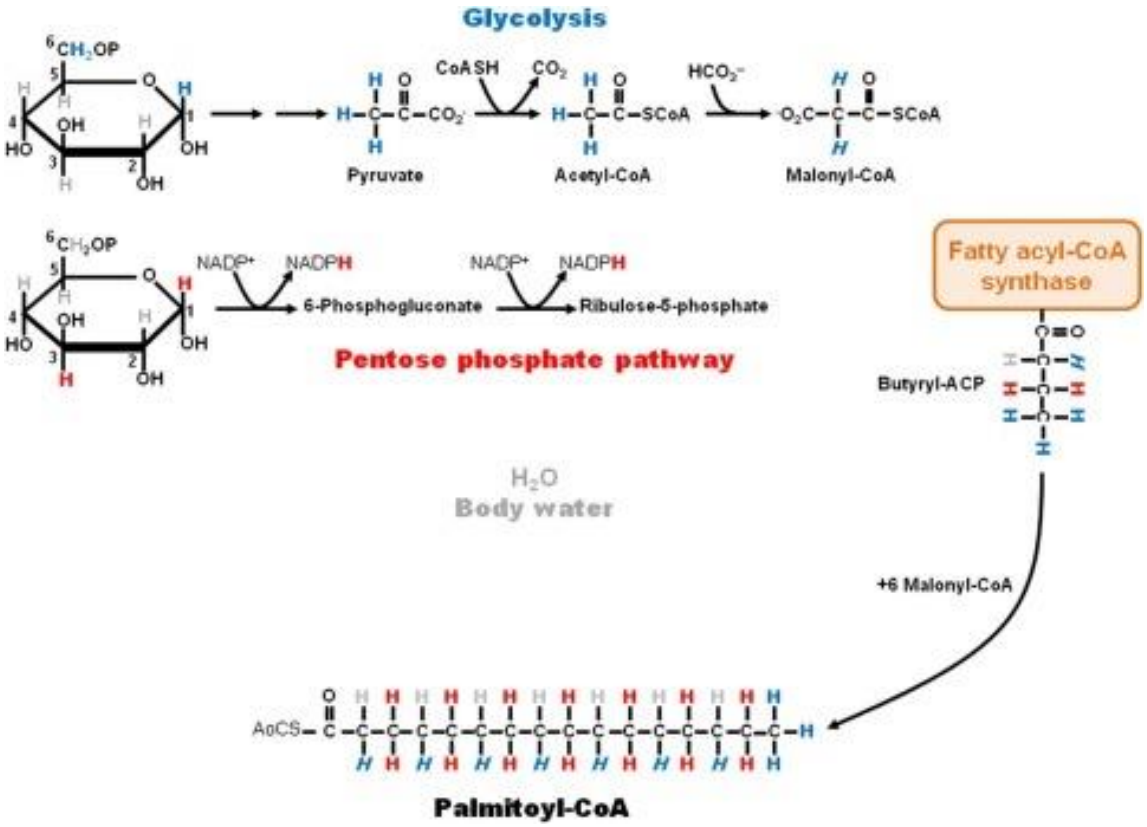

Figure 5: *Sources of hydrogens for the synthesis of palmitoyl-CoA from glucose and body water via fatty acyl-CoA synthase, with the butyryl acyl carrier protein (Butyryl-ACP) intermediate also shown. When glucose is metabolized via glycolysis, hydrogens 1 and 6 (shown in blue) are transferred to pyruvate and then to acetyl-CoA and malonyl-CoA (represented by blue italic). During the first cycle of fatty acid synthesis, acetyl-CoA and malonyl-CoA hydrogens are incorporated into the terminal methyl group and one of the position 2 hydrogens of butyryl-ACP, respectively. In the palmitoyl-CoA product, this corresponds to the terminal methyl hydrogens and one of the methylene hydrogens attached to each even-numbered carbon. When glucose is metabolized via the pentose phosphate pathway (PPP), hydrogens 1 and 3 (shown in red) are transferred to NADPH. During the first cycle of fatty acid synthesis, these are incorporated into both position 3 hydrogens of butyryl-ACP and subsequently into both methylene hydrogens attached to each odd-numbered carbon of palmitoyl-CoA. The remaining hydrogen in position 2 of butyryl-ACP is derived from body*

water (shown in gray) and is incorporated into one of the methylene hydrogens attached to each even-numbered carbon of palmitoyl-CoA. The color scheme indicates possible labeling sites only and is not meant to represent the stoichiometry of hydrogen transfer.

A less than theoretical ^{2}H enrichment of the fatty acids implies that hydrogen exchange is incomplete, but to what degree this occurs for each of the metabolic precursors is not known. To address this, we provided mice with [U-$^{2}H_{7}$]glucose and performed ^{2}H NMR analysis of liver triglyceride (T. C. Delgado et al., 2009; Duarte et al., 2014; Viegas et al., 2016) to determine the extent to which the ^{2}H were transferred into positions 2 and 3 and the terminal methyl hydrogens of hepatic fatty acids: each position reflecting ^{2}H transfer from glucose via malonyl-CoA, NADPH, and acetyl-CoA, respectively. Our data indicate that there was a substantial transfer of glucose hydrogen to newly synthesized fatty acids via NADPH, corresponding to a limited exchange with water hydrogen, but relatively low transfer via malonyl-CoA and acetyl-CoA intermediates, indicating extensive hydrogen exchange at these loci of the DNL pathway.

2. METHODS

2.1. Materials

[U-$^{2}H_{7}$]- and [U-$^{13}C_{6}$]glucose at 98–99% enrichment were obtained from Sigma-Aldrich. [3-^{2}H]glucose at 98% enrichment was obtained from Omicron Biochemicals, South Bend, IN, USA.

2.2. Animal studies

Animal studies were approved by the University of Coimbra Ethics Committee on Animal Studies (ORBEA) and the Portuguese National Authority for Animal Health (DGAV), approval code 0421/000/000/2013. Adult male C57BL/6J mice were obtained from Charles River Laboratories, Barcelona, Spain, and housed at the University of Coimbra Faculty of Medicine Bioterium, where they were maintained with a 12 hours light/12 hours dark cycle. Upon delivery to the Bioterium, mice were provided a 2 week interval for acclimation, with free access to water and standard chow. Following acclimation, the drinking water was supplemented with glucose and fructose (15.0 g of each sugar to 100 g of water). In the first set of studies, the glucose was enriched to 20% each with [U-$^{2}H_{7}$]glucose and [U-$^{13}C_{6}$]glucose. In a second set of studies, glucose was enriched to 16% each with [3-^{2}H]glucose and [U-$^{13}C_{6}$]glucose. In the third set of experiments, mice were administered an intraperitoneal injection of 99.9% $^{2}H_{2}O$ containing 9 mg NaCl per milliliter at a dose of 4 g/100 g body mass at the start of the dark period. For these animals, the drinking water was enriched to 5% with $^{2}H_{2}O$ and the glucose was enriched to 50% with [U-$^{13}C_{6}$]glucose but not with ^{2}H. Animals were allowed to feed and drink *ad libitum* during the entire 12 hour dark period and were euthanized by cervical dislocation the following morning. Livers and adipose tissue depots

were freeze-clamped and stored at −80°C until further processing for triglyceride extraction and purification.

2.3. Triglyceride extraction and purification

Liver triglyceride was extracted and purified as previously described (Viegas et al., 2016). Briefly, livers were powdered under liquid nitrogen and then rapidly mixed with HPLC-grade methanol (4.6 ml/g) followed by methyl-tert-butyl ether (MTBE) (15.4 ml/g). The mixture was placed in a shaker for 1 hour at room temperature and then centrifuged at 13,000 *g* for 10 min. The liquid fraction was collected and phase separation was induced by adding 4 ml of distilled water to the liquid fraction and letting it rest at room temperature for 10 min. The liquid was then centrifuged for 10 min at 1,000 *g*. The upper organic phase containing the lipids was carefully separated and dried under nitrogen gas in a dark glass vial. Triglycerides from the dried lipid extracts were purified with a solid phase extraction (SPE) process. Discovery DSC-Si SPE cartridges (2 g/12 ml) were washed with 8 ml of hexane/MTBE (96/4; v/v) followed by 24 ml of hexane. The dried lipids were re-suspended in 800 µl of hexane/MTBE (200/3; v/v) and added to the column after washing. The lipid vials were washed with a further 500 µl solvent to quantitatively transfer the lipids to the column. Triglycerides were eluted with 32 ml of hexane/MTBE (96/4; v/v), collected in 4 ml fractions. Fractions containing triglycerides were identified by thin-layer chromatography (TLC). A few microliters of the eluted fractions were spotted on the TLC plate alongside triglyceride standards and the plate was developed with petroleum ether/diethyl ether/acetic acid (7.0/1.0/0.1; v/v/v). After drying, lipid spots were visualized by iodine vapor. The triglyceride-containing fractions were pooled and dried under nitrogen gas and stored at −20°C until ready for NMR analysis.

2.4. NMR analysis

Purified triglycerides were dissolved in ~0.5 ml $CHCl_3$. To these, 25 µl of a pyrazine standard enriched to 1% with pyrazine-d_4 and dissolved in $CHCl_3$ (0.07 g pyrazine/1 g $CHCl_3$), and 50 µl of C_6F_6 were added. ^1H and ^2H NMR spectra were acquired with an 11.7 T Bruker Avance III HD system using a dedicated 5 mm ^2H-probe with ^{19}F lock and ^1H-decoupling coil as previously described. ^1H spectra at 500.1 MHz were acquired with a 90° pulse, 10 kHz spectral width, 3 seconds acquisition time, and 5 seconds pulse delay. Sixteen free-induction decays (fid) were collected for each spectrum. ^2H NMR spectra at 76.7 MHz were obtained with a 90° pulse, a 1,230 Hz sweep width, an acquisition time of 0.37 seconds, and a pulse delay of 0.1 seconds. Between 10,000 and 20,000 fid were acquired for each spectrum. Correction factors were applied to all ^2H triglyceride signals to adjust their intensities relative to the partially saturated ^2H pyrazine standard signal. These were obtained as mean values from a set of seven liver triglyceride samples obtained from mice administered with ^2H_2O. For each sample, a spectrum was acquired with the described parameters and immediately followed by a spectrum acquired under the same parameters with the exception of the acquisition time and pulse delay, which were set to 1 s and 8 s, respectively. The correction factors for the ^2H signals in fatty acid position 2, position 3, and methyl hydrogens were 0.51, 0.52, and 0.88, respectively. For ^{13}C isotopomer analysis by ^{13}C NMR, dried triglyceride samples were dissolved in 0.2 ml 99.96% enriched $CDCl_3$ (Sigma-Aldrich) and placed in 3 mm NMR tubes. ^{13}C NMR spectra were acquired at 150.8 MHz with an Agilent V600 spectrometer equipped with a 3 mm broadband probe. Spectra were acquired with a 70° pulse, an acquisition time of 2.5 s, and a 0.5 s pulse delay. For each spectrum, 2,000–4,000 fid were collected.

2.5. Quantification of triglyceride positional ^{2}H and ^{13}C enrichments

Positional ^{2}H enrichments of triglyceride fatty acids were quantified by analysis of ^{1}H and ^{2}H NMR triglyceride spectra as previously described (Duarte et al., 2014; Viegas et al., 2016). From the methyl and carboxyl ^{13}C NMR resonances, positional ^{13}C enrichments of fatty acids were estimated from the ratio of ^{13}C-^{13}C-spin-coupled doublet signals (representing positional isotopomers derived from [1,2-$^{13}C_2$]acetyl-CoA) to the singlet signal, representing the 1.11% natural abundance ^{13}C (see Figure 6). From the methyl singlet and doublet ^{13}C NMR signals, the ^{13}C enrichment of fatty acids from [1,2-$^{13}C_2$]acetyl-CoA in the methyl position was calculated as follows:

Excess ^{13}C-enrichment of fatty acid methyls (%) = **Methyl D**/**Methyl S** × 1.11

Where Methyl D and Methyl S are the doublet and singlet components, respectively, of the ^{13}C-signal of the fatty acid terminal methyls and 1.11 represents the background ^{13}C enrichment (%).

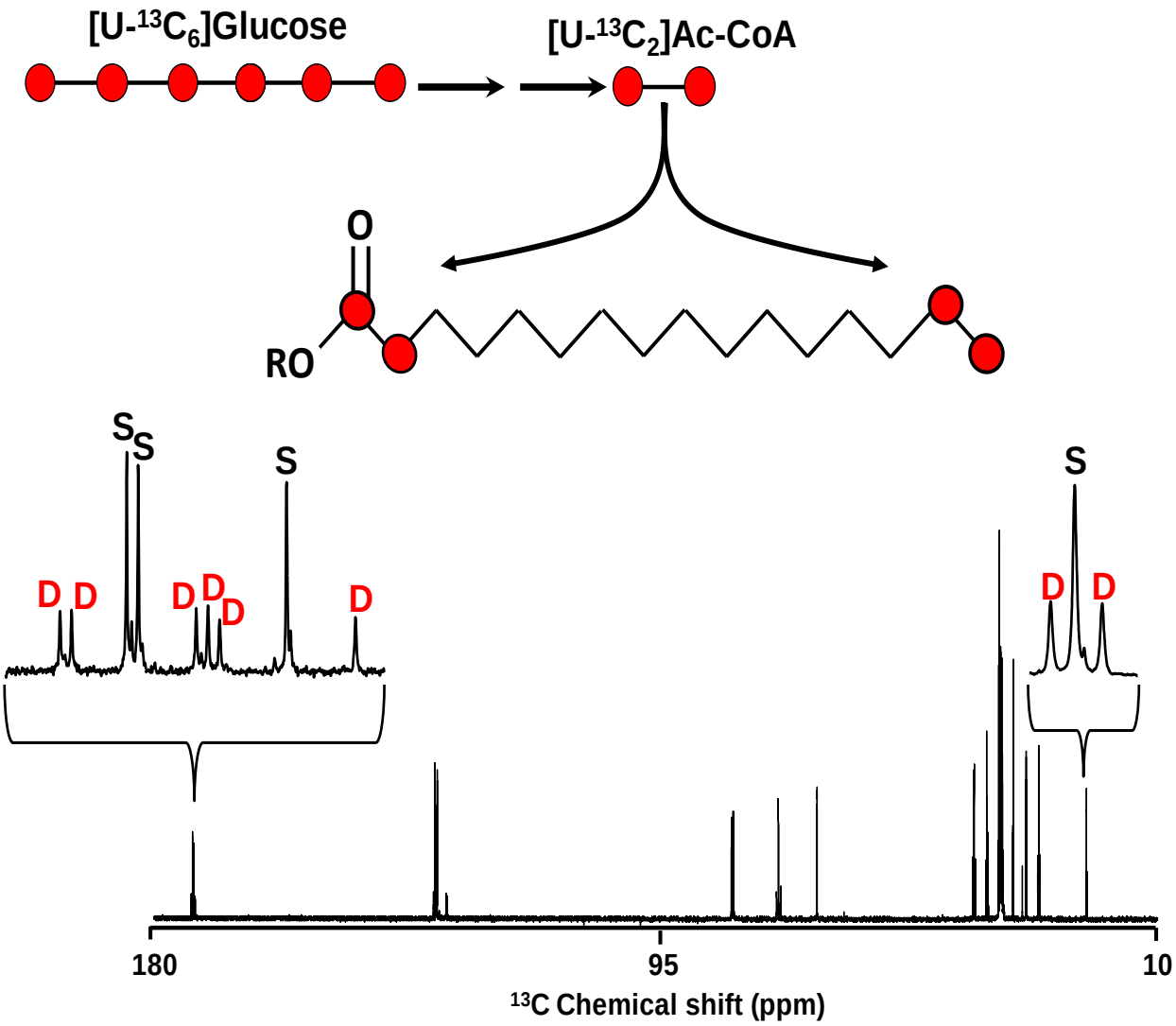

Figure 6: *Representative ^{13}C NMR spectrum of liver triglyceride isolated from a mouse that ingested glucose enriched with [U-$^{13}C_6$]- and [U-$^{2}H_7$]glucose. The insets show the ^{13}C-^{13}C-spin-coupled doublets for the fatty acid methyl and position 1 sn1,3 carboxyls enriched with [U-$^{13}C_2$]acetyl-CoA derived from [U-$^{13}C_6$]glucose metabolism (**D**) and natural-abundance singlets from fatty acids that were not enriched (**S**). Under these conditions, excess ^{13}C-enrichment of positions 1 and 2 are equivalent therefore position 2 enrichment can be inferred from analysis of the position 1 signals.*

Assuming that fatty acid enrichment from [1,2-$^{13}C_2$]acetyl-CoA via elongation was limited to position 1 and 2 carbons, enrichment of carbon 3 was assumed to be equivalent to that of the terminal methyl carbon.

From analysis of the fatty acid singlet and doublet carboxyl ^{13}C-signals, excess enrichment of the position 1 of fatty acids from [1,2-$^{13}C_2$]acetyl-CoA was estimated as follows:

Position 1 Excess ^{13}C-enrichment (%) = $\mathbf{\Sigma\ D/\Sigma\ S} \times 1.11$

Where ΣD and ΣS are the summed doublet and singlet components, respectively, of the ^{13}C-carboxyl resonances and 1.11 represents the background ^{13}C enrichment (%). Excess enrichment of the fatty acid position 2 carbon was assumed to be equal to that of position 1.

For determining the fractional rate of [U-$^{2}H_7$]glucose transfer into acetyl- and malonyl-CoA relative to that of [U-$^{13}C_6$]glucose, the $^{2}H/^{13}C$ enrichment ratios of the terminal methyl and carbon 2 positions were divided by 1.5 to account for the fact that there are three ^{2}H for every two ^{13}C in the initial glucose mixture. For estimating the fractional rate of [U-$^{2}H_7$]glucose transfer into NADPH relative to the lipogenic utilization of [U-$^{13}C_6$]glucose, we assumed that two ^{2}H were transferred per glucose molecule corresponding to one ^{2}H per acetyl-CoA derived from glucose.

2.6. Statistics

All results are presented as mean ± standard error and comparisons were made by an unpaired two-tailed Student's *t*-test performed with Microsoft Excel.

3. RESULTS

Mice that were provided with the mix of [U-$^{2}H_{7}$]- and [U-$^{13}C_{6}$]glucose yielded liver triglycerides that were enriched in both ^{13}C and ^{2}H (Table 2). Both ^{2}H and ^{13}C NMR spectra featured composite signals of the inner fatty acid methylenes and well-resolved resonances representing both ends of the fatty acid chain (Figure 6, Figure 7A). Enrichment from [U-$^{13}C_{6}$]glucose was relatively uniform between terminal and proximal carbons indicating that DNL was the main route for incorporation of glucose carbons into fatty acids with elongation playing a relatively insignificant role [3]. In comparison, enrichment of fatty acid sites from [U-$^{2}H_{7}$]glucose was highly heterogeneous, as seen by the very different intensities of positions 2 and 3 and the terminal methyl resonances (Figure 7A) and the excess ^{2}H enrichments estimated from these signals (Table 2). Normalizing the fatty acid enrichment from [U-$^{2}H_{7}$]glucose to that of [U-$^{13}C_{6}$]glucose provides a measure of the fractional retention of the [U-$^{2}H_{7}$]glucose ^{2}H atoms in a given position (Table 3). These data revealed that for those fatty acids that were synthesized from exogenous glucose, far more ^{2}H was transferred into the position 3 hydrogens compared with either position 2 or the terminal methyl hydrogens. This indicates a greater exchange of ^{2}H and water hydrogens during the conversion of [U-$^{2}H_{7}$]glucose to acetyl-CoA and malonyl-CoA compared with hydrogen transfer via pentose phosphate pathway (PPP) oxidation and NADPH. Only one of the fatty acid position 2 hydrogens is derived from malonyl-CoA, the other originates from body water. Therefore, based on the observed fatty acid position 2 $^{2}H/^{13}C$ enrichment ratio of 6%, we can infer that the $^{2}H/^{13}C$ enrichment ratio of the malonyl-CoA precursor was 12%. This is similar to the 14% estimated for the initial acetyl-CoA pool recruited by fatty acyl-CoA synthase (FAS).

[3] If elongation had been a significant route for [U-$^{13}C_{6}$]glucose incorporation, enrichment of the proximal fatty acid carbons would be significantly higher than that of the terminal carbons.

Table 2: *Fatty acid ^{13}C and ^{2}H enrichments from mice provided with glucose enriched with [U-$^{13}C_6$]- and [U-$^{2}H_7$]glucose and [U-$^{13}C_6$]- and [3-^{2}H]glucose.*

Experiment	***Isotope***	**Fatty acid Positional enrichment**		
		Methyl	*Position 2*	*Position 3*
20% [U-$^{13}C_6$]glucose + 20% [U-$^{2}H_7$]glucose (n=11)	^{13}C	0.99 ± 0.06	1.04 ± 0.07#	0.99 ± 0.06*
	^{2}H	0.23 ± 0.02	0.09 ± 0.01	0.49 ± 0.05
16% [U-$^{13}C_6$]glucose + 16% [3-^{2}H]glucose (n=5)	^{13}C	0.77 ± 0.02	0.83 ± 0.03	0.77 ± 0.02
	^{2}H	0.01 ± 0.01	n.d.	0.17 ± 0.02

Fatty acid ^{13}C and ^{2}H enrichments from a group of eleven mice provided with glucose enriched to 20% with [U-$^{13}C_6$]- and [U-$^{2}H_7$]glucose and a second group of five mice provided with glucose enriched to 16% with [U-$^{13}C_6$]- and [3-^{2}H]glucose.

n.d., not detected (signal-to-noise ratio <3:1).

^{13}C-excess enrichment of fatty acid position 1 carboxyl carbons was assumed to be equivalent to that of position 2.

* ^{13}C-excess enrichment of fatty acid position 3 was assumed to be equivalent to that of the methyl carbon.

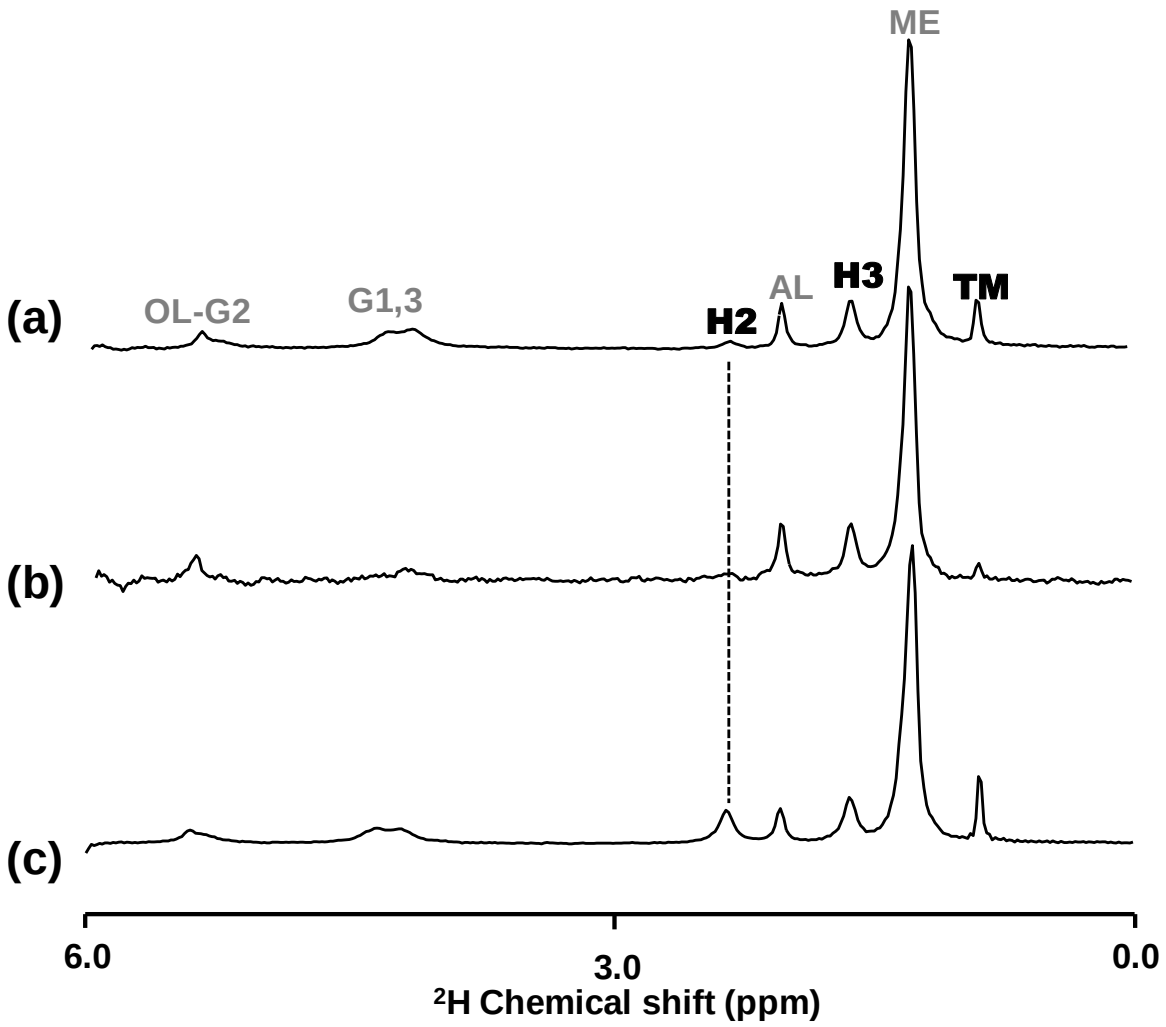

Figure 7: A: *A representative ^{2}H NMR spectrum of purified liver triglyceride acquired from a mouse provided with glucose enriched with equimolar amounts of [U-$^{2}H_{7}$]glucose and [U-$^{13}C_{6}$]glucose.* ***B:*** *A ^{2}H NMR spectrum of triglyceride acquired from a mouse provided with glucose enriched with equimolar amounts of [3-^{2}H]glucose and [U-$^{13}C_{6}$]glucose.* ***C****: A ^{2}H NMR spectrum of triglyceride acquired from a mouse provided with $^{2}H_{2}O$ and [U-$^{13}C_{6}$]glucose. For the spectra, the signals corresponding to ^{2}H in the fatty acid terminal methyl (**TM**) as well as in fatty acid position 2 (**H2**) and position 3 (**H3**) are indicated in bold. Also indicated are signals from ^{2}H in fatty acid olefinic sites and glyceryl position 2 (OL-G2), ^{2}H from glycerol* sn*1,3 positions (G1,3), ^{2}H bound to the allylic carbon of monounsaturated fatty acids (AL), and ^{2}H bound to the inner methylene carbons (ME).*

We performed an additional a set of studies where [U-$^{13}C_6$]glucose was accompanied by [3-^{2}H]glucose, where incorporation of ^{2}H into fatty acids from this precursor occurs exclusively via NADPH. Taking into account the lower $^{2}H/^{13}C$ precursor enrichment (16% versus 20% for the [U-$^{2}H_7$]glucose/[U-$^{13}C_6$]glucose experiments), the fatty acid ^{13}C enrichment distributions were consistent with those of the [U-$^{2}H_7$]glucose/[U-$^{13}C_6$]glucose study. This indicates that for both studies, exogenous glucose had been utilized to the same extent for DNL. Figure 7B shows a representative ^{2}H NMR spectrum of liver triglyceride from a mouse provided with the [3-^{2}H]glucose/[U-$^{13}C_6$]glucose mixture. In accordance with the predicted metabolic fate of the ^{2}H label, fatty acids were enriched in position 3, while enrichment of position 2 was not detectable and the terminal methyl had a vestigial ^{2}H signal. Given the substantial transfer of glucose hydrogens into the position 3 of fatty acid relative to position 2, it might be expected that for mice administered with $^{2}H_2O$, enrichment of fatty acid position 3 would also be less than that of position 2. However, as shown by Figure 7C, the intensities of position 2 and 3 signals were similar, and there was no significant difference between the ^{2}H enrichments quantified for each site (1.79 ± 0.19% and 1.81 ± 0.19% for positions 2 and 3, respectively).

Table 3: *$^{2}H/^{13}C$ enrichment ratios for fatty acid position 2, position 3, and terminal methyl*

	Fatty acid positional $^{2}H/^{13}C$ enrichment ratios		
	Position 2	*Position 3*	*Methyl*
[U-$^{2}H_7$]/[U-$^{13}C_6$]glucose	0.06 ± 0.01*	0.46 ± 0.04**	0.14 ± 0.01
[3-^{2}H]/[U-$^{13}C_6$]glucose	Not determined	0.22 ± 0.02	Not determined

$^{13}C/^{2}H$ enrichment ratios for fatty acid positions 2 and 3 and methyls estimated from the group of eleven mice provided with [U-$^{2}H_7$]- and [U-$^{13}C_6$]glucose and that of fatty position 3 from the group of five mice provided with [3-^{2}H]- and [U-$^{13}C_6$]glucose.

*$p < 0.005$ compared to methyl.

**$p < 10^{-5}$ compared to methyl.

4. DISCUSSION

Since the pioneering studies of Beylot and coworkers (F. Diraison et al., 1996, 1997), $^{2}H_{2}O$ has been extensively used as a tracer for quantifying fractional DNL rates. From the beginning, it was understood that ^{2}H incorporation into fatty acids might be limited by *a*) incomplete exchange of body water and metabolite hydrogens and/or *b*) discrimination against the incorporation of ^{2}H into these precursors or intermediates of FAS due to kinetic isotope effects. In the present study, by quantifying fatty acid positional enrichments corresponding to the transfer of ^{2}H from [U-$^{2}H_{7}$]glucose via acetyl-CoA, malonyl-CoA, and NADPH, the extent of glucose hydrogen exchange during its conversion to fatty acids via each intermediate was evaluated.

4.1. Exchange of glucose ^{2}H during the formation of acetyl-CoA and malonyl-CoA

Glycolysis of [U-$^{2}H_{7}$]glucose yields one pyruvate with a single ^{2}H and a second pyruvate with two ^{2}H in the methyl position. Therefore, there are 1.5 equivalents of ^{2}H for each pyruvate. If this pyruvate is recruited for lipogenesis via acetyl-CoA, citrate, and cytosolic acetyl-CoA, one of the methyl hydrogens undergoes obligatory exchange with water, resulting in one equivalent of ^{2}H per cytosolic acetyl-CoA. While pyruvate methyl hydrogens can undergo extensive exchange with water via alanine aminotransferase (WALTER et al., 1975), there is evidence that not all intracellular pyruvate participates in this process. For example, in perfused rat hearts supplied with [3-$^{2}H_{3}$,1-^{13}C]pyruvate, Funk et al. observed a significantly higher retention of ^{2}H in lactate compared with alanine at 3 and 6 min of perfusion (Funk et al., 2019). Moreover, pyruvate molecules with ^{2}H in the methyl position may be metabolized at different rates to those without ^{2}H. In the same setting, [U-$^{2}H_{7}$, U-$^{13}C_{6}$]glucose was less efficiently incorporated

into the Krebs cycle compared with [U-$^{13}C_6$]glucose (Funk et al., 2017), suggesting that the presence of ^2H in the methyl hydrogens of acetyl-CoA was attenuating its conversion to citrate via citrate synthase. Thus, while there is an efficient exchange mechanism for incorporating ^2H from water into the methyl sites of pyruvate, there may be intracellular pyruvate pools that do not experience this exchange. Moreover, pyruvate molecules that do become enriched with ^2H may be transformed into citrate and cytosolic acetyl-CoA at slower rates in comparison to their non-deuterated counterparts. In our study, we found that for the initial FAS-bound acetyl-CoA that was derived from exogenous [U-$^2H_7$]glucose, 86% of ^2H had been exchanged for ^1H. From analysis of cytosolic acetyl-CoA ^2H enrichment from ^2H_2O via chemical biopsy, Duarte et al. concluded that exchange between the methyl hydrogens of this precursor and body water was ~100% (Duarte et al., 2014). In our experimental setting, exogenous glucose contributes a minor fraction (~10%) of hepatic DNL (J. C. P. Silva et al., 2019). In the presence of ^2H_2O, it is probable that endogenous DNL sources, including acetyl-CoA derived from fructose, lactate, and microbial acetate, will be already enriched to a significant extent with ^2H prior to being recruited for DNL. For these reasons, we believe that the overall hydrogen exchange fraction of the lipogenic acetyl-CoA pool is closer to 100% than to 86%. Thus, in our experimental setting, animals provided with ^2H_2O would be expected to have near-equivalent ^2H enrichments of acetyl-CoA methyl hydrogens and body water. For [U-$^2H_7$]glucose that was metabolized to fatty acid via malonyl-CoA, exchange of ^2H with ^1H was similar to that observed for acetyl-CoA. Therefore, enrichment of malonyl-CoA from ^2H_2O would also be expected to approach that of body water.

4.2. ^{2}H transfer from glucose to fatty acids via NADPH

^{2}H that were metabolized from glucose to fatty acids via NADPH were more highly retained in comparison to those transferred via acetyl-CoA and malonyl-CoA. During PPP oxidation, the first and third hydrogens of glucose are transferred to NADPH, hence [U-$^{2}H_{7}$]glucose contributes two ^{2}H, while [3-^{2}H]glucose only contributes one. In accordance, transfer of ^{2}H to fatty acid position 3 from [U-$^{2}H_{7}$]glucose was found to be approximately twice that from [3-^{2}H]glucose (46% vs. 22%, see Table 3). This indicates that under our study conditions, there was no additional loss of ^{2}H from glucose position 1 compared with position 3, for example, by exchange of glucose-6-phosphate with fructose-6-phosphate and mannose-6-phosphate (Chandramouli et al., 1999). Direct studies of intracellular NADPH enrichment from $^{2}H_{2}O$ report a greater degree of exchange between the reducing hydrogen and body water than might be expected based on our observations (Z. Zhang et al., 2017). One explanation for this is that the PPP is not the sole source of intracellular NADPH, as illustrated by Figure 8. In mitochondria, NADPH can be generated from NADH by nicotinamide nucleotide transhydrogenase. In mitochondria as well as cytosol, NADPH can also be generated via $NADP^{+}$-malic enzyme and $NADP^{+}$-isocitrate dehydrogenase. In all of these cases, the likelihood that the hydrogen that was transferred to $NADP^{+}$ had previously exchanged with body water is high. For NADPH formed via the $NADP^{+}$-malic enzyme, the reducing hydrogen originates from hydrogen 2 of malate, which in turn originated from water during the hydration of fumarate. If the malate is metabolized via the Krebs cycle to citrate and isocitrate, this hydrogen is transferred to NADPH via $NADP^{+}$-isocitrate dehydrogenase. The bulk of mitochondrial NADH hydrogens are also derived from Krebs cycle intermediates, such as malate, whose hydrogens are highly exchanged with those of water. In addition, NADPH and water hydrogens may also be exchanged via $NADP^{+}$-linked redox enzymes (J. Fan et al., 2014;

Z. Zhang et al., 2017). Another consideration, and an important caveat of our assessment of hydrogen exchange at the level of NADPH, is that fatty acid ^{2}H enrichment from [U-$^{2}H_{7}$]glucose via this pathway was quantified relative to [U-$^{13}C_{6}$]glucose conversion to fatty acid via malonyl-CoA. If the rate of glucose oxidation by the PPP was different to that of its conversion to fatty acid via malonyl-CoA, then the fractional rate of $^{2}H/^{1}H$ exchange at the level of NADPH would also differ from the $^{2}H/^{13}C$ ratio of fatty acid position 3[4]. However, this does not alter the conclusion that the relative amounts of ^{2}H transferred from glucose to fatty acid via NADPH were significantly higher than those transferred via acetyl-CoA and malonyl-CoA intermediates.

[4] For example, if the rate of glucose oxidation via PPP was twice the rate of glucose conversion to fatty acid via malonyl-CoA, then NADPH ^{2}H enrichment would be one-half of the fatty acid position 3 $^{2}H/^{13}C$ ratio (i.e 23% compared to 46%).

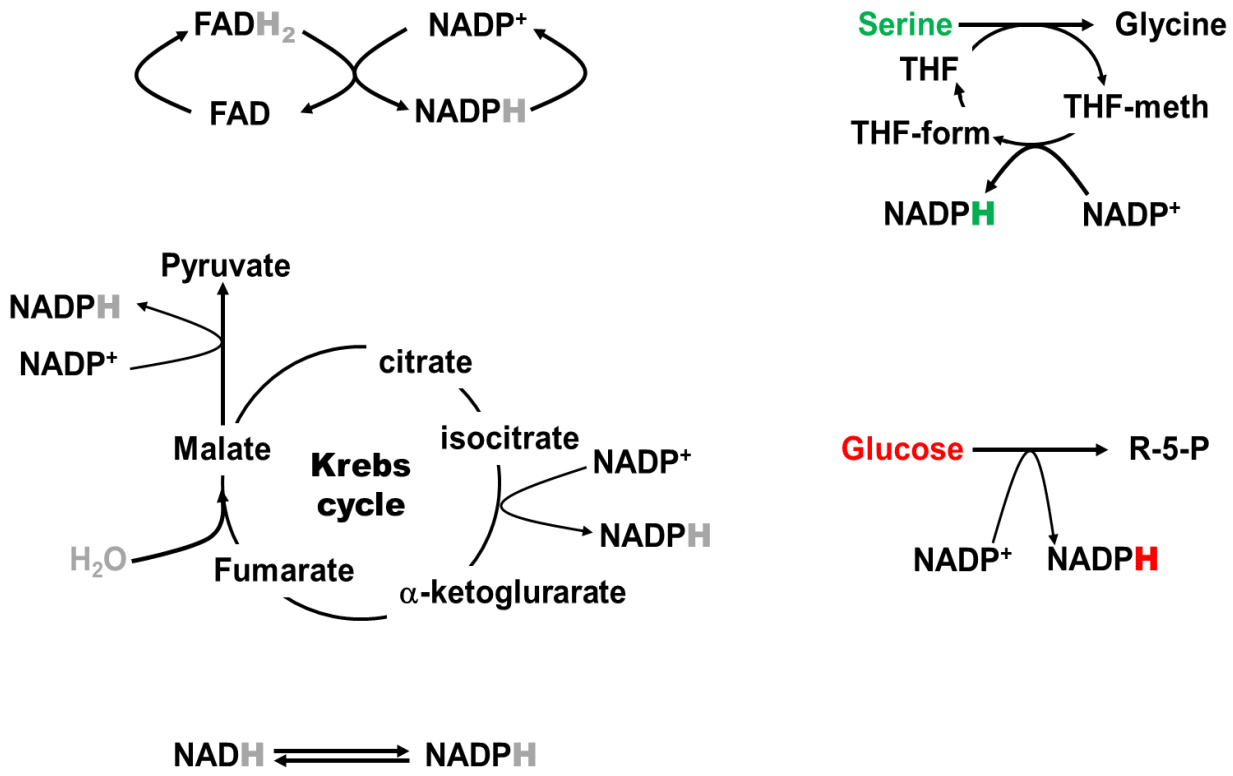

Figure 8: *Schematic of intracellular NADPH hydrogen sources. On the left-hand side are the pathways that are involved in the transfer of water hydrogen to NADPH (depicted in gray). These include cycling between NADPH and other redox cofactors such as FAD whose hydrogens are exchanged with those of water; generation of NADPH from malate and isocitrate via NADP$^+$-malic enzyme and NADP$^+$-isocitrate dehydrogenase, respectively; and exchange of NADH and NADPH via transhydrogenase. On the right-hand side are the two principal pathways that transfer hydrogens to NADPH from nutrient substrates, namely, glucose and serine. Abbreviations: FAD/FADH$_2$, Flavin adenine dinucleotide; NADH/NADPH, Non-protonated nicotinamide adenine dinucleotide phosphate*

Our observation of extensive ^{2}H transfer from glucose to fatty acid synthesis via NADPH suggests that this process is tightly coupled to the extent that NADPH generated by the PPP does not fully mix with other intracellular NADPH pools. This apparent compartmentation of

PPP and lipogenic NADPH metabolism has also been reported in other laboratories using different isotopic approaches and models. In mice with fatty liver, hepatic PPP fluxes measured by a ^{13}C-isotopomer approach were found to be highly correlated with lipogenesis but were not associated with antioxidant activity (Jin et al., 2018). This suggests that in the postprandial liver, NADPH derived from the PPP is prioritized for DNL rather than being utilized for antioxidant defense, such as the reduction of oxidized glutathione. In the H1299 tumor cell line supplied with various ^{2}H-enriched substrates, Lewis et al. also demonstrated a substantial transfer of ^{2}H label from [3-^{2}H]glucose to fatty acids, while fatty acid ^{2}H enrichment via NADPH from [2,3,3-$^{2}H_3$]serine was much more limited (C. A. Lewis et al., 2014).

4.3. Fatty acid enrichment from $^{2}H_2O$

We observed extensive exchange of exogenous glucose hydrogens with water during its conversion to fatty acids via both acetyl- and malonyl-CoA. In contrast, glucose hydrogens that were transferred to fatty acids via NADPH experienced more limited exchange. Based on these observations, it would be anticipated that enrichment of the fatty acid position 2 hydrogens from $^{2}H_2O$ (derived from water and malonyl-CoA) would be equivalent to those of body water, while those of position 3 (derived via NADPH) would be significantly less enriched. Instead, we observed that positions 2 and 3 were enriched to the same level. As mentioned previously, exogenous glucose is a minor contributor of acetyl-CoA to DNL in our experimental setting (although it may have a more substantial contribution to the NADPH equivalents for DNL). Moreover, following $^{2}H_2O$ administration under both fed and fasted conditions, hepatic glucose-6-phosphate becomes highly enriched with ^{2}H in all positions due to extensive cycling between glucose-6-phosphate and gluconeogenic precursors (Ii. R. Bederman et al., 2009; Teresa C. Delgado et al., 2013). Under these conditions, NADPH derived from PPP oxidation

of glucose-6-phosphate will also become highly enriched with ^{2}H and this will be transferred to the respective fatty acid positions.

4.4. Implications for estimating the number of deuterium atoms incorporated per fatty acid

Under our study conditions, the number of deuterium atoms incorporated per fatty acid molecule (N) appears to approach the theoretical value (i.e., 31 for palmitate). Therefore, in this instance, no correction needs to be applied to the observed fatty acid ^{2}H enrichment from $^{2}H_2O$. This differs from previous studies in rats, where N was estimated to be 21 and 22 out of 31 (68% and 71% of the theoretical value) by mass isotopomer distribution analysis for plasma and liver triglyceride palmitate, respectively (F. Diraison et al., 1996; W. N. P. Lee, Bassilian, Ajie, et al., 1994) To our knowledge, N has not been determined in the mouse by mass isotopomer distribution analysis, but given its smaller size and higher basal metabolic rate, it might be expected to be higher compared with the rat. The mice in our study also ingested significant amounts of fructose, a sugar that is rapidly metabolized via triose phosphate intermediates to glucose-6-phosphate, lactate, and acetyl-CoA, thereby further promoting ^{2}H enrichment of these metabolites from $^{2}H_2O$. It is possible that for mice fed a standard chow diet featuring maltose as the main carbohydrate component, whose digestion yields unlabeled glucose, there could be less complete ^{2}H incorporation from $^{2}H_2O$ into fatty acids, particularly via NADPH. In cultured cells, N for palmitate was estimated to be 17 (W. N. P. Lee, Bassilian, Guo, et al., 1994). This is 55% of the theoretical value and is also substantially lower than that determined for in vivo rat studies. Our data for mice indicate that if glucose was the sole source of DNL in vivo, the value of N would be 24 based on ^{2}H transfer from exogenous [U-$^{2}H_7$]glucose to fatty acids via acetyl-CoA, malonyl-CoA, and

NADPH[5]. Because there is more opportunity for the loss of glucose ^{2}H by Cori cycling and other inter-organ transfer of glucose metabolites in vivo compared with in vitro, we anticipate that there would be a greater degree of transfer of ^{2}H from glucose to fatty acids in vitro, corresponding to a lower N value.

In conclusion, N may vary considerably according to the type of organism as well as the substrates that were utilized for DNL. Our study indicates that transfer of hydrogen from unlabelled glucose to fatty acids via NADPH is an important factor in the nonstoichiometric incorporation of ^{2}H into fatty acids during DNL. For the measurement of DNL with $^{2}H_2O$, the ratio of ^{2}H enrichment in fatty acid positions 2 and 3 as measured by ^{2}H NMR provides a convenient internal check for assessing the extent to which this might have occurred.

[5] For palmitate, this is calculated as 31 – [(3× 0.14) + (14 × 0.46) + (7 × 0.06)].

CHAPTER THREE

ESTIMATING PENTOSE PHOSPHATE PATHWAY ACTIVITY FROM THE ANALYSIS OF HEPATIC GLYCOGEN ^{13}C-ISOTOPOMERS DERIVED FROM [U-^{13}C]FRUCTOSE AND [U-^{13}C]GLUCOSE

1. INTRODUCTION

When carbohydrate intake surpasses the capacity for oxidation and storage, the additional energy is converted to endogenous triglycerides within the liver by passing through the hepatic de novo lipogenesis process. Though this process may benefit short-term glucose homeostasis, it may have the adverse effect of elevating triglyceride accumulation and thus contributing to hepatic steatosis, oxidative stress and liver injury. In the process of the development of oxidative stress and fat accumulation, nicotinamide adenine dinucleotide phosphate (NADPH) plays a vital role in both reductive biosynthesis and protection from oxidative damage (Jin et al., 2018).The pentose phosphate pathway (PPP) plays a critical role in intermediary metabolism by providing the reduced form of nicotinamide adenine dinucleotide phosphate (NADPH) for both biosynthetic activities and regeneration of reduced glutathione as well as ribose-5-phosphate for nucleotide biosynthesis. In the liver, there is high interest in the role of the PPP in the pathogenesis of diseases, such as non-alcoholic fatty liver disease (NAFLD), where PPP activity may be linked to elevated rates of *de novo* lipogenesis (Jin et al., 2018), and hepatocellular carcinoma, where among other things, *de novo* synthesis of nucleotides is upregulated (Kowalik et al., 2017).

Recently, a stable-isotope tracer method for quantifying hepatic PPP activity by analysis of plasma glucose ^{13}C-isotopomers generated from [U-^{13}C]glycerol was reported (Jin et al., 2014, 2016, 2018). The ^{13}C-labeling arrays deliver an important source of information about the

multiple pathways including triglyceride synthesis, gluconeogenesis, glycogenesis, the PPP, and tricarboxylic acid (TCA) cycle activity (Jin et al., 2016). The ^{13}C-label reaches glucose-6-Phosphate via gluconeogenesis and the glucose ^{13}C-isotopomer distribution reports the proportion of ^{13}C-enriched glucose-6-Phosphate that was directly converted to glucose, *versus* the fraction that had cycled through the PPP beforehand (See Figure 9). Previously, in most cases, PPP fluxes had been evaluated with a labeled glucose precursor by analyzing the label distribution in a downstream glycolytic product, such as lactate (Delgada et al., 2004; M. H. Lee et al., 2019; Ross et al., 1994). In the liver, glucose-6-Phosphate enrichment from both glucose and gluconeogenic ^{13}C-tracers is transferred to glycogen via the so-called direct and indirect pathways (Newgard et al., 1983). Therefore, we applied the hexose ^{13}C-isotopomer analysis developed by Jin et al. (Jin et al., 2014, 2016, 2018) to liver glycogen to determine the extent of PPP metabolism of exogenous [U-^{13}C]glucose and [U-^{13}C]fructose destined for hepatic glycogen synthesis (Figure 9).

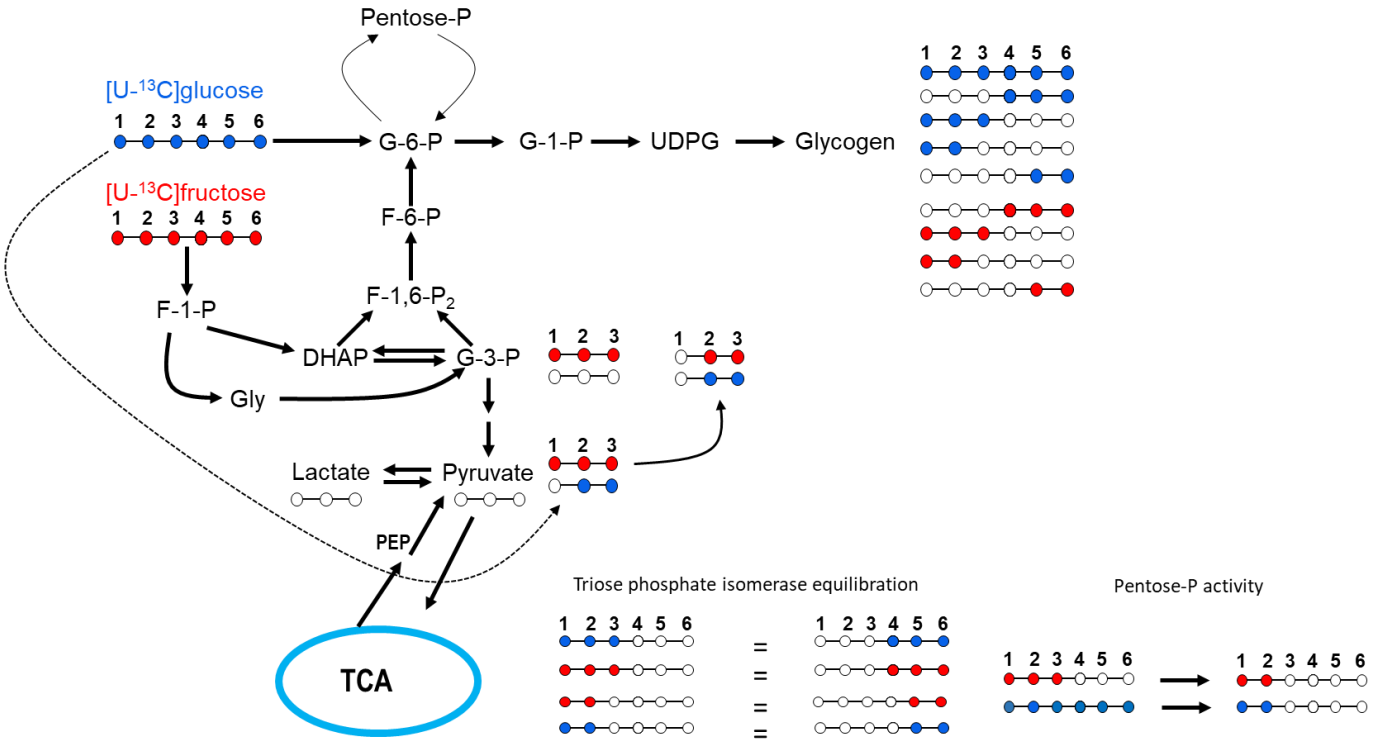

Figure 9: *Schematic of glycogen isotopomer formation from exogenous [U-^{13}C]glucose and [U-^{13}C]fructose, including TCA cycle and Pentose-P effects. PPP converts both the [1,2,3-$^{13}C_3$]glucose-6-P from fructose and [U-^{13}C]glucose-6-P from [U-^{13}C]glucose to [1,2-$^{13}C_2$]glucose-6-P.*

2. METHODS

2.1. Materials:

[U-^{13}C]fructose at 99% enrichment was obtained from Omicron Biochemicals Inc., IN, USA and [U-^{13}C]glucose at 99% enrichment was manufactured by Cambridge Isotopes Limited, Cambridge, MA, USA and purchased through Tracertec, Madrid, Spain.

2.2. Animal Studies

Animal studies were approved by the University of Coimbra Ethics Committee on Animal Studies (ORBEA) and the Portuguese National Authority for Animal Health (DGAV), approval code 0421/000/000/2013. Adult male C57BL/6 mice were obtained from Charles River Labs, Barcelona, Spain, and housed at the UC Biotech Bioterium. They were maintained in a well-ventilated environment, and a 12 hour light/12 hour dark cycle. Upon delivery to the Bioterium, mice were provided a two week interval for acclimation, with free access to water and standard chow, comprising of 60% mixed carbohydrate, 16% protein and 3% lipid. After this period, the drinking water was supplemented with a 55/45 mixture of fructose and glucose. This mixture was present at a concentration of 30% w/v and was provided for a period of 18 weeks. On the ultimate evening, the fructose/glucose mixture was replaced with a mixture, where the fructose was enriched to 20% with [U-^{13}C]fructose for six of the mice, with the remaining six provided with a mixture, where the glucose was enriched to 20% with [U-^{13}C]glucose. As part of a separate study on triglyceride and glycogen synthesis sources, the mice also received 99.8% deuterated water ($^{2}H_2O$) with 0.9% NaCl as an intraperitoneal loading dose (4 g/100 g body weight). At the end of this dark cycle, mice were deeply

anesthetized with ketamine/xylazine and sacrificed by cardiac puncture. Livers were freeze-clamped and stored at -80ºC until further analysis.

2.3. Glycogen extraction and monoacetone glucose synthesis

Samples were prepared as described previously by Rito et al. (Rito et al., 2018). Briefly, glycogen was extracted from frozen liver powder after basic digestion with 30% KOH (2 ml/g of liver) at 70°C for one hour. The mixture was treated with 6% Na_2SO_4 (1 ml/g of liver) and glycogen precipitated with ethanol (7 ml/g of liver). After centrifugation, the solid residue was dried and resuspended in acetate buffer (0.05 M, pH = 4.5). Aqueous solution containing 20 U of amyloglucosidase from *Aspergillus niger* (Glucose-free preparation, Sigma-Aldrich, Germany) was added and incubated overnight at 55ºC. The supernatant was lyophilized and mixed with 5 ml ^{2}H-enriched acetone prepared as described (J. Jones et al., 2006) and 4% sulfuric acid enriched to 2% with $^2H_2SO_4$ (v/v). The mixture was stirred overnight at room temperature. The reaction was quenched with water (5 ml, enriched to 2% with ^2H_2O), the pH adjusted with HCl (pH = 2.0) and the mixture incubated at 40ºC for 5 hours. The solution pH was adjusted to 8 with $NaHCO_3$ and the samples evaporated to dryness. Monoacetone glucose (MAG) in the residue was extracted with boiling ethyl acetate. Ethyl acetate was evaporated, the residue dissolved in H_2O and purified by solid phase Discovery® DSC-18 3 mL/500 mg disposable columns (Sigma-Aldrich) as previously described (Rito et al., 2018). MAG samples were dissolved in 0.2 ml 99.9% ^2H_2O for ^{13}C NMR analysis.

2.4. NMR analysis:

Proton-decoupled ^{13}C NMR spectra were obtained with a Varian VNMRS 600 MHz NMR (Agilent) spectrometer equipped with a 3-mm broadband probe. ^{13}C NMR spectra were acquired at 25 ºC using a 60º pulse, 30.5 kHz spectral width, and 4.1 seconds of recycling time (4.0 seconds of acquisition time and 0.1 second pulse delay). The number of acquisitions ranged from 2,000 to 12,000. The spectra were processed with 0.2 Hz line-broadening before Fourier transformation. Spectra were analyzed using NUTS PC-based NMR spectral analysis software (Acorn NMR Inc., USA).

2.5. Quantification of PPP fluxes

PPP fluxes were quantified from the analysis of glycogen carbon 2 and carbon 5 ^{13}C-isotopomer multiplets based on the method of Jin et al. for [U-^{13}C]glycerol (Jin et al., 2014, 2016). Translating this method to [U-^{13}C]fructose is straightforward since this sugar is metabolized to the same triose-P intermediates as glycerol (Figure 11). In the case of [U-^{13}C]glucose, although the initial pentose phosphate intermediates are uniformly enriched following the oxidative removal of carbon 1, the subsequent transaldolase/transketolase exchange pathways generate [1,2-$^{13}C_2$]fructose-6-P that is stoichiometric with the oxidative PPP step (Figure 10). Thus, quantification of the resulting [1,2-$^{13}C_2$]glycogen isotopomer from the ^{13}C NMR doublet 12 signal component ($D12_{PPP}$) with correction for contributions from non-PPP activity (Jin et al., 2014, 2016, 2018), can yield fractional PPP rates relative to the conversion of [U-^{13}C]glucose to glycogen.

$$D12_{PPP} = D12_{total} - D12_{KC} \quad (1)$$

Where $D12_{total}$ is the observed doublet fraction relative to all other carbon 2 signals and $D12_{KC}$ is the doublet contribution from Krebs cycle sources. $D12_{KC}$ was estimated as follows (Jin et al., 2014, 2016, 2018):

$$D12_{KC} = D23 \times D56/D45 \quad (2)$$

Where D23 is the area of the 2,3-^{13}C doublet relative to the total carbon 2 signal and D56 and D45 are the areas of the 5,6-^{13}C and 4,5-^{13}C doublet signals relative to the total carbon 5 signal, respectively.

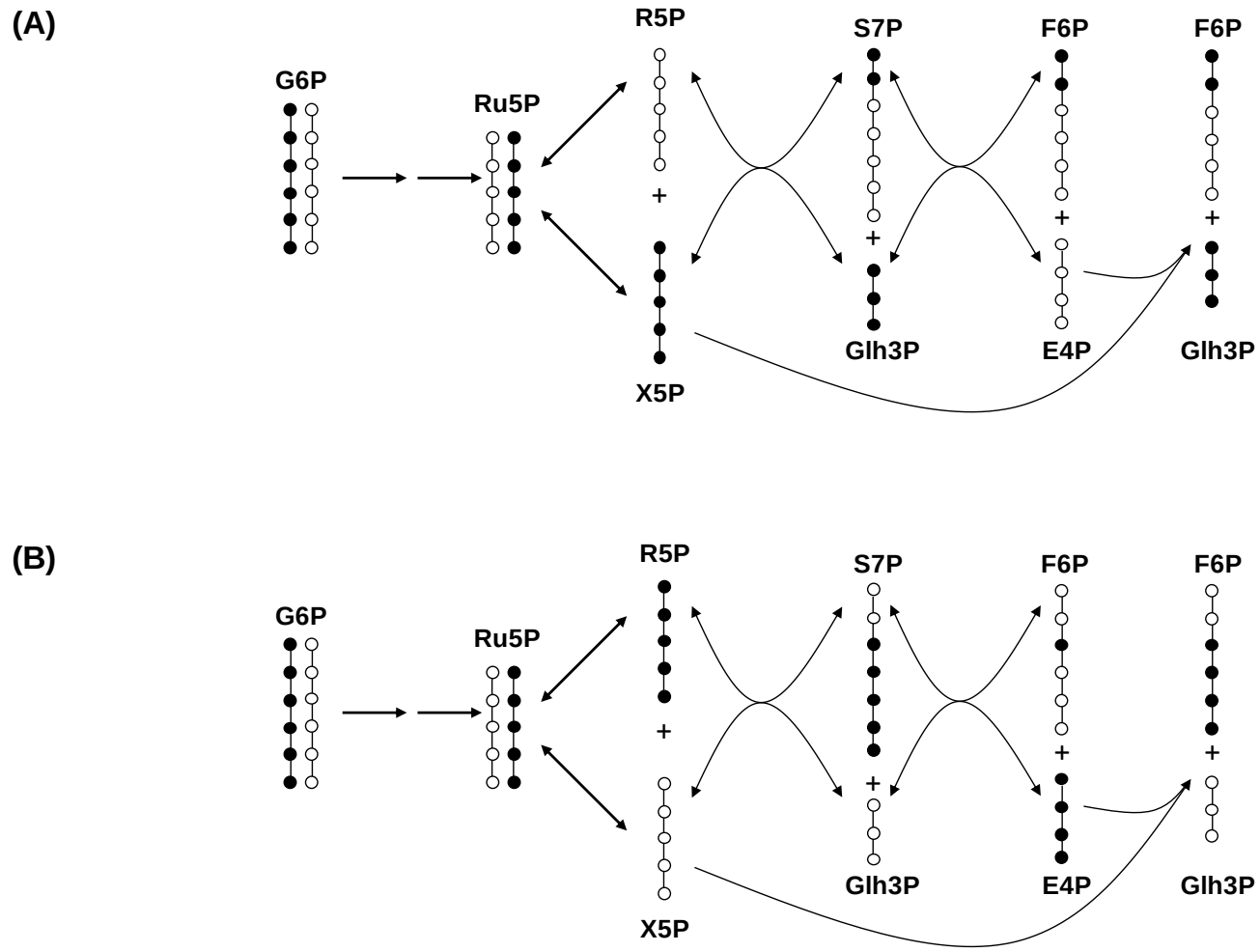

Figure 10: *Schematic of [U-13C]glucose-6-P conversion to fructose-6-P through the PPP with the carbon skeleton passing via xylulose-5-phosphate* ***(A)*** *or ribose-5-phosphate* ***(B)****. It is assumed that there is sufficient dilution of* ^{13}C *by* ^{12}C *such that the probability of two [U-*^{13}C*]pentose-P precursors interacting with each other is negligible*

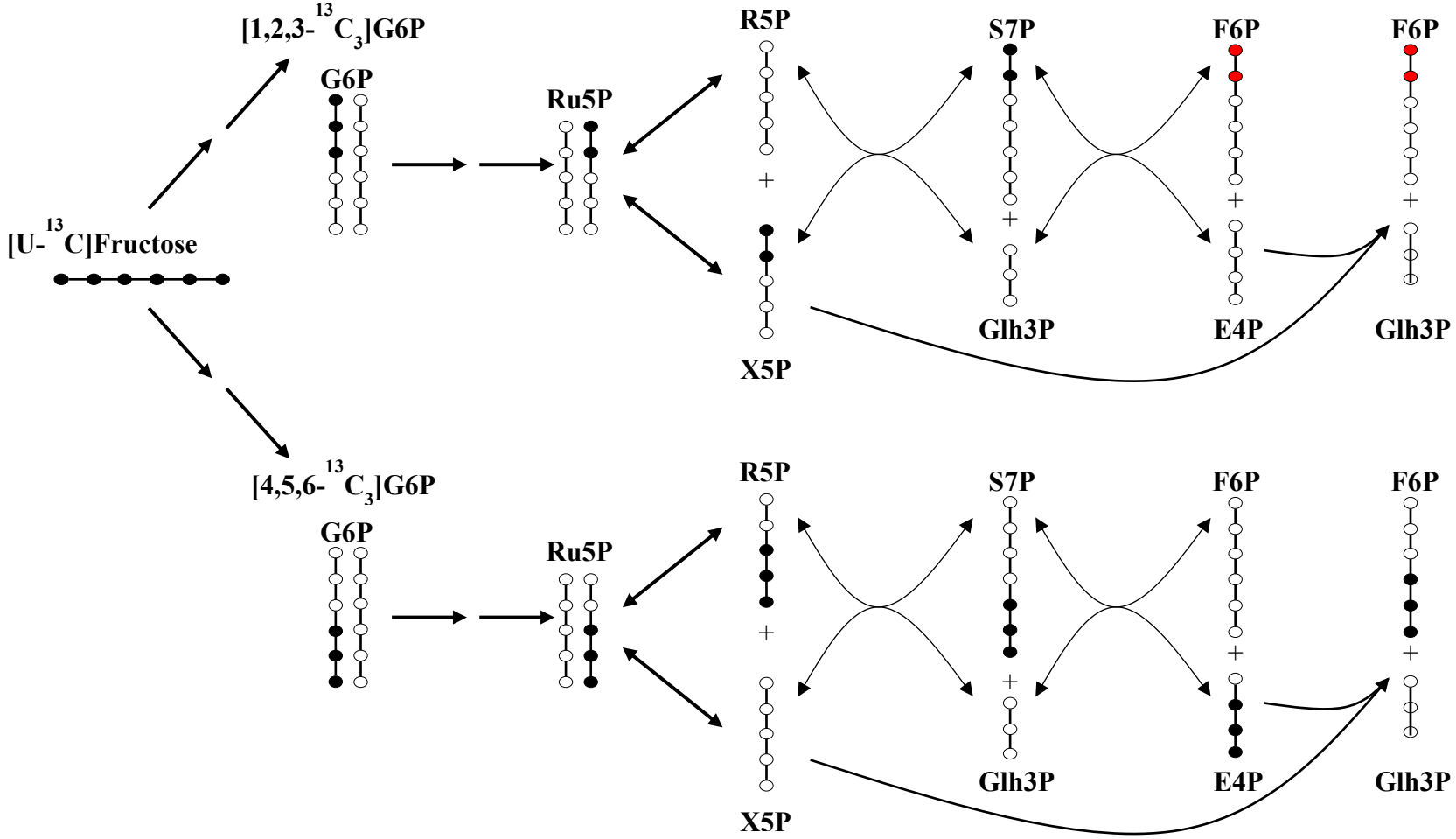

Figure 11: *Schematic of glycogen enrichment from exogenous [U-13C]fructose, via the PPP. In the presence of unlabeled glucose-6-phosphate (G6P), it initially forms a mixture of [1,2,3-$^{13}C_3$]- and [4,5,6-$^{13}C_3$]G6P. Metabolism through the PPP leads to the formation of [1,2-$^{13}C_2$]fructose-6-P (in red) which becomes [1,2-$^{13}C_2$]glycogen . Smaller amounts of [1,2-$^{13}C_2$]fructose-6-P can also be formed if the ^{13}C-label from fructose is metabolized through glycolysis and the Krebs cycle and back into G6P (not shown).*

The ^{13}C-fractional enrichment of the $D12_{PPP}$ component was estimated as follows:

$D12_{PPP}$ fractional ^{13}C-enrichment (%) = $D12_{PPP}$ signal area/carbon 2 singlet area × 1.11 (3)

The fraction of [U-^{13}C]glucose utilized by the pentose phosphate pathway relative to that entering the direct pathway was estimated from the ratios of glycogen $D12_{PPP}$ and [U-^{13}C]glycogen fractional ^{13}C-enrichments as follows:

[U-^{13}C]glucose PPP fraction = 100 × $D12_{PPP}$ /[U-^{13}C]glycogen fractional ^{13}C-enrichment (4)

Where the [U-^{13}C]glucose fractional ^{13}C-enrichment was calculated from the MAG carbon 1 multiplet as previously described (Perdigoto et al., 2003; Rito et al., 2018).

The fraction of [U-^{13}C]fructose utilized by the pentose phosphate pathway relative to that entering glycogen via the indirect pathway was estimated from the ratios of glycogen $D12_{PPP}$ and [4,5,6-^{13}C]glycogen fractional ^{13}C-enrichments as follows:

[U-^{13}C]fructose PPP fraction = $D12_{PPP}$/[4,5,6-^{13}C]glycogen fractional ^{13}C-enrichment (5)

The [4,5,6-^{13}C]glycogen fractional ^{13}C-enrichment was measured from the ratio of the carbon 5 quartet and singlet as follows:

[4,5,6-^{13}C]glycogen fractional ^{13}C-enrichment (%) = carbon 5 quartet/singlet × 1.11 (6)

2.6. Statistics

All results are presented as means ± standard error and comparisons were made by an unpaired t-test (two tailed) performed using Microsoft Excel. Statistical significance was defined by *p* values of < 0.05.

3. RESULTS

The ^{13}C NMR signals of carbons 2 and 5 of MAG derived from hepatic glycogen of a mouse provided with [U-^{13}C]glucose are shown in Figure 12. The multiplet (M) component of the carbon 2 signal represents a mixture of [U-^{13}C]glucose and [1,2,3-$^{13}C_3$]glucose isotopomers while the M component of the carbon 5 resonance represents a mixture of [U-^{13}C]glucose and [4,5,6-$^{13}C_3$]glucose isotopomers. Its complex structure reflects the presence of long-range ^{13}C-^{13}C couplings within the [U-^{13}C]glucose moiety between carbons 5 and 1, carbons 5 and 2, and carbons 5 and 3 (Perdigoto et al., 2003). Likewise, the M component of carbon 2 features long-range ^{13}C-^{13}C couplings between carbon 2 and 4, and carbons 2 and 5 (Perdigoto et al., 2003). The low intensities of the D45 and D56 components relative to M reflect the minor proportion of ^{13}C-isotopomers that were formed via the indirect pathway and Krebs cycle relative to direct pathway conversion of [U-^{13}C]glucose to glycogen. In the carbon 2 resonance, the D23 contribution, which also represents ^{13}C-Krebs cycle isotopomers, was correspondingly low in relation to the M signals. In comparison, the D12 signal was substantially stronger, indicative of PPP metabolism of the [U-^{13}C]glucose precursor.

The carbon 2 and 5 resonances of MAG obtained from a mouse provided with a mixture of unlabeled glucose and [U-^{13}C]fructose are also shown in Figure 12. Qualitatively, the main difference between these resonances and those derived from [U-^{13}C]glucose is the presence of well-resolved quartet structures for both carbons 2 and 5 reflecting the presence of discrete [1,2,3-$^{13}C_3$]- and [4,5,6-$^{13}C_3$]glycogen isotopomers. This resembles the glucose carbon 2 and carbon 5 multiplet structures observed in rats that were administered with [U-^{13}C]glycerol (Jin et al., 2014, 2016, 2018).

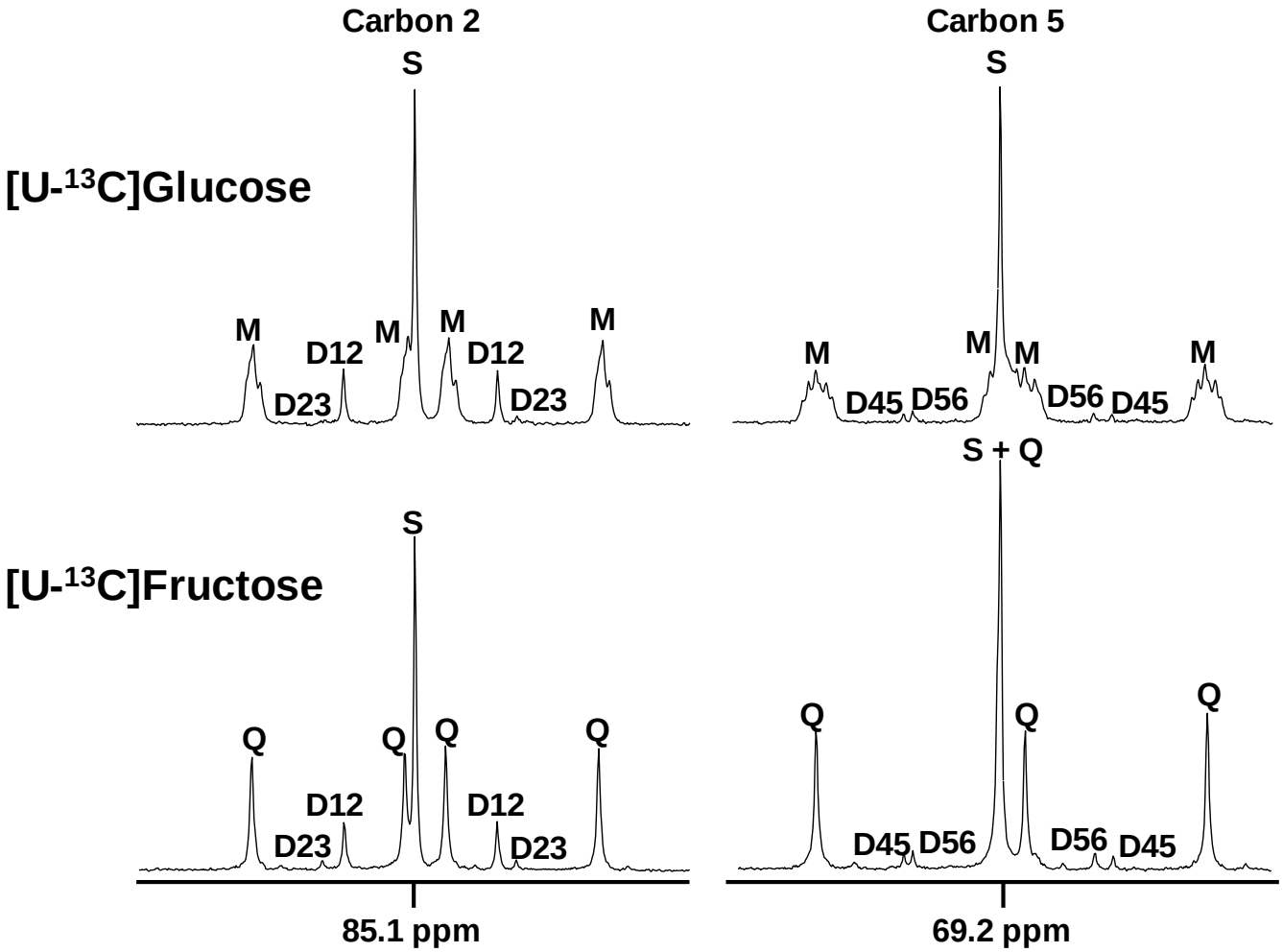

Figure 12: *Carbon 2 and carbon 5 resonances of glycogen following derivatization to MAG from a mouse administered with [U-^{13}C]glucose (top) and a mouse administered with [U-^{13}C]fructose (bottom). The multiplet components are indicated as follows:* ***S*** *= natural-abundance singlet,* ***M*** *= multiplet representing [1,2,3-$^{13}C_3$]- plus [U-^{13}C]glycogen in carbon 2 and [4,5,6-$^{13}C_3$]- plus [U-^{13}C]glycogen in carbon 5,* ***D12*** *= doublet representing [1,2-$^{13}C_2$]glycogen$_{total}$,* ***D23*** *= doublet representing [2,3-$^{13}C_2$]glycogen,* ***D45*** *= doublet representing [4,5-$^{13}C_2$]glycogen,* ***D56*** *= doublet representing [5,6-$^{13}C_2$]glycogen,* ***Q*** *= quartet representing [1,2,3-$^{13}C_3$]glycogen in carbon 2 and [4,5,6-$^{13}C_3$]glycogen in carbon 5.*

Quantitatively, direct pathway metabolism of [U-^{13}C]glucose and indirect pathway metabolism of [U-^{13}C]fructose via triose-P yielded similar enrichments of [U-^{13}C]glycogen and [4,5,6-$^{13}C_3$]glycogen isotopomers (see Table 4). Considering the abundance of these primary isotopomers plus pentose phosphate pathway contributions ([1,2-$^{13}C_2$]glycogen$_{ppp}$), exogenous fructose and glucose contributed almost equally to hepatic glycogen synthesis with 15 ± 1% derived from fructose and 14 ± 2% from glucose. For the [U-^{13}C]fructose experiments, while the proportion of ^{13}C-isotopomers derived via the Krebs cycle was small in comparison to those derived via triose-P, it was nevertheless substantially higher compared to that from the [U-^{13}C]glucose experiments (see Table 4). Thus, the ratio of [2,3-$^{13}C_2$]/[4,5,6-$^{13}C_3$]glycogen from the [U-^{13}C]fructose study is approximately 0.036 while the ratio of [2,3-$^{13}C_2$]/[U-^{13}C]glycogen from the [U-^{13}C]glucose study is only 0.008. This resulted in substantially higher Krebs cycle contributions to the observed [1,2-$^{13}C_2$]glycogen enrichment for mice administered with [U-^{13}C]fructose compared to those given [U-^{13}C]glucose. As a result, the difference between [1,2-$^{13}C_2$]glycogen$_{total}$ and [1,2-$^{13}C_2$]glycogen$_{PPP}$ abundance was more pronounced in the [U-^{13}C]fructose compared to the [U-^{13}C]glucose studies. Finally, the ^{13}C-isotopomer data revealed that a significantly larger proportion of exogenous glucose metabolized to glycogen via the direct pathway had been recruited by the PPP in comparison to that from fructose converted glycogen via the indirect pathway (Table 4).

Table 4: *Selected liver glycogen 13C-isotopomers from mice provided with fructose/glucose mixture in their drinking water enriched with either [U-13C]fructose or [U-13C]glucose. The values represent means and standard errors of six mice for each condition.*

Glycogen ^{13}C-isotopomers from mice provided with [U-^{13}C]glucose and unlabeled fructose					
[U-^{13}C]GLY (%)	**[1,2-$^{13}C_2$]GLY$_{TOT}$ (%)**	**[2,3-$^{13}C_2$]GLY (%)**	**D56/D45**	**[1,2-$^{13}C_2$]GLY$_{PPP}$ (%)**	**Fraction of direct pathway glucose metabolized via PPP (%)**
2.57	0.39	0.02	1.18	0.36	14
(0.32)	(0.04)	(0.01)	(0.02)	(0.04)	(1)
Glycogen ^{13}C-isotopomers from mice provided with [U-^{13}C]fructose and unlabeled glucose					
[4,5,6-$^{13}C_3$]GLY (%)	**[1,2-$^{13}C_2$]GLY$_{TOT}$ (%)**	**[2,3-$^{13}C_2$]GLY (%)**	**D56/D45**	**[1,2-$^{13}C_2$]GLY$_{PPP}$ (%)**	**Fraction of indirect pathway fructose metabolized via PPP (%)**
2.51	0.38	0.09	1.60	0.24	10*
(0.10)	(0.03)	(0.01)	(0.10)	(0.02)	(1)

*p = 0.00032 compared to PPP fraction from glucose

4. DISCUSSION

In the liver, the PPP plays a critical role in the conversion of exogenous sugars to fat by providing the necessary NADPH equivalents for fatty acid biosynthesis. While glucose is the canonical substrate for the PPP, any substrate that is converted to glucose-6-P, including glycerol and lactate, can also in principle provide carbon skeletons for this pathway (Jin et al., 2014). Our study took a recently developed assay of hepatic PPP flux based on analysis of plasma glucose ^{13}C-isotopomers derived from [U-13C]glycerol (Jin et al., 2014, 2016, 2018) and adapted it to read PPP flux from other substrates, including the canonical glucose substrate. By reading ^{13}C-isotopomers of hepatic glycogen instead of plasma glucose, our approach allowed PPP utilization of glucose-6-P derived from direct pathway metabolism of glucose to be specifically measured and compared to glucose-6-P derived from gluconeogenesis. The main significance of our work is the finding that glucose-6-P formed from glucose via the direct pathway was more heavily utilized by the PPP compared to glucose-6-P derived from fructose via gluconeogenesis

The fraction of [U-^{13}C]fructose that underwent PPP cycling prior to being converted to glycogen (10%) in our study was similar to the reported fraction of [U-^{13}C]glycerol that underwent PPP utilization prior to being converted to glucose in fed rats (8%) (Jin et al., 2014). Jin et al also measured PPP recruitment of glucose-6-P that had been synthesized from [U-^{13}C]lactate and found this contribution to be less than that from [U-^{13}C]glycerol (Jin et al., 2014). The results of our study indicates that a significantly larger fraction of glucose-6-P derived via the direct pathway was recruited by the PPP compared to glucose-6-P generated by indirect pathway metabolism of fructose. Glucose-6-P derived via the direct pathway is synthesized via glucokinase, while indirect pathway glucose-6-P is generated by glucose-6-

phosphate isomerase. In the fed condition, glucokinase activation is highly coupled to upregulation of the main pathways of glucose disposal such as glycogen synthesis and *de novo* lipogenesis (Petersen et al., 2017). This may involve the co-ordinated activation of glucokinase and glucose-6-phosphate disposal pathways by upstream effectors such as insulin, as well as intracellular co-localization of glucokinase with the enzymes of pathways involved in glucose-6-P disposal, such as glycogen synthase (Agius et al., 1996). Under essentially the same conditions as that of the present study, we demonstrated a strong coupling of *de novo* lipogenesis from exogenous glucose with PPP activity as seen by a high fractional transfer of exogenous glucose hydrogens to newly-synthesized fatty acids via the PPP (Belew et al., 2019). Others have shown that hepatic PPP activity is more closely linked with lipogenic activity than with mitigation of oxidative stress – a process that potentially competes with biosynthetic pathways for intracellular NADPH (Jin et al., 2018). To what extent the activity and/or intracellular location of glucose-6-phosphate dehydrogenase - the committing enzyme of the PPP - is co-ordinated with that of glucokinase and glycogen synthesis is unclear. Frederiks et al. reported that glucose-6-phosphate dehydrogenase in rat liver parenchymal cells was associated with the ribosomes of granular endoplasmic reticulum (Frederiks & Vreeling-Sindelárová, 2001). Agius et al. concluded that the very strong control exerted by glucokinase on the conversion of glucose to glycogen suggests that active glucokinase and glycogen synthase exist in close proximity to each other in the cell (Agius et al., 1996). Moreover, glucose-6-phosphate derived from sources other than glucokinase is utilized to a lesser extent by glycogen synthase (Seoane et al., 1996). Since glycogen synthesis is also initiated in the endoplasmic reticulum (Prats et al., 2018), this raises the possibility that glucokinase, glycogen synthase and glucose-6-phosphate dehydrogenase could be in close proximity to each other thereby explaining the higher recruitment of glucokinase-derived glucose-6-P for PPP activity as well as for glycogen synthesis. Whether glucose-6-P derived from glucokinase is always

highly utilized by the PPP is unclear. For example, in the initial stages of refeeding, glucokinase may be active while transcription of lipogenesis pathway enzymes may be incomplete. Under these conditions, demand for NADPH formation via PPP may be temporarily low; hence, the fraction of glucose-6-P consumed by the PPP might be small.

Jin et al have successfully translated their methodology into humans with the procedure involving ingestion of a few grams of [U-^{13}C]glycerol followed by blood sampling and analysis of glucose ^{13}C-isotopomers (Jin et al., 2016). While this procedure can be used for [U-^{13}C]fructose, it cannot be applied to [U-^{13}C]glucose. This is because [U-^{13}C]glucose that participated in hepatic metabolism and was returned to the blood via glucose-glucose-6-P cycling cannot be distinguished from [U-^{13}C]glucose that appeared via absorption and was not metabolized by the liver. Alternatively, hepatic UDP-glucose ^{13}C-isotopomers, which provide equivalent information to those of glycogen, can be noninvasively assayed following conversion of UDP-glucose to glucuronide and clearance into urine. This so-called "chemical biopsy" approach involves ingestion of acetaminophen or other glucuronidation agent and can be integrated with oral ^{13}C-tracer administration in human studies (Barosa et al., 2012; Mendes et al., 2006).

In conclusion, we applied the hepatic PPP analysis originally developed by Jin et al. to study PPP utilization of glucose and fructose that are destined for glycogen synthesis. From the analysis of glycogen ^{13}C-isotopomers derived from [U-^{13}C]glucose, PPP recruitment of glucose-6-phosphate derived specifically from glucokinase can be evaluated. Our results suggest that this source of glucose-6-P is preferentially utilized for PPP flux compared to glucose-6-P obtained from indirect pathway precursors such as [U-^{13}C]fructose.

CHAPTER FOUR

QUANTIFYING THE EFFECTS OF HIGH FAT, HIGH SUGAR AND A COMBINATION OF HIGH FAT AND HIGH SUGAR FEEDING ON HEPATIC TRIGLYCERIDE SYNTHESIS AND SOURCES IN THE MOUSE MODEL

1. INTRODUCTION

Non-alcoholic fatty liver disease, one of the most prevalent chronic liver disease globally in current times, is characterized as an irregular accumulation of triglycerides in hepatocytes (García-Ruiz et al., 2014; Hardy et al., 2016; Priore et al., 2015). It has repeatedly been associated with many metabolic disorders including obesity, type 2 diabetes mellitus (T2DM), insulin resistance (IR) and hyperlipidemia that are considered as the main aspects of the metabolic syndrome (Abenavoli et al., 2016). Even though genetic predisposition expressed in metabolic derangement situation has been suggested to influence the pathogenic endpoint of NAFLD, in the metabolic sense, the occurrence and development of NAFLD is a result of an excessive lipid accumulation in the liver mostly from a surplus consumption of fat and/or carbohydrate (Abenavoli et al., 2016; Diehl & Day, 2017; Friedman et al., 2018).

In Western countries, an increased fructose consumption either as part of sucrose or in the form of high-fructose corn syrup, is implicated in the surge of non-alcoholic fatty liver disease (NAFLD) (Musso et al., 2008). Since fructose is assumed to be largely metabolized in liver, its role in promoting NAFLD has been to date explained by its unregulated conversion to fatty acids via de novo lipogenesis, which in turn promotes hyperlipidemia and lipotoxicity. Moreover, in a typical of the so-called Western diet, high fructose ingestion is regularly accompanied by high consumption of fat specifically high levels of saturated fat, which has

also been associated with insulin resistance, dyslipidemia and other metabolic/cardiovascular diseases (Lian et al., 2020; Parks et al., 2008; Stanhope, 2012; Yki-Järvinen, 2010). However, to what extent fructose per se accentuates the already high NAFLD risk from fat overnutrition is unclear. Also, animal models of fructose feeding show different responses to this sugar compared to humans. Many mouse models of high fructose feeding fail to induce weight gain and adiposity (Nunes et al., 2014; Tillman et al., 2014). Also, different mouse strains show different susceptibility to developing NAFLD from high fructose diets (Montgomery et al., 2015). So far, the C57BL/6J mouse strain has been shown to be more susceptible to diet-induced obesity compared to other strains (Montgomery et al., 2015).

Therefore, in the current study, we established mouse models, using previously suggested approaches (Marin et al., 2016; Sellmann et al., 2015), for studying fructose metabolism and the contribution of increased dietary fructose intake with and without high dietary fat to *de novo* synthesis of liver triglyceride in diet induced mice models of NAFLD under normal feeding condition of stayed for about 18 weeks of feeding trial study. The mice under different feeding trial conditions were provided with a combination of deuterated water (^2H_2O) (T. C. Delgado et al., 2009; Duarte et al., 2014; Soares et al., 2012) and/or [U-^{13}C]fructose tracers (F Carvalho et al., 2011; J. C. P. Silva et al., 2019) to quantify the enrichment level, where enrichment from ^2H_2O revealed the fractional synthetic rates of TG-fatty acids and glycerol from all lipogenic precursors (Duarte et al., 2014), while enrichment [U-^{13}C]fructose provided the specific contribution of exogenous fructose to the processes. The contribution of the ^{13}C-enriched fructose to *de novo* synthesis of TG-fatty acid and glycerol can be estimated from ^{13}C NMR analysis of hepatic TG ^{13}C-isotopomers (Figure 4). The positional ^{2}H-enrichment and ^{13}C-isotopomer distributions of TG can be resolved and quantified by sequential ^{2}H and ^{13}C nuclear magnetic resonance (NMR) spectroscopy which constitutes an innovative

integration method developed by our lab group (J. C. P. Silva et al., 2019). Moreover, the ^{13}C NMR spectrum of TG yields a riches of information on the identity and position of individual fatty acids (Gouk et al., 2012; Siddiqui et al., 2003; Tengku-Rozaina & Birch, 2014; Vlahov et al., 2010), which provided a detailed compositional analysis of the TG sample as well as allowed to resolve the contribution of the ^{13}C-enriched sugar to the synthesis of specific fatty acids or fatty acid classes.

2. MATERIALS AND METHODS

2.1. Materials

Unless otherwise specified, [U-^{13}C]fructose at 99% enrichment was obtained from Omicron Biochemicals Inc., IN, USA and purchased through Tracertec, Madrid, Spain. Non-deuterated chloroform ($CHCl_3$) used to prepare TG extracts for $^1H/^2H$ NMR spectroscopy had a purity of 99.8% and contained 100–200 ppm amylenes as stabilizers (Sigma-Aldrich). ^2H_2O at 99.8% isotopic enrichment was also manufactured by Cambridge Isotopes Limited and purchased through Tracertec, Madrid, Spain.

2.2. Animal Studies

Animal studies were approved by the University of Coimbra Ethics Committee on Animal Studies (ORBEA) and the Portuguese National Authority for Animal Health (DGAV), approval code 0421/000/000/2013. Moreover, all animal procedures hereby described were accomplished in full accordance with DGAV guidelines and European regulations (European Union Directive 2010/63/EU). Forty six adult male C57BL/6 mice were obtained from Charles River Labs, Barcelona, Spain, and housed at the University of Coimbra (UC) Biotech Bioterium. They were maintained in a controlled and well-ventilated environment, and a twelve hour light/twelve hour dark cycle. Upon arrival to the Bioterium, mice were provided a two week interval for acclimation, with free access to water and standard chow, comprising of 60% mixed carbohydrate, 16% protein and 3% lipid by weight. After this period, the mice were distributed among four groups according to diet. The first group (n =11) was fed a high-fat diet (HFD) group provided with chow where fat accounted for 30% by weight, while the second group (n = 11) was fed a high-fat and high-sugar diet (HFHSD) where the high-fat chow was supplemented with drinking water containing a 55/45 mixture of fructose and glucose at a

concentration of 30% w/v. The third group (n =12) was fed a high-sugar diet (HSD) where standard chow was supplemented with drinking water containing the same 55/45 mixture of fructose and glucose as for the HFHSD group. Lastly, a fourth group (n=12) designated as control (CTL) was maintained on standard chow. The mice were maintained on the diets for 18 weeks.

On the starting of the ultimate evening, all the mice were received 99.8% deuterated water (^2H_2O) containing 0.9% NaCl as an intraperitoneal (IP) loading dose (4 ml/100 g body weight) and the drinking water was enriched to 5% with ^2H_2O. For the twenty three mice that were provided with fructose/glucose mixture in their drinking water, this was replaced with mixture of same composition, yet, the fructose was enriched to 20% with [U-^{13}C]fructose in their drinking water. The mice were allowed to feed and drink for the entire dark period. At the end of this dark cycle, mice were deeply anesthetized with ketamine/xylazine and sacrificed by cardiac puncture and cervical dislocation. Both hepatic portal and arterial blood were collected and immediately centrifuged and plasma was isolated and stored at − 80 °C for further experimental analysis including for the analysis of body water ^{2}H-enrichment. Livers and other tissues including adipose tissues depots were freeze-clamped and stored at -80ºC until further processing for TG extraction and purification.

2.3. Liver triglyceride extraction and purification

Liver TGs were extracted and purified as previously described (Belew et al., 2019; Matyash et al., 2008; J. C. P. Silva et al., 2019; Viegas et al., 2016). Briefly, livers were powdered under liquid nitrogen and then rapidly mixed with HPLC-grade methanol (4.6 mL/g) followed by methyl-tert-butyl ether (MTBE) (15.4 mL/g). The mixture was placed in a shaker for 1 hour at room temperature then centrifuged at 13,000 *g* for 10 min. The liquid fraction was collected,

and phase separation was induced by adding 4 mL of distilled water to the liquid fraction and letting it rest at room temperature for 10 min. The liquid was then centrifuged for 10 min at 1000 *g*. The upper organic phase containing the lipids was carefully separated and dried under nitrogen gas in an amber glass vial. The triglycerides from the dried organic fraction were purified with a solid phase extraction (SPE) process. Discovery DSC-Si SPE cartridges (2 g/12 ml) were washed with 8 ml of hexane/MTBE (96/4; v/v) followed by 24 ml of hexane. The dried lipids were re-suspended in 800 µl of hexane/MTBE (200/3; v/v) and added into the column after washing. The lipid vials were washed with a further 500 µl of solvent to quantitatively transfer the lipids to the column. Triglycerides were eluted with 32 ml of hexane/MTBE (96/4; v/v), collected in 4 ml fractions. TGs were eluted with 32 ml of hexane/MTBE (96/4; v/v), collected in 4 mL fractions. Fractions containing TGs were identified by thin-layer chromatography (TLC) (Hamilton & Comai, 1988). A few microliters of the eluted fractions were spotted on the TLC plate alongside TG standards and the plate was developed with petroleum ether/diethyl ether/acetic acid (7.0/1.0/0.1; v/v/v). After drying, lipid spots were visualized under iodine vapor. The TG-containing fractions were pooled and dried under nitrogen gas and stored at −20 °C until NMR analysis.

2.4. NMR analysis

The analysis plasma body water ^{2}H-enrichments were determined from 10 µl aliquots by ^{2}H NMR as previously described (J. G. Jones et al., 2001). In details, triplicate 10 µl of plasma samples were mixed with 1 ml acetone of each and ~0.5 ml were loaded in a 5 mm NMR tube to which 50 µl C_6F_6 were added. ^{2}H NMR spectra of these samples were acquired with a 23° pulse angle, 922 Hz spectral width, 4 s acquisition time and 8 s pulse delay (J. G. Jones et al., 2001; J. C. P. Silva et al., 2019). Sixteen fid were collected for each spectrum and water ^{2}H-enrichment was estimated from a calibration curve calculated from ^{2}H-enriched water

standards (J. G. Jones et al., 2001; J. C. P. Silva et al., 2019). Purified liver triglycerides were dissolved in ~0.5 ml $CHCl_3$. To these, 25 µl of a pyrazine standard enriched to 1% with pyrazine-d_4 and dissolved in $CHCl_3$ (0.07 g pyrazine/1 g $CHCl_3$), and 50 µl of C_6F_6 were added. ^1H and ^2H NMR spectra were acquired with an 11.7 T Bruker Avance III HD system using a dedicated 5 mm ^2H-probe with ^{19}F lock and ^1H-decoupling coil as previously described (Belew et al., 2019; J. C. P. Silva et al., 2019; Viegas et al., 2016). ^1H spectra at 500.1 MHz were acquired with a 90-degree pulse, 10 kHz spectral width, 3 seconds of acquisition time, and 5 seconds of pulse delay. Sixteen fid were collected for each spectrum. ^2H NMR spectra at 76.7 MHz were obtained with a 90-degree pulse, a 1230 Hz spectral width, an acquisition time of 0.37 seconds, and a pulse delay of 0.1 seconds. Approximately 16,000 to 20,000 fid were acquired for each spectrum. Quantification of liver triglyceride ^2H-enrichments were determined from the ^1H and ^2H NMR spectra by measuring the ^1H and ^2H intensities of selected signals relative to the ^1H and ^2H intensities of a pyrazine standard, as previously described (Belew et al., 2019; Duarte et al., 2014; J. C. P. Silva et al., 2019; Viegas et al., 2016).

For ^{13}C isotopomer analysis by ^{13}C NMR, dried triglyceride samples were dissolved in 0.2 ml 99.96% enriched $CDCl_3$ (Sigma-Aldrich) and placed in 3 mm NMR tubes. Proton-decoupled ^{13}C NMR spectra were acquired at 150.8 MHz with an Agilent V600 spectrometer equipped with a 3 mm broadband probe. Spectra were acquired with a 70° pulse, an acquisition time of 2.5 s, and a 0.5 s pulse delay. For each spectrum, between 8,000–14,000 fid were collected. The spectra were processed with 0.2 Hz line-broadening before Fourier transformation. Spectra were analyzed using NUTS PC-based NMR spectral analysis software (Acorn NMR Inc., USA).

2.5. Estimation of body fat fraction

The analysis of body composition measurement from ^{2}H body water in mice were determined as previously described (McCabe et al., 2006). The ^{2}H labeling of plasma water was determined as described above, and the degree of dilution of a known 99.8% $^{2}H_2O$ bolus after administration is a function of total body water (TBW). Assuming that the body weight (total body mass) is composed of fat mass (FM) and fat-free mass (FFM), FM can be calculated using the following equations:

FM (g) = body weight – [TBW (g) + FFM (g)] (McCabe et al., 2006)

And, because TBW can be determined via ^{2}H dilution and there is a constant relationship between FFM and body water, FM can then be calculated from the ^{2}H dilution space;

FM (g) = TBM (g) - [^{2}H dilution space (ml) x 1.23]

Where,

^{2}H Dilution space = $^{2}H_2O$ injected (ml) / ^{2}H enrichment of plasma

"1.23" is the total correction factors that accounted for the overestimate of body water by ^{2}H dilution and a hydration constant, and 1 ml of water is equal to 1 g (McCabe et al., 2006; Speakman, 2001; Wolfe & Chinkes, 2004).

The main caveat when applying this analysis to our typical studies is that the mice drink water *ad libitum* with the maintenance enrichment of ^{2}H (usually 5%) so this will alter the body water enrichment to some extent as well as changing the amount of $^{2}H_2O$ entering the body. For overnight period this is typically a relatively small effect. If a more precise measurement is

required, then the mouse should be sampled for blood in an environment free of food or water 15-20 min after $^{2}H_2O$ administration.

2.6. ^{13}C-chemical shift assignments and quantification of FAs abundance

The ^{13}C chemical shifts of FA carbons are sensitive to their overall concentration in the NMR sample (Mannina et al., 2000). Therefore, ^{13}C-chemical shifts of individual FAs were verified with a mixture of five TG standards whose FAs collectively compromise 90–95% of TG FAs in mouse hepatic and adipose tissue (Angrish et al., 2013; Nelson, 1962). The mixture was based on the reported composition of TG FAs in mouse and human adipose tissues (Angrish et al., 2013; Garaulet et al., 2001) and consisted of glyceryl tripalmitate (16:0) (21 mol%), trioleate (18:1) (52 mol%), tristearate (18:0) (4 mol%), tripalmitoleate (16:1) (4 mol%) and trilinoleate (18:2) (19 mol%). The relative abundance of TG FAs was determined from the relative areas of their ω-2 ^{13}C signals. No corrections were made for differential longitudinal relaxation times or nuclear Overhauser effects (J. C. P. Silva et al., 2019).

2.7. Quantification of TG positional ^{2}H-enrichments and estimates of FA and glycerol fractional synthetic rates:

TG positional ^{2}H-enrichments in the glycerol and FA moieties were quantified by analysis of ^{1}H and ^{2}H NMR TG spectra as previously described (Duarte et al., 2014; J. C. P. Silva et al., 2019; Viegas et al., 2016). Fractional synthetic rates for the TG glycerol (**FSR_{Gly}**) and FA moieties (**FSR_{FA}**) over the overnight feeding period when $^{2}H_2O$ was administered were estimated from the ^{2}H-enrichments of the 1,3-glycerol and FA ω-1 hydrogens and those of

body water as previously described (Duarte et al., 2014; J. C. P. Silva et al., 2019; Viegas et al., 2016).

Quantification of TG ^{13}C-enrichment from [U-^{13}C]fructose in the drinking water and its contribution to TG glycerol and FA synthesis as previously described (J. C. P. Silva et al., 2019):

From the ω-1 singlet and doublet ^{13}C NMR signals, which are a composite of all saturated fatty acids (SFA) and monounsaturated fatty acids (MUFA) species, the weighted mean excess ^{13}C-enrichment of all SFA + MUFA species in the ω-1 position from [1,2–$^{13}C_2$]acetyl-CoA was calculated as follows:

Weighted mean excess ^{13}C-enrichment of SFA + MUFA (%) = **ω-1D**/**ω-1 S** × 1.11 -------- (1)

Where **ω-1 D** and **ω-1 S** are the doublet and singlet components, respectively, of the ω-1 ^{13}C resonance and 1.11 represents the background ^{13}C-enrichment (%).

Enrichments of individual FAs, oleate and palmitoleate, as well as that of SFA were estimated from their resolved ω-2 ^{13}C-resonances as follows:

Excess ^{13}C-enrichment of FA *x* (%) = $\mathbf{\omega\text{-}2\ D_x/\omega\text{-}2\ S_x}$ × 1.11 ---------- (2)

Where $\mathbf{\omega\text{-}2\ D_x}$ and $\mathbf{\omega\text{-}2\ S_x}$ are the ω-2 doublet and singlet components of fatty acyl ***x***, and 1.11 represents the background ^{13}C-enrichment (%).

Enrichment of the glycerol moiety from ^{13}C-enriched Triose-P precursors was estimated as follows:

Glycerol ^{13}C-enrichment (%) = **GLY^{13}C-Doublet**/**GLY^{13}C-Singlet** × 1.11 ---------- (3)

Where **GLY^{13}C-Doublet** is the glycerol carbon 1 and carbon 3 (C1,C3) doublet signal originating from [U-^{13}C]Triose-P + [2,3–$^{13}C_2$]- or [1,2–$^{13}C_2$]Triose-P[6] incorporation into glycerol and **GLY^{13}C-Singlet** is the singlet signal representing the 1.11% background ^{13}C-enrichment of C1,C3.

The fractional contribution of fructose in the drinking water to the TG FA and glycerol moieties was calculated as follows:

Fructose contribution to FA (%) = **^{13}C-FA** /**^{13}C-Fructose** × 100 ---------- (4)

Where **^{13}C-FA** is the ^{13}C-excess enrichment of the ω-1, ω-2 FA moiety given by Equations (1), (2), and **^{13}C-Fructose** is the enrichment of fructose in the drinking water.

Fructose contribution to glycerol (%) = **^{13}C-Glycerol**/**^{13}C-Fructose** × 100 ---------- (5)

Where **^{13}C-Glycerol** is the enrichment of the glycerol moiety given by Equation (3) and **^{13}C-Fructose** is the enrichment of fructose in the drinking water.

[6] Triose-P isotopomers with ^{13}C in carbons 1 and 2 and/or carbons 2 and 3 are generated by pentose pathway activity and/or carbon cycling between triose-P and the Krebs cycle. They have a minor contribution (10–15%) to the total Triose-P isotopomer population.

The contribution of fructose in the drinking water to newly-synthesized glyceryl and fatty acyl TG moieties (i.e. formed during the period when [U-^{13}C]fructose and $^{2}H_2O$ tracers were administered) were estimated as follows:

Fructose contribution to new glyceryl (%) = **^{13}C-Glyceryl**/**^{13}C-Fructose** × 100/**FSR_{Gly}** × 100% ----------(6)

Fructose contribution to new fatty acyl (%) = **^{13}C-acyl**/**^{13}C-Fructose** × 100/**FSR_{FA}** × 100% ----------(7)

2.8. Statistics

Data from different subject groups (CTL, HFD, HSD and HFHSD) are represented as box and whisker plots with the box spanning the 25th to 75th percentiles the whiskers extending to the lowest and highest value and the center line representing the median value. According to the variables number different tests were applied. One-way ANOVA followed by Tukey's multiple comparison for single variables (with more than two groups) or two-way ANOVA with Tukey's multiple comparison for two variables. If in the presence of interaction between both variables, analysis proceeded separately for each one of them: two-tailed t-tests for variable pair comparison (two groups) or one-way ANOVA followed by Tukey's multiple comparisons (more than two groups). Differences were considered statistically significant by a p value < 0.05. Analyses were performed with GraphPad Prism 9 software.

3. RESULTS

3.1. Effects of the diets on body weight, adiposity and liver TG

We performed an 18-week feeding study with 46 young adult male C57BL/6 mice. In comparison to CTL mice, significant gains in both weight and adiposity were recorded for HFD and HFHSD mice, whereas HSD mice showed a significant increase in body weight gain from the 8th week onwards compared to CTL mice (see Figure 13). Among the diet groups, HFHSD mice had significantly higher weight gain and adiposity compared to all the other groups. Likewise, the highest body water enrichment and fat mass accumulation were recorded in HFHSD mice followed by HFD mice (Figure 13). Liver TG concentrations in both HSD and HFHSD mice were significantly elevated over CTL mice. In contrast, HFD mice did not have significantly elevated liver TG over CTL mice although there was a tendency towards this (p = 0.1786).

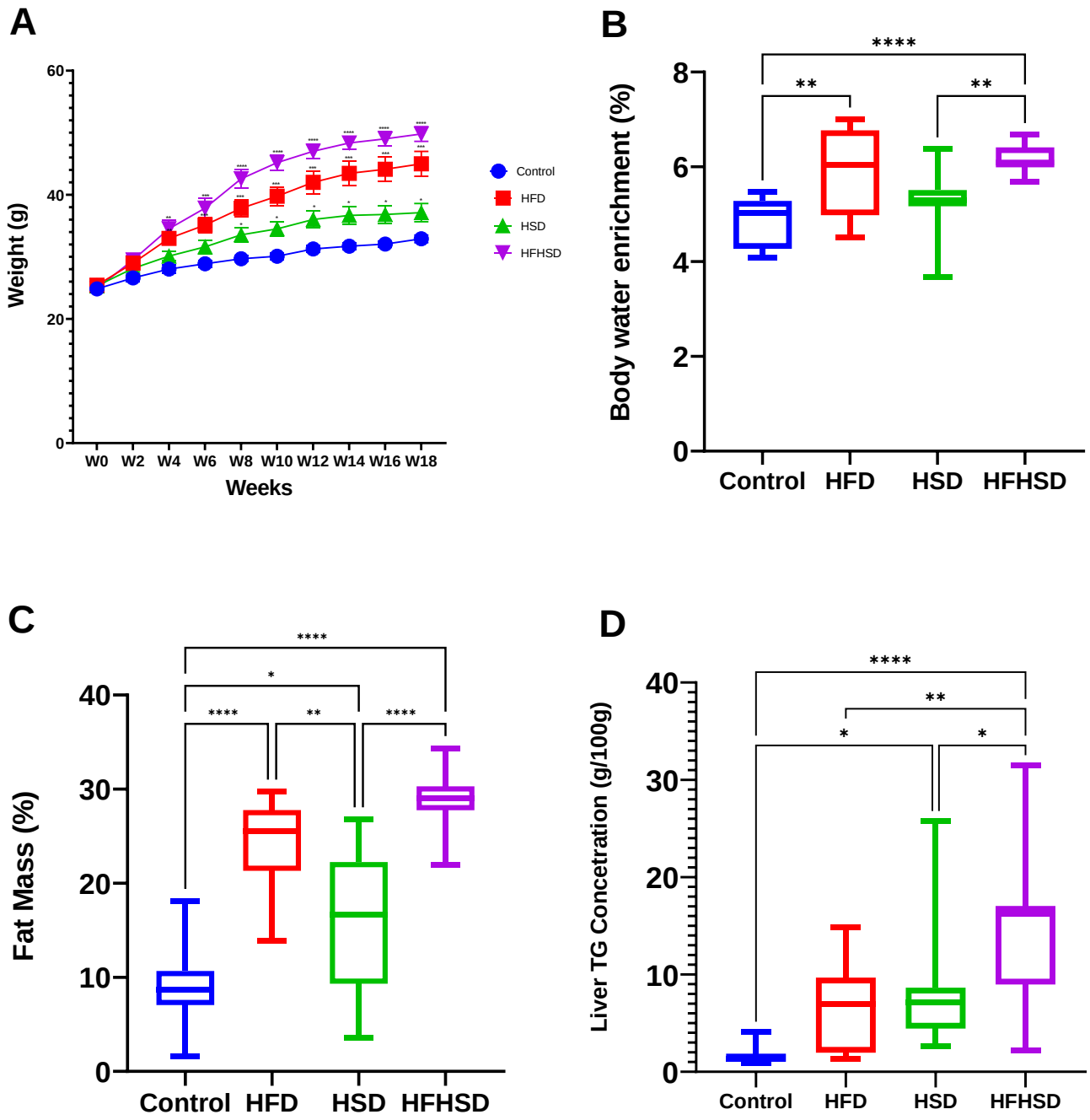

Figure 13: *Effects of the diets on body weight, adiposity and liver TG. Effects of 18 weeks of feeding with standard chow diet (**CTRL**, n=12), high-fat chow diet (**HFD** n=11), standard chow diet supplemented with HFCS-55 formulation in the drinking water (**HSD** n=12), and high-fat chow diet supplemented with HFCS-55 formulation in the drinking water (**HFHSD** n=11) on the following parameters: **(A)**, body weight evolution, **(B)**, body water enrichment from a standardized dose of $^{2}H_2O$, **(C)**, body weight fat fraction, and **(D)**, liver triglyceride concentration.*

3.2. Effects of the diets on hepatic triglyceride lipidomics

The natural-abundance ^{13}C NMR spectrum of intact triglyceride informs the relative abundance of different fatty acid classes, including some individual fatty acid species within a class (for example oleate and palmitoleate within MUFA and linoleic acid within PUFA), as well as the distributions of SFA, MUFA and PUFA between the *sn*1,3 and *sn*2 positions of the glycerol moiety (Gouk et al., 2012; Mannina et al., 2000; Siddiqui et al., 2003; J. C. P. Silva et al., 2019; Tengku-Rozaina & Birch, 2014; Vlahov et al., 2010; Willker & Leibfritz, 1998). These characteristics were compared between feeding trial mice groups; CTL, HFD, HSD, and HFHSD. Fatty acid abundances and positional distributions for the four diet groups are described in Figures 16 and 17**,** and Tables 5 and 6. Saturated fatty acid, poly-and monounsaturated fatty acid, and the special cases of linoleic, ω-3 fatty acids, and DHA were distinguishable by $^{1}H/\ ^{2}H$ and ^{13}C NMR spectra of liver tissue extracts (Figure 14 and 15). For all the diet groups studied, oleate and SFA were the main FA constituents, followed by linoleate and palmitoleate (see Figure 16 and Table 5). HSD mice had significantly lower fractions of linoleate, ω-*3* fatty acids and DHA compared to the other three diet groups. HFD mice had the lowest levels of palmitoleate and the highest abundance of linoleate, ω-*3* fatty acids, and DHA compared to the other three diet groups (Figure 16A and B).

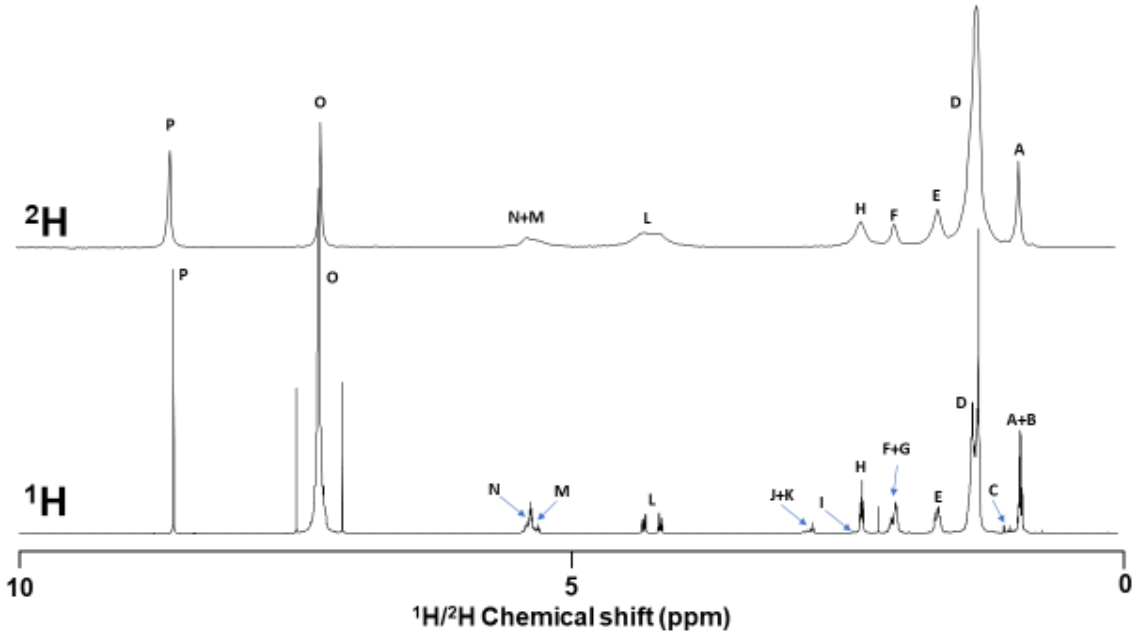

Figure 14: *^{2}H (upper) and ^{1}H (lower) NMR spectra of a purified triglyceride fraction obtained from a* ***HFHSD*** *mouse provided with a mixture of $^{2}H_2O$ and a combination of [U-^{13}C]fructose and unlabelled glucose.* ***A****: Non ω-3 methyl;* ***B****: Partial ω-6 methyl;* ***C****: ω-3 methyl;* ***D****: Aliphatic chain;* ***E****: α3 aliphatic;* ***F****: Protons adjacent to monounsaturated olefinic;* ***G****: protons adjacent to polyunsaturated olefinic;* ***H****: α2 aliphatic;* ***I****: DHA α2 and α3 ally;* ***J****: Linoleic acid bisallylic;* ***K****: Other bisallylic;* ***L****: sn1,sn3 of esterified glycerol;* ***M****: sn2 of esterified glycerol;* ***N****: Olefinic;* ***O****: Chloroform;* ***P****:Pyrazine standard.*

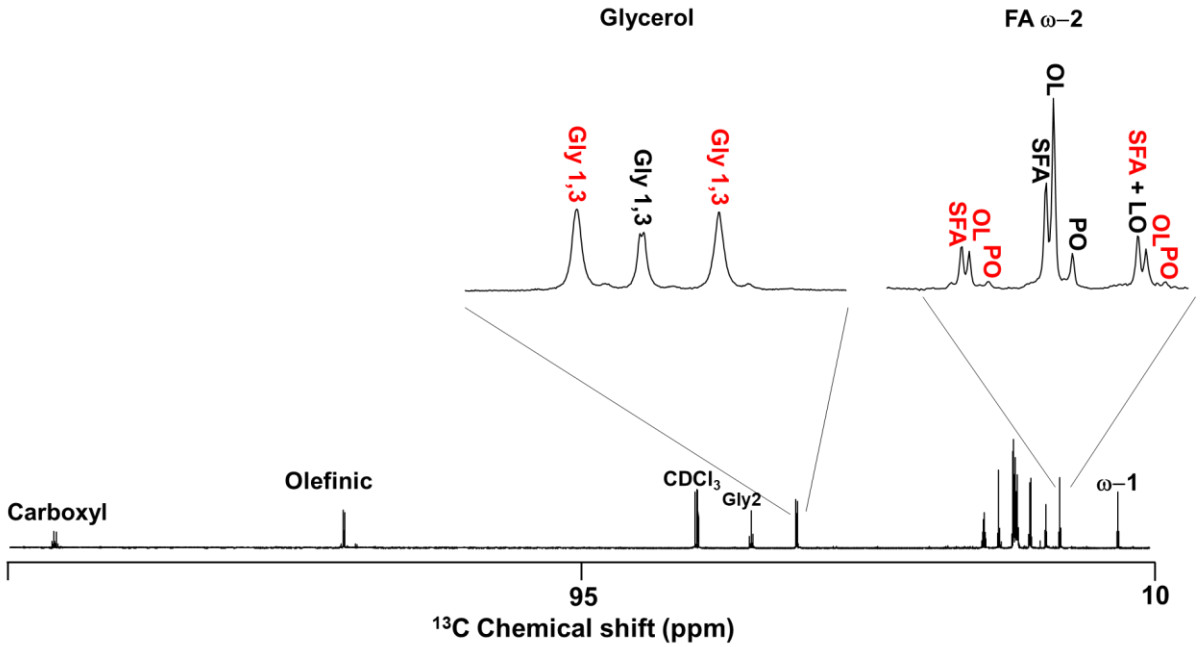

Figure 15: *^{13}C NMR spectrum of hepatic TG obtained from a **HFHSD** mouse provided with a mixture of [U-^{13}C]fructose and unlabeled glucose. The FA ω-2 signals and the glyceryl signal corresponding to carbons 1 and 3 (Gly-sn1,3) are shown in expanded form. For the FA ω-2 resonances; **SFA** = saturated FAs natural abundance singlet, **SFA** = saturated FAs ^{13}C-^{13}C spin-coupled doublet, **OL** = oleate natural abundance singlet, **OL** = oleate ^{13}C-^{13}C spin-coupled doublet, **PO** = palmitoleate natural abundance singlet, **PO** = palmitoleate ^{13}C-^{13}C spin-coupled doublet. For the Gly-sn1,3 signals, **Gly 1,3** = natural abundance singlet and **Gly 1,3** = ^{13}C-^{13}C spin coupled doublet.*

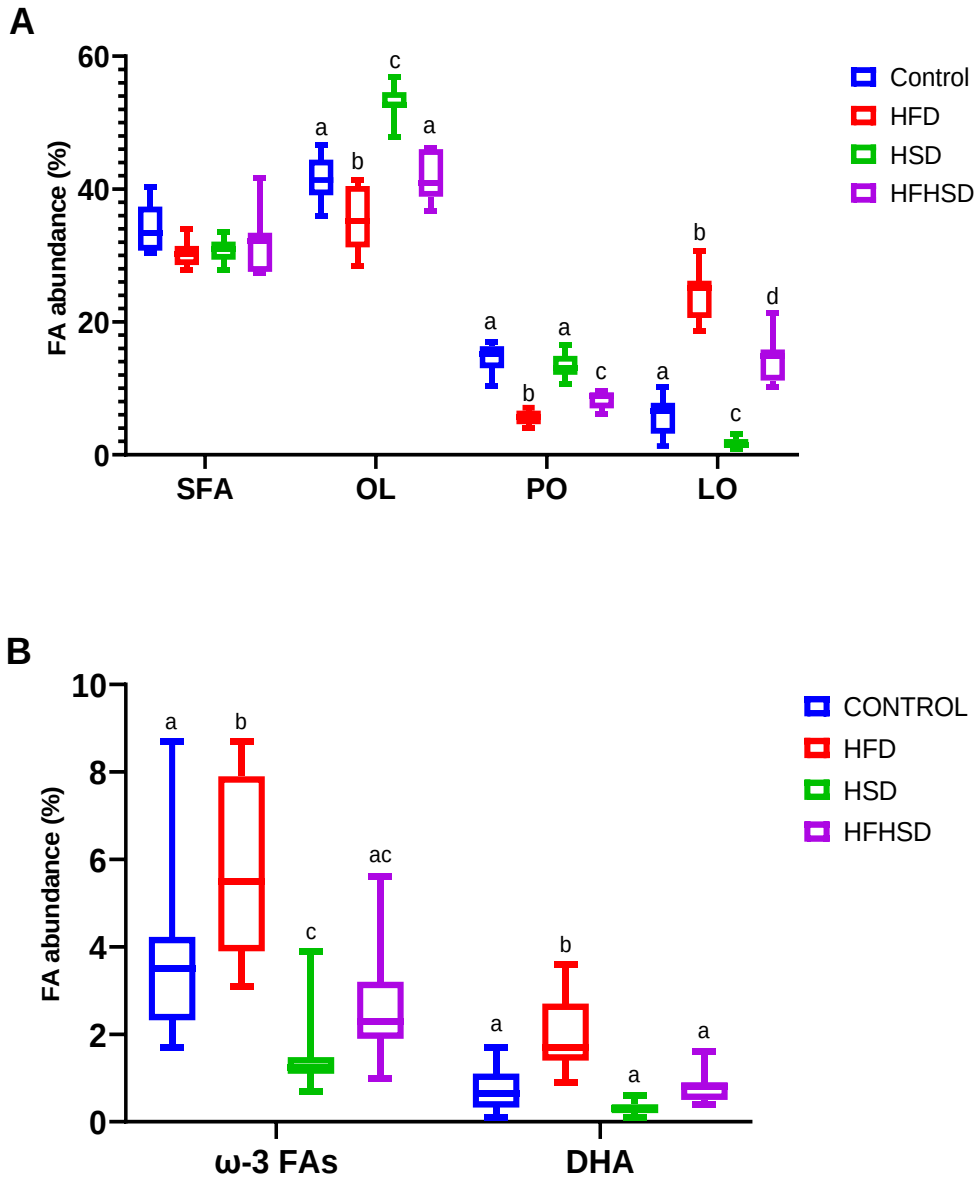

Figure 16: *Hepatic triglyceride fatty acid profiles for mice fed normal chow (**CTRL, n=12**), high-fat chow diet (**HFD n=11**), standard chow diet supplemented with HFCS-55 formulation in the drinking water (**HSD n=12**), and high-fat chow diet supplemented with HFCS-55 formulation in the drinking water (**HFHSD n=11**): The fatty acid species resolved by ^{13}C NMR are shown in (**A**) and include saturated fatty acids (**SFA**), oleate (**OL**), palmitoleate (**PO**) and linoleate (**LO**). The fatty acid species resolved by ^{1}H NMR are shown in (**B**) and include the total fraction of ω-3 fatty acids (**ω-3 FA**) and the fraction of docosahexaenoic acid (DHA).*

Table 5: *Results from one-way ANOVA (p-values) applied to data representing on Figure 16 "Hepatic triglyceride fatty acid profiles" among different diet based groups of mice: normal chow (**CTRL**), high fat chow (**HFD**), high sugar diets (**HSD**), and high fat and high sugar diet (**HFHSD**).*

	One-way ANOVA (n=46)	*Tukey's multiple comparisons*					
		Control vs HFD	**Control vs HSD**	**Control vs HFHSD**	**HFD vs. HSD**	**HFD vs. HFHSD**	**HSD vs. HFHSD**
SFA	*p = 0.0784*	*p = 0.0922*	*p = 0.1420*	*p = 0.6538*	*p = 0.9833*	*p = 0.6291*	*p = 0.7974*
Oleate	*p < 0.0001*	*p = 0.0141*	*p < 0.0001*	*p = 0.9953*	*p < 0.0001*	*p = 0.0130*	*p < 0.0001*
PO	*p < 0.0001*	*p < 0.0001*	*p = 0.4288*	*p < 0.0001*	*p < 0.0001*	*p = 0.0285*	*p < 0.0001*
LO	*p < 0.0001*	*p < 0.0001*	*p = 0.0251*	*p < 0.0001*	*p < 0.0001*	*p < 0.0001*	*p < 0.0001*
ω–3FA	*p = 0.1281*	*p = 0.0177*	*P = 0.0065*	*P = 0.4383*	*p < 0.0001*	*p < 0.0003*	*P = 0.2537*
DHA	*p < 0.0001*	*p < 0.0001*	*P = 0.1957*	*P = 0.9828*	*p < 0.0001*	*p < 0.0001*	*P = 0.1038*

For all diet groups, ^{13}C NMR revealed a markedly non-uniform distribution of fatty acid classes between *sn*2 and *sn*1,3 sites among the different diet groups (Figure 17 A, B and C and Table 6). The majority of SFA were bound to the *sn*1,3 positions with only minor quantities at the *sn*2 site. In contrast, both MUFA and PUFA were more abundant in the *sn*2 compared to *sn*1,3 sites. The fraction of MUFA in the *sn*2 position was significantly higher in HSD mice, whereas the PUFA fraction in the *sn*2 position was significantly more abundant in HFD mice compared to the other dietary groups (Figure 17 B and C).

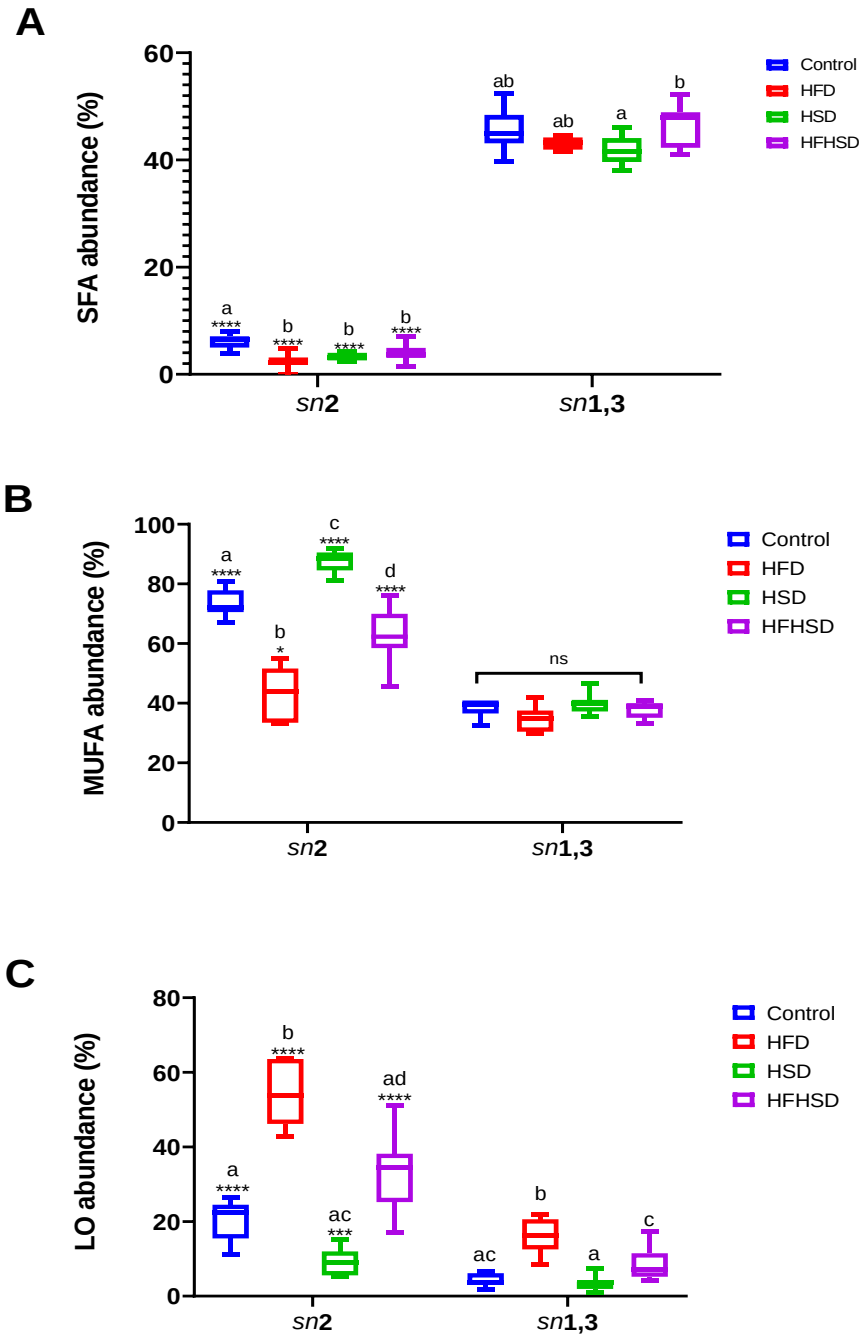

Figure 17: *The distribution of different fatty acid classes in the glycerol sn1,3 and sn2 positions of hepatic triglyceride resolved by ^{13}C NMR for mice fed normal chow (**Control, n=12**), high-fat chow diet (**HFD n=11**), standard chow diet supplemented with HFCS-55 formulation in the drinking water (**HSD n=12**), and high-fat chow diet supplemented with HFCS-55 formulation in the drinking water (**HFHSD n=11**): Distributions of saturated fatty acids (**SFA**), monounsaturated fatty acids (**MUFA**) and linoleate (**LO**) are shown in panels **A**, **B** and **C**,*

respectively. *The fatty acid abundances in different dietary groups within each sn site are represented by letters (one-way ANOVA; $p < 0.05$). For each dietary group fatty acid, differences between sn2 and sn1,3 positions are indicated by asterisks (t-test; * $p < 0.05$, ** $p < 0.01$ *** $p < 0.001$, **** $p < 0.0001$)*

Table 6: *Results from one-way ANOVA (p values) applied to data on Figure 17 representing FAs distribution in each position – sn2 or sn1,3 – for the four different analyzed diet groups. Previous analysis under a two-way ANOVA for the two variables (diet; position) showed significant interactions for MUFA and LO but not for SFA:* ***MUFA*** *– Interaction (p < 0.0001), position (p < 0.0001), diet (p < 0.0001);* ***LO*** *– Interaction (p < 0.0001), position (p < 0.0001), diet (p < 0.0001);* ***SFA*** *– Interaction (p = 0.1522), position ((p < 0.0001), diet (p < 0.0001). Due to interactions separate analysis were applied: one-way ANOVA for FA differences in each position; t-test for sn2 vs sn1,3 in each FA for each diet group*

	One-way ANOVA (n=46)	*Tukey's multiple comparisons*					
		Control vs HFD	**Control vs HSD**	**Control vs HFHSD**	**HFD vs HSD**	**HFD vs HFHSD**	**HSD vs HFHSD**
				A (SFA)			
sn2	*p = 0.0003*	*p = 0.0003*	*p = 0.0095*	*p = 0.0113*	*p = 0.4104*	*p = 0.3762*	*p = 0.9999*
				B (MUFA)			
	p < 0.0001	*p < 0.0001*	*p = 0.0008*	*p = 0.0145*	*p < 0.0001*	*p < 0.0001*	*p < 0.0001*
				C (LO)			
	p < 0.0001	*p < 0.0001*	*p = 0.0125*	*p = 0.0037*	*p < 0.0001*	*p < 0.0001*	*p < 0.0001*
				A (SFA)			
sn1,3	*p = 0.0201*	*p = 0.3655*	*p = 0.0620*	*p = 0.9927*	*p = 0.8545*	*p = 0.2456*	*p = 0.0335*
				B (MUFA)			
	p = 0.0423	*p = 0.1272*	*p = 0.8889*	*p = 0.9874*	*p = 0.5234*	*p = 0.2235*	*p = 0.7231*
				C (LO)			
	p < 0.0001	*p < 0.0001*	*p = 0.9095*	*p = 0.0501*	*p < 0.0001*	*p = 0.0004*	*p = 0.0103*

	t-test (n=46)	*sn2 vs sn1,3*		
		SFA	**MUFA**	**LO**
Control		*p < 0.0001*	*p < 0.0001*	*p < 0.0001*
HFD		*p < 0.0001*	*p = 0.0317*	*p < 0.0001*
HSD		*p < 0.0001*	*p < 0.0001*	*p = 0.0004*
HFHSD		*p < 0.0001*	*p < 0.0001*	*p < 0.0001*

3.3. Effects of the diets on hepatic triglyceride lipid fluxes

Among all the diet trial study groups, ^{2}H incorporation from body water into fatty acid and glycerol moieties of hepatic TG was resolved by ^{2}H NMR spectroscopy. The fractional synthetic rate (FSR) of fatty acids was significantly higher in CTL and HSD compared to the other two diet groups (Figure 18A and Table 7). However, when fatty acid FSR was adjusted for total liver triglyceride levels (Figure 19A and Table 8), there was a clear progression in fatty acid FSR with the lowest rates found for CTL and HFD with significantly higher values for both HSD and HFHSD. Similar trends were observed for fatty acid elongation and desaturation rates (Figure 19B and 19C, respectively). Glycerol synthesis rates were not significantly different between CTL, HFD and HSD while for HFHSD mice, these rates were significantly higher relative to the other three diet conditions (Figure 19D).

Table 7: *Results from one-way ANOVA (p-values) applied to data on Figure 18 representing the effect of diets on hepatic triglyceride lipid fluxes (%) for the four different analyzed diet groups, normal chow (**CTRL**), high fat chow (**HFD**), high sugar diets (**HSD**), and high fat and high sugar diet (**HFHSD**) groups.*

^{2}H Liver TG lipid fluxes ($^{2}H_2O$ and *[U-^{13}C]fructose + unlabeled glucose (n=46)*						
%	CTL vs HFD	CTL vs HSD	CTL vs HFHSD	HFD vs HSD	HFD vs HFHSD	HSD vs HFHSD
DNL	*p < 0.0001*	*p = 0.5036*	*p = 0.0013*	*p = 0.0002*	*p = 0.2018*	*p = 0.0541*
Elongation	*p < 0.0001*	*p = 0.0002*	*p < 0.0001*	*p = 0.3700*	*p = 0.7904*	*p = 0.0618*
Desaturation	*p < 0.0001*	*p = 0.0005*	*p < 0.0001*	*p = 0.0043*	*p = 0.2677*	*p = 0.3202*
Glyceroneogenesis	*p = 0.1161*	*p = 0.1253*	*p = 0.0016*	*p = 0.9998*	*p = 0.3781*	*p = 0.3152*

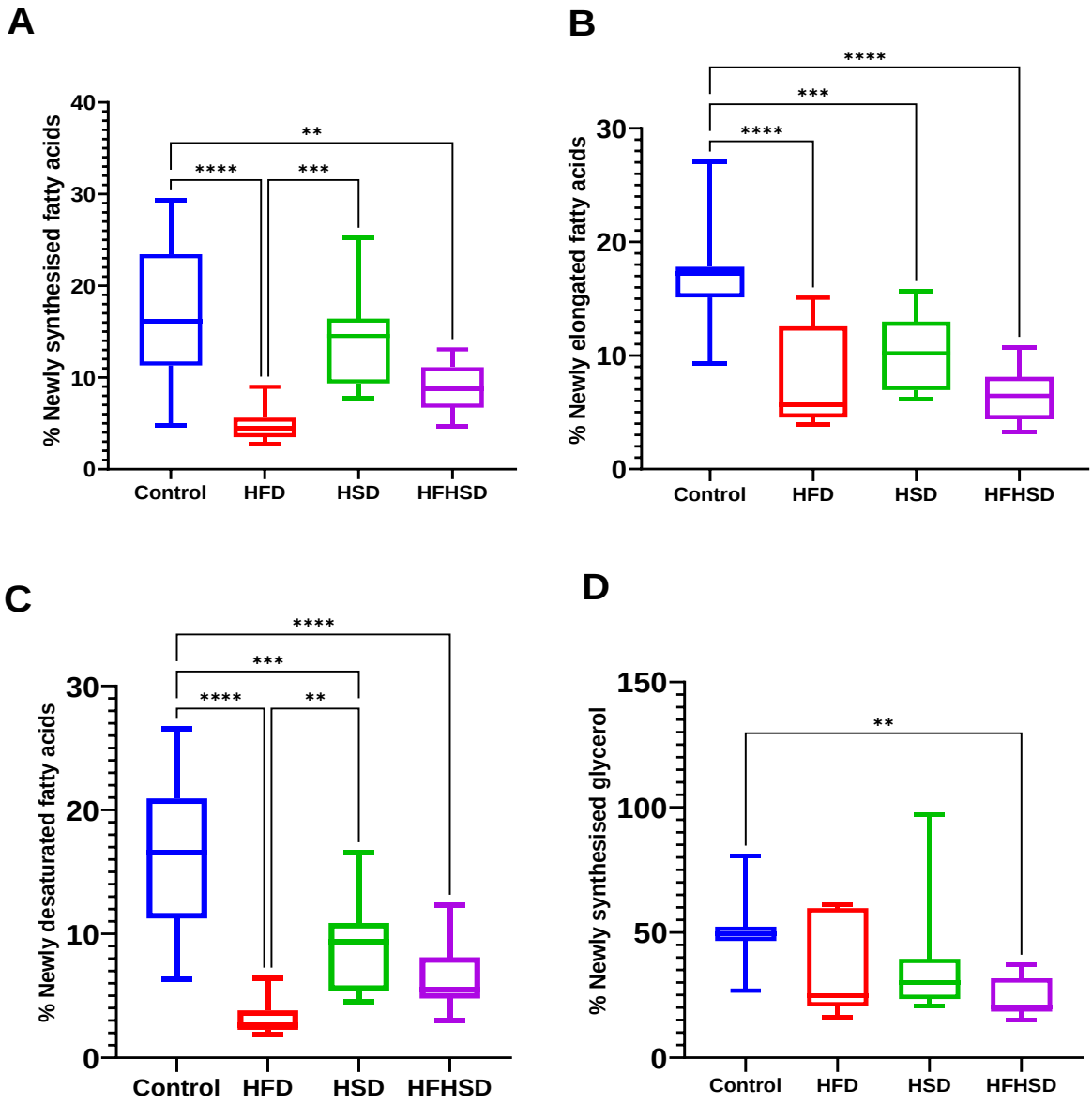

***Figure 18**: Fractional rates of fatty acid synthesis (A), fatty acid elongation (B), fatty acid desaturation (C) and glycerol synthesis (D) of hepatic triglyceride for mice fed normal chow (**Control, n=12**), high-fat chow diet (**HFD n=11**), standard chow diet supplemented with HFCS-55 formulation in the drinking water (**HSD n=12**), and high-fat chow diet supplemented with HFCS-55 formulation in the drinking water (**HFHSD n=11**):*

Table 8: *Results from one-way ANOVA (p-values) applied to data on Figure 19 representing the effect of diets on hepatic triglyceride lipid fluxes (g/100g of tissue) for the four different analysed diet groups, mice fed normal chow (**CTRL**), high fat chow (**HFD**), high sugar diets (**HSD**), and high fat and high sugar diet (**HFHSD**).*

^{2}H Liver TG lipid fluxes ($^{2}H_2O$ and *[U-^{13}C]fructose + unlabeled glucose (n=46)*						
g/100g	CTL vs HFD	CTL vs HSD	CTL vs HFHSD	HFD vs HSD	HFD vs HFHSD	HSD vs HFHSD
DNL	*p > 0.9999*	*p = 0.0009*	*p < 0.0001*	*p = 0.0010*	*p < 0.0001*	*p = 0.2109*
Elongation	*p = 0.8559*	*p = 0.0041*	*p < 0.0001*	*p = 0.0414*	*p = 0.0002*	*p = 0.1934*
Desaturation	*p = 0.9220*	*p = 0.0079*	*p < 0.0001*	*p = 0.0016*	*p < 0.0001*	*p = 0.0811*
Glyceroneogenesis	*p = 0.1391*	*p = 0.0631*	*p < 0.0001*	*p = 0.9891*	*p = 0.0018*	*p = 0.0036*

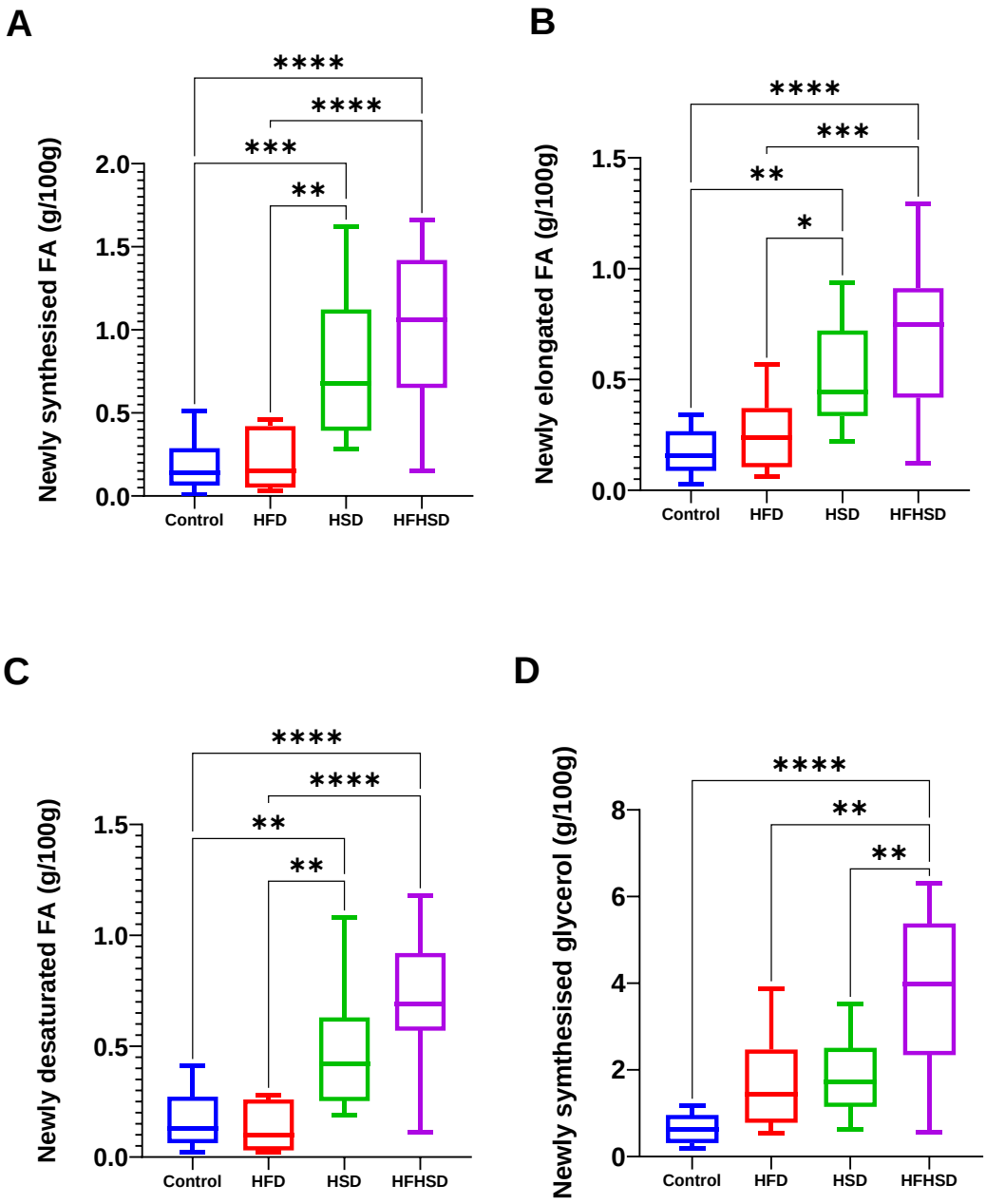

Figure 19: *Fractional mass of newly synthesized fatty acid* ***(A)****, fatty acid elongation mass* ***(B)****, desaturated fatty acid mass* ***(C)*** *and newly synthesized glycerol mass* ***(D)*** *of hepatic triglyceride for mice fed normal chow (****Control, n=12****), high-fat chow diet (****HFD, n=11****), standard chow diet supplemented with HFCS-55 formulation in the drinking water (****HSD, n=12****), and high-fat chow diet supplemented with HFCS-55 formulation in the drinking water (****HFHSD, n=11****):*

3.4. Effects of a high fat background on HFCS-55 fructose metabolism into hepatic triglyceride fatty acids and glycerol.

As described by Silva et al. (J. C. P. Silva et al., 2019), we applied ^{13}C-isotopomer analysis to the TG samples to estimate the contribution of the dietary fructose component to selected newly-synthesized triglyceride fatty acids and to glycerol in HSD and HFHSD mice (Figure 20 and Table 10). Also, the ^{2}H enrichment of TG ω-1 and glycerol *C1, C3* hydrogens in HSD and HFHSD mice group provided with $^{2}H_2O$ and [U-^{13}C]fructose in their drinking water presented in Table 9. In HSD mice, fructose contributed 28 ± 4% of acetyl-CoA to the synthesis of SFA compared to 16 ± 3% to oleate synthesis (p = 0.054 vs. SFA) and 18 ± 3% to palmitoleate synthesis (p = 0.118 vs. SFA). For HFHSD mice, fructose contributed 18 ± 3% of acetyl-CoA to the synthesis of SFA compared to 7 ± 2% towards oleate synthesis (p = 0.002 vs. SFA) and 7 ± 2% to palmitoleate synthesis (p = 0.003 vs. SFA). Moreover, the exogenous fructose contributed more for the synthesis of selective FAs in HSD group as compared to HFHSD. It accounted for 30-40% of newly synthesized glycerol, with a tendency for a higher contribution in HSD compared to HFHSD.

Table 9: *^{2}H Enrichment of the TG ω-1 and glycerol sn1, sn3 hydrogens in mice group provided with $^{2}H_2O$ and the combinations of [U-^{13}C]fructose and unlabeled glucose in their drinking water*.

^{2}H Liver TG enrichment ($^{2}H_2O$ and *[U-^{13}C]fructose + unlabeled glucose (n=23)*			
	FA ω-1	***sn1,3-Glyceryl***	***Body water***
HSD	0.15 ± 0.02	0.38 ± 0.07	5.24 ± 0.18
HFHSD	0.09 ± 0.01	0.23 ± 0.02	6.14 ± 0.08

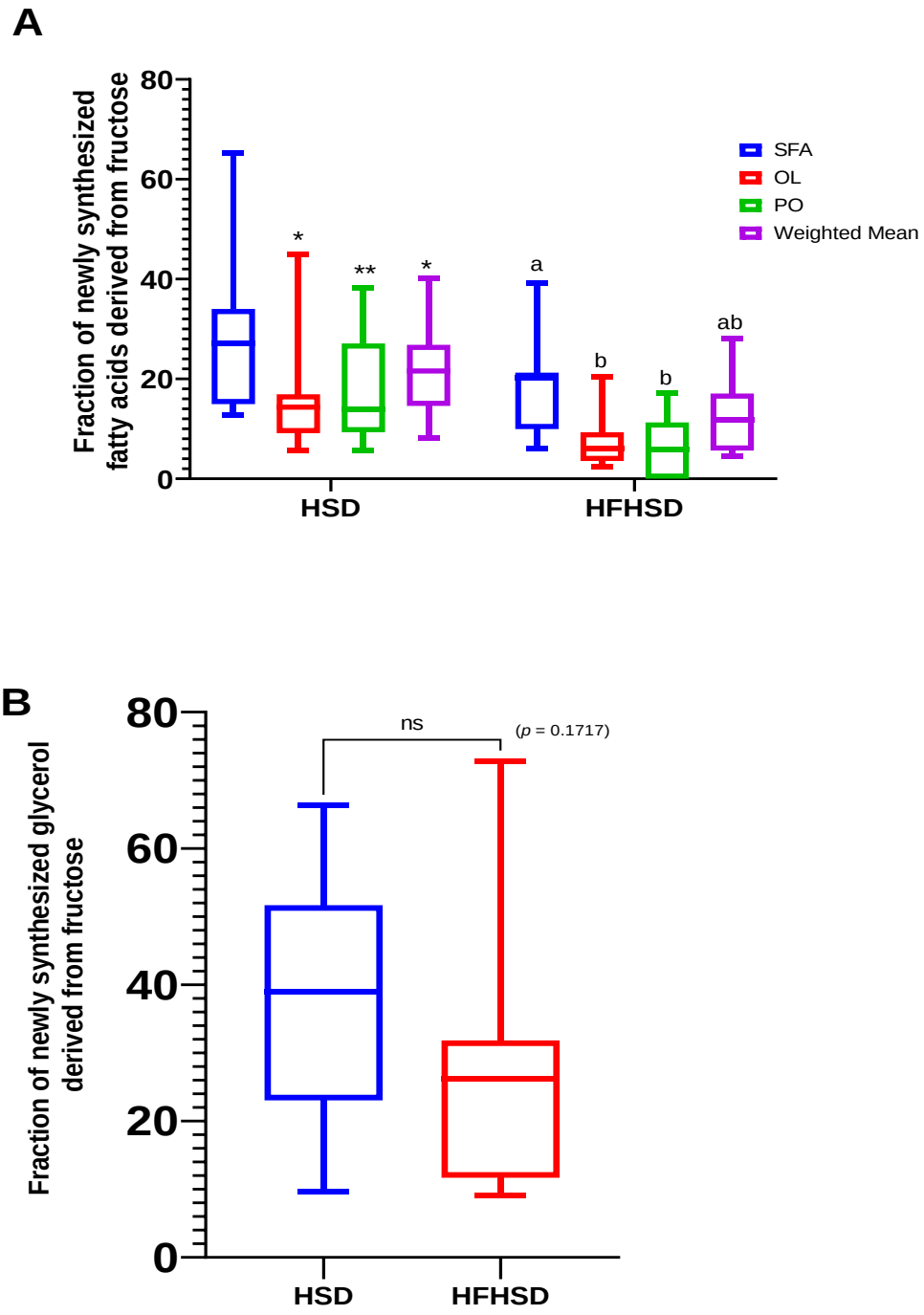

Figure 20: *Contribution of dietary fructose to the synthesis of fatty acid* ***(A)*** *and glycerol* ***(B)*** *components of hepatic triglyceride for mice fed standard chow diet supplemented with HFCS-55 formulation in the drinking water (**HSD n=12**), and high-fat chow diet supplemented with HFCS-55 formulation in the drinking water (**HFHSD n=11**): The fatty acid abundances in different dietary groups are represented by letters (one-way*

*ANOVA; $p < 0.05$). For each fatty acid, differences between HFD and HFHSD are indicated by asterisks (t-test; * $p < 0.05$, ** $p < 0.01$ *** $p < 0.001$, **** $p < 0.0001$) (Figure 20 A)*

***Table 10:** Results from one-way ANOVA (p-values) applied on data from specific contributions [U-^{13}C]fructose to newly synthesized fractions of FA in each diet group (high sugar diets (**HSD**), and high fat and high sugar diet (**HFHSD**)), and two-tailed t-tests on specific contributions [U-^{13}C] fructose to newly synthesized fractions of glycerol and FA between the diets (**HSD vs HFHSD**).*

One-way ANOVA **(n = 23)**	*Tukey's multiple comparisons*					
	SFA vs OL	SFA vs PO	SFA vs Mean	OL vs PO	OL vs Mean	PO vs Mean
HSD *p = 0.0635*	*p = 0.0627*	*p = 0.1479*	*p = 0.5985*	*p = 0.9775*	*p = 0.5543*	*p = 0.7952*
HFHSD *p = 0.0015*	*p = 0.0042*	*p = 0.0032*	*p = 0.2184*	*p = 0.9996*	*p = 0.3537*	*p = 0.3027*

t-test	**FA**				**Glycerol**
(n = 23)	**SFA**	**OL**	**PO**	**Mean weighted**	
HSD vs HFHSD	*p = 0.0804*	*p = 0.0245*	*p = 0.0078*	*p = 0.0101*	*p = 0.1717*

4. DISCUSSION

4.1. Influence of the diet on liver adiposity and fat levels

Numerous studies of C57BL6 mice have demonstrated that overall adiposity in general and hepatic fat levels in particular are increased following an extended interval of feeding with chow that is highly enriched with lipid (García-Ruiz et al., 2014), refined sugar (Mock et al., 2017; Montgomery et al., 2015; Tillman et al., 2014), or both (Asgharpour et al., 2016; Jensen et al., 2018). This accumulation of lipid is a consequence of increased inflow of dietary fatty acids as well as increased DNL rates. In terms of overall adiposity and liver fat levels, our data indicate that the combination of high fat and high sugar feeding was more obesogenic that either high sugar or high fat supplementation alone. This likely reflects an overall increased caloric intake for HFHSD mice compared to either HF or HSD mice, and an additive effect of lipogenic conversion of sugar to fat and increased dietary fat absorption.

4.2. Influence of the diets on hepatic triglyceride lipidomics:

High fat and high sugar feeding resulted in distinctive lipidomic phenotypes, with HSD mice featuring significantly higher levels of oleate and a depletion in linoleate and other essential fatty acids relative to controls. In contrast, HFD mice had lower amounts of oleate and higher abundances of linoleate and other essential fatty acids. The differences in oleate levels are well correlated with the systematically higher rates of DNL, elongation and desaturation for HSD compared to HFD mice (Figure 19). Given that palmitate (16:0) is the principal fatty acid product of DNL, elongation and desaturation would

generate stearate (18:0) and oleate (18:1), respectively. Linoleate is exclusively derived from dietary lipid and will therefore be ingested in higher amounts by HFD compared to CTL. In contrast, HSD mice derive a significant fraction of their caloric intake from the sugar-enriched drinking water, therefore they have a reduced intake of dietary lipid from the standard chow even compared to CTL. The lipid profile of HFHSD mice lies in-between that of HSD and HFD reflecting a partial dilution of dietary lipids with de-novo synthesized fatty acids generated from the dietary sugar. The differences in positional distributions of different fatty acid classes (SFA, MUFA and LO) appear to be directly related to their overall abundances. As previously reported (J. C. P. Silva et al., 2019), we found a strong preference for MUFA and LO to be bound to the glyceryl *sn*2 position while the large majority of SFA were esterified at the *sn*1,3 sites.

4.3. Influence of the diets on hepatic lipogenesis and triglyceride synthesis rates:

The enrichment of triglyceride fatty acids from $^{2}H_2O$ provides a measure of the fraction of newly synthesized fatty acids relative to the total triglyceride pool. In order to translate fractional synthetic rates (FSR) to absolute synthetic rates, the total pool size needs to be known. In the absence of this information, similar FSR rates measured under conditions where the TG pool sizes are very different may in fact disguise highly significant changes in absolute synthetic rates. Thus, the fractional synthetic rate estimates shown in Figure 18, which are not adjusted for hepatic TG pool size, show apparent decreases in lipogenic activity for each of the HFD, HS and HFHSD groups relative to CTL. When these data were adjusted for hepatic TG concentrations (Figure 19), significant increases in lipogenic activity were found for both HS and HFHSD compared to CTL, with HFD

yielding similar rates to CTL. However, this adjustment comes with an important caveat. The hepatic TG pool is undergoing constant turnover, with newly formed TG being exported as very-low density lipoproteins (VLDL). Thus, alterations in hepatic lipid levels can reflect changes in both inflow and outflow fluxes and elevations in hepatic TG concentrations may not necessarily reflect absolute increases in DNL and/or fatty acid import rates. Indeed, the elevation in hepatic TG in mice fed methionine and choline-deficient diets is explained by a reduction in VLDL export capacity due to a deficiency in hepatic lipoprotein synthesis (Postic & Girard, 2008; Rinella et al., 2008) The relationship between hepatic fat accumulation and VLDL export rates may in part depend on the diet. Martins et al. found that increased hepatic TG levels in rats fed a high sucrose diet was accompanied by proportionally higher VLDL export rates (Martins et al., 2015). On the other hand, mice that were fed a diet high in saturated fat had significant elevations in hepatic TG levels but unchanged VLDL export rates (Oosterveer et al., 2009). Another study comparing mice fed a high-fat versus a low-fat diet showed that increased hepatic TG levels were accompanied by significantly lower VLDL export rates (Ono-Moore et al., 2017). In the case of high fat and sugar feeding, Gasparin et al. showed proportionate increases in liver TG concentrations and VLDL export rates for male mice fed a "cafeteria diet" high in both refined sugar and saturated fat compared to mice fed standard chow (Gasparin et al., 2018). Thus, in summary, hepatic VLDL export rates are not altered or may even be decreased by high fat feeding, while high sugar or high fat-high sugar diets promote higher VLDL export rates over normal chow. The implications for our study are that the adjusted FSR data for HFD mice may somewhat overstate absolute lipogenesis rate for HFD mice, but likely understate absolute rates for both HSD and HFHSD mice. Taking this into account, the results indicate that lipogenesis rates in the HFHSD are comparable to those of HSD mice and several-fold higher than that of CTL mice.

Meanwhile, despite a significantly lower FSR, after adjusting for hepatic TG levels the lipogenesis rates of HFD mice are similar to CTL mice. Thus, in the case of HFHSD, the increased liver TG levels and adiposity reflect an additive effect of increased dietary lipid intake and increased lipogenic activity secondary to the high intake of sugar.

4.4. Contribution of dietary fructose to hepatic TG synthesis during high sugar and high sugar + high fat feeding:

Dietary fructose is considered to be a highly lipogenic sugar in comparison to dietary glucose and in a previous study where a 50/50 fructose/glucose mixture was ingested over a single night by mice that were otherwise on a normal chow diet, it provided a significantly higher fraction of acetyl-CoA for both newly synthesized fatty acids and glycerol compared to the glucose component (J. C. P. Silva et al., 2019). In the current study, we emulated the widely used HFCS-55 sweetener with a 55/45 mix of fructose and glucose and measured the contribution of the fructose component only to fatty acid and glycerol synthesis. For the HSD mice, the fraction of acetyl-CoA derived from fructose (~25%) was somewhat less than the ~30% reported for the study of Silva et al. while for HFHSD mice, its contribution tended to be lower, averaging about 15% of the lipogenic acetyl-CoA pool. Given that the adjusted DNL rates of HSD and HFHSD were similar (see Figure 19A) the lower contribution of fructose carbons to lipogenic acetyl-CoA production in HFHSD relative to HSD represents a shift in the sourcing of lipogenic acetyl-CoA towards other substrates. Fructose also contributed substantially to liver TG glycerol synthesis in both HSD and HFHSD mice, accounting for 30-40% of glycerol that was synthesized overnight. This is consistent with the efficient entry of fructose carbons

into the hepatic triose phosphate pool via the ketohexokinase, aldolase and triokinase enyzmes. The study of Silva et al. not only revealed that fructose was more lipogenic than glucose overall, but also demonstrated that fructose contributed a greater fraction of acetyl-CoA to synthesized SFA compared to oleate (J. C. P. Silva et al., 2019). In the current study, which included data from palmitoleic acid as well as oleic acid, there was a tendency for a higher fructose contribution to the synthesis of SFA over oleate or palmitoleate for HSD mice while for HFHSD mice these differences were statistically significant. Given that the SFA component is mainly palmitate (Angrish et al., 2013; Garaulet et al., 2001), then elongation activity could account for a lower ^{13}C-enrichment of oleate ω-1, ω-2 compared to that of SFA (Oosterveer et al., 2009). However, this does not explain the difference between SFA and oleate enrichment from [U-^{13}C]fructose. Fructose is efficiently extracted by the liver implying that a significant concentration gradient exists across the hepatic lobule. We speculate that this could result in a heterogeneous enrichment of hepatic acetyl-CoA pools with those used for SFA synthesis having a higher enrichment of [U-^{13}C]acetyl-CoA compared to those used for *de novo* oleate synthesis. Based on analysis of lipogenesis pathway enzyme activities such as ATP-isocitrate lyase, acetyl-CoA carboxylase and fatty acid synthase, lipogenesis is considered to occur predominantly in the perivenous region (Postic & Girard, 2008). As far as we know, there have been no reported data on the localization of fatty acid elongases and desaturases in relation to those of the DNL pathway. Since DNL contributes fatty acid precursors for elongation and desaturation, from a teleological perspective, these enzymes would be expected to be located downstream of the DNL ones.

In conclusion, high-fat, high sugar and a combination of high sugar and high fat diets provided over an 18 week period resulted in significant increases in adiposity over standard chow for adult male C57BL6/J mice. High sugar and high fat plus high sugar feeding resulted in significant increased hepatic TG levels as well. The increased liver TG from high sugar feeding was associated with elevated lipogenesis rates, with the fructose component contributing sizable fractions of both acetyl-CoA and glycerol-3-phosphate precursors. This lipogenic activity and the contributions from fructose were not significantly diminished in a diet where high sugar was accompanied by high fat. Thus, the fat and sugar components of this diet contribute to overall adiposity and hepatic steatosis in an additive manner.

CHAPTER FIVE

GENERAL CONCLUSIONS AND FUTURE PERSPECTIVES

1. GENERAL CONCLUSION

Deuterated water (^2H_2O) is a widely used tracer for quantifying fatty-acid synthesis. However, a major uncertainty of this method is that exchange of water hydrogens with those of fatty acid precursors and/or NADPH is considered to be incomplete. Due to this, a correction factor based on an estimate of the average number of ^2H hydrogens incorportated into palmitate (*N*) is applied for the calculation of DNL. In our study, we monitored transfer of ^2H and ^{13}C from glucose into fatty-acid position-2 (^2H originating via malonyl-CoA), position-3 (^2H originating via NADPH), and methyl (^2H originating via acetyl-CoA) in feeding mice. Our study indicates that glucose ^2H are transferred at different fractional rates into different fatty-acid sites during lipogenesis, with transfer via NADPH being the most extensive, and therefore the most implicated in the potential for reduced incorporation of ^2H from ^2H_2O into fatty acids during DNL. Interestingly, for mice administered with ^2H_2O, this process did not result in a significantly reduced enrichment of fatty acid position 3 hydrogens relative to those of position 2 as measured by ^2H NMR. This may be explained by extensive ^2H-enrichment of circulating glucose and exchange of NADPH hydrogens via cofactors. This information allows better modelling of lipid enrichment from ^2H_2O and also provides insight on NADPH sources for lipogenesis. The *N* value for palmitate that was calculated from our ^2H retention data in mice is consistent with that calculated from a previous MIDA analysis of palmitate enrichment from ^2H_2O in rats (F. Diraison et al., 1996), nevertheless, *N* may vary

considerably according to the type of organism as well as the substrates that were utilized for DNL.

In the fed state, sugar phosphate flux through the pentose phosphate pathway is a key requirement for *de novo* lipogenesis since it generates NADPH equivalents for fatty acid synthesis and/or elongation. In our study, we applied an elegant ^{13}C-NMR analysis approach to exogenous [U-^{13}C]fructose and [U-^{13}C]glucose precursors originally developed by Jin et al to study the PPP utilization of fructose and glucose that are destined for glycogen synthesis (Jin et al., 2018). Hepatic PPP fluxes from both [U-^{13}C]glucose and [U-^{13}C]fructose precursors were assessed by ^{13}C NMR analysis of glycogen ^{13}C-isotopomers. PPP recruitment of glucose-6-phosphate derived specifically from glucokinase can be evaluated from the analysis of glycogen ^{13}C-isotopomers derived from [U-^{13}C]glucose. Our results suggest that this source of glucose-6-P is preferentially utilized for PPP flux compared to glucose-6-P obtained from indirect pathway precursors, such as [U-^{13}C]fructose, indicating that the PPP was active under our experimental conditions. Our study also revealed that the PPP has preferentially utilized the glucose-6 phosphate generated via glucokinase and the direct pathway. Fructose is considered to be a highly lipogenic sugar and it has been previously shown to contribute substantially to *de novo* lipogenesis in mouse models. In this dissertation, we demonstrate for the first time that it also supports PPP activity, thereby contributing NADPH for the reductive formation of fatty acids during *de novo* lipogenesis.

An increased consumption of fat and/or fructose either as part of sucrose or in the form of high-fructose corn syrup composed of 55/45 fructose/glucose (HFCS-55) results an excessive accumulation of lipid in the liver. In this study, we determined the impact of

high dietary fat levels on the contribution of the HFCS-55 fructose component to *de novo* synthesis of liver triglyceride. Our study demonstrate that high-fat, high sugar and a combination of high sugar and high fat diets provided over an 18 week period resulted in significant increases in adiposity over standard chow for adult male C57BL6/J mice. Moreover, high sugar and high fat plus high sugar feeding resulted in significantly increased hepatic TG levels as well. The increased liver TG from high sugar feeding was associated with elevated lipogenesis rates, with the fructose component contributing sizable fractions of both acetyl-CoA and glycerol-3-phosphate precursors. This lipogenic activity and the contributions from fructose were not significantly diminished in a diet where HFCS-55 was accompanied by high fat. Furthermore, our study documented that for mice fed a normal chow diet supplemented with HFCS-55, there was a tendency for higher contributions of fructose to SFA synthesis in comparison to oleate or palmitoleate, while for mice fed high-fat diets that were supplemented with HFCS-55, fructose contributed significantly more acetyl-CoA to SFA synthesis than to either oleate or palmitoleate synthesis thereby promoting a more lipotoxic lipid profile. Thus, the fat and sugar components of this diet contribute to overall adiposity and hepatic steatosis in an additive manner.

2. FUTURE PERSPECTIVES

Given the steep parallel increases in obesity rates and NAFLD in most Westernized societies, there is a pressing need for a better understanding of the metabolic mechanisms that contribute to lipid overload, of which DNL is likely a key component. Over-nutrition, accompanied by hyperinsulinemia and hyperglycemia, drives DNL activity. However, despite the clear association between elevated DNL activity and increased hepatic triglyceride levels, surprisingly little is known about the sources of acetyl-CoA that fuel this process. Our study indicates that while dietary fructose does contribute carbons to DNL, it is not an overwhelmingly large fraction. Thus, it will be important to identify the remaining acetyl-CoA sources that supply the majority of DNL carbons. These likely include products of intestinal microflora fermentation such as short-chain fatty acids (SCFA) and ethanol. The more important role lipogenic role of fructose may be in activating lipogenic transcription factors such as ChREPB that in turn upregulate expression of DNL pathway enzymes thereby creating conditions where acetyl-CoA derived from other substrates are recruited for DNL.

The development of the therapeutic landscape in NAFLD is progressing rapidly although there are still no currently approved drugs specifically for this condition. A large and diverse number of agents are currently being investigated for the treatment of NAFLD. They include glucose lowering agents/anti-diabetic agents, lipid lowering agents. Moreover, there are also several drugs that target the liver. In addition, some of the therapies target hepatic lipid synthesis (e.g. Acetyl-Coenzyme A Carboxylase (ACC) Inhibition, Stearoyl coenzyme A desaturase 1 (SCD1) inhibition, for the treatment of

NAFLD. In addition to targeting ACC, considering other lipogenic enzymes such as fatty acid synthase (FAS), and diacylglycerol O-acyltransferase (DGAT) will be other potential pharmacologic agents to reduce steatosis and lipotoxicity. Our methodologies will allow better evaluation of the effects of these and other medications on DNL activity and substrate selection, in particular during the early development phase which is typically performed in rodent models.

We observed strong coupling between DNL and the pentose phosphate pathway (PPP) in mice fed a high sugar diet. Whether this applies in humans and the extent to which it is depends on the diet will be important to elucidate. PPP activity is also an important characteristic of tumour cells, and a key future question to be addressed is to what extent PPP fluxes are remodelled during the development of hepatocellular carcinoma in the setting of NAFLD. It may well be that hepatic PPP fluxes are "trained" by high sugar feeding in such a way as to facilitate subsequent tumour development. Our methodologies will allow such changes, should they exist, to be observed and quantified.

BIBLIOGRAPHY

Aarsland, A., Chinkes, D., & Wolfe, R. R. (1996). Contributions of de novo synthesis of fatty acids to total VLDL- triglyceride secretion during prolonged hyperglycemia/hyperinsulinemia in normal man. *Journal of Clinical Investigation*, *98*(9), 2008–2017. https://doi.org/10.1172/JCI119005

Abdelmalek, M. F., Suzuki, A., Guy, C., Unalp-Arida, A., Colvin, R., Johnson, R. J., & Diehl, A. M. (2010). Increased fructose consumption is associated with fibrosis severity in patients with nonalcoholic fatty liver disease. *Hepatology*, *51*(6), 1961–1971. https://doi.org/10.1002/hep.23535

Abenavoli, L., Milic, N., Di Renzo, L., Preveden, T., Medic-Stojanoska, M., & De Lorenzo, A. (2016). Metabolic aspects of adult patients with nonalcoholic fatty liver disease. In *World Journal of Gastroenterology* (Vol. 22, Issue 31, pp. 7006–7016). Baishideng Publishing Group Co. https://doi.org/10.3748/wjg.v22.i31.7006

Abid, A., Taha, O., Nseir, W., Farah, R., Grosovski, M., & Assy, N. (2009). Soft drink consumption is associated with fatty liver disease independent of metabolic syndrome. *Journal of Hepatology*, *51*(5), 918–924. https://doi.org/10.1016/j.jhep.2009.05.033

Abu-Elheiga, L., Brinkley, W. R., Zhong, L., Chirala, S. S., Woldegiorgis, G., & Wakil, S. J. (2000). The subcellular localization of acetyl-CoA carboxylase 2. *Proceedings of the National Academy of Sciences of the United States of America*, *97*(4), 1444–1449. https://doi.org/10.1073/pnas.97.4.1444

Agius, L., Peak, M., Newgard, C. B., Gomez-Foix, A. M., & Guinovart, J. J. (1996). *Evidence for a Role of Glucose-induced Translocation of Glucokinase in the Control of Hepatic Glycogen Synthesis**. https://doi.org/10.1074/jbc.271.48.30479

Aithal, G. P., Thomas, J. A., Kaye, P. V., Lawson, A., Ryder, S. D., Spendlove, I., Austin, A. S., Freeman, J. G., Morgan, L., & Webber, J. (2008). Randomized, Placebo-Controlled Trial of Pioglitazone in Nondiabetic Subjects With Nonalcoholic Steatohepatitis. *Gastroenterology*, *135*(4), 1176–1184. https://doi.org/10.1053/j.gastro.2008.06.047

Akuta, N., Kawamura, Y., Watanabe, C., Nishimura, A., Okubo, M., Mori, Y., Fujiyama, S., Sezaki, H., Hosaka, T., Kobayashi, M., Kobayashi, M., Saitoh, S., Suzuki, F., Suzuki, Y., Arase, Y., Ikeda, K., & Kumada, H. (2019). Impact of

sodium glucose cotransporter 2 inhibitor on histological features and glucose metabolism of non-alcoholic fatty liver disease complicated by diabetes mellitus. *Hepatology Research*, *49*(5), 531–539. https://doi.org/10.1111/hepr.13304

Alang, N., & Kelly, C. R. (2015). Weight gain after fecal microbiota transplantation. *Open Forum Infectious Diseases*, *2*(1). https://doi.org/10.1093/ofid/ofv004

Ameer, F., Scandiuzzi, L., Hasnain, S., Kalbacher, H., & Zaidi, N. (2014). De novo lipogenesis in health and disease. In *Metabolism: Clinical and Experimental* (Vol. 63, Issue 7, pp. 895–902). W.B. Saunders. https://doi.org/10.1016/j.metabol.2014.04.003

Angrish, M. M., Dominici, C. Y., & Zacharewski, T. R. (2013). TCDD-Elicited effects on liver, serum, and adipose lipid composition in C57BL/6 mice. *Toxicological Sciences*, *131*(1), 108–115. https://doi.org/10.1093/toxsci/kfs277

Anstee, Q. M., Seth, D., & Day, C. P. (2016). Genetic Factors That Affect Risk of Alcoholic and Nonalcoholic Fatty Liver Disease. *Gastroenterology*, *150*(8), 1728-1744.e7. https://doi.org/10.1053/j.gastro.2016.01.037

Armstrong, M. J., Houlihan, D. D., Rowe, I. A., Clausen, W. H. O., Elbrønd, B., Gough, S. C. L., Tomlinson, J. W., & Newsome, P. N. (2013). Safety and efficacy of liraglutide in patients with type 2 diabetes and elevated liver enzymes: Individual patient data meta-analysis of the LEAD program. *Alimentary Pharmacology and Therapeutics*, *37*(2), 234–242. https://doi.org/10.1111/apt.12149

Armstrong, Matthew J., Hull, D., Guo, K., Barton, D., Hazlehurst, J. M., Gathercole, L. L., Nasiri, M., Yu, J., Gough, S. C., Newsome, P. N., & Tomlinson, J. W. (2016a). Glucagon-like peptide 1 decreases lipotoxicity in non-alcoholic steatohepatitis. *Journal of Hepatology*, *64*(2), 399–408. https://doi.org/10.1016/j.jhep.2015.08.038

Armstrong, Matthew J., Hull, D., Guo, K., Barton, D., Hazlehurst, J. M., Gathercole, L. L., Nasiri, M., Yu, J., Gough, S. C., Newsome, P. N., & Tomlinson, J. W. (2016b). Glucagon-like peptide 1 decreases lipotoxicity in non-alcoholic steatohepatitis. *Journal of Hepatology*, *64*(2), 399–408. https://doi.org/10.1016/j.jhep.2015.08.038

Arsov, T., Larter, C. Z., Nolan, C. J., Petrovsky, N., Goodnow, C. C., Teoh, N. C., Yeh, M. M., & Farrell, G. C. (2006). Adaptive failure to high-fat diet characterizes steatohepatitis in Alms1 mutant mice. *Biochemical and Biophysical Research Communications*, *342*(4), 1152–1159. https://doi.org/10.1016/j.bbrc.2006.02.032

Asgharpour, A., Cazanave, S. C., Pacana, T., Seneshaw, M., Vincent, R., Banini, B. A.,

Kumar, D. P., Daita, K., Min, H. K., Mirshahi, F., Bedossa, P., Sun, X., Hoshida, Y., Koduru, S. V., Contaifer, D., Warncke, U. O., Wijesinghe, D. S., & Sanyal, A. J. (2016). A diet-induced animal model of non-alcoholic fatty liver disease and hepatocellular cancer. *Journal of Hepatology*, *65*(3), 579–588. https://doi.org/10.1016/j.jhep.2016.05.005

Assy, N., Nasser, G., Kamayse, I., Nseir, W., Beniashvili, Z., Djibre, A., & Grosovski, M. (2008). Soft drink consumation linked with fatty liver in the absence of traditional risk factors. *Canadian Journal of Gastroenterology*, *22*(10), 811–816. https://doi.org/10.1155/2008/810961

Azrad, M., Turgeon, C., & Demark-Wahnefried, W. (2013). Current evidence linking polyunsaturated fatty acids with cancer risk and progression. In *Frontiers in Oncology: Vol. 3 SEP*. Front Oncol. https://doi.org/10.3389/fonc.2013.00224

Baba, C. S., Alexander, G., Kalyani, B., Pandey, R., Rastogi, S., Pandey, A., & Choudhuri, G. (2006). Effect of exercise and dietary modification on serum aminotransferase levels in patients with nonalcoholic steatohepatitis. *Journal of Gastroenterology and Hepatology (Australia)*, *21*(1 PART1), 191–198. https://doi.org/10.1111/j.1440-1746.2005.04233.x

Bajaj, H. S., Brown, R. E., Bhullar, L., Sohi, N., Kalra, S., & Aronson, R. (2018). SGLT2 inhibitors and incretin agents: Associations with alanine aminotransferase activity in type 2 diabetes. *Diabetes and Metabolism*, *44*(6), 493–499. https://doi.org/10.1016/j.diabet.2018.08.001

Ballestri, S., Nascimbeni, F., Baldelli, E., Marrazzo, A., Romagnoli, D., & Lonardo, A. (2017). NAFLD as a Sexual Dimorphic Disease: Role of Gender and Reproductive Status in the Development and Progression of Nonalcoholic Fatty Liver Disease and Inherent Cardiovascular Risk. In *Advances in Therapy* (Vol. 34, Issue 6, pp. 1291–1326). Springer Healthcare. https://doi.org/10.1007/s12325-017-0556-1

Barosa, C., Almeida, M., Caldeira, M. M., Gomes, F., & Jones, J. G. (2010). Contribution of proteolytic and metabolic sources to hepatic glutamine by 2H NMR analysis of urinary phenylacetylglutamine 2H-enrichment from 2H2O. *Metabolic Engineering*, *12*(1), 53–61. https://doi.org/10.1016/j.ymben.2009.08.009

Barosa, C., Silva, C., Fagulha, A., Barros, L., Caldeira, M. M., Carvalheiro, M., & Jones, J. G. (2012). Sources of hepatic glycogen synthesis following a milk-containing breakfast meal in healthy subjects. *Metabolism: Clinical and*

Experimental, *61*(2), 250–254. https://doi.org/10.1016/j.metabol.2011.06.022

Barrows, B. R., & Parks, E. J. (2006). Contributions of different fatty acid sources to very low-density lipoprotein-triacylglycerol in the fasted and fed states. *Journal of Clinical Endocrinology and Metabolism*, *91*(4), 1446–1452. https://doi.org/10.1210/jc.2005-1709

Bassuk, S. S., & Manson, J. A. E. (2005). Epidemiological evidence for the role of physical activity in reducing risk of type 2 diabetes and cardiovascular disease. In *Journal of Applied Physiology* (Vol. 99, Issue 3, pp. 1193–1204). J Appl Physiol (1985). https://doi.org/10.1152/japplphysiol.00160.2005

BasuRay, S., Smagris, E., Cohen, J. C., & Hobbs, H. H. (2017). The PNPLA3 variant associated with fatty liver disease (I148M) accumulates on lipid droplets by evading ubiquitylation. *Hepatology*, *66*(4), 1111–1124. https://doi.org/10.1002/hep.29273

Bederman, I. R., Kasumov, T., Reszko, A. E., David, F., Brunengraber, H., & Kelleher, J. K. (2004). In vitro modeling of fatty acid synthesis under conditions simulating the zonation of lipogenic [13C]acetyl-CoA enrichment in the liver. *Journal of Biological Chemistry*, *279*(41), 43217–43226. https://doi.org/10.1074/jbc.M403837200

Bederman, I. R., Reszko, A. E., Kasumov, T., David, F., Wasserman, D. H., Kelleher, J. K., & Brunengraber, H. (2004). Zonation of labeling of lipogenic acetyl-CoA across the liver: Implications for studies of lipogenesis by mass isotopomer analysis. *Journal of Biological Chemistry*, *279*(41), 43207–43216. https://doi.org/10.1074/jbc.M403838200

Bederman, Ii. R., Foy, S., Chandramouli, V., Alexander, J. C., & Previs, S. F. (2009). Triglyceride synthesis in epididymal adipose tissue. Contribution of glucose and non-glucose carbon sources. *Journal of Biological Chemistry*, *284*(10), 6101–6108. https://doi.org/10.1074/jbc.M808668200

Bedogni, G., Bellentani, S., Miglioli, L., Masutti, F., Passalacqua, M., Castiglione, A., & Tiribelli, C. (2006). The fatty liver index: A simple and accurate predictor of hepatic steatosis in the general population. *BMC Gastroenterology*, *6*. https://doi.org/10.1186/1471-230X-6-33

Beer, N. L., Tribble, N. D., McCulloch, L. J., Roos, C., Johnson, P. R. V., Orho-Melander, M., & Gloyn, A. L. (2009). The P446L variant in GCKR associated

with fasting plasma glucose and triglyceride levels exerts its effect through increased glucokinase activity in liver. *Human Molecular Genetics*, *18*(21), 4081–4088. https://doi.org/10.1093/hmg/ddp357

Belew, G. D., Silva, J., Rito, J., Tavares, L., Viegas, I., Teixeira, J., Oliveira, P. J., Macedo, M. P., & Jones, J. G. (2019). Transfer of glucose hydrogens via acetyl-CoA, malonyl-CoA, and NADPH to fatty acids during de novo lipogenesis. *Journal of Lipid Research*, *60*(12), 2050–2056. https://doi.org/10.1194/jlr.RA119000354

Belfort, R., Harrison, S. A., Brown, K., Darland, C., Finch, J., Hardies, J., Balas, B., Gastaldelli, A., Tio, F., Pulcini, J., Berria, R., Ma, J. Z., Dwivedi, S., Havranek, R., Fincke, C., DeFronzo, R., Bannayan, G. A., Schenker, S., & Cusi, K. (2006). A Placebo-Controlled Trial of Pioglitazone in Subjects with Nonalcoholic Steatohepatitis. *New England Journal of Medicine*, *355*(22), 2297–2307. https://doi.org/10.1056/nejmoa060326

Ben-Shlomo, S., Zvibel, I., Shnell, M., Shlomai, A., Chepurko, E., Halpern, Z., Barzilai, N., Oren, R., & Fishman, S. (2011). Glucagon-like peptide-1 reduces hepatic lipogenesis via activation of AMP-activated protein kinase. *Journal of Hepatology*, *54*(6), 1214–1223. https://doi.org/10.1016/j.jhep.2010.09.032

Bergen, W. G., & Mersmann, H. J. (2005). Comparative aspects of lipid metabolism: Impact on contemporary research and use of animal models. In *Journal of Nutrition* (Vol. 135, Issue 11, pp. 2499–2502). American Society for Nutrition. https://doi.org/10.1093/jn/135.11.2499

Bergheim, I., Weber, S., Vos, M., Krämer, S., Volynets, V., Kaserouni, S., McClain, C. J., & Bischoff, S. C. (2008). Antibiotics protect against fructose-induced hepatic lipid accumulation in mice: Role of endotoxin. *Journal of Hepatology*, *48*(6), 983–992. https://doi.org/10.1016/j.jhep.2008.01.035

Bernard Zinman, Christoph Wanner, J. M. L., David Fitchett, Erich Bluhmki, S. H., Michaela Mattheus, Dipl. Biomath., T. D., Odd Erik Johansen, Hans J. Woerle, U. C. B., & and Silvio E. Inzucchi, for the E.-R. O. I. (2015). Empagliflozin, cardiovascular outcomes, and mortality in type 2 diabetes. *N Engl J Med*, *373*(22), 2117-28. https://doi.org/10.1056/nejmoa1504720

Bourgeois, C. S., Wiggins, D., Hems, R., & Gibbons, G. F. (1995). VLDL output by hepatocytes from obese Zucker rats is resistant to the inhibitory effect of insulin.

American Journal of Physiology - Endocrinology and Metabolism, *269*(2 32-2). https://doi.org/10.1152/ajpendo.1995.269.2.e208

Bradshaw, P. C. (2019). Cytoplasmic and mitochondrial NADPH-coupled Redox systems in the regulation of aging. In *Nutrients* (Vol. 11, Issue 3). MDPI AG. https://doi.org/10.3390/nu11030504

Brandt, T. (1990). Positional and positioning vertigo and nystagmus. *Journal of the Neurological Sciences*, *95*(1), 3–28. https://doi.org/10.1016/0022-510X(90)90113-2

Camastra, S., Astiarraga, B., Tura, A., Frascerra, S., Ciociaro, D., Mari, A., Gastaldelli, A., & Ferrannini, E. (2017). Effect of exenatide on postprandial glucose fluxes, lipolysis, and ß-cell function in non-diabetic, morbidly obese patients. *Diabetes, Obesity and Metabolism*, *19*(3), 412–420. https://doi.org/10.1111/dom.12836

Capanni, M., Calella, F., Biagini, M. R., Genise, S., Raimondi, L., Bedogni, G., Svegliati-Baroni, G., Sofi, F., Milani, S., Abbate, R., Surrenti, C., & Casini, A. (2006). Prolonged n-3 polyunsaturated fatty acid supplementation ameliorates hepatic steatosis in patients with non-alcoholic fatty liver disease: A pilot study. *Alimentary Pharmacology and Therapeutics*, *23*(8), 1143–1151. https://doi.org/10.1111/j.1365-2036.2006.02885.x

Carvalho, F, Gonçalves, A., Barra, J., Caldeira, M., Duarte, J., & Jones, J. (2011). Noninvasive sampling of murine hepatic acetyl-CoA enrichment with p-amino benzoic acid. *Diabetologia*, *54*, S284–S284.

Carvalho, Filipa, Duarte, J., Simoes, A. R., Cruz, P. F., & Jones, J. G. (2013). Noninvasive measurement of murine hepatic acetyl-CoA C 13 -enrichment following overnight feeding with C 13 -enriched fructose and glucose. *BioMed Research International*, *2013*. https://doi.org/10.1155/2013/638085

Cersosimo, E., Gastaldelli, A., Cervera, A., Wajcberg, E., Sriwijilkamol, A., Fernandez, M., Zuo, P., Petz, R., Triplitt, C., Musi, N., & DeFronzo, R. A. (2011). Effect of exenatide on splanchnic and peripheral glucose metabolism in type 2 diabetic subjects. *Journal of Clinical Endocrinology and Metabolism*, *96*(6), 1763–1770. https://doi.org/10.1210/jc.2010-2146

Chalasani, N., Younossi, Z., Lavine, J. E., Charlton, M., Cusi, K., Rinella, M., Harrison, S. A., Brunt, E. M., & Sanyal, A. J. (2018a). The diagnosis and management of nonalcoholic fatty liver disease: Practice guidance from the American Association

for the Study of Liver Diseases. *Hepatology*, *67*(1), 328–357. https://doi.org/10.1002/hep.29367

Chalasani, N., Younossi, Z., Lavine, J. E., Charlton, M., Cusi, K., Rinella, M., Harrison, S. A., Brunt, E. M., & Sanyal, A. J. (2018b). The diagnosis and management of nonalcoholic fatty liver disease: Practice guidance from the American Association for the Study of Liver Diseases. *Hepatology*, *67*(1), 328–357. https://doi.org/10.1002/hep.29367

Chandramouli, V., Ekberg, K., Schumann, W. C., Wahren, J., & Landau, B. R. (1999). Origins of the hydrogen bound to carbon i of glucose in fasting: Significance in gluconeogenesis quantitation. *American Journal of Physiology - Endocrinology and Metabolism*, *277*(4 40-4). https://doi.org/10.1152/ajpendo.1999.277.4.e717

Chen, W., Chang, B., Li, L., & Chan, L. (2010). Patatin-like phospholipase domain-containing 3/adiponutrin deficiency in mice is not associated with fatty liver disease. *Hepatology*, *52*(3), 1134–1142. https://doi.org/10.1002/hep.23812

Choi, Y. J., Shin, H. S., Choi, H. S., Park, J. W., Jo, I., Oh, E. S., Lee, K. Y., Lee, B. H., Johnson, R. J., & Kang, D. H. (2014). Uric acid induces fat accumulation via generation of endoplasmic reticulum stress and SREBP-1c activation in hepatocytes. *Laboratory Investigation*, *94*(10), 1114–1125. https://doi.org/10.1038/labinvest.2014.98

Chwalibog, A., & Thorbek, G. (2001). Energy expenditure by de novo lipogenesis . *British Journal of Nutrition*, *86*(2), 309–309. https://doi.org/10.1079/bjn2001401

Clapper, J. R., Hendricks, M. D., Gu, G., Wittmer, C., Dolman, C. S., Herich, J., Athanacio, J., Villescaz, C., Ghosh, S. S., Heilig, J. S., Lowe, C., & Roth, J. D. (2013). Diet-induced mouse model of fatty liver disease and nonalcoholic steatohepatitis reflecting clinical disease progression and methods of assessment. *American Journal of Physiology - Gastrointestinal and Liver Physiology*, *305*(7). https://doi.org/10.1152/ajpgi.00079.2013

Clarke, S. D., & Jump, D. B. (1996). Polyunsaturated fatty acid regulation of hepatic gene transcription. *Lipids*, *31*(3 SUPPL.). https://doi.org/10.1007/bf02637044

Cortez-Pinto, H., Jesus, L., Barros, H., Lopes, C., Moura, M. C., & Camilo, M. E. (2006). How different is the dietary pattern in non-alcoholic steatohepatitis patients? *Clinical Nutrition*, *25*(5), 816–823. https://doi.org/10.1016/j.clnu.2006.01.027

Cusi, K., Bril, F., Barb, D., Polidori, D., Sha, S., Ghosh, A., Farrell, K., Sunny, N. E., Kalavalapalli, S., Pettus, J., Ciaraldi, T. P., Mudaliar, S., & Henry, R. R. (2019). Effect of canagliflozin treatment on hepatic triglyceride content and glucose metabolism in patients with type 2 diabetes. *Diabetes, Obesity and Metabolism*, *21*(4), 812–821. https://doi.org/10.1111/dom.13584

Cusi, K., Orsak, B., Bril, F., Lomonaco, R., Hecht, J., Ortiz-Lopez, C., Tio, F., Hardies, J., Darland, C., Musi, N., Webb, A., & Portillo-Sanchez, P. (2016). Long-term pioglitazone treatment for patients with nonalcoholic steatohepatitis and prediabetes or type 2 diabetes mellitus a randomized trial. *Annals of Internal Medicine*, *165*(5), 305–315. https://doi.org/10.7326/M15-1774

Dai, G., Liu, P., Li, X., Zhou, X., & He, S. (2019). Association between PNPLA3 rs738409 polymorphism and nonalcoholic fatty liver disease (NAFLD) susceptibility and severity: A meta-analysis. In *Medicine (United States)* (Vol. 98, Issue 7). Lippincott Williams and Wilkins. https://doi.org/10.1097/MD.0000000000014324

Davies, M. J., D'Alessio, D. A., Fradkin, J., Kernan, W. N., Mathieu, C., Mingrone, G., Rossing, P., Tsapas, A., Wexler, D. J., & Buse, J. B. (2018). Management of hyperglycemia in type 2 diabetes, 2018. A consensus report by the American Diabetes Association (ADA) and the european association for the study of diabetes (EASD). In *Diabetes Care* (Vol. 41, Issue 12, pp. 2669–2701). American Diabetes Association Inc. https://doi.org/10.2337/dci18-0033

De Vadder, F., Kovatcheva-Datchary, P., Goncalves, D., Vinera, J., Zitoun, C., Duchampt, A., Bäckhed, F., & Mithieux, G. (2014). Microbiota-generated metabolites promote metabolic benefits via gut-brain neural circuits. *Cell*, *156*(1–2), 84–96. https://doi.org/10.1016/j.cell.2013.12.016

Delgada, T. C., Castra, M. M., Geraldes, C. F., & Jones, J. G. (2004). Quantitation of erythrocyte pentose pathway flux with [2- 13C]glucose and 1H NMR analysis of the lactate methyl signal. *Magnetic Resonance in Medicine*, *51*(6), 1283–1286. https://doi.org/10.1002/mrm.20096

Delgado, T. C., Pinheiro, D., Caldeira, M., Castro, M. M. C. A., Geraldes, C. F. G. C., López-Larrubia, P., Cerdán, S., & Jones, J. G. (2009). Sources of hepatic triglyceride accumulation during high-fat feeding in the healthy rat. *NMR in Biomedicine*, *22*(3), 310–317. https://doi.org/10.1002/nbm.1327

Delgado, Teresa C., Martins, F. O., Carvalho, F., Gonçalves, A., Scott, D. K., O'Doherty, R., Paula Macedo, M., & Jones, J. G. (2013). 2H enrichment distribution of hepatic glycogen from 2H2O reveals the contribution of dietary fructose to glycogen synthesis. *American Journal of Physiology - Endocrinology and Metabolism*, *304*(4). https://doi.org/10.1152/ajpendo.00185.2012

Diehl, A. M., & Day, C. (2017). Cause, Pathogenesis, and Treatment of Nonalcoholic Steatohepatitis. *New England Journal of Medicine*, *377*(21), 2063–2072. https://doi.org/10.1056/nejmra1503519

Ding, S., Chi, M. M., Scull, B. P., Rigby, R., Schwerbrock, N. M. J., Magness, S., Jobin, C., & Lund, P. K. (2010). High-fat diet: Bacteria interactions promote intestinal inflammation which precedes and correlates with obesity and insulin resistance in mouse. *PLoS ONE*, *5*(8). https://doi.org/10.1371/journal.pone.0012191

Diraison, F., Moulin, P. H., & Beylot, M. (2003). Contribution of hepatic de novo lipogenesis and reesterification of plasma non esterified fatty acids to plasma triglyceride synthesis during non-alcoholic fatty liver disease. *Diabetes and Metabolism*, *29*(5), 478–485. https://doi.org/10.1016/S1262-3636(07)70061-7

Diraison, F., Pachiaudi, C., & Beylot, M. (1996). In vivo measurement of plasma cholesterol and fatty acid synthesis with deuterated water: Determination of the average number of deuterium atoms incorporated. *Metabolism: Clinical and Experimental*, *45*(7), 817–821. https://doi.org/10.1016/S0026-0495(96)90152-3

Diraison, F., Pachiaudi, C., & Beylot, M. (1997). Measuring lipogenesis and cholesterol synthesis in humans with deuterated water: Use of simple gas chromatographic/mass spectrometric techniques. *Journal of Mass Spectrometry*, *32*(1), 81–86. https://doi.org/10.1002/(SICI)1096-9888(199701)32:1<81::AID-JMS454>3.0.CO;2-2

Diraison, Frédérique, Yankah, V., Letexier, D., Dusserre, E., Jones, P., & Beylot, M. (2003). Differences in the regulation of adipose tissue and liver lipogenesis by carbohydrates in humans. *Journal of Lipid Research*, *44*(4), 846–853. https://doi.org/10.1194/jlr.M200461-JLR200

Donati, B., Dongiovanni, P., Romeo, S., Meroni, M., McCain, M., Miele, L., Petta, S., Maier, S., Rosso, C., De Luca, L., Vanni, E., Grimaudo, S., Romagnoli, R., Colli, F., Ferri, F., Mancina, R. M., Iruzubieta, P., Craxi, A., Fracanzani, A. L., …

Valenti, L. (2017). MBOAT7 rs641738 variant and hepatocellular carcinoma in non-cirrhotic individuals. *Scientific Reports*, *7*(1). https://doi.org/10.1038/s41598-017-04991-0

Donati, B., Motta, B. M., Pingitore, P., Meroni, M., Pietrelli, A., Alisi, A., Petta, S., Xing, C., Dongiovanni, P., del Menico, B., Rametta, R., Mancina, R. M., Badiali, S., Fracanzani, A. L., Craxì, A., Fargion, S., Nobili, V., Romeo, S., & Valenti, L. (2016). The rs2294918 E434K variant modulates patatin-like phospholipase domain-containing 3 expression and liver damage. *Hepatology*, *63*(3), 787–798. https://doi.org/10.1002/hep.28370

Dongiovanni, P., Donati, B., Fares, R., Lombardi, R., Mancina, R. M., Romeo, S., & Valenti, L. (2013). PNPLA3 I148M polymorphism and progressive liver disease. In *World Journal of Gastroenterology* (Vol. 19, Issue 41, pp. 6969–6978). Baishideng Publishing Group Co. https://doi.org/10.3748/wjg.v19.i41.6969

Dongiovanni, P., Petta, S., Maglio, C., Fracanzani, A. L., Pipitone, R., Mozzi, E., Motta, B. M., Kaminska, D., Rametta, R., Grimaudo, S., Pelusi, S., Montalcini, T., Alisi, A., Maggioni, M., Kärjä, V., Borén, J., Käkelä, P., Di Marco, V., Xing, C., … Valenti, L. (2015). Transmembrane 6 superfamily member 2 gene variant disentangles nonalcoholic steatohepatitis from cardiovascular disease. *Hepatology*, *61*(2), 506–514. https://doi.org/10.1002/hep.27490

Dongiovanni, P., Romeo, S., & Valenti, L. (2015). Genetic factors in the pathogenesis of nonalcoholic fatty liver and steatohepatitis. In *BioMed Research International* (Vol. 2015). Hindawi Publishing Corporation. https://doi.org/10.1155/2015/460190

Donnan, J. R., Grandy, C. A., Chibrikov, E., Marra, C. A., Aubrey-Bassler, K., Johnston, K., Swab, M., Hache, J., Curnew, D., Nguyen, H., & Gamble, J. M. (2019). Comparative safety of the sodium glucose co-transporter 2 (SGLT2) inhibitors: A systematic review and meta-analysis. In *BMJ Open* (Vol. 9, Issue 1). BMJ Publishing Group. https://doi.org/10.1136/bmjopen-2018-022577

Donnelly, K. L., Smith, C. I., Schwarzenberg, S. J., Jessurun, J., Boldt, M. D., & Parks, E. J. (2005). Sources of fatty acids stored in liver and secreted via lipoproteins in patients with nonalcoholic fatty liver disease. *Journal of Clinical Investigation*, *115*(5), 1343–1351. https://doi.org/10.1172/JCI23621

Dowman, J. K., Hopkins, L. J., Reynolds, G. M., Nikolaou, N., Armstrong, M. J., Shaw,

J. C., Houlihan, D. D., Lalor, P. F., Tomlinson, J. W., Hübscher, S. G., & Newsome, P. N. (2014). Development of hepatocellular carcinoma in a murine model of nonalcoholic steatohepatitis induced by use of a high-fat/fructose diet and sedentary lifestyle. *American Journal of Pathology*, *184*(5), 1550–1561. https://doi.org/10.1016/j.ajpath.2014.01.034

Duarte, J. A. G., Carvalho, F., Pearson, M., Horton, J. D., Browning, J. D., Jones, J. G., & Burgess, S. C. (2014). A high-fat diet suppresses de novo lipogenesis and desaturation but not elongation and triglyceride synthesis in mice. *Journal of Lipid Research*, *55*(12), 2541–2553. https://doi.org/10.1194/jlr.M052308

El-Agroudy, N. N., Kurzbach, A., Rodionov, R. N., O'Sullivan, J., Roden, M., Birkenfeld, A. L., & Pesta, D. H. (2019). Are Lifestyle Therapies Effective for NAFLD Treatment? In *Trends in Endocrinology and Metabolism* (Vol. 30, Issue 10, pp. 701–709). Elsevier Inc. https://doi.org/10.1016/j.tem.2019.07.013

Eriksson, J. W., Lundkvist, P., Jansson, P. A., Johansson, L., Kvarnström, M., Moris, L., Miliotis, T., Forsberg, G. B., Risérus, U., Lind, L., & Oscarsson, J. (2018). Effects of dapagliflozin and n-3 carboxylic acids on non-alcoholic fatty liver disease in people with type 2 diabetes: a double-blind randomised placebo-controlled study. *Diabetologia*, *61*(9), 1923–1934. https://doi.org/10.1007/s00125-018-4675-2

Eslam, M., Sanyal, A. J., George, J., Sanyal, A., Neuschwander-Tetri, B., Tiribelli, C., Kleiner, D. E., Brunt, E., Bugianesi, E., Yki-Järvinen, H., Grønbæk, H., Cortez-Pinto, H., Fan, J., Valenti, L., Abdelmalek, M., Romero-Gomez, M., Rinella, M., Arrese, M., Bedossa, P., … Younossi, Z. (2020). MAFLD: A Consensus-Driven Proposed Nomenclature for Metabolic Associated Fatty Liver Disease. *Gastroenterology*, *158*(7), 1999-2014.e1. https://doi.org/10.1053/j.gastro.2019.11.312

Estadella, D., Da Penha Oller Do Nascimento, C. M., Oyama, L. M., Ribeiro, E. B., Dâmaso, A. R., & De Piano, A. (2013). Lipotoxicity: Effects of dietary saturated and transfatty acids. In *Mediators of Inflammation* (Vol. 2013). Mediators Inflamm. https://doi.org/10.1155/2013/137579

Fan, J. G., Zhu, J., Li, X. J., Chen, L., Li, L., Dai, F., Li, F., & Chen, S. Y. (2005). Prevalence of and risk factors for fatty liver in a general population of Shanghai, China. *Journal of Hepatology*, *43*(3), 508–514.

https://doi.org/10.1016/j.jhep.2005.02.042

Fan, J., Ye, J., Kamphorst, J. J., Shlomi, T., Thompson, C. B., & Rabinowitz, J. D. (2014). Quantitative flux analysis reveals folate-dependent NADPH production. *Nature*, *510*(7504), 298–302. https://doi.org/10.1038/nature13236

Febbraio, M. A., Reibe, S., Shalapour, S., Ooi, G. J., Watt, M. J., & Karin, M. (2019). Preclinical Models for Studying NASH-Driven HCC: How Useful Are They? In *Cell Metabolism* (Vol. 29, Issue 1, pp. 18–26). Cell Press. https://doi.org/10.1016/j.cmet.2018.10.012

Fechner, A., Kiehntopf, M., & Jahreis, G. (2014). The formation of short-chain fatty acids is positively associated with the blood lipid-lowering effect of lupin kernel fiber in moderately hypercholesterolemic adults. *Journal of Nutrition*, *144*(5), 599–607. https://doi.org/10.3945/jn.113.186858

Feng, W., Gao, C., Bi, Y., Wu, M., Li, P., Shen, S., Chen, W., Yin, T., & Zhu, D. (2017). Randomized trial comparing the effects of gliclazide, liraglutide, and metformin on diabetes with non-alcoholic fatty liver disease. *Journal of Diabetes*, *9*(8), 800–809. https://doi.org/10.1111/1753-0407.12555

Filipova, E., Uzunova, K., Kalinov, K., & Vekov, T. (2017). Pioglitazone and the Risk of Bladder Cancer: A Meta-Analysis. In *Diabetes Therapy* (Vol. 8, Issue 4, pp. 705–726). Springer Healthcare. https://doi.org/10.1007/s13300-017-0273-4

Forcheron, F., Cachefo, A., Thevenon, S., Pinteur, C., & Beylot, M. (2002). Mechanisms of the triglyceride- and cholesterol-lowering effect of fenofibrate in hyperlipidemic type 2 diabetic patients. *Diabetes*, *51*(12), 3486–3491. https://doi.org/10.2337/diabetes.51.12.3486

Foster, D. W. (2012). Malonyl-CoA: The regulator of fatty acid synthesis and oxidation. In *Journal of Clinical Investigation* (Vol. 122, Issue 6, pp. 1958–1959). J Clin Invest. https://doi.org/10.1172/JCI63967

Frederiks, W. M., & Vreeling-Sindelárová, H. (2001). Localization of glucose-6-phosphate dehydrogenase activity on ribosomes of granular endoplasmic reticulum, in peroxisomes and peripheral cytoplasm of rat liver parenchymal cells. *Histochemical Journal*, *33*(6), 345–353. https://doi.org/10.1023/A:1012427224822

Friedman, S. L., Neuschwander-Tetri, B. A., Rinella, M., & Sanyal, A. J. (2018). Mechanisms of NAFLD development and therapeutic strategies. *Nat Med*, *24*(7), 908–922. https://doi.org/10.1038/s41591-018-0104-9

Frøssing, S., Nylander, M., Chabanova, E., Frystyk, J., Holst, J. J., Kistorp, C., Skouby, S. O., & Faber, J. (2018). Effect of liraglutide on ectopic fat in polycystic ovary syndrome: A randomized clinical trial. *Diabetes, Obesity and Metabolism*, *20*(1), 215–218. https://doi.org/10.1111/dom.13053

Fu, J. F., Fang, Y. L., Liang, L., Wang, C. L., Hong, F., & Dong, G. P. (2009). A rabbit model of pediatric nonalcoholic steatohepatitis: The role of adiponectin. *World Journal of Gastroenterology*, *15*(8), 912–918. https://doi.org/10.3748/wjg.15.912

Fujii, M., Shibazaki, Y., Wakamatsu, K., Honda, Y., Kawauchi, Y., Suzuki, K., Arumugam, S., Watanabe, K., Ichida, T., Asakura, H., & Yoneyama, H. (2013). A murine model for non-alcoholic steatohepatitis showing evidence of association between diabetes and hepatocellular carcinoma. *Medical Molecular Morphology*, *46*(3), 141–152. https://doi.org/10.1007/s00795-013-0016-1

Funk, A. M., Anderson, B. L., Wen, X., Hever, T., Khemtong, C., Kovacs, Z., Sherry, A. D., & Malloy, C. R. (2017). The rate of lactate production from glucose in hearts is not altered by per-deuteration of glucose. *Journal of Magnetic Resonance*, *284*, 86–93. https://doi.org/10.1016/j.jmr.2017.09.007

Funk, A. M., Wen, X., Hever, T., Maptue, N. R., Khemtong, C., Sherry, A. D., & Malloy, C. R. (2019). Effects of deuteration on transamination and oxidation of hyperpolarized 13 C-Pyruvate in the isolated heart. *Journal of Magnetic Resonance*, *301*, 102–108. https://doi.org/10.1016/j.jmr.2019.03.003

Garaulet, M., Pérez-Llamas, F., Pérez-Ayala, M., Martínez, P., Sánchez De Medina, F., Tebar, F. J., & Zamora, S. (2001). Site-specific differences in the fatty acid composition of abdominal adipose tissue in an obese population from a mediterranean area: Relation with dietary fatty acids, plasma lipid profile, serum insulin, and central obesity. *American Journal of Clinical Nutrition*, *74*(5), 585–591. https://doi.org/10.1093/ajcn/74.5.585

García-Ruiz, I., Solís-Muñoz, P., Fernández-Moreira, D., Grau, M., Colina, F., Muñoz-Yagüe, T., & Solís-Herruzo, J. A. (2014). High-fat diet decreases activity of the oxidative phosphorylation complexes and causes nonalcoholic steatohepatitis in mice. *DMM Disease Models and Mechanisms*, *7*(11), 1287–1296. https://doi.org/10.1242/dmm.016766

Gasparin, F. R. S., Carreño, F. O., Mewes, J. M., Gilglioni, E. H., Pagadigorria, C. L. S., Natali, M. R. M., Utsunomiya, K. S., Constantin, R. P., Ouchida, A. T., Curti,

C., Gaemers, I. C., Elferink, R. P. J. O., Constantin, J., & Ishii-Iwamoto, E. L. (2018). Sex differences in the development of hepatic steatosis in cafeteria diet-induced obesity in young mice. *Biochimica et Biophysica Acta - Molecular Basis of Disease*, *1864*(7), 2495–2509. https://doi.org/10.1016/j.bbadis.2018.04.004

Gastaldelli, A., & Cusi, K. (2019). From NASH to diabetes and from diabetes to NASH: Mechanisms and treatment options. *JHEP Reports*, *1*(4), 312–328. https://doi.org/10.1016/j.jhepr.2019.07.002

Gastaldelli, A., Gaggini, M., Daniele, G., Ciociaro, D., Cersosimo, E., Tripathy, D., Triplitt, C., Fox, P., Musi, N., DeFronzo, R., & Iozzo, P. (2016). Exenatide improves both hepatic and adipose tissue insulin resistance: A dynamic positron emission tomography study. *Hepatology*, *64*(6), 2028–2037. https://doi.org/10.1002/hep.28827

Giles, D. A., Moreno-Fernandez, M. E., Stankiewicz, T. E., Graspeuntner, S., Cappelletti, M., Wu, D., Mukherjee, R., Chan, C. C., Lawson, M. J., Klarquist, J., Sünderhauf, A., Softic, S., Kahn, C. R., Stemmer, K., Iwakura, Y., Aronow, B. J., Karns, R., Steinbrecher, K. A., Karp, C. L., … Divanovic, S. (2017). Thermoneutral housing exacerbates nonalcoholic fatty liver disease in mice and allows for sex-independent disease modeling. *Nature Medicine*, *23*(7), 829–838. https://doi.org/10.1038/nm.4346

Ginsberg, H. N., Zhang, Y. L., & Hernandez-Ono, A. (2005). Regulation of plasma triglycerides in insulin resistance and diabetes. In *Archives of Medical Research* (Vol. 36, Issue 3, pp. 232–240). Arch Med Res. https://doi.org/10.1016/j.arcmed.2005.01.005

Gluud, L. L., Knop, F. K., & Vilsbøll, T. (2014). Effects of lixisenatide on elevated liver transaminases: Systematic review with individual patient data meta-analysis of randomised controlled trials on patients with type 2 diabetes. *BMJ Open*, *4*(12). https://doi.org/10.1136/bmjopen-2014-005325

Goffredo, M., Mass, K., Parks, E. J., Wagner, D. A., McClure, E. A., Graf, J., Savoye, M., Pierpont, B., Cline, G., & Santoro, N. (2016). Role of gut microbiota and short chain fatty acids in modulating energy harvest and fat partitioning in youth. *Journal of Clinical Endocrinology and Metabolism*, *101*(11), 4367–4376. https://doi.org/10.1210/jc.2016-1797

Gouk, S. W., Cheng, S. F., Ong, A. S. H., & Chuah, C. H. (2012). Rapid and direct

quantitative analysis of positional fatty acids in triacylglycerols using 13C NMR. *European Journal of Lipid Science and Technology*, *114*(5), 510–519. https://doi.org/10.1002/ejlt.201100074

Gross, B., Pawlak, M., Lefebvre, P., & Staels, B. (2017). PPARs in obesity-induced T2DM, dyslipidaemia and NAFLD. In *Nature Reviews Endocrinology* (Vol. 13, Issue 1, pp. 36–49). Nature Publishing Group. https://doi.org/10.1038/nrendo.2016.135

Hamblin, P. S., Wong, R., Ekinci, E. I., Fourlanos, S., Shah, S., Jones, A. R., Hare, M. J. L., Calder, G. L., Epa, D. S., George, E. M., Giri, R., Kotowicz, M. A., Kyi, M., Lafontaine, N., Macisaac, R. J., Nolan, B. J., O'Neal, D. N., Renouf, D., Varadarajan, S., … Bach, L. A. (2019). SGLT2 Inhibitors Increase the Risk of Diabetic Ketoacidosis Developing in the Community and during Hospital Admission. *Journal of Clinical Endocrinology and Metabolism*, *104*(8), 3077–3087. https://doi.org/10.1210/jc.2019-00139

Hamilton, J. G., & Comai, K. (1988). Rapid separation of neutral lipids, free fatty acids and polar lipids using prepacked silica sep-Pak columns. *Lipids*, *23*(12), 1146–1149. https://doi.org/10.1007/BF02535281

Hardy, T., Oakley, F., Anstee, Q. M., & Day, C. P. (2016). Nonalcoholic Fatty Liver Disease: Pathogenesis and Disease Spectrum. *Annual Review of Pathology: Mechanisms of Disease*, *11*, 451–496. https://doi.org/10.1146/annurev-pathol-012615-044224

He, Y. L., Haynes, W., Meyers, C. D., Amer, A., Zhang, Y., Mahling, P., Mendonza, A. E., Ma, S., Chutkow, W., & Bachman, E. (2019). The effects of licogliflozin, a dual SGLT1/2 inhibitor, on body weight in obese patients with or without diabetes. *Diabetes, Obesity and Metabolism*, *21*(6), 1311–1321. https://doi.org/10.1111/dom.13654

Hellerstein, M. K. (1999). De novo lipogenesis in humans: Metabolic and regulatory aspects. *European Journal of Clinical Nutrition*, *53*, s53–s65. https://doi.org/10.1038/sj.ejcn.1600744

Hellerstein, M. K., Kletke, C., Kaempfer, S., Wu, K., & Shackleton, C. H. L. (1991). Use of mass isotopomer distributions in secreted lipids to sample lipogenic acetyl-CoA pool in vivo in humans. *American Journal of Physiology - Endocrinology and Metabolism*, *261*(4 24-4). https://doi.org/10.1152/ajpendo.1991.261.4.e479

Hellerstein, M. K., & Neese, R. A. (1992). Mass isotopomer distribution analysis: A technique for measuring biosynthesis and turnover of polymers. *American Journal of Physiology - Endocrinology and Metabolism*, *263*(5 26-5). https://doi.org/10.1152/ajpendo.1992.263.5.e988

Hickman, I. J., Jonsson, J. R., Prins, J. B., Ash, S., Purdie, D. M., Clouston, A. D., & Powell, E. E. (2004). Modest weight loss and physical activity in overweight patients with chronic liver disease results in sustained improvements in alanine aminotransferase, fasting insulin, and quality of life. *Gut*, *53*(3), 413–419. https://doi.org/10.1136/gut.2003.027581

Higuchi, N., Kato, M., Shundo, Y., Tajiri, H., Tanaka, M., Yamashita, N., Kohjima, M., Kotoh, K., Nakamuta, M., Takayanagi, R., & Enjoji, M. (2008). Liver X receptor in cooperation with SREBP-1c is a major lipid synthesis regulator in nonalcoholic fatty liver disease. *Hepatology Research*, *38*(11), 1122–1129. https://doi.org/10.1111/j.1872-034X.2008.00382.x

Hooper, A. J., Adams, L. A., & Burnett, J. R. (2011). Thematic review series: Genetics of human lipid diseases - Genetic determinants of hepatic steatosis in man. In *Journal of Lipid Research* (Vol. 52, Issue 4, pp. 593–617). American Society for Biochemistry and Molecular Biology Inc. https://doi.org/10.1194/jlr.R008896

Horie, Y., Suzuki, A., Kataoka, E., Sasaki, T., Hamada, K., Sasaki, J., Mizuno, K., Hasegawa, G., Kishimoto, H., Iizuka, M., Naito, M., Enomoto, K., Watanabe, S., Mak, T. W., & Nakano, T. (2004). Hepatocyte-specific Pten deficiency results in steatohepatitis and hepatocellular carcinomas. *Journal of Clinical Investigation*, *113*(12), 1774–1783. https://doi.org/10.1172/JCI20513

Huang, Z., Guo, X., Zhang, G., Liang, L., & Nong, B. (2019). Correlation between PNPLA3 rs738409 polymorphism and hepatocellular carcinoma: a meta-analysis of 10,330 subjects. *International Journal of Biological Markers*, *34*(2), 117–122. https://doi.org/10.1177/1724600818812471

Hummel, K. P., Dickie, M. M., & Coleman, D. L. (1966). Diabetes, a new mutation in the mouse. *Science*, *153*(3740), 1127–1128. https://doi.org/10.1126/science.153.3740.1127

Ibrahim, S. H., Hirsova, P., Malhi, H., & Gores, G. J. (2016). Animal Models of Nonalcoholic Steatohepatitis: Eat, Delete, and Inflame. In *Digestive Diseases and Sciences* (Vol. 61, Issue 5, pp. 1325–1336). Springer New York LLC.

https://doi.org/10.1007/s10620-015-3977-1

Ito, D., Shimizu, S., Inoue, K., Saito, D., Yanagisawa, M., Inukai, K., Akiyama, Y., Morimoto, Y., Noda, M., & Shimada, A. (2017). Comparison of Ipragliflozin and Pioglitazone effects on Nonalcoholic fatty liver disease in patients with type 2 diabetes: A randomized, 24-week, open-label, active-controlled trial. *Diabetes Care*, *40*(10), 1364–1372. https://doi.org/10.2337/dc17-0518

Jensen, V. S., Hvid, H., Damgaard, J., Nygaard, H., Ingvorsen, C., Wulff, E. M., Lykkesfeldt, J., & Fledelius, C. (2018). Dietary fat stimulates development of NAFLD more potently than dietary fructose in Sprague–Dawley rats. *Diabetology & Metabolic Syndrome*, *10*(1), 4. https://doi.org/10.1186/s13098-018-0307-8

Jin, E. S., Lee, M. H., Murphy, R. E., & Malloy, C. R. (2018). Pentose phosphate pathway activity parallels lipogenesis but not antioxidant processes in rat liver. *American Journal of Physiology - Endocrinology and Metabolism*, *314*(6), E543–E551. https://doi.org/10.1152/ajpendo.00342.2017

Jin, E. S., Sherry, A. D., & Malloy, C. R. (2014). Interaction between the pentose phosphate pathway and gluconeogenesis from glycerol in the liver. *Journal of Biological Chemistry*, *289*(47), 32593–32603. https://doi.org/10.1074/jbc.M114.577692

Jin, E. S., Sherry, A. D., & Malloy, C. R. (2016). An oral load of [13C3]glycerol and blood NMR analysis detect fatty acid esterification, pentose phosphate pathway, and glycerol metabolism through the tricarboxylic acid cycle in human liver. *Journal of Biological Chemistry*, *291*(36), 19031–19041. https://doi.org/10.1074/jbc.M116.742262

Johnson, N. A., Sachinwalla, T., Walton, D. W., Smith, K., Armstrong, A., Thompson, M. W., & George, J. (2009). Aerobic exercise training reduces hepatic and visceral lipids in obese individuals without weight loss. *Hepatology*, *50*(4), 1105–1112. https://doi.org/10.1002/hep.23129

Jones, J., Barosa, C., Gomes, F., Carina Mendes, A., Delgado, T., Diogo, L., Garcia, P., Bastos, M., Barros, L., Fagulha, A., Baptista, C., Carvalheiro, M., & Madalena Caldeira, M. (2006). NMR Derivatives for quantification of 2H and 13C-enrichment of human glucuronide from metabolic tracers. *Journal of Carbohydrate Chemistry*, *25*(2–3), 203–217. https://doi.org/10.1080/07328300600732840

Jones, J. G. (2014). Identifying Sources of Hepatic Lipogenic Acetyl-CoA Using Stable

Isotope Tracers and NMR. *Advances in Radiology*, *2014*, 1–9. https://doi.org/10.1155/2014/109252

Jones, J. G., Merritt, M., Malloy, C., Nell, M., & Rogers, R. B. (2001). Quantifying Tracer Levels of 2 H 2 O Enrichment From Microliter Amounts of Plasma and Urine by 2 H NMR. In *Magnetic Resonance in Medicine* (Vol. 45). https://doi.org/10.1002/1522-2594

Kalavalapalli, S., Bril, F., Guingab, J., Vergara, A., Garrett, T. J., Sunny, N. E., & Cusi, K. (2019). Impact of exenatide on mitochondrial lipid metabolism in mice with nonalcoholic steatohepatitis. *Journal of Endocrinology*, *241*(3), 293–305. https://doi.org/10.1530/JOE-19-0007

Kammoun, H. L., Allen, T. L., Henstridge, D. C., Kraakman, M. J., Peijs, L., Rose-John, S., & Febbraio, M. A. (2017). Over-expressing the soluble gp130-Fc does not ameliorate methionine and choline deficient diet-induced non alcoholic steatohepatitis in mice. *PLoS ONE*, *12*(6). https://doi.org/10.1371/journal.pone.0179099

Kawano, Y., & Cohen, D. E. (2013). Mechanisms of hepatic triglyceride accumulation in non-alcoholic fatty liver disease. In *Journal of Gastroenterology* (Vol. 48, Issue 4, pp. 434–441). J Gastroenterol. https://doi.org/10.1007/s00535-013-0758-5

Keating, S. E., Hackett, D. A., George, J., & Johnson, N. A. (2012). Exercise and non-alcoholic fatty liver disease: A systematic review and meta-analysis. *Journal of Hepatology*, *57*(1), 157–166. https://doi.org/10.1016/j.jhep.2012.02.023

Kechagias, S., Emersson, Å., Dahlqvist, O., Lundberg, P., Lindström, T., & Nystrom, F. H. (2008). Fast-food-based hyper-alimentation can induce rapid and profound elevation of serum alanine aminotransferase in healthy subjects. *Gut*, *57*(5), 649–654. https://doi.org/10.1136/gut.2007.131797

Khan, R. S., Bril, F., Cusi, K., & Newsome, P. N. (2019). Modulation of Insulin Resistance in Nonalcoholic Fatty Liver Disease. In *Hepatology* (Vol. 70, Issue 2, pp. 711–724). John Wiley and Sons Inc. https://doi.org/10.1002/hep.30429

Kim, D. S., Jackson, A. U., Li, Y. K., Stringham, H. M., Kuusisto, J., Kangas, A. J., Soininen, P., Ala-Korpela, M., Burant, C. F., Salomaa, V., Boehnke, M., Laakso, M., & Speliotes, E. K. (2017). Novel association of TM6SF2 rs58542926 genotype with increased serum tyrosine levels and decreased apoB-100 particles in finns. *Journal of Lipid Research*, *58*(7), 1471–1481. https://doi.org/10.1194/jlr.P076034

Kim, H. J., Takahashi, M., & Ezaki, O. (1999). Fish oil feeding decreases mature sterol regulatory element-binding protein 1 (SREBP-1) by down-regulation of SREBP-1c mRNA in mouse liver. A possible mechanism for down-regulation of lipogenic enzyme mRNAs. *Journal of Biological Chemistry*, *274*(36), 25892–25898. https://doi.org/10.1074/jbc.274.36.25892

Kintscher, U. (2008). Pharmacological Differences of Glitazones. Does Peroxisome Proliferator-Activated Receptor-α Activation Make the Difference?**Editorials published in the Journal of the American College of Cardiology reflect the views of the authors and do not necessarily represent the views of JACC or the American College of Cardiology. In *Journal of the American College of Cardiology* (Vol. 52, Issue 10, pp. 882–884). J Am Coll Cardiol. https://doi.org/10.1016/j.jacc.2008.06.012

Knebel, B., Haas, J., Hartwig, S., Jacob, S., Köllmer, C., Nitzgen, U., Muller-Wieland, D., & Kotzka, J. (2012). Liver-specific expression of transcriptionally active srebp-1c is associated with fatty liver and increased visceral fat mass. *PLoS ONE*, *7*(2). https://doi.org/10.1371/journal.pone.0031812

Kohjima, M., Enjoji, M., Higuchi, N., Kato, M., Kotoh, K., Yoshimoto, T., Fujino, T., Yada, M., Yada, R., Harada, N., Takayanagi, R., & Nakamuta, M. (2007). Re-evaluation of fatty acid metabolism-related gene expression in nonalcoholic fatty liver disease. *International Journal of Molecular Medicine*, *20*(3), 351–358. https://doi.org/10.3892/ijmm.20.3.351

Kotronen, A., Peltonen, M., Hakkarainen, A., Sevastianova, K., Bergholm, R., Johansson, L. M., Lundbom, N., Rissanen, A., Ridderstråle, M., Groop, L., Orho-Melander, M., & Yki-Järvinen, H. (2009). Prediction of Non-Alcoholic Fatty Liver Disease and Liver Fat Using Metabolic and Genetic Factors. *Gastroenterology*, *137*(3), 865–872. https://doi.org/10.1053/j.gastro.2009.06.005

Kotronen, A., Velagapudi, V. R., Yetukuri, L., Westerbacka, J., Bergholm, R., Ekroos, K., Makkonen, J., Taskinen, M. R., Orešič, M., & Yki-Järvinen, H. (2009). Serum saturated fatty acids containing triacylglycerols are better markers of insulin resistance than total serum triacylglycerol concentrations. *Diabetologia*, *52*(4), 684–690. https://doi.org/10.1007/s00125-009-1282-2

Kowalik, M. A., Columbano, A., & Perra, A. (2017). Emerging role of the pentose phosphate pathway in hepatocellular carcinoma. In *Frontiers in Oncology* (Vol. 7,

Issue MAY). Frontiers Media S.A. https://doi.org/10.3389/fonc.2017.00087

Kozlitina, J., Smagris, E., Stender, S., Nordestgaard, B. G., Zhou, H. H., Tybjærg-Hansen, A., Vogt, T. F., Hobbs, H. H., & Cohen, J. C. (2014). Exome-wide association study identifies a TM6SF2 variant that confers susceptibility to nonalcoholic fatty liver disease. *Nature Genetics*, *46*(4), 352–356. https://doi.org/10.1038/ng.2901

Kuchay, M. S., Krishan, S., Mishra, S. K., Farooqui, K. J., Singh, M. K., Wasir, J. S., Bansal, B., Kaur, P., Jevalikar, G., Gill, H. K., Choudhary, N. S., & Mithal, A. (2018). Effect of empagliflozin on liver fat in patients with type 2 diabetes and nonalcoholic fatty liver disease: A randomized controlled trial (E-LIFT Trial). *Diabetes Care*, *41*(8), 1801–1808. https://doi.org/10.2337/dc18-0165

Lai, C. Y., Lin, C. Y., Hsu, C. C., Yeh, K. Y., & Her, G. M. (2018). Liver-directed microRNA-7a depletion induces nonalcoholic fatty liver disease by stabilizing YY1-mediated lipogenic pathways in zebrafish. *Biochimica et Biophysica Acta - Molecular and Cell Biology of Lipids*, *1863*(8), 844–856. https://doi.org/10.1016/j.bbalip.2018.04.009

Lambert, J. E., Ramos-Roman, M. A., Browning, J. D., & Parks, E. J. (2014). Increased de novo lipogenesis is a distinct characteristic of individuals with nonalcoholic fatty liver disease. *Gastroenterology*, *146*(3), 726–735. https://doi.org/10.1053/j.gastro.2013.11.049

Lamonte, M. J., Blair, S. N., & Church, T. S. (2005). Physical activity and diabetes prevention. In *Journal of Applied Physiology* (Vol. 99, Issue 3, pp. 1205–1213). J Appl Physiol (1985). https://doi.org/10.1152/japplphysiol.00193.2005

Lanaspa, M. A., Sanchez-Lozada, L. G., Choi, Y. J., Cicerchi, C., Kanbay, M., Roncal-Jimenez, C. A., Ishimoto, T., Li, N., Marek, G., Duranay, M., Schreiner, G., Rodriguez-Iturbe, B., Nakagawa, T., Kang, D. H., Sautin, Y. Y., & Johnson, R. J. (2012). Uric acid induces hepatic steatosis by generation of mitochondrial oxidative stress: Potential role in fructose-dependent and -independent fatty liver. *Journal of Biological Chemistry*, *287*(48), 40732–40744. https://doi.org/10.1074/jbc.M112.399899

Latva-Rasku, A., Honka, M. J., Kullberg, J., Mononen, N., Lehtimäki, T., Saltevo, J., Kirjavainen, A. K., Saunavaara, V., Iozzo, P., Johansson, L., Oscarsson, J., Hannukainen, J. C., & Nuutila, P. (2019). The SGLT2 inhibitor dapagliflozin

reduces liver fat but does not affect tissue insulin sensitivity: A randomized, double-blind, placebo-controlled study with 8-week treatment in type 2 diabetes patients. *Diabetes Care*, *42*(5), 931–937. https://doi.org/10.2337/dc18-1569

Lawitz, E. J., Coste, A., Poordad, F., Alkhouri, N., Loo, N., McColgan, B. J., Tarrant, J. M., Nguyen, T., Han, L., Chung, C., Ray, A. S., McHutchison, J. G., Subramanian, G. M., Myers, R. P., Middleton, M. S., Sirlin, C., Loomba, R., Nyangau, E., Fitch, M., … Hellerstein, M. (2018). Acetyl-CoA Carboxylase Inhibitor GS-0976 for 12 Weeks Reduces Hepatic De Novo Lipogenesis and Steatosis in Patients With Nonalcoholic Steatohepatitis. *Clinical Gastroenterology and Hepatology*, *16*(12), 1983-1991.e3. https://doi.org/10.1016/j.cgh.2018.04.042

Leamy, A. K., Egnatchik, R. A., & Young, J. D. (2013). Molecular mechanisms and the role of saturated fatty acids in the progression of non-alcoholic fatty liver disease. In *Progress in Lipid Research* (Vol. 52, Issue 1, pp. 165–174). Prog Lipid Res. https://doi.org/10.1016/j.plipres.2012.10.004

Lee, L., Alloosh, M., Saxena, R., Van Alstine, W., Watkins, B. A., Klaunig, J. E., Sturek, M., & Chalasani, N. (2009). Nutritional model of steatohepatitis and metabolic syndrome in the Ossabaw miniature swine. *Hepatology*, *50*(1), 56–67. https://doi.org/10.1002/hep.22904

Lee, M. H., Malloy, C. R., Corbin, I. R., Li, J., & Jin, E. S. (2019). Assessing the pentose phosphate pathway using [2, 3-13C2]glucose. *NMR in Biomedicine*, *32*(6). https://doi.org/10.1002/nbm.4096

Lee, W. N. P., Bassilian, S., Ajie, H. O., Schoeller, D. A., Edmond, J., Bergner, E. A., & Byerley, L. O. (1994). In vivo measurement of fatty acids and cholesterol synthesis using D2O and mass isotopomer analysis. *American Journal of Physiology - Endocrinology and Metabolism*, *266*(5 29-5). https://doi.org/10.1152/ajpendo.1994.266.5.e699

Lee, W. N. P., Bassilian, S., Guo, Z., Schoeller, D., Edmond, J., Bergner, E. A., & Byerley, L. O. (1994). Measurement of fractional lipid synthesis using deuterated water (2H2O) and mass isotopomer analysis. *American Journal of Physiology - Endocrinology and Metabolism*, *266*(3 29-3). https://doi.org/10.1152/ajpendo.1994.266.3.e372

Leitch, C. A., & Jones, P. J. H. (1993). Measurement of human lipogenesis using deuterium incorporation. *Journal of Lipid Research*, *34*(1), 157–163.

https://doi.org/10.1016/s0022-2275(20)41329-x

Lepage, P., Hösler, R., Spehlmann, M. E., Rehman, A., Zvirbliene, A., Begun, A., Ott, S., Kupcinskas, L., Doré, J., Raedler, A., & Schreiber, S. (2011). Twin study indicates loss of interaction between microbiota and mucosa of patients with ulcerative colitis. *Gastroenterology*, *141*(1), 227–236. https://doi.org/10.1053/j.gastro.2011.04.011

Lewis, C. A., Parker, S. J., Fiske, B. P., McCloskey, D., Gui, D. Y., Green, C. R., Vokes, N. I., Feist, A. M., Vander Heiden, M. G., & Metallo, C. M. (2014). Tracing Compartmentalized NADPH Metabolism in the Cytosol and Mitochondria of Mammalian Cells. *Molecular Cell*, *55*(2), 253–263. https://doi.org/10.1016/j.molcel.2014.05.008

Lewis, G. F., Carpentier, A., Adeli, K., & Giacca, A. (2002). Disordered fat storage and mobilization in the pathogenesis of insulin resistance and type 2 diabetes. In *Endocrine Reviews* (Vol. 23, Issue 2, pp. 201–229). Endocrine Society. https://doi.org/10.1210/edrv.23.2.0461

Lian, C. Y., Zhai, Z. Z., Li, Z. F., & Wang, L. (2020). High fat diet-triggered non-alcoholic fatty liver disease: A review of proposed mechanisms. In *Chemico-Biological Interactions* (Vol. 330, p. 109199). Elsevier Ireland Ltd. https://doi.org/10.1016/j.cbi.2020.109199

Library, W. O., Ka, J., Lau, C., Zhang, X., & Yu, J. (2017). Animal models of non-alcoholic fatty liver disease: current perspectives and recent advances. *Journal of Pathology J Pathol*, *241*, 36–44. https://doi.org/10.1002/path.4829

Lim, J. S., Mietus-Snyder, M., Valente, A., Schwarz, J. M., & Lustig, R. H. (2010). The role of fructose in the pathogenesis of NAFLD and the metabolic syndrome. In *Nature Reviews Gastroenterology and Hepatology* (Vol. 7, Issue 5, pp. 251–264). Nature Publishing Group. https://doi.org/10.1038/nrgastro.2010.41

Liss, K. H. H., & Finck, B. N. (2017). PPARs and nonalcoholic fatty liver disease. In *Biochimie* (Vol. 136, pp. 65–74). Elsevier B.V. https://doi.org/10.1016/j.biochi.2016.11.009

Liu, Y. L., Reeves, H. L., Burt, A. D., Tiniakos, D., McPherson, S., Leathart, J. B. S., Allison, M. E. D., Alexander, G. J., Piguet, A. C., Anty, R., Donaldson, P., Aithal, G. P., Francque, S., Van Gaal, L., Clement, K., Ratziu, V., Dufour, J. F., Day, C. P., Daly, A. K., & Anstee, Q. M. (2014). TM6SF2 rs58542926 influences hepatic

fibrosis progression in patients with non-alcoholic fatty liver disease. *Nature Communications*, *5*. https://doi.org/10.1038/ncomms5309

Liu, Z., Que, S., Zhou, L., & Zheng, S. (2015). Dose-response Relationship of Serum Uric Acid with Metabolic Syndrome and Non-alcoholic Fatty Liver Disease Incidence: A Meta-analysis of Prospective Studies. *Scientific Reports*, *5*. https://doi.org/10.1038/srep14325

Lomonaco, R., Ortiz-Lopez, C., Orsak, B., Webb, A., Hardies, J., Darland, C., Finch, J., Gastaldelli, A., Harrison, S., Tio, F., & Cusi, K. (2012). Effect of adipose tissue insulin resistance on metabolic parameters and liver histology in obese patients with nonalcoholic fatty liver disease. *Hepatology*, *55*(5), 1389–1397. https://doi.org/10.1002/hep.25539

Loomba, R., Kayali, Z., Noureddin, M., Ruane, P., Lawitz, E. J., Bennett, M., Wang, L., Harting, E., Tarrant, J. M., McColgan, B. J., Chung, C., Ray, A. S., Subramanian, G. M., Myers, R. P., Middleton, M. S., Lai, M., Charlton, M., & Harrison, S. A. (2018). GS-0976 Reduces Hepatic Steatosis and Fibrosis Markers in Patients With Nonalcoholic Fatty Liver Disease. *Gastroenterology*, *155*(5), 1463-1473.e6. https://doi.org/10.1053/j.gastro.2018.07.027

Lupsa, B. C., & Inzucchi, S. E. (2018). Use of SGLT2 inhibitors in type 2 diabetes: weighing the risks and benefits. In *Diabetologia* (Vol. 61, Issue 10, pp. 2118–2125). Springer Verlag. https://doi.org/10.1007/s00125-018-4663-6

Luukkonen, P. K., Zhou, Y., Hyötyläinen, T., Leivonen, M., Arola, J., Orho-Melander, M., Orešič, M., & Yki-Järvinen, H. (2016). The MBOAT7 variant rs641738 alters hepatic phosphatidylinositols and increases severity of non-alcoholic fatty liver disease in humans. In *Journal of Hepatology* (Vol. 65, Issue 6, pp. 1263–1265). Elsevier B.V. https://doi.org/10.1016/j.jhep.2016.07.045

Luukkonen, P. K., Zhou, Y., Nidhina Haridas, P. A., Dwivedi, O. P., Hyötyläinen, T., Ali, A., Juuti, A., Leivonen, M., Tukiainen, T., Ahonen, L., Scott, E., Palmer, J. M., Arola, J., Orho-Melander, M., Vikman, P., Anstee, Q. M., Olkkonen, V. M., Orešič, M., Groop, L., & Yki-Järvinen, H. (2017). Impaired hepatic lipid synthesis from polyunsaturated fatty acids in TM6SF2 E167K variant carriers with NAFLD. *Journal of Hepatology*, *67*(1), 128–136. https://doi.org/10.1016/j.jhep.2017.02.014

Ma, J., Fox, C. S., Jacques, P. F., Speliotes, E. K., Hoffmann, U., Smith, C. E., Saltzman, E., & McKeown, N. M. (2015). Sugar-sweetened beverage, diet soda,

and fatty liver disease in the Framingham Heart Study cohorts. *Journal of Hepatology*, *63*(2), 462–469. https://doi.org/10.1016/j.jhep.2015.03.032

Machado, M. V., Michelotti, G. A., Xie, G., De Almeida, T. P., Boursier, J., Bohnic, B., Guy, C. D., & Diehl, A. M. (2015). Mouse models of diet-induced nonalcoholic steatohepatitis reproduce the heterogeneity of the human disease. *PLoS ONE*, *10*(5). https://doi.org/10.1371/journal.pone.0127991

Maersk, M., Belza, A., Stødkilde-Jørgensen, H., Ringgaard, S., Chabanova, E., Thomsen, H., Pedersen, S. B., Astrup, A., & Richelsen, B. (2012). Sucrose-sweetened beverages increase fat storage in the liver, muscle, and visceral fat depot: A 6-mo randomized intervention study. *American Journal of Clinical Nutrition*, *95*(2), 283–289. https://doi.org/10.3945/ajcn.111.022533

Mahady, S. E., Webster, A. C., Walker, S., Sanyal, A., & George, J. (2011). The role of thiazolidinediones in non-alcoholic steatohepatitis - A systematic review and meta analysis. *Journal of Hepatology*, *55*(6), 1383–1390. https://doi.org/10.1016/j.jhep.2011.03.016

Mancina, R. M., Dongiovanni, P., Petta, S., Pingitore, P., Meroni, M., Rametta, R., Borén, J., Montalcini, T., Pujia, A., Wiklund, O., Hindy, G., Spagnuolo, R., Motta, B. M., Pipitone, R. M., Craxì, A., Fargion, S., Nobili, V., Käkelä, P., Kärjä, V., … Romeo, S. (2016). The MBOAT7-TMC4 Variant rs641738 Increases Risk of Nonalcoholic Fatty Liver Disease in Individuals of European Descent. *Gastroenterology*, *150*(5), 1219-1230.e6. https://doi.org/10.1053/j.gastro.2016.01.032

Mannina, L., Luchinat, C., Patumi, M., Emanuele, M. C., Rossi, E., & Segre, A. (2000). Concentration dependence of 13C NMR spectra of triglycerides: Implications for the NMR analysis of olive oils. *Magnetic Resonance in Chemistry*, *38*(10), 886–890. https://doi.org/10.1002/1097-458X(200010)38:10<886::AID-MRC738>3.0.CO;2-J

Mantovani, A., Byrne, C. D., Bonora, E., & Targher, G. (2018). Nonalcoholic fatty liver disease and risk of incident type 2 diabetes: A meta-analysis. *Diabetes Care*, *41*(2), 372–382. https://doi.org/10.2337/dc17-1902

Marchesini, G., Day, C. P., Dufour, J. F., Canbay, A., Nobili, V., Ratziu, V., Tilg, H., Roden, M., Gastaldelli, A., Yki-Jarvinen, H., Schick, F., Vettor, R., Fruhbeck, G., & Mathus-Vliegen, L. (2016). EASL-EASD-EASO Clinical Practice Guidelines

for the management of non-alcoholic fatty liver disease. *Journal of Hepatology*, *64*(6), 1388–1402. https://doi.org/10.1016/j.jhep.2015.11.004

Marin, V., Rosso, N., Dal Ben, M., Raseni, A., Boschelle, M., Degrassi, C., Nemeckova, I., Nachtigal, P., Avellini, C., Tiribelli, C., & Gazzin, S. (2016). An animal model for the juvenile non-alcoholic fatty liver disease and non-alcoholic steatohepatitis. *PLoS ONE*, *11*(7), e0158817. https://doi.org/10.1371/journal.pone.0158817

Marjot, T., Moolla, A., Cobbold, J. F., Hodson, L., & Tomlinson, J. W. (2020). Nonalcoholic Fatty Liver Disease in Adults: Current Concepts in Etiology, Outcomes, and Management. *Endocrine Reviews*, *41*(1), 66–117. https://doi.org/10.1210/endrev/bnz009

Marques-Lopes, I., Ansorena, D., Astiasaran, I., Forga, L., & Martínez, J. A. (2001). Postprandial de novo lipogenesis and metabolic changes induced by a high-carbohydrate, low-fat meal in lean and overweight men. *American Journal of Clinical Nutrition*, *73*(2), 253–261. https://doi.org/10.1093/ajcn/73.2.253

Martins, F., Campos, D. H. S., Pagan, L. U., Martinez, P. F., Okoshi, K., Okoshi, M. P., Padovani, C. R., de Souza, A. S., Cicogna, A. C., & de Oliveira-Junior, S. A. (2015). Dieta hiperlipídica promove remodelação cardíaca em modelo experimental de obesidade. *Arquivos Brasileiros de Cardiologia*, *105*(5), 479–486. https://doi.org/10.5935/abc.20150095

Matsumoto, M., Hada, N., Sakamaki, Y., Uno, A., Shiga, T., Tanaka, C., Ito, T., Katsume, A., & Sudoh, M. (2013). An improved mouse model that rapidly develops fibrosis in non-alcoholic steatohepatitis. *International Journal of Experimental Pathology*, *94*(2), 93–103. https://doi.org/10.1111/iep.12008

Matyash, V., Liebisch, G., Kurzchalia, T. V., Shevchenko, A., & Schwudke, D. (2008). Lipid extraction by methyl-terf-butyl ether for high-throughput lipidomics. *Journal of Lipid Research*, *49*(5), 1137–1146. https://doi.org/10.1194/jlr.D700041-JLR200

McCabe, B. J., Bederman, I. R., Croniger, C., Millward, C., Norment, C., & Previs, S. F. (2006). Reproducibility of gas chromatography-mass spectrometry measurements of 2H labeling of water: Application for measuring body composition in mice. *Analytical Biochemistry*, *350*(2), 171–176. https://doi.org/10.1016/j.ab.2006.01.020

McCarthy, E. M., & Rinella, M. E. (2012). The Role of Diet and Nutrient Composition

in Nonalcoholic Fatty Liver Disease. *Journal of the Academy of Nutrition and Dietetics*, *112*(3), 401–409. https://doi.org/10.1016/j.jada.2011.10.007

McGarry, J. D., Mannaerts, G. P., & Foster, D. W. (1977). A possible role for malonyl CoA in the regulation of hepatic fatty acid oxidation and ketogenesis. *Journal of Clinical Investigation*, *60*(1), 265–270. https://doi.org/10.1172/JCI108764

McGarry, J. D., Takabayashi, Y., & Foster, D. W. (1978). The role of malonyl-CoA in the coordination of fatty acid synthesis and oxidation in isolated rat hepatocytes. *Journal of Biological Chemistry*, *253*(22), 8294–8300. https://doi.org/10.1016/s0021-9258(17)34395-8

Mendes, A. C., Caldeira, M. M., Silva, C., Burgess, S. C., Merritt, M. E., Gomes, F., Barosa, C., Delgado, T. C., Franco, F., Monteiro, P., Providencia, L., & Jones, J. G. (2006). Hepatic UDP-glucose 13C isotopomers from [U-13C] glucose: A simple analysis by 13C NMR of urinary menthol glucuronide. *Magnetic Resonance in Medicine*, *56*(5), 1121–1125. https://doi.org/10.1002/mrm.21057

Mock, K., Lateef, S., Benedito, V. A., & Tou, J. C. (2017). High-fructose corn syrup-55 consumption alters hepatic lipid metabolism and promotes triglyceride accumulation. *Journal of Nutritional Biochemistry*, *39*, 32–39. https://doi.org/10.1016/j.jnutbio.2016.09.010

Montgomery, M. K., Fiveash, C. E., Braude, J. P., Osborne, B., Brown, S. H. J., Mitchell, T. W., & Turner, N. (2015). Disparate metabolic response to fructose feeding between different mouse strains. *Scientific Reports*, *5*. https://doi.org/10.1038/srep18474

Moon, Y. A., Liang, G., Xie, X., Frank-Kamenetsky, M., Fitzgerald, K., Koteliansky, V., Brown, M. S., Goldstein, J. L., & Horton, J. D. (2012). The Scap/SREBP pathway is essential for developing diabetic fatty liver and carbohydrate-induced hypertriglyceridemia in animals. *Cell Metabolism*, *15*(2), 240–246. https://doi.org/10.1016/j.cmet.2011.12.017

Murphy, E. J. (2006). Stable isotope methods for the in vivo measurement of lipogenesis and triglyceride metabolism. In *Journal of animal science: Vol. 84 Suppl.* J Anim Sci. https://doi.org/10.2527/2006.8413_supplE94x

Musselman, L. P., Fink, J. L., Ramachandran, P. V., Patterson, B. W., Okunade, A. L., Maier, E., Brent, M. R., Turk, J., & Baranski, T. J. (2013). Role of fat body lipogenesis in protection against the effects of caloric overload in drosophila.

Journal of Biological Chemistry, *288*(12), 8028–8042. https://doi.org/10.1074/jbc.M112.371047

Musso, G., Gambino, R., Bo, S., Uberti, B., Biroli, G., Pagano, G., & Cassader, M. (2008). Should nonalcoholic fatty liver disease be included in the definition of metabolic syndrome? A cross-sectional comparison with Adult Treatment Panel III criteria in nonobese nondiabetic subjects. *Diabetes Care*, *31*(3), 562–568. https://doi.org/10.2337/dc07-1526

Musso, G., Gambino, R., De Michieli, F., Cassader, M., Rizzetto, M., Durazzo, M., Fagà, E., Silli, B., & Pagano, G. (2003). Dietary habits and their relations to insulin resistance and postprandial lipemia in nonalcoholic steatohepatitis. *Hepatology*, *37*(4), 909–916. https://doi.org/10.1053/jhep.2003.50132

Nakagawa, H., Umemura, A., Taniguchi, K., Font-Burgada, J., Dhar, D., Ogata, H., Zhong, Z., Valasek, M. A., Seki, E., Hidalgo, J., Koike, K., Kaufman, R. J., & Karin, M. (2014). ER Stress Cooperates with Hypernutrition to Trigger TNF-Dependent Spontaneous HCC Development. *Cancer Cell*, *26*(3), 331–343. https://doi.org/10.1016/j.ccr.2014.07.001

Nakayama, H., Otabe, S., Ueno, T., Hirota, N., Yuan, X., Fukutani, T., Hashinaga, T., Wada, N., & Yamada, K. (2007). Transgenic mice expressing nuclear sterol regulatory element-binding protein 1c in adipose tissue exhibit liver histology similar to nonalcoholic steatohepatitis. *Metabolism: Clinical and Experimental*, *56*(4), 470–475. https://doi.org/10.1016/j.metabol.2006.11.004

Nauck, M. A., Meier, J. J., Cavender, M. A., El Aziz, M. A., & Drucker, D. J. (2017). Cardiovascular actions and clinical outcomes with glucagon-like peptide-1 receptor agonists and dipeptidyl peptidase-4 inhibitors. *Circulation*, *136*(9), 849–870. https://doi.org/10.1161/CIRCULATIONAHA.117.028136

Neal, B., Perkovic, V., Mahaffey, K. W., de Zeeuw, D., Fulcher, G., Erondu, N., Shaw, W., Law, G., Desai, M., & Matthews, D. R. (2017). Canagliflozin and Cardiovascular and Renal Events in Type 2 Diabetes. *New England Journal of Medicine*, *377*(7), 644–657. https://doi.org/10.1056/nejmoa1611925

Nelson, G. J. (1962). The lipid composition of normal mouse liver. *Journal of Lipid Research*, *3*(2), 256–262. https://doi.org/10.1016/s0022-2275(20)40438-9

Newgard, C. B., Hirsch, L. J., Foster, D. W., & McGarry, J. D. (1983). Studies on the mechanism by which exogenous glucose is converted into liver glycogen in the rat.

A direct or an indirect pathway? *Journal of Biological Chemistry*, *258*(13), 8046–8052. https://doi.org/10.1016/s0021-9258(20)82025-0

Nielsen, S. J., & Popkin, B. M. (2004). Changes in beverage intake between 1977 and 2001. *American Journal of Preventive Medicine*, *27*(3), 205–210. https://doi.org/10.1016/j.amepre.2004.05.005

Nolan, C. J., & Larter, C. Z. (2009). Lipotoxicity: Why do saturated fatty acids cause and monounsaturates protect against it? In *Journal of Gastroenterology and Hepatology (Australia)* (Vol. 24, Issue 5, pp. 703–706). Blackwell Publishing. https://doi.org/10.1111/j.1440-1746.2009.05823.x

Nunes, P. M., Wright, A. J., Veltien, A., Van Asten, J. J. A., Tack, C. J., Jones, J. G., & Heerschap, A. (2014). Dietary lipids do not contribute to the higher hepatic triglyceride levels of fructose-compared to glucose-fed mice. *FASEB Journal*, *28*(5), 1988–1997. https://doi.org/10.1096/fj.13-241208

O'Sullivan, T. A., Oddy, W. H., Bremner, A. P., Sherriff, J. L., Ayonrinde, O. T., Olynyk, J. K., Beilin, L. J., Mori, T. A., & Adams, L. A. (2014). Lower fructose intake may help protect against development of nonalcoholic fatty liver in adolescents with obesity. *Journal of Pediatric Gastroenterology and Nutrition*, *58*(5), 624–631. https://doi.org/10.1097/MPG.0000000000000267

Oana, F., Takeda, H., Hayakawa, K., Matsuzawa, A., Akahane, S., Isaji, M., & Akahane, M. (2005). Physiological difference between obese (fa/fa) Zucker rats and lean Zucker rats concerning adiponectin. *Metabolism: Clinical and Experimental*, *54*(8), 995–1001. https://doi.org/10.1016/j.metabol.2005.02.016

Oddy, W. H., Herbison, C. E., Jacoby, P., Ambrosini, G. L., O'Sullivan, T. A., Ayonrinde, O. T., Olynyk, J. K., Black, L. J., Beilin, L. J., Mori, T. A., Hands, B. P., & Adams, L. A. (2013). The western dietary pattern is prospectively associated with nonalcoholic fatty liver disease in adolescence. *American Journal of Gastroenterology*, *108*(5), 778–785. https://doi.org/10.1038/ajg.2013.95

Ono-Moore, K. D., Ferguson, M., Blackburn, M. L., Issafras, H., & Adams, S. H. (2017). Application of an in vivo hepatic triacylglycerol production method in the setting of a high-fat diet in mice. *Nutrients*, *9*(1). https://doi.org/10.3390/nu9010016

Oosterveer, M. H., & Schoonjans, K. (2014). Hepatic glucose sensing and integrative pathways in the liver. In *Cellular and Molecular Life Sciences* (Vol. 71, Issue 8,

pp. 1453–1467). Birkhauser Verlag AG. https://doi.org/10.1007/s00018-013-1505-z

Oosterveer, M. H., van Dijk, T. H., Tietge, U. J. F., Boer, T., Havinga, R., Stellaard, F., Groen, A. K., Kuipers, F., & Reijngoud, D. J. (2009). High fat feeding induces hepatic fatty acid elongation in mice. *PLoS ONE*, *4*(6). https://doi.org/10.1371/journal.pone.0006066

Orasanu, G., Ziouzenkova, O., Devchand, P. R., Nehra, V., Hamdy, O., Horton, E. S., & Plutzky, J. (2008). The Peroxisome Proliferator-Activated Receptor-γ Agonist Pioglitazone Represses Inflammation in a Peroxisome Proliferator-Activated Receptor-α-Dependent Manner In Vitro and In Vivo in Mice. *Journal of the American College of Cardiology*, *52*(10), 869–881. https://doi.org/10.1016/j.jacc.2008.04.055

Ouyang, X., Cirillo, P., Sautin, Y., McCall, S., Bruchette, J. L., Diehl, A. M., Johnson, R. J., & Abdelmalek, M. F. (2008). Fructose consumption as a risk factor for non-alcoholic fatty liver disease. *Journal of Hepatology*, *48*(6), 993–999. https://doi.org/10.1016/j.jhep.2008.02.011

Paglialunga, S., & Dehn, C. A. (2016). Clinical assessment of hepatic de novo lipogenesis in non-alcoholic fatty liver disease. In *Lipids in Health and Disease* (Vol. 15, Issue 1). BioMed Central Ltd. https://doi.org/10.1186/s12944-016-0321-5

Pälve, K. S., Pahkala, K., Suomela, E., Aatola, H., Hulkkonen, J., Juonala, M., Lehtimäki, T., Rönnemaa, T., Viikari, J. S. A., Kähönen, M., Hutri-Kähönen, N., Telama, R., Tammelin, T., & Raitakari, O. T. (2017). Cardiorespiratory Fitness and Risk of Fatty Liver: The Young Finns Study. *Medicine and Science in Sports and Exercise*, *49*(9), 1834–1841. https://doi.org/10.1249/MSS.0000000000001288

Panjwani, N., Mulvihill, E. E., Longuet, C., Yusta, B., Campbell, J. E., Brown, T. J., Streutker, C., Holland, D., Cao, X., Baggio, L. L., & Drucker, D. J. (2013). GLP-1 receptor activation indirectly reduces hepatic lipid accumulation but does not attenuate development of atherosclerosis in diabetic male ApoE -/- mice. *Endocrinology*, *154*(1), 127–139. https://doi.org/10.1210/en.2012-1937

Park, J., Lemieux, S., Lewis, G. F., Kuksis, A., & Steiner, G. (1997). Chronic exogenous insulin and chronic carbohydrate supplementation increase de novo VLDL triglyceride fatty acid production in rats. *Journal of Lipid Research*, *38*(12),

2529–2536. https://doi.org/10.1016/s0022-2275(20)30037-7

Park, S. H., Jeon, W. K., Kim, S. H., Kim, H. J., Park, D. I., Cho, Y. K., Sung, I. K., Sohn, C. I., Keum, D. K., & Kim, B. I. (2006). Prevalence and risk factors of non-alcoholic fatty liver disease among Korean adults. *Journal of Gastroenterology and Hepatology (Australia)*, *21*(1 PART1), 138–143. https://doi.org/10.1111/j.1440-1746.2005.04086.x

Park, S. Y., Kim, H. J., Wang, S., Higashimori, T., Dong, J., Kim, Y. J., Cline, G., Li, H., Prentki, M., Shulman, G. I., Mitchell, G. A., & Kim, J. K. (2005). Hormone-sensitive lipase knockout mice have increased hepatic insulin sensitivity and are protected from short-term diet-induced insulin resistance in skeletal muscle and heart. *American Journal of Physiology - Endocrinology and Metabolism*, *289*(1 52-1). https://doi.org/10.1152/ajpendo.00251.2004

Park, Y. K., & Yetley, E. A. (1993). Intakes and food sources of fructose in the United States. *American Journal of Clinical Nutrition*, *58*(5 SUPPL.). https://doi.org/10.1093/ajcn/58.5.737S

Parks, E. J., Krauss, R. M., Christiansen, M. P., Neese, R. A., & Hellerstein, M. K. (1999). Effects of a low-fat, high-carbohydrate diet on VLDL-triglyceride assembly, production, and clearance. *Journal of Clinical Investigation*, *104*(8), 1087–1096. https://doi.org/10.1172/JCI6572

Parks, E. J., Skokan, L. E., Timlin, M. T., & Dingfelder, C. S. (2008). Dietary sugars stimulate fatty acid synthesis in adults. *Journal of Nutrition*, *138*(6), 1039–1046. https://doi.org/10.1093/jn/138.6.1039

Patterson, E., Wall, R., Fitzgerald, G. F., Ross, R. P., & Stanton, C. (2012). Health implications of high dietary omega-6 polyunsaturated fatty acids. In *Journal of Nutrition and Metabolism* (Vol. 2012). Hindawi Limited. https://doi.org/10.1155/2012/539426

Perdigoto, R., Rodrigues, T. B., Furtado, A. L., Porto, A., Geraldes, C. F. G. C., & Jones, J. G. (2003). Integration of [U-13C]glucose and 2H2O for quantification of hepatic glucose production and gluconeogenesis. *NMR in Biomedicine*, *16*(4), 189–198. https://doi.org/10.1002/nbm.826

Perry, R. J., Peng, L., Barry, N. A., Cline, G. W., Zhang, D., Cardone, R. L., Petersen, K. F., Kibbey, R. G., Goodman, A. L., & Shulman, G. I. (2016). Acetate mediates a microbiome-brain-β-cell axis to promote metabolic syndrome. *Nature*,

534(7606), 213–217. https://doi.org/10.1038/nature18309

Petersen, M. C., Vatner, D. F., & Shulman, G. I. (2017). Regulation of hepatic glucose metabolism in health and disease. In *Nature Reviews Endocrinology* (Vol. 13, Issue 10, pp. 572–587). Nature Publishing Group. https://doi.org/10.1038/nrendo.2017.80

Petit, J. M., Cercueil, J. P., Loffroy, R., Denimal, D., Bouillet, B., Fourmont, C., Chevallier, O., Duvillard, L., & Vergès, B. (2017). Effect of liraglutide therapy on liver fat content in patients with inadequately controlled type 2 diabetes: The Lira-NAFLD study. In *Journal of Clinical Endocrinology and Metabolism* (Vol. 102, Issue 2, pp. 407–415). Endocrine Society. https://doi.org/10.1210/jc.2016-2775

Petta, S., Miele, L., Bugianesi, E., Cammà, C., Rosso, C., Boccia, S., Cabibi, D., Di Marco, V., Grimaudo, S., Grieco, A., Pipitone, R. M., Marchesini, G., & Craxì, A. (2014). Glucokinase regulatory protein gene polymorphism affects liver fibrosis in non-alcoholic fatty liver disease. *PLoS ONE*, *9*(2). https://doi.org/10.1371/journal.pone.0087523

Pettinelli, P., del Pozo, T., Araya, J., Rodrigo, R., Araya, A. V., Smok, G., Csendes, A., Gutierrez, L., Rojas, J., Korn, O., Maluenda, F., Diaz, J. C., Rencoret, G., Braghetto, I., Castillo, J., Poniachik, J., & Videla, L. A. (2009). Enhancement in liver SREBP-1c/PPAR-α ratio and steatosis in obese patients: Correlations with insulin resistance and n-3 long-chain polyunsaturated fatty acid depletion. *Biochimica et Biophysica Acta - Molecular Basis of Disease*, *1792*(11), 1080–1086. https://doi.org/10.1016/j.bbadis.2009.08.015

Pingitore, P., Dongiovanni, P., Motta, B. M., Meroni, M., Lepore, S. M., Mancina, R. M., Pelusi, S., Russo, C., Caddeo, A., Rossi, G., Montalcini, T., Pujia, A., Wiklund, O., Valenti, L., & Romeo, S. (2016). PNPLA3 overexpression results in reduction of proteins predisposing to fibrosis. *Human Molecular Genetics*, *25*(23), 5212–5222. https://doi.org/10.1093/hmg/ddw341

Pingitore, P., Pirazzi, C., Mancina, R. M., Motta, B. M., Indiveri, C., Pujia, A., Montalcini, T., Hedfalk, K., & Romeo, S. (2014). Recombinant PNPLA3 protein shows triglyceride hydrolase activity and its I148M mutation results in loss of function. *Biochimica et Biophysica Acta - Molecular and Cell Biology of Lipids*, *1841*(4), 574–580. https://doi.org/10.1016/j.bbalip.2013.12.006

Pirazzi, C., Valenti, L., Motta, B. M., Pingitore, P., Hedfalk, K., Mancina, R. M., Burza,

M. A., Indiveri, C., Ferro, Y., Montalcini, T., Maglio, C., Dongiovanni, P., Fargion, S., Rametta, R., Pujia, A., Andersson, L., Ghosal, S., Levin, M., Wiklund, O., … Romeo, S. (2014). PNPLA3 has retinyl-palmitate lipase activity in human hepatic stellate cells. *Human Molecular Genetics*, *23*(15), 4077–4085. https://doi.org/10.1093/hmg/ddu121

Pirola, C. J., & Sookoian, S. (2015). The dual and opposite role of the TM6SF2-rs58542926 variant in protecting against cardiovascular disease and conferring risk for nonalcoholic fatty liver: A meta-analysis. *Hepatology*, *62*(6), 1742–1756. https://doi.org/10.1002/hep.28142

Postic, C., & Girard, J. (2008). Contribution of de novo fatty acid synthesis to hepatic steatosis and insulin resistance: Lessons from genetically engineered mice. *Journal of Clinical Investigation*, *118*(3), 829–838. https://doi.org/10.1172/JCI34275

Prats, C., Graham, T. E., & Shearer, J. (2018). The dynamic life of the glycogen granule. In *Journal of Biological Chemistry* (Vol. 293, Issue 19, pp. 7089–7098). American Society for Biochemistry and Molecular Biology Inc. https://doi.org/10.1074/jbc.R117.802843

Priore, P., Cavallo, A., Gnoni, A., Damiano, F., Gnoni, G. V., & Siculella, L. (2015). Modulation of hepatic lipid metabolism by olive oil and its phenols in nonalcoholic fatty liver disease. In *IUBMB Life* (Vol. 67, Issue 1, pp. 9–17). Blackwell Publishing Ltd. https://doi.org/10.1002/iub.1340

Pyke, C., Heller, R. S., Kirk, R. K., Ørskov, C., Reedtz-Runge, S., Kaastrup, P., Hvelplund, A., Bardram, L., Calatayud, D., & Knudsen, L. B. (2014). GLP-1 receptor localization in monkey and human tissue: Novel distribution revealed with extensively validated monoclonal antibody. *Endocrinology*, *155*(4), 1280–1290. https://doi.org/10.1210/en.2013-1934

Rich, N. E., Oji, S., Mufti, A. R., Browning, J. D., Parikh, N. D., Odewole, M., Mayo, H., & Singal, A. G. (2018). Racial and Ethnic Disparities in Nonalcoholic Fatty Liver Disease Prevalence, Severity, and Outcomes in the United States: A Systematic Review and Meta-analysis. *Clinical Gastroenterology and Hepatology*, *16*(2), 198-210.e2. https://doi.org/10.1016/j.cgh.2017.09.041

Rinella, M. E., Elias, M. S., Smolak, R. R., Fu, T., Borensztajn, J., & Green, R. M. (2008). Mechanisms of hepatic steatosis in mice fed a lipogenic methionine choline-deficient diet. *Journal of Lipid Research*, *49*(5), 1068–1076.

https://doi.org/10.1194/jlr.M800042-JLR200

Rito, J., Viegas, I., Pardal, M. A., Metón, I., Baanante, I. V., & Jones, J. G. (2018). Disposition of a Glucose Load into Hepatic Glycogen by Direct and Indirect Pathways in Juvenile Seabass and Seabream. *Scientific Reports*, *8*(1). https://doi.org/10.1038/s41598-017-19087-y

Romeo, S., Kozlitina, J., Xing, C., Pertsemlidis, A., Cox, D., Pennacchio, L. A., Boerwinkle, E., Cohen, J. C., & Hobbs, H. H. (2008). Genetic variation in PNPLA3 confers susceptibility to nonalcoholic fatty liver disease. *Nature Genetics*, *40*(12), 1461–1465. https://doi.org/10.1038/ng.257

Romero-Gómez, M., Zelber-Sagi, S., & Trenell, M. (2017). Treatment of NAFLD with diet, physical activity and exercise. In *Journal of Hepatology* (Vol. 67, Issue 4, pp. 829–846). Elsevier B.V. https://doi.org/10.1016/j.jhep.2017.05.016

Ross, B. D., Kingsley, P. B., & Ben-Yoseph, O. (1994). Measurement of pentose phosphate-pathway activity in a single incubation with [1,6-13C2,6,6-2H2]glucose. *Biochemical Journal*, *302*(1), 31–38. https://doi.org/10.1042/bj3020031

Ruderman, N. B., Saha, A. K., & Kraegen, E. W. (2003). Minireview: Malonyl CoA, AMP-Activated Protein Kinase, and Adiposity. In *Endocrinology* (Vol. 144, Issue 12, pp. 5166–5171). Endocrinology. https://doi.org/10.1210/en.2003-0849

Ryu, S., Chang, Y., Jung, H. S., Yun, K. E., Kwon, M. J., Choi, Y., Kim, C. W., Cho, J., Suh, B. S., Cho, Y. K., Chung, E. C., Shin, H., & Kim, Y. S. (2015). Relationship of sitting time and physical activity with non-alcoholic fatty liver disease. *Journal of Hepatology*, *63*(5), 1229–1237. https://doi.org/10.1016/j.jhep.2015.07.010

Santhekadur, P. K., Kumar, D. P., & Sanyal, A. J. (2018). PRECLINICAL MODELS OF NONALCOHOLIC FATTY LIVER DISEASE HHS Public Access. *J Hepatol*, *68*(2), 230–237. https://doi.org/10.1016/j.jhep.2017.10.031

Santoro, N., Zhang, C. K., Zhao, H., Pakstis, A. J., Kim, G., Kursawe, R., Dykas, D. J., Bale, A. E., Giannini, C., Pierpont, B., Shaw, M. M., Groop, L., & Caprio, S. (2012). Variant in the glucokinase regulatory protein (GCKR) gene is associated with fatty liver in obese children and adolescents. *Hepatology*, *55*(3), 781–789. https://doi.org/10.1002/hep.24806

Sanyal, A. J., Chalasani, N., Kowdley, K. V., McCullough, A., Diehl, A. M., Bass, N. M., Neuschwander-Tetri, B. A., Lavine, J. E., Tonascia, J., Unalp, A., Van Natta,

M., Clark, J., Brunt, E. M., Kleiner, D. E., Hoofnagle, J. H., & Robuck, P. R. (2010). Pioglitazone, Vitamin E, or Placebo for Nonalcoholic Steatohepatitis. *New England Journal of Medicine*, *362*(18), 1675–1685. https://doi.org/10.1056/nejmoa0907929

Sanyal, A. J., & Pacana, T. (2015). A Lipidomic Readout of Disease Progression in A Diet-Induced Mouse Model of Nonalcoholic Fatty Liver Disease. *Transactions of the American Clinical and Climatological Association*, *126*, 271–288. https://pubmed.ncbi.nlm.nih.gov/26330688/

Saponaro, C., Gaggini, M., & Gastaldelli, A. (2015). Nonalcoholic Fatty Liver Disease and Type 2 Diabetes: Common Pathophysiologic Mechanisms. In *Current Diabetes Reports* (Vol. 15, Issue 6, pp. 1–13). Current Medicine Group LLC 1. https://doi.org/10.1007/s11892-015-0607-4

Sattar, N., Fitchett, D., Hantel, S., George, J. T., & Zinman, B. (2018). Empagliflozin is associated with improvements in liver enzymes potentially consistent with reductions in liver fat: results from randomised trials including the EMPA-REG OUTCOME® trial. *Diabetologia*, *61*(10), 2155–2163. https://doi.org/10.1007/s00125-018-4702-3

Schierwagen, R., Maybüchen, L., Zimmer, S., Hittatiya, K., Bäck, C., Klein, S., Uschner, F. E., Reul, W., Boor, P., Nickenig, G., Strassburg, C. P., Trautwein, C., Plat, J., Lütjohann, D., Sauerbruch, T., Tacke, F., & Trebicka, J. (2015). Seven weeks of Western diet in apolipoprotein-E-deficient mice induce metabolic syndrome and non-alcoholic steatohepatitis with liver fibrosis. *Scientific Reports*, *5*. https://doi.org/10.1038/srep12931

Schoenheimer, R., & Rittenberg, D. (1936). DEUTERIUM AS AN INDICATOR IN THE STUDY OF INTERMEDIARY METABOLISM. *Journal of Biological Chemistry*, *114*(2), 381–396. https://doi.org/10.1016/s0021-9258(18)74810-2

Schwarz, J. M., Neese, R. A., Turner, S., Dare, D., & Hellerstein, M. K. (1995). Short-term alterations in carbohydrate energy intake in humans. Striking effects on hepatic glucose production, de novo lipogenesis, lipolysis, and whole-body fuel selection. *Journal of Clinical Investigation*, *96*(6), 2735–2743. https://doi.org/10.1172/JCI118342

Schwarz, Jean Marc, Linfoot, P., Dare, D., & Aghajanian, K. (2003). Hepatic de novo lipogenesis in normoinsulinemic and hyperinsulinemic subjects consuming high-

fat, low-carbohydrate and low-fat, high-carbohydrate isoenergetic diets. *American Journal of Clinical Nutrition*, *77*(1), 43–50. https://doi.org/10.1093/ajcn/77.1.43

Seko, Y., Nishikawa, T., Umemura, A., Yamaguchi, K., Moriguchi, M., Yasui, K., Kimura, M., Iijima, H., Hashimoto, T., Sumida, Y., Okanoue, T., & Itoh, Y. (2018). Efficacy and safety of canagliflozin in type 2 diabetes mellitus patients with biopsy-proven nonalcoholic steatohepatitis classified as stage 1–3 fibrosis. *Diabetes, Metabolic Syndrome and Obesity: Targets and Therapy*, *11*, 835–843. https://doi.org/10.2147/DMSO.S184767

Sellmann, C., Priebs, J., Landmann, M., Degen, C., Engstler, A. J., Jin, C. J., Gärttner, S., Spruss, A., Huber, O., & Bergheim, I. (2015). Diets rich in fructose, fat or fructose and fat alter intestinal barrier function and lead to the development of nonalcoholic fatty liver disease over time. *Journal of Nutritional Biochemistry*, *26*(11), 1183–1192. https://doi.org/10.1016/j.jnutbio.2015.05.011

Seoane, J., Gómez-Foix, A. M., O'Doherty, R. M., Gómez-Ara, C., Newgard, C. B., & Guinovart, J. J. (1996). Glucose 6-phosphate produced by glucokinase, but not hexokinase I, promotes the activation of hepatic glycogen synthase. *Journal of Biological Chemistry*, *271*(39), 23756–23760. https://doi.org/10.1074/jbc.271.39.23756

Shen, J. H., Li, Y. L., Li, D., Wang, N. N., Jing, L., & Huang, Y. H. (2015). The rs738409 (I148M) variant of the PNPLA3 gene and cirrhosis: A meta-analysis. *Journal of Lipid Research*, *56*(1), 167–175. https://doi.org/10.1194/jlr.M048777

Shibuya, T., Fushimi, N., Kawai, M., Yoshida, Y., Hachiya, H., Ito, S., Kawai, H., Ohashi, N., & Mori, A. (2018). Luseogliflozin improves liver fat deposition compared to metformin in type 2 diabetes patients with non-alcoholic fatty liver disease: A prospective randomized controlled pilot study. *Diabetes, Obesity and Metabolism*, *20*(2), 438–442. https://doi.org/10.1111/dom.13061

Siddiqui, N., Sim, J., Silwood, C. J. L., Toms, H., Iles, R. A., & Grootveld, M. (2003). Multicomponent analysis of encapsulated marine oil supplements using high-resolution 1H and 13C NMR techniques. *Journal of Lipid Research*, *44*(12), 2406–2427. https://doi.org/10.1194/jlr.D300017-JLR200

Silva, A. M., Martins, F., Jones, J. G., & Carvalho, R. (2011). 2H2O incorporation into hepatic acetyl-CoA and de novo lipogenesis as measured by Krebs cycle-mediated 2H-enrichment of glutamate and glutamine. *Magnetic Resonance in Medicine*,

66(6), 1526–1530. https://doi.org/10.1002/mrm.22955

Silva, J. C. P., Marques, C., Martins, F. O., Viegas, I., Tavares, L., Macedo, M. P., & Jones, J. G. (2019). Determining contributions of exogenous glucose and fructose to de novo fatty acid and glycerol synthesis in liver and adipose tissue. *Metabolic Engineering*, *56*(August), 69–76. https://doi.org/10.1016/j.ymben.2019.08.018

Simopoulos, A. P. (2002). The importance of the ratio of omega-6/omega-3 essential fatty acids. *Biomedicine and Pharmacotherapy*, *56*(8), 365–379. https://doi.org/10.1016/S0753-3322(02)00253-6

Singal, A. G., Manjunath, H., Yopp, A. C., Beg, M. S., Marrero, J. A., Gopal, P., & Waljee, A. K. (2014). The effect of PNPLA3 on fibrosis progression and development of hepatocellular carcinoma: A meta-analysis. *American Journal of Gastroenterology*, *109*(3), 325–334. https://doi.org/10.1038/ajg.2013.476

Soares, A. F., Carvalho, R. A., Veiga, F. J., Alves, M. G., Martins, F. O., Viegas, I., González, J. D., Metón, I., Baanante, I. V., & Jones, J. G. (2012). Restoration of direct pathway glycogen synthesis flux in the STZ-diabetes rat model by insulin administration. *American Journal of Physiology - Endocrinology and Metabolism*, *303*(7). https://doi.org/10.1152/ajpendo.00161.2012

Soccio, R. E., Chen, E. R., & Lazar, M. A. (2014). Thiazolidinediones and the promise of insulin sensitization in type 2 diabetes. In *Cell Metabolism* (Vol. 20, Issue 4, pp. 573–591). Cell Press. https://doi.org/10.1016/j.cmet.2014.08.005

Softic, S., Cohen, D. E., & Kahn, C. R. (2016). Role of Dietary Fructose and Hepatic De Novo Lipogenesis in Fatty Liver Disease. In *Digestive Diseases and Sciences* (Vol. 61, Issue 5, pp. 1282–1293). Springer New York LLC. https://doi.org/10.1007/s10620-016-4054-0

Soni, H. (2016). Peptide-based GLP-1/glucagon co-agonists: A double-edged sword to combat diabesity. *Medical Hypotheses*, *95*, 5–9. https://doi.org/10.1016/j.mehy.2016.08.005

Speakman, J. R. (2001). *Body composition analysis of animals: a handbook of non-destructive methods*. Cambridge University Press.

Stanhope, K. L. (2012). Role of fructose-containing sugars in the epidemics of obesity and metabolic syndrome. In *Annual Review of Medicine* (Vol. 63, pp. 329–343). Annu Rev Med. https://doi.org/10.1146/annurev-med-042010-113026

Subramanian, S., Goodspeed, L., Wang, S., Kim, J., Zeng, L., Ioannou, G. N., Haigh,

W. G., Yeh, M. M., Kowdley, K. V., O'Brien, K. D., Pennathur, S., & Chait, A. (2011). Dietary cholesterol exacerbates hepatic steatosis and inflammation in obese LDL receptor-deficient mice. *Journal of Lipid Research*, *52*(9), 1626–1635. https://doi.org/10.1194/jlr.M016246

Sullivan, S., Kirk, E. P., Mittendorfer, B., Patterson, B. W., & Klein, S. (2012). Randomized trial of exercise effect on intrahepatic triglyceride content and lipid kinetics in nonalcoholic fatty liver disease. *Hepatology*, *55*(6), 1738–1745. https://doi.org/10.1002/hep.25548

Suvitaival, T., Bondia-Pons, I., Yetukuri, L., Pöhö, P., Nolan, J. J., Hyötyläinen, T., Kuusisto, J., & Orešič, M. (2018). Lipidome as a predictive tool in progression to type 2 diabetes in Finnish men. *Metabolism: Clinical and Experimental*, *78*, 1–12. https://doi.org/10.1016/j.metabol.2017.08.014

Suzuki, A., Lindor, K., Saver, J. S., Lymp, J., Mendes, F., Muto, A., Okada, T., & Angulo, P. (2005). Effect of changes on body weight and lifestyle in nonalcoholic fatty liver disease. *Journal of Hepatology*, *43*(6), 1060–1066. https://doi.org/10.1016/j.jhep.2005.06.008

Svegliati-Baroni, G., Saccomanno, S., Rychlicki, C., Agostinelli, L., de Minicis, S., Candelaresi, C., Faraci, G., Pacetti, D., Vivarelli, M., Nicolini, D., Garelli, P., Casini, A., Manco, M., Mingrone, G., Risaliti, A., Frega, G. N., Benedetti, A., & Gastaldelli, A. (2011). Glucagon-like peptide-1 receptor activation stimulates hepatic lipid oxidation and restores hepatic signalling alteration induced by a high-fat diet in nonalcoholic steatohepatitis. *Liver International*, *31*(9), 1285–1297. https://doi.org/10.1111/j.1478-3231.2011.02462.x

Takahashi, K., Nishida, A., Fujimoto, T., Fujii, M., Shioya, M., Imaeda, H., Inatomi, O., Bamba, S., Andoh, A., & Sugimoto, M. (2016). Reduced Abundance of Butyrate-Producing Bacteria Species in the Fecal Microbial Community in Crohn's Disease. *Digestion*, *93*(1), 59–65. https://doi.org/10.1159/000441768

Takahashi, Y., Soejima, Y., & Fukusato, T. (2012). Animal models of nonalcoholic fatty liver disease/ nonalcoholic steatohepatitis. In *World Journal of Gastroenterology* (Vol. 18, Issue 19, pp. 2300–2308). Baishideng Publishing Group Co. https://doi.org/10.3748/wjg.v18.i19.2300

Tan, J., McKenzie, C., Potamitis, M., Thorburn, A. N., Mackay, C. R., & Macia, L. (2014). The Role of Short-Chain Fatty Acids in Health and Disease. In *Advances*

in Immunology (Vol. 121, pp. 91–119). Academic Press Inc. https://doi.org/10.1016/B978-0-12-800100-4.00003-9

Tengku-Rozaina, T. M., & Birch, E. J. (2014). Positional distribution of fatty acids on hoki and tuna oil triglycerides by pancreatic lipase and 13C NMR analysis. *European Journal of Lipid Science and Technology*, *116*(3), 272–281. https://doi.org/10.1002/ejlt.201300357

Thivel, D., Tremblay, A., Genin, P. M., Panahi, S., Rivière, D., & Duclos, M. (2018). Physical Activity, Inactivity, and Sedentary Behaviors: Definitions and Implications in Occupational Health. *Frontiers in Public Health*, *6*. https://doi.org/10.3389/fpubh.2018.00288

Tilg, H., Moschen, A. R., & Roden, M. (2017). NAFLD and diabetes mellitus. In *Nature Reviews Gastroenterology and Hepatology* (Vol. 14, Issue 1, pp. 32–42). Nature Publishing Group. https://doi.org/10.1038/nrgastro.2016.147

Tillman, E. J., Morgan, D. A., Rahmouni, K., & Swoap, S. J. (2014). Three months of high-fructose feeding fails to induce excessive weight gain or leptin resistance in mice. *PLoS ONE*, *9*(9), e107206. https://doi.org/10.1371/journal.pone.0107206

Timlin, M. T., Barrows, B. R., & Parks, E. J. (2005). Increased dietary substrate delivery alters hepatic fatty acid recycling in healthy men. *Diabetes*, *54*(9), 2694–2701. https://doi.org/10.2337/diabetes.54.9.2694

Trovato, F. M., Martines, G. F., & Catalano, D. (2018). Addressing Western dietary pattern in obesity and NAFLD. *Nutrire*, *43*(1), 1–6. https://doi.org/10.1186/s41110-018-0067-0

Tsuchida, T., Lee, Y. A., Fujiwara, N., Ybanez, M., Allen, B., Martins, S., Fiel, M. I., Goossens, N., Chou, H. I., Hoshida, Y., & Friedman, S. L. (2018). A simple diet- and chemical-induced murine NASH model with rapid progression of steatohepatitis, fibrosis and liver cancer. *Journal of Hepatology*, *69*(2), 385–395. https://doi.org/10.1016/j.jhep.2018.03.011

Turnbaugh, P. J., Ley, R. E., Mahowald, M. A., Magrini, V., Mardis, E. R., & Gordon, J. I. (2006). An obesity-associated gut microbiome with increased capacity for energy harvest. *Nature*, *444*(7122), 1027–1031. https://doi.org/10.1038/nature05414

Valenti, L., Alisi, A., & Nobili, V. (2012). Unraveling the genetics of fatty liver in obese children: Additive effect of P446L GCKR and I148M PNPLA3

polymorphisms. In *Hepatology* (Vol. 55, Issue 3, pp. 661–663). Hepatology. https://doi.org/10.1002/hep.25617

Valenti, L., & Dongiovanni, P. (2017). Mutant PNPLA3 I148M protein as pharmacological target for liver disease. In *Hepatology* (Vol. 66, Issue 4, pp. 1026–1028). John Wiley and Sons Inc. https://doi.org/10.1002/hep.29298

Vallim, T., & Salter, A. M. (2010). Regulation of hepatic gene expression by saturated fatty acids. *Prostaglandins Leukotrienes and Essential Fatty Acids*, *82*(4–6), 211–218. https://doi.org/10.1016/j.plefa.2010.02.016

Vedala, A., Wang, W., Neese, R. A., Christiansen, M. P., & Hellerstein, M. K. (2006). Delayed secretory pathway contributions to VLDL-triglycerides from plasma NEFA, diet, and de novo lipogenesis in humans. *Journal of Lipid Research*, *47*(11), 2562–2574. https://doi.org/10.1194/jlr.M600200-JLR200

Verma, S., & McMurray, J. J. V. (2018). SGLT2 inhibitors and mechanisms of cardiovascular benefit: a state-of-the-art review. In *Diabetologia* (Vol. 61, Issue 10, pp. 2108–2117). Springer Verlag. https://doi.org/10.1007/s00125-018-4670-7

Vernon, G., Baranova, A., & Younossi, Z. M. (2011). Systematic review: The epidemiology and natural history of non-alcoholic fatty liver disease and non-alcoholic steatohepatitis in adults. In *Alimentary Pharmacology and Therapeutics* (Vol. 34, Issue 3, pp. 274–285). Aliment Pharmacol Ther. https://doi.org/10.1111/j.1365-2036.2011.04724.x

Viegas, I., Jarak, I., Rito, J., Carvalho, R. A., Metón, I., Pardal, M. A., Baanante, I. V., & Jones, J. G. (2016). Effects of dietary carbohydrate on hepatic de novo lipogenesis in European seabass (Dicentrarchus labrax L.). *Journal of Lipid Research*, *57*(7), 1264–1272. https://doi.org/10.1194/jlr.M067850

Vilar Gomez, E., Rodriguez De Miranda, A., Gra Oramas, B., Arus Soler, E., Llanio Navarro, R., Calzadilla Bertot, L., Yasells Garcia, A., & Del Rosario Abreu Vazquez, M. (2009). Clinical trial: A nutritional supplement Viusid, in combination with diet and exercise, in patients with nonalcoholic fatty liver disease. *Alimentary Pharmacology and Therapeutics*, *30*(10), 999–1009. https://doi.org/10.1111/j.1365-2036.2009.04122.x

Viscoli, C. M., Inzucchi, S. E., Young, L. H., Insogna, K. L., Conwit, R., Furie, K. L., Gorman, M., Kelly, M. A., Lovejoy, A. M., & Kernan, W. N. (2017). Pioglitazone and risk for bone fracture: Safety data from a randomized clinical trial. *Journal of*

Clinical Endocrinology and Metabolism, *102*(3), 914–922. https://doi.org/10.1210/jc.2016-3237

Vlahov, G., Giuliani, A. A., & Del Re, P. (2010). 13C NMR spectroscopy for determining the acylglycerol positional composition of lampante olive oils. Chemical shift assignments and their dependence on sample concentration. *Analytical Methods*, *2*(7), 916–923. https://doi.org/10.1039/c0ay00028k

Vos, M. B., Kimmons, J. E., Gillespie, C., Welsh, J., & Blank, H. M. (2008). Dietary fructose consumption among US children and adults: The Third National Health and Nutrition Examination Survey CME. *MedGenMed Medscape General Medicine*, *10*(7), 160. /pmc/articles/PMC2525476/

Voshol, P. J., Haemmerle, G., Ouwens, D. M., Zimmermann, R., Zechner, R., Teusink, B., Maassen, J. A., Havekes, L. M., & Romijn, J. A. (2003). Increased hepatic insulin sensitivity together with decreased hepatic triglyceride stores in hormone-sensitive lipase-deficient mice. *Endocrinology*, *144*(8), 3456–3462. https://doi.org/10.1210/en.2002-0036

WALTER, U., LUTHE, H., SÖLING, H. -D, & GERHART, F. (1975). Hydrogen Exchange at the β-Carbon of Amino Acids during Transamination. *European Journal of Biochemistry*, *59*(2), 395–403. https://doi.org/10.1111/j.1432-1033.1975.tb02467.x

Welsh, J. A., Sharma, A. J., Grellinger, L., & Vos, M. B. (2011). Consumption of added sugars is decreasing in the United States. *American Journal of Clinical Nutrition*, *94*(3), 726–734. https://doi.org/10.3945/ajcn.111.018366

Wiggins, D., Hems, R., & Gibbons, G. F. (1995). Decreased sensitivity to the inhibitory effect of insulin on the secretion of very-low-density lipoprotein in cultured hepatocytes from fructose-fed rats. *Metabolism*, *44*(7), 841–847. https://doi.org/10.1016/0026-0495(95)90235-X

Willker, W., & Leibfritz, D. (1998). Assignment of mono- and polyunsaturated fatty acids in lipids of tissues and body fluids. *Magnetic Resonance in Chemistry*, *36*(998), 79–84. https://doi.org/10.1002/(sici)1097-458x(199806)36:13<s79::aid-omr294>3.3.co;2-q

Wiviott, S. D., Raz, I., Bonaca, M. P., Mosenzon, O., Kato, E. T., Cahn, A., Silverman, M. G., Zelniker, T. A., Kuder, J. F., Murphy, S. A., Bhatt, D. L., Leiter, L. A., McGuire, D. K., Wilding, J. P. H., Ruff, C. T., Gause-Nilsson, I. A. M.,

Fredriksson, M., Johansson, P. A., Langkilde, A.-M., & Sabatine, M. S. (2019). Dapagliflozin and Cardiovascular Outcomes in Type 2 Diabetes. *New England Journal of Medicine*, *380*(4), 347–357. https://doi.org/10.1056/nejmoa1812389

Wolf, M. J., Adili, A., Piotrowitz, K., Abdullah, Z., Boege, Y., Stemmer, K., Ringelhan, M., Simonavicius, N., Egger, M., Wohlleber, D., Lorentzen, A., Einer, C., Schulz, S., Clavel, T., Protzer, U., Thiele, C., Zischka, H., Moch, H., Tschöp, M., … Heikenwalder, M. (2014). Metabolic activation of intrahepatic CD8+ T cells and NKT cells causes nonalcoholic steatohepatitis and liver cancer via cross-talk with hepatocytes. *Cancer Cell*, *26*(4), 549–564. https://doi.org/10.1016/j.ccell.2014.09.003

Wolfe, R. R., & Chinkes, D. L. (2004). *Isotope tracers in metabolic research: principles and practice of kinetic analysis*. John Wiley & Sons.

Xanthakos, S., Miles, L., Bucuvalas, J., Daniels, S., Garcia, V., & Inge, T. (2006). Histologic spectrum of nonalcoholic fatty liver disease in morbidly obese adolescents. *Clinical Gastroenterology and Hepatology*, *4*(2), 226–232. https://doi.org/10.1016/S1542-3565(05)00978-X

Ye, P., Cheah, I. K., & Halliwell, B. (2013). High fat diets and pathology in the guinea pig. Atherosclerosis or liver damage? In *Biochimica et Biophysica Acta - Molecular Basis of Disease* (Vol. 1832, Issue 2, pp. 355–364). Biochim Biophys Acta. https://doi.org/10.1016/j.bbadis.2012.11.008

Yki-Järvinen, H. (2010). Nutritional modulation of nonalcoholic fatty liver disease and insulin resistance: Human data. In *Current Opinion in Clinical Nutrition and Metabolic Care* (Vol. 13, Issue 6, pp. 709–714). Curr Opin Clin Nutr Metab Care. https://doi.org/10.1097/MCO.0b013e32833f4b34

Yki-Järvinen, H. (2014). Non-alcoholic fatty liver disease as a cause and a consequence of metabolic syndrome. In *The Lancet Diabetes and Endocrinology* (Vol. 2, Issue 11, pp. 901–910). Lancet Publishing Group. https://doi.org/10.1016/S2213-8587(14)70032-4

Younossi, Z. ., Koenig, A. B., Abdelatif, D., Fazel, Y., Henry, L., & Wymer, M. (2016). Global epidemiology of nonalcoholic fatty liver disease—Meta-analytic assessment of prevalence, incidence, and outcomes. *Hepatology*, *64*(1), 73–84. https://doi.org/10.1002/hep.28431

Younossi, Z., Anstee, Q. M., Marietti, M., Hardy, T., Henry, L., Eslam, M., George, J.,

& Bugianesi, E. (2018). Global burden of NAFLD and NASH: Trends, predictions, risk factors and prevention. *Nature Reviews Gastroenterology and Hepatology*, *15*(1), 11–20. https://doi.org/10.1038/nrgastro.2017.109

Younossi, Z., Stepanova, M., Negro, F., Hallaji, S., Younossi, Y., Lam, B., & Srishord, M. (2012). Nonalcoholic fatty liver disease in lean individuals in the United States. *Medicine (United States)*, *91*(6), 319–327. https://doi.org/10.1097/MD.0b013e3182779d49

Zelber-Sagi, S., Nitzan-Kaluski, D., Goldsmith, R., Webb, M., Blendis, L., Halpern, Z., & Oren, R. (2007). Long term nutritional intake and the risk for non-alcoholic fatty liver disease (NAFLD): A population based study. *Journal of Hepatology*, *47*(5), 711–717. https://doi.org/10.1016/j.jhep.2007.06.020

Zhang, L., Wu, X., Liao, S., Li, Y., Zhang, Z., Chang, Q., Xiao, R., & Liang, B. (2016). Tree shrew (Tupaia belangeri chinensis), a novel non-obese animal model of non-Alcoholic fatty liver disease. *Biology Open*, *5*(10), 1545–1552. https://doi.org/10.1242/bio.020875

Zhang, Y., Proenca, R., Maffei, M., Barone, M., Leopold, L., & Friedman, J. M. (1994). Positional cloning of the mouse obese gene and its human homologue. *Nature*, *372*(6505), 425–432. https://doi.org/10.1038/372425a0

Zhang, Z., Chen, L., Liu, L., Su, X., & Rabinowitz, J. D. (2017). Chemical Basis for Deuterium Labeling of Fat and NADPH. *Journal of the American Chemical Society*, *139*(41), 14368–14371. https://doi.org/10.1021/jacs.7b08012

Zhou, Y., Wei, F., & Fan, Y. (2016). High serum uric acid and risk of nonalcoholic fatty liver disease: A systematic review and meta-analysis. In *Clinical Biochemistry* (Vol. 49, Issues 7–8, pp. 636–642). Elsevier Inc. https://doi.org/10.1016/j.clinbiochem.2015.12.010

Zivkovic, A. M., German, J. B., & Sanyal, A. J. (2007). Comparative review of diets for the metabolic syndrome: Implications for nonalcoholic fatty liver disease. In *American Journal of Clinical Nutrition* (Vol. 86, Issue 2, pp. 285–300). American Society for Nutrition. https://doi.org/10.1093/ajcn/86.2.285